BIOLOGICAL IDENTIFICATION SYSTEM WITH INTEGRATED SENSOR CHIP

[0001] This application claims the benefit of U.S. Provisional Patent Application Serial No. 60/201,603, filed May 3, 2000.

Statement Regarding Federally Sponsored Research Or Development

[0002] This invention was made with Government support under Grant No. N66001-96-C-8632 awarded by the Department of the Navy. The Government has certain rights in this invention.

Field Of The Invention

[0003] The field of the present invention relates generally to apparatus and methods for sensing or detecting various target analytes, including ionic molecules (e.g. iron, chromium, lead, copper, calcium or potassium) and macromolecules (e.g. DNA, RNA or protein) and in particular, to biosensors, methods of using the biosensors, and methods for making the biosensors.

Background Of The Invention

[0004] A variety of biosensors have been developed for the detection of biological material, such as pathogenic bacteria. Conventional methods for detecting bacteria usually involve a morphological evaluation of the organisms and rely on (or often require) growing the number of organisms needed for such an evaluation; such methods are time consuming and are typically impractical under field conditions. The need for rapid detection as well as portability has led to the development of systems that couple pathogen recognition with signal transduction. Both optical and electrochemical detection of bacteria have been reported (Ivnitski, et. al., 1999, T. Wang, et. al., 2000). (Full citations to the literature cited herein are given at the end of the specification.) However, the present inventive entity has determined that electrochemical methods have an advantage in that they are more amenable to miniaturization.

[0005] Requirements for an ideal detector include high specificity and high sensitivity using a protocol that can be completed in a relatively short time. Moreover, systems that can be miniaturized and automated offer a significant advantage over current technology, especially if detection is needed in the field.

[0006] The electrochemical methods use the principle of electrical circuit completion. To complete the electrical circuit, a counter electrode is used to provide a return path to the sample solution or reagent and a reference electrode is used as a reference point against which the

potential of another electrode or electrodes are determined (typically that of the working electrode or measuring electrode). Since this contact must be provided by electrochemical means, i.e. a metal electrode immersed in a chemical solution or reagent, it is impossible to avoid generating an electrical potential in series with the potential developed by the electrode. The conventional theory in the electrochemical methods is that it is essential for the reference electrode potential to be very stable and not be affected by chemical changes in the solution. Thus, silver/silver chloride reference electrodes, which provide a very stable reference potential, are the most common type of electrode used for reference electrodes today.

[0007] Referring to Fig. 1, the typical silver/silver chloride reference electrode 10 contains a chloridised silver wire 1 (a layer of silver chloride coated on silver wire) immersed in a solution 5 of potassium chloride (3.5M KCl) saturated with silver chloride (AgCl). This internal filling solution 5 slowly seeps out of the electrode 10 through a porous ceramic junction 20 and acts as an electrical connection between the reference element 1 and the sample. Potassium chloride is used because it is inexpensive and does not normally interfere with the measurement. The solution 5 also includes silver chloride to prevent dissolution of the coating on the reference element 1. It is therefore necessary to maintain the level of solution 5 in the electrode 10 using a filling solution hole 40.

[0008] The present inventive entity, however, has determined that robust and precise biological detection can be achieved using electrochemical methods, and more precisely using redox (reduction-oxidation) methods, without the need of a two-layered reference electrode (e.g., silver chloride coated on silver) having a known reference electrode potential described above.

[0009] Referring now to Fig. 2, the electrochemical methods also required a potentiostat 50, which is a control amplifier with the test cell placed in the feedback loop. The objective is to control the potential difference between a test electrode (working electrode) 60 and a reference electrode 70 by the application of a current via the third, auxiliary electrode (counter electrode) 80. In practice a fairly good potentiostat may be built using a minimum of components. In the circuit shown here, 90A and 90B are 1.22V bandgap reference diodes connected between the positive and negative power rails. Potentiometer 100 is then used to set the required cell polarization, applied to the non-inverting input of the main amplifier 110. The working electrode

60 connects to the ground of the circuit and the reference electrode 70 to the inverting input of the main amplifier 110. In order to boost the output capability somewhat (most operational amplifiers are limited to about 20 mA and do not tolerate capacitative loads well) a unity gain buffer amplifier 120 is used. Preferably, gain buffer amplifier 120 has a much higher bandwidth than amplifier 110, otherwise the circuit is likely to oscillate when driving a capacitative cell. The output of the buffer amplifier 120 connects to the auxiliary electrode 80 via a current measuring resistor 140. Differential amplifier 130 is then used to measure the voltage drop across this resistor 140 and to convert it to a ground referenced output voltage.

[0010] Microelectromechanical systems (MEMS) technology provides transducers to perform sensing and actuation in various engineering applications. The significance of MEMS technology is that it makes possible mechanical parts of micron size that can be integrated with electronics and batch fabricated in large quantities. MEMS devices are fabricated through the process of micromachining, a batch production process employing lithography. Micromachining relies heavily on the use of lithographic methods to create 3-dimensional structures using pre-designed resist patterns (masks) (Ho and Tai, 1996, 1998). MEMS is one suitable technology for making microfabricated devices or aspects thereof. Microfabricated devices are generally defined as devices fabricated by using MEMS and/or integrated circuit (IC) technology. An integrated circuit (IC) is defined as a tiny chip of substrate material upon which is etched or imprinted a complex of electronic components and their interconnections.

[0011] The present inventive entity has determined that miniaturization and portability features are inherent in electrochemical methods make these methods excellent candidates for integration into MEMS devices, and, further that it would be advantageous to integrate MEMS technology with biosensing methods to detect various ionic molecules and macromolecules (DNA, RNA or protein).

[0012] The present inventive entity has also determined that in the area of biosensing of bacteria, one of the most effective means of achieving high specificity is to detect the bacteria's genetic material (e.g. rRNA, mRNA, denatured DNA). By choosing a single-stranded DNA (ssDNA) probe whose sequence is complementary only to the target bacteria's rRNA or ssDNA, monitoring the hybridization event allows selective sensing of target cells. To maximize sensitivity, coupling the hybridization event with an enzymatic reaction leads to signal

amplification, as each substrate-to-product turnover contributes to the overall signal. Biosensing to detect DNA hybridizations that are amplified by enzymatic reaction can still be completed within a reasonably short time according to the invention.

[0013] Thus, a prototype amperometric detector for Escherichia coli (E. coli) has been developed based on the above determinations and technologies (Chen, et. al., 2000, Gau, et. al., 2000). The technologies of MEMS, self-assembled monolayers (SAMs), DNA hybridization, and enzyme amplification all contribute to the design of a miniaturized, specific, and sensitive E. coli detector. DNA electrochemical probes have been reported previously (Wang, et al., 1997, Marrazza, et al., 1999), with graphite or carbon electrodes typically used. Commercial units for amperometric detection of DNA from E. coli using screen-printed carbon electrodes on disposable test strips are also available. Screen-printing has the advantage of low cost; however, achieving high dimensional precision is not easy. Thus, the present inventive entity has determined a need to develop a method of using lithography to accurately pattern in μm size dimensions a wide range of materials such as metals (e.g. Au, Ag) and carbon. Moreover, utilizing a surface modification, such as self-assembly monolayer (SAM) of biotin-DAD-C12-SH dodecanamide, is a preferred method of selectively immobilizing molecules on MEMS surfaces. The formation of SAMs on Au, Ag and other metals has been well studied (Revell, et al., 1998, Motesharei, et al., 1998, Xia, et al., 1998, Lahiri, et al., 1999), and proteins and other biomolecules can be easily immobilized onto surfaces such as Au using SAMs (Ostuni, et al., 1999, Kane, et al., 1999, Spinke, et al., 1993, Haussling, et al., 1991). Amperometric methods using SAMs on electrodes have demonstrated the ability to detect target analytes successfully (Sun, et al., 1998, Hou, et al., 1998, Murthy, et al., 1998).

[0014] In the instant E. coli detection system, the present invention identifies and takes advantage of certain benefits inherent in each technology. Using DNA hybridization and enzyme amplification, the present invention achieves the required specificity and sensitivity. Using MEMS and SAMs, the present inventive entity fabricated a miniaturized system that can be developed into a portable instrument. Finally, the invention demonstrates that the present detection system is applicable to a broad range of pathogenic bacteria. For example, the detection module and assay protocol can be adapted to detect uropathogenic E. coli and identify microorganisms causing otitis media (middle ear infection).

[0015] Accordingly, it is an object of the invention to provide novel biosensors, novel methods of using the biosensors, and novel methods for making the biosensors. This object is solved by the combination of the features of the main claim, and the sub-claims disclose further advantageous embodiments of the invention.

Summary of the Invention

[0016] This summary of the invention does not necessarily describe all necessary features detailed in the specification, and the invention may also reside in a sub-combination of features described here and elsewhere in the specification.

[0017] A first aspect of the present invention provides an apparatus and method for sensing or detecting various target analytes, including especially macromolecules (e.g. DNA, RNA or protein) and ionic molecules (e.g. iron, chromium, lead, copper, calcium or potassium) using a biosensor incorporated on a single substrate (silicon, glass, plastic, etc.). The substrated biosensor system comprises at least two electrodes that are typically fabricated together as a single series microfabrication process step on the substrate. However, successive microfabrication steps may also be employed to fabricate the system.

[0018] In a preferred embodiment, the electrodes are all made out of pure metal (as opposed to the Ag/AgC1 electrodes of the prior art, for exmple). In another preferred embodiment, the substrated biosensor system comprises a working electrode, a reference electrode and a counter (auxiliary) electrode. Preferably the substrated biosensor system has the same electrochemical performance as a conventional electrochemical biosensor. In addition, the substrated biosensor system should be compatible with integrated circuit (IC) and/or MEMS fabrication processes and be capable of being constructed in a small area.

[0019] A second aspect of the present invention provides an apparatus and method for confinement of reagent and/or solution in a biosensor using surface tension at small scale. The reagent and/or solution contain the necessary electrolytes and/or analytes needed for biological sensing.

[0020] In a preferred embodiment, the apparatus and method in the present invention allow for each electrode used for sensing or detecting various ionic molecules (e.g. iron, chromium, lead,

copper, calcium or potassium) and macromolecules (e.g. DNA, RNA or protein) to be in selective contact with the reagent and/or solution when the electrolytes and/or analytes are needed by using controllable surface properties and surface tension forces at small scale.

[0021] In another preferred embodiment, the apparatus and method for confinement of reagent and/or solution (and thus the electrolytes and/or analytes in the reagent and/or solution) using surface tension is incorporated with a portable or handheld device and is immune to shaking of the device. In addition, the reagent and/or solution should be held firmly in position by the biosensor using surface tension even when the biosensor is flipped upside down.

[0022] A third aspect of the present invention provides an apparatus and method for integrating the components of an electrochemical sensor and/or sensors (e.g. electrodes) and additional required electronic circuit components (e.g. amplifiers) in an electrochemical sensor or sensors with integrated circuit (IC) technologies. The entire sensor system and/or systems can be incorporated on a single IC substrate or chip, such as a single semiconductor (e.g. silicon or gallium arsenide) substrate or chip. Preferably, no or much fewer external components and/or instruments are required to complete the system or systems. The sensor and/or sensors are preferably fabricated using the IC process.

[0023] In any of the embodiments used for macromolecule electrochemical detection, a preferred feature of the invention is to modify the surface on at least one of the electrodes. Preferably, the surface is modified for anchoring macromolecules on the surface. Preferably, the surface is modified using a self-assembly monolayer (SAM) such as biotin-streptavidin. Preferably, the SAM is placed on the surface of a working electrode in an electrochemical sensor. Optionally, materials such as solgel and/or carbon paste may be used to modify the surface (as a replacement for SAM or in combination with SAM).

[0024] The above "summary of the invention" presents only examples and not limitations. Further embodiments as well as sub-combinations, modifications, variations and enhancements of the invention will become apparent in the detailed description of the invention, which follows herein.

Brief Description of the Drawings

[0025] In the drawings, wherein the same reference number indicates the same element throughout the several views:

[0026] Fig. 1 is a schematic of an embodiment of a conventional reference electrode.

[0027] Fig. 2 is a schematic of an embodiment of a potentiostat used in the electrochemical methods.

[0028] Fig. 3 is a schematic of an embodiment of a plurality of electrochemical biosensors on a circular substrate wafer according to the present invention.

[0029] Fig. 4 is a schematic of alternative embodiment of a plurality of electrochemical biosensors on a square substrate according to the present invention.

[0030] Fig. 5 is a schematic of another embodiment of an electrochemical biosensor on a substrate according to the present invention.

[0031] Fig. 6 is a graph of Cyclic Voltammetry (CV) scan potential over time.

[0032] Fig. 7 is a one-cycle Cyclic Voltammetry (current vs. bias potential) taken by a biosensor according to the present invention.

[0033] Fig. 8. is a Cyclic Voltammetry (current vs. bias potential) at different scan rate taken by a biosensor according to the present invention.

[0034] Fig. 9. is a graph of the square root of scan rate vs. peak current taken by a biosensor according to the present invention.

[0035] Fig. 10 is a Cyclic Voltammetry (current vs. bias potential) on a plurality of cycles at constant scan rate taken by a biosensor according to the present invention.

[0036] Figs 11(a), (b) and (c) are diagrams showing reagent and/or solution confinement by surface tension and treatment according to the present invention.

[0037] Fig. 12 is a diagram showing reagent and/or solution confinement selectively over only a working electrode on a biosensor according to the present invention.

[0038] Fig. 13 is a diagram showing reagent and/or solution confinement over all electrodes on a biosensor according to the present invention.

[0039] Fig. 14 is a side view diagram showing the first step of how an embodiment of a biosensor of the present invention can be fabricated.

[0040] Fig. 15 is a diagram showing the second step of how the biosensor can be fabricated.

[0041] Fig. 16 is a diagram showing the third step of how the biosensor can be fabricated.

[0042] Fig. 17 is a diagram showing the fourth step of how the biosensor can be fabricated.

[0043] Fig. 18 is a diagram showing the fifth step of how the biosensor can be fabricated.

[0044] Fig. 19 is a diagram showing the sixth step of how the biosensor can be fabricated.

[0045] Fig. 20 is a diagram showing how the surface of an embodiment of the present biosensor can be modified to prevent non-specific binding.

[0046] Fig. 21 is a diagram showing the final result on the biosensor surface of the surface modification process in Fig. 20.

[0047] Fig. 22 is a sectional diagram of an embodiment of the present invention of a biosensor system with a biosensor integrated with integrated circuit components.

[0048] Fig. 23 is a diagram of an embodiment of the present invention of a plurality of biosensors integrated with integrated circuit components.

[0049] Fig. 24 is a sectional diagram of a biosensor unit that, together with other similar units, makes up the plurality of biosensors integrated with the integrated circuit components in Fig. 24.

[0050] Fig. 25 is a diagram showing the first step of how an embodiment of a biosensor (sensor-chip) of the present invention can be fabricated by integrated circuit (IC) technology with a CMOS device integrated on the biosensor (sensor-chip) itself.

[0051] Fig. 26 is a diagram showing the second step of how the biosensor (sensor-chip) can be fabricated by integrated circuit (IC) technology.

[0052] Fig. 27 is a diagram showing the third step of how the biosensor (sensor-chip) can be fabricated by IC technology.

[0053] Fig. 28 is a diagram showing the fourth step of how the biosensor (sensor-chip) can be fabricated by IC technology.

[0054] Fig. 29 is a diagram showing the fifth step of how the biosensor (sensor-chip) can be fabricated by IC technology.

[0055] Fig. 30 is a diagram showing the sixth step of how the biosensor (sensor-chip) can be fabricated by IC technology.

[0056] Fig. 31 is a diagram showing how an embodiment of a biosensor of the present invention can be use to detect ionic analytes (or molecules).

[0057] Fig. 32 is Cyclic Voltammetry (CV) (current vs. bias potential) graph taken by the sensor of Fig. 31.

[0058] Fig. 33 is a diagram showing the first step of how an embodiment of a biosensor of the present invention can be used to detect macromolecules (e.g. DNS, RNA, protein).

[0059] Fig. 34 is a diagram showing the second step of the detection of the macromolecules.

[0060] Fig. 35 is a diagram showing the third step of the detection of the macromolecules.

Detailed Description of the Preferred Embodiment

[0061] Although specific embodiments of the invention will now be described with reference to the drawings, it should be understood that various changes and modifications may be made without departing from the spirit, scope and contemplation of the invention. Indeed, the drawings and description herein are provided by way of examples, and not by way of limitations.

[0062] The first aspect of the invention relates to detection of various target analytes, especially ionic molecules (e.g. iron, chromium, lead, copper, calcium or potassium) and macromolecules (e.g. DNA, RNA or protein), using the principles of electrochemical detection. The principles of electrochemical detection require the use of a redox cell and an electrochemical reaction in the cell.

[0063] The redox cell is a device that converts chemical energy into electrical energy or vice versa when a chemical reaction occurs in the cell. Typically, the cell consists of three electrodes immersed into an aqueous solution (electrolyte) with electrode reactions occurring at the electrode-solution surfaces.

[0064] The cell consists of two electronically conducting phases (e.g., solid or liquid metals, semiconductors, etc.) connected by an ionically conducting phase (e.g. aqueous or nonaqueous solution, molten salt, ionically conducting solid). As an electrical current passes, it must change mode from electronic current to ionic current and back to electronic current. These changes of conduction mode are accompanied by reduction-oxidation reactions. Each mode changing reaction is called a half-cell.

[0065] Each electrochemical reaction is reduction-oxidation (redox) reaction that occurs in the redox cell. For example, in a spontaneous "chemical reaction" during the oxidation of hydrogen by oxygen to water, electrons are passed directly from the hydrogen to the oxygen. In contrast,

in the spontaneous electrochemical reaction in the redox cell, two separate electrode reactions occur substantially simultaneously or in tandem.

[0066] An important feature of the redox cell is that the simultaneously occurring -reduction-oxidation reactions are spatially separated. The hydrogen, for example, is oxidized at the anode electrode by transferring electrons to the anode electrode and the oxygen is reduced at the cathode electrode by accepting electrons from the cathode electrode. The overall electrochemical reaction is the sum of the two electrode reactions. The ions produced in the electrode reactions, in this case positive hydrogen ions and negative hydroxyl ions, will recombine in the solution to form the final product of the reaction: water.

[0067] During this process the electrons are conducted from the anode electrode to the cathode electrode through an outside electric circuit where the electronic current can be measured. The reaction can also be reversed; water can be decomposed into hydrogen and oxygen by the application of electrical power in an electrolytic cell.

[0068] A three-electrode system of the invention is an electrochemical cell containing a working electrode, a counter electrode (or auxiliary electrode), and a reference electrode. A current may flow between the working and counter electrodes, while the potential of the working electrode is measured against the reference electrode. This setup can be used in basic research to investigate the kinetics and mechanism of the electrode reaction occurring on the working electrode surface, or in electroanalytical applications. The detection module in the preferred embodiment in the instant invention is based of a three-electrode system.

[0069] The counter electrode is used to make an electrical connection to the electrolyte so that a current can be applied to the working electrode. The counter electrode is usually made of inert materials (noble metals or carbon/graphite) to avoid its dissolution. It has been observed in connection with the present invention that a small feature or small cross-section at the counter electrode will heat up the surrounding solution when a large current is pulled out from the counter electrode. Bubbles will be generated if the current is continuously overflowed, and ultimately dissolution of the electrode occurs. Thus, the bubble formation can be avoided by controlling the current and/or the electrode size. In a preferred embodiment of the present invention, the width of the counter electrode is large enough to avoid this heat up problem even at large current.

[0070] The reference electrode is used as a reference point against which the potential of other electrodes (typically that of the working electrode or measuring electrode) can be measured in an electrochemical cell. The few commonly used (and usually commercially available) electrode assemblies all have an electrode potential independent of the electrolyte used in the cell, such as a silver/silver-chloride electrode, calomel electrode, or hydrogen electrode. However, the present inventive entity has determined that a single layer electrode, such as a single layer of gold electrode, can fulfill the requirement for a reference electrode.. In addition, other materials such as silver, copper, platinum, chromium, aluminum, titanium, nickel may also work as a single layer reference electrode under the right conditions.

[0071] The working electrode plays a central role in the electrochemical biosensors of the invention. The reaction occurring at the working electrode may be used to perform an electrochemical analysis of the electrolyte solution. It can serve either as an anode or a cathode, depending on the applied polarity. One of the electrodes in some "classical two-electrode" cells can also be considered a "working" ("measuring," "indicator," or "sensing") electrode, e.g., in a potentiometric electroanalytical setup where the potential of the measuring electrode (against a reference electrode) is a measure of the concentration of a species in the solution.

[0072] In a preferred three-electrode embodiment, the counter and reference electrodes are configured to extend generally about the periphering of the working electrode of the biosensor. Suitability configurations are seen in, for example, Figs. 3, 4, 5, 12, 13 and 23.

[0073] In a preferred embodiment, the electrochemical biosensor is fabricated using microelectromechanical systems (MEMS) technology. Referring now to Fig. 3, a layer of silicon dioxide (SiO_2, 1000Å) is deposited on a bare silicon wafer 200 (prime grade, p-type <100>, thickness 500-550. μm) and served as a pad layer underneath the silicon nitride (Si_3N_4, 1000Å) to release stress and improve adhesion. A plurality of MEMS biosensors (such as biosensor 210) were fabricated with working electrodes of various dimensions (such as working electrode 220). Preferably each of the working electrodes is etched to form a well up to 350. μm in depth.

[0074] The nitride-coated silicon wafer 200 was patterned and bulk etched using KOH along the [111] and [100] crystal planes, and the depth of the well was controlled by KOH etching time and temperature. The 100. μm wide auxiliary (such as auxiliary electrode 230) and reference

(such as reference electrode 240) electrodes are separated from their corresponding working electrode 220 by 200 μm. Fig. 3 shows a schematic of the pattern used in generating the MEMS biosensors (such as biosensor 210).

[0075] The nitride and oxide were removed by HF etching to release internal stress, and another oxide layer (5000Å) was deposited for electrical isolation. Electrodes were patterned by PR5214 photo resist reverse imaging and lift-off process with electron beam deposition of Au(2000Å)/Cr(200Å). Finally the wafer 200 was bathed in hexamethyldisilazane (HMDS) vapor for three minutes after ten minutes of a 150°C hot bake to generate a hydrophobic surface on the surrounding Si areas. The hydrophobic nature of the surrounding area, along with the 3-dimensional nature of the working electrode (such as working electrode 220), allows containment of a liquid droplet on the working electrode 220 during the initial sensing step of immobilizing to the working electrode molecules of interest in the solution. This design effectively minimized non-specific binding of biomolecules to other areas of the MEMS array.

[0076] Preferably the material used for all the electrochemical electrodes is gold (Au). Several conducting materials, available in MEMS technology, were patterned on a silicon substrate by the lift-off process, and the characteristics of the three-electrode system were tested by cyclic voltammetry with ferricyanide solution. Different combinations of gold, platinum, titanium and aluminum electrodes were tested and the Au/Au/Au three-electrode system gave the best C-V curve and redox characteristics.

[0077] Fig. 4 shows an embodiment of biosensors fabricated on a square substrate 300 (such as silicon, gallium arsenide, plastic and/or glass) having a plurality of circular biosensors, such as biosensor 310. The biosensor 310 comprises a working electrode 320, a reference electrode 330, and a counter (auxiliary) electrode 340. As previously mentioned, preferably the electrodes are constructed out of a single layer of conducting materials, available in MEMS technology. Furthermore, all of the electrodes should preferably be constructed out of gold (Au).

[0078] Fig. 5 shows yet another preferred embodiment of the present invention. The biosensor 410 comprises a working electrode 420, a reference electrode 430 and a counter (auxiliary) electrode 440 fabricated on the substrate. Preferably, the electrodes are made out of gold. The working electrode 420 is formed in a built-in well 450 in the substrate up to 350 μm in depth.

The well 450 is designed for confining a desired reagent within the well-defined space. As shown in Fig. 5, the well 450 fabricated by the microfabrication methods described herein, is bordered by (111) silicon planes after KOH etching. The working electrode 420, defined by the microfabrication methods described above, covers the entire well 450 surface.

[0079] In operation, the above embodiments have the advantage of being easy to fabricate and can be fabricated together as a single series microfabrication process step on the substrate. However, successive microfabrication steps may also be employed for fabrication. Furthermore, as the following analysis and experiments below show, these low-cost and easy-to-fabricate biosensors are reusable and have the same robust and reversible electrochemical performance as conventional biosensors.

[0080] In one experiment, Cyclic Voltammetry (CV) analytical technique is used. CV is one of the most versatile analytical techniques used in the study of electroactive species and the characterization of biosensors. It is widely used as both an industrial and academic research tool in the fundamental characterization of electrochemical systems. In Cyclic Voltammetry, the potential is ramped from an initial potential (E_o) to a maximum potential (E_m) at a controlled (and typically fixed) sweep rate (V/sec.).

Fig. 6 illustrates this concept. Repeated cycles of reduction and oxidation of the analyte generate alternating anodic and cathodic currents in and out of the working electrode. Since the solution and/or reagent is not stirred, diffusion effects are observed at different analyte concentrations and different scan rates.

[0081] Separation of the anodic (i_{pa}) and cathodic (i_{pc}) current peaks can be used to predict the number of electrons involved in the redox reaction. The peak current is also directly proportional to the analyte concentration, C and scan rate, v. Experimental results are usually plotted as current versus potential, similar to the graph shown in Fig. 7.

[0082] In the CV scan shown in Fig. 7, the potential is graphed along the x-axis with more positive (or oxidizing) potentials plotted to the right, and more negative (or reducing) potentials to the left. The current is plotted on the y-axis with cathodic (i.e., reducing) currents plotted down along the negative direction, and anodic (i.e. oxidizing) currents plotted in the positive direction.

[0083] The analyte used in the following control experiment was potassium ferricyanide, $K_3Fe(CN)_6$ (329.26 g/mol), which contains an iron atom in the +3 oxidation state (Fe^{III}) in a buffer solution of potassium nitrate, KNO_3 (101.11 g/mol). At the surface of a working electrode, a single electron can be added to the ferricyanide anion. This will cause it to be reduced to the ferricyanide anion, $Fe^{II}(CN)_6^{4-}$, which contains an iron atom in the +2 oxidation state (Fe^{II}). This simple, one electron exchange between the analyte and the electrode is a well behaved, reversible reaction. This means that the analyte can be easily reduced to $Fe^{II}(CN)_6^{4-}$ and then easily oxidized back to $Fe^{III}(CN)_6^{3-}$.

[0084] A redox couple is a pair of analytes differing only in oxidation state. The electrochemical half-reaction for the $Fe^{III}(CN)_6^{3-}$ / $Fe^{II}(CN)_6^{4-}$ redox couple can be written as follows:

$$Fe^{III}(CN)_6^{3-} + e^- \Leftrightarrow Fe^{II}(CN)_6^{4-} \qquad E_o = +0.358V(NHE). \qquad \textbf{(1)}$$

The voltammogram shown in Fig. 8 exhibits two asymmetric peaks, one cathodic (i_{pc}) and the other anodic (i_{pa}). Using a standard reference electrode, such as the normal hydrogen electrode (NHE), the formal potential associated with this half-reaction is near *+358* mV. If the working electrode is held at a potential more positive than *+400* mV, then the analyte tends to be oxidized to the $Fe^{III}(CN)_6^{3-}$ form. This oxidation at the working electrode causes electrons to go into the electrode from the solution resulting in an anodic current. At potentials more negative than *+400* mV, the analyte tends to be reduced to $Fe^{III}(CN)_6^{4-}$. This reduction at the working electrode causes electrons to flow out of the electrode into the solution resulting in a cathodic current. Since the preferred sensor design embodiment of the present invention does not utilize a standard reference electrode like NHE, silver/silver chloride (Ag/AgCl) or saturated calomel electrode (SCE), and since all three electrodes are gold (Au), the rest (unbiased) potential in this experiment is close to zero volts.

[0085] The important parameters of a cyclic voltammogram are the magnitudes of the cathodic and anodic peak currents (i_{pc} and i_{pa}, respectively) and the potentials at which these currents are observed (E_{pc} and E_{pa}, respectively). Using these parameters, it is possible to calculate the formal reduction potential (E_o – which is centered between E_{pa} and E_{pc}) and the number of electrons (n) transferred in the charge transfer reaction.

[0086] The peak current (i_{pa} or i_{pc}) can be expressed by the Randles-Sevcik equation:

$$i_p = 0.4463nFAC\left(\frac{nF\nu D}{RT}\right)^{\frac{1}{2}} \quad (2)$$

where, n = number of electrons appearing in half-reaction for the redox couple

F = Faraday's constant (96,485 C/ mol)

A = electrode area (cm^2)

ν = rate at which the potential is swept (V/sec)

D = analyte's diffusion coefficient (cm^2/sec)

R = universal gas constant (8.314 J / mol K)

T = absolute temperature (K)

At 25°C, the Randles-Sevcik equation can be reduced to the following:

$$i_p = (2.687 \times 10^5)n^{3/2}\nu^{1/2}D^{1/2}AC \quad (3)$$

where the constant has units (i.e., 2.687×10^5 C mol^{-1} $V^{-1/2}$).

[0087] The Randles-Sevcik equation predicts that the peak current should be proportional to the square root of the sweep rate when voltammograms are taken at different scan rates. As shown in Fig. 9, the plot of peak current versus the square root of sweep rate yields a straight line. The Randles-Sevcik equation can be modified to give an expression for the slope of this straight line as follows,

$$Slope = (2.687 \times 10^5 Cmol^{-1}V^{-1/2})n^{3/2}D^{1/2}AC \quad (4)$$

The scan rate dependence of the peak potentials and peak currents are used to evaluate the number of electrons participating in the redox reaction as well as provide a qualitative account of the degree of reversibility in the overall reaction. The number of electrons transferred in the electrode reaction (n) for a reversible redox couple is determined from the separation between the peak potentials ($\Delta Ep = Epa - Epc$). For a simple, reversible (fast) redox couple, the ratio of the anodic and cathodic peak currents should be equal to one. The results of the experiment using the preferred sensor design deviate only slightly from unity. Large deviations would indicate interfering chemical reactions coupled to the electrode processes, but slight deviations from unity merely suggest a non-ideal system. Fig. 10 shows the CV scan for 12 consecutive cycles with minor deviations from the first cycle. These results clearly indicate a highly reversible system and robust cell design.

[0088] Besides being easy and cheap to fabricate while having the same performance as the conventional sensor, the above embodiments of the present invention also have the advantages of being compatible with the integrated circuit (IC) and the MEMS fabrication process. Furthermore, as shown in Figs. 3 and 4 these embodiments are capable of being constructed in an array of biosensors and in a small area.

[0089] A second aspect of the present invention relates to confinement of a reagent and/or solution in a biosensor using surface tension at small scale. The reagent and/or solution contains the target analyte(s) and/or the chemical(s) needed for biosensing.

[0090] A biosensor's performance is mainly determined by its specificity and sensitivity. The concept of confining the reagent on a substrate, such as silicon, was discovered in investigations relating to the present invention to be a solution for reducing the high level of detection noise caused by the non-specific binding of the analyte or other reagent or solution components, such as Horseradish Peroxidase (HRP), onto regions arund the periphery of the working electrode and causing high detection noises and creating high false positive rates. HRP is used in the instant embodiment as a signaling enzyme. To verify that noise does come from the HRP residual at the surface, a simple test was done to estimate the contribution of this unwanted binding. HRP was introduced to a bare silicon chip, followed with several wash steps before the addition of the substrate solution. A very high level of enzymatic reaction was observed immediately after adding the substrate solution.

[0091] As expected, HRP, like other proteins, sticks to the silicon surface easily and tightly. Several commercial wash solutions and blocking protein were tested without any significant improvement of reducing non-specific binding. Thus, it was determined that the best way to avoid the effects ofundesirable binding is to prevent it from happening in the first place. The area outside the working electrode of the biosensor of the invention need not encounter the HRP solution in order to achieve biological sensing. In the prior art, however, it is conventional to immerse all three electrodes in aqueous system all the time and all the reagents would flow through all the surface area.

[0092] The simplest way, discovered by the present inventive entity, to confine certain reagents within a well-defined space is to form a well in the biosenser. As shown in Fig. 5, a microfabricated well is bordered by silicon crystal planes 400 after KOH etching. The working

electrode 420 defined by a lift-off process covers the whole well surface. Thus, a reagent or solution containing components capable of non-specific binding (e.g. HRP) may initially be confined to the well area to achieve the desired binding to the electrode in the well (preferably the working electrode), while avoiding non-specific binding to the periphery region of the biosensor. The reagent or solution can then be washed off the biosensor and additional reagents and/or solutions later added to complete the sensing process.

[0093] The importance of surface and material science cannot be underestimated when designing a biosensor. An unacceptable amount of non-specific binding may still occur during the washing process while the diluted reagent is flowing around the wafer surface. The time for the wash solution containing HRP, for example, to stay on the periphery region is much longer than the binding time constant. Therefore, besides fabricating the well structure, the surface of the periphery area preferably should be protected by other mechanisms.

[0094] Thus, another way to keep the surface from contacting undesired reagents or binding components is to make it hydrophobic. Silanation of silicon surface is widely used to prevent suspended structures from sticking to substrate by surface tension. This approach was used here to prevent the direct contact of biomolecules to the periphery area of the silicon substrate.

[0095] Silane-based molecules with various functional terminal groups have been used to modify surface properties of silicon wafers, silicon nitride chips, and atomic force microscopy (AFM) tips. Silane compounds for the surface modification form robust monolayers chemically tethered to silicon oxide surfaces as a result of hydrolysis of terminal $Si(Cl)_n$ or $SiO\text{-}C_2H_5$ groups.

[0096] The performance of artificial materials in contact with biological systems is determined by the surface interactions of the two materials. Since the surface interaction could result in noise increasing and structure damage, surface modification is one way to avoid this problem. The easiest way is to change the surface property of the structure or by using plastic. By converting the surface into a biocompatible or bio-inert surface, non-specific interaction will be limited to a minimum or eliminated by the fabrication of a molecular layer firmly tethered to the surface. The most widely implemented approach uses a self-assembly monolayer (SAM) from thiol molecules by chemisorption onto a gold surface and silane molecules to form SAM on a silicon oxide surface according to well-established procedures developed in the 80's mostly by

C. D. Bain, and G. M. Whitesides. Other materials such as sol gel and carbon paste may also be used to modify the surface.

[0097] In operation, referring now to Fig. 11(a), the reagent is shaped by the hydrophilic working electrode and a droplet is nicely formed over the Au working electrode surface. Fig. 11(b) demonstrates that with increasing volume of the reagent, the area covered by the reagent will gradually expand and then cover the other two electrodes. Fig. 11(c) shows that when an excess stream of reagent is administered by pipette, a ball 465 of reagent will be formed instead of spreading out on the hydrophobic silicon substrate.

[0098] Turning now to Figs. 12 and 13, each individual electrode will be in contact with electrolyte and/or analyte and other components 509 only when needed by using controllable surface property and surface tension force at small scale. Referring now only to Fig. 13, for electrochemical detection, all electrodes have to be immersed in the electrolyte and/or analyte 509 only at detection time. For most applications, the majority of time is spent on sample preparation as depicted in Fig. 12 to immobilize the electrolyte and/or analyte 509 onto working electrode 510. In this embodiment as shown in Figs. 12 and 13, the coverage of the electrolyte and/or analyte 509 over the electrodes is controlled by surface property and reagent volume 520.

[0100] Thus, the above embodiments take advantage of surface tension at small scale to confine the electrolytes and/or analytes and other components. In addition, the above embodiments require much less reagent (in the order of pL to mL); and eliminate the need for bulk solution. Furthermore, because of the small amount of reagent use, the above embodiments have the advantages of having the analyte close to the electrodes (pm to mm), whereby adequate exposure of analyte to the electrodes can be achieved using diffusion effects alone, and the need for stirring or other mixing is eliminated. Another advantage of the above embodiments is the ease of the control and/or change of the coverage of electrolyte and/or analyte over the electrodes. Moreover, the above reagent and/or solution confinement embodiments reduce the loss of target analytes and improve the sensitivity of the biosensor by greatly reduce non-specific binding. In addition, the above embodiments are relatively immune to shaking of the biosensor and are suitable for portable or handheld systems. Lastly, due to the surface tension confinement effect, the reagent will be held firmly by surface tension even the sensor is flipped upside down.

[0101] Optionally, as shown in Figs. 12 and 13, the biosensor embodiments can be equipped with a reaction well 530 to help hold the reagent 520 in place and to control the shape of the reagent 520. However, such a well 530 is not required and the confinement of the reagent 520 can be achieved by a simple flat surface.

[0102] Referring now to Fig. 14, this shows the first step of a preferred fabrication of an embodiment of the present biosensor (sensor-chip).As shown in Fig. 14, a layer of silicon dioxide (SiO_2, 1000Å) 620 is first deposited on a bare Si wafer 610 (prime grade or test grade, p-type or n-type <100>, thickness 500-550 μm). The silicon dioxide 620 serves as a pad layer underneath the silicon nitride 630 (Si_3N_4, 1000Å) to release stress and improve adhesion.

[0103] Next, referring to Figs. 15 and 16, the nitride wafer 600 is patterned (Fig. 15) by mask 640 and bulk etched using KOH along the [111] and [100] crystal planes (Fig. 16). The etching creates a well 650 and the depth of the well 650 (up to 350 μm) is controlled by KOH etching time and temperature.

[0104] Referring now to Fig. 17, the nitride 630 and oxide 620 were then removed by HF etching to release internal stress, and another oxide 660 layer (5000Å) is deposited for electrical isolation. Figure 17.

[0105] Figs. 18 and 19 show a lift-off process for the fabrication of the necessary electrodes. The electrodes for biosensing are patterned on substrate 610 by using PR5214 photo resist layer 670 on silicon dioxide layer 660. Next, a mask 671 is used to transfer a desired pattern onto photo resist layer 670 by using reverse imaging process (which includes the removal unwanted photo resist layer 670). A layer of gold Au (2000Å) 680 is electron-beam deposited on silicon dioxide layer 660 with the desired photo resist pattern layer 670. Preferably, a deposition of an adhesive 690, such as chromium (Cr 200Å) occurs before the deposition of Au(2000Å) 680 to improve the adhesion of the Au onto the silicon dioxide layer 660. In addition, other materials such as titanium or glue may also work as an adhesive. Lastly, referring to Fig. 19, any photo resist 670 and unwanted Au 680 and Cr 690 are removed by dissolving the photo resist pattern layer 670.

[0106] Finally the wafer 600 is bathed in hexamethyldisilazane (HMDS) vapor for three minutes after ten minutes of a 150°C hot bake to generate a hydrophobic surface on the surrounding silicon areas.

[0107] Preferably, the surface of the biosensor (sensor chip) is modified by a surface modification step to prevent non-specific binding. As an example, referring to Fig. 20, a macromolecule biosensor's surface can be modified by the steps of first cleaning the Au surfaces 680 with concentrated "Piranha" solution (70 vol% H_2SO_4, 30 vol% H_2O_2) and thoroughly rinsed with deionized water (dH_2O). Next, referring to Fig. 20, surface modification material such as SAM of biotin-DAD-C12-SH (12-mercapto(8-biotinamide-3,6-dioxaoctyl)dodecanamide) Roche GmBH, Germany is deposited. For depositing a SAM of biotin-DAD-C12-SH), the procedure of Spinke, et al. (1993) was used wherein samples were incubated for ~18 hours in a 50mM solution of biotin-DAD-C12-SH in ethanol with 4.5x10-4M 11-mercapto-1-undecanol (Aldrich Chemical Co., 44,752-8) and rinsed with ethanol and water. Finally, referring to Fig. 21, the biotin-coated Au surfaces 700 were then exposed to a 1.0 mg/ml streptavidin solution for ~10 minutes and rinsed again with dH_2O to form a streptavidin-coated Au surface 710.

[0108] A third aspect of the present invention relates to the integration of an entire electrochemical (redox) biosensor onto a single integrated circuit (IC) chip. An integrated circuit (IC) is defined as a tiny wafer of substrate material upon which is etched or imprinted a complex of electronic components and their interconnections.

[0109] MEMS devices have distinctive properties as a result of small features but the signal level from MEMS-based sensor is relatively low compared to a conventional sensor. Sensitivity can be improved by using an off-chip amplification module but it also increases the noise and the system size. Thus, the present inventive entity designed an on-chip amplification circuitry (amplification circuit incorporated on the biosensor chip itself) and detection circuitry (such as providing bias potential, current measurement, sequential control and signal processing) to reduce the inter-chip interference. Both the detection circuitry and the amplification circuitry can be provided by using bipolar transistor (BJT) and/or complementary metal-oxide-semiconductor (CMOS) devices.

[0110] In a present embodiment, an on-chip amplification device is equipped underneath the working electrode, which is typically the largest area of the electrochemical sensor cell. Analogous to the open-base bipolar (BJT) photosensor, the base region receives the current from the transducer with the current gain beta β, which ranges from 80-150. There are two types of BJT which can be implemented with an electrochemical cell, vertical BJT and horizontal BJT.

The current gain is determined by the length of base region. In vertical BJT, this is a function of ion implementation energy and doping concentration. In horizontal BJT, the length is a function of lithography resolution, ion implementation angle and thermal diffusion. For these reasons the vertical BJT is more reliable in terms of chip-to-chip or in-chip gain uniformity.

[0111] Fig. 22 shows in cross-section an embodiment of in-chip amplifier circuitry that preferably includes a biosensor comprising three metal electrodes used for electrochemical sensing. Preferably, the three electrodes are fabricated using integrated circuit (IC) processes and have a relatively large area for interconnection and isolation. The entire biosensor chip 700 can be stacked in two stages (electrochemical sensing stage 730 and bipolar transistor (BJT) amplifying stage 720) and the Au working electrode 710 can act as an electromagnetic shield for the BJT device 720. The working electrode contacts (such as contacts 733, 734, 735, 736, 737 and 738) make contact to a contact interface 740 and also increase the surface area of the working electrode 710 for higher signal. All contact and electrode structures can be made with a single layer of metal such as gold. In addition, biosensor chip 700 comprises a silicon substrate 744. Substrate 744 includes a base region 743, a collector 742 and an emitter 741. Base region 743 receives electron flux from working electrode 710. Collector 742 is connected to a power source and provides the current gain under certain base conditions for amplification reasons. A resulting current from base 743 and collector 742 is then measured at emitter 741.

[0112] Referring still to Fig. 22, metal interconnect 750 is connected to signal output (not shown) and emitter 741. Gold working electrode 710 connects to base region 743 through a first layer 760 of silicon dioxide via etching. A second layer of silicon dioxide 770 isolates the BJT 720 and signal line while first layer 760 isolates the three electrodes (working electrode 710, reference electrode 780, and counter electrode 790). The contacts (such as contacts 733, 734, 735, 736, 737 and 738) on working electrode 710 increase the surface area and also form a solid contact with BJT 720. The dimension of the contacts (about a few tenths μm each) is much larger than the size of the optional protein SAM (about a few tenths Å) on working electrode 710 so the protein adsorption will not be affected.

[0113] Fig. 24 shows a sectional view of another preferred embodiment of a biosensor unit 800 representing a preferred embodiment of a plurality of biosensors on a substrate 805 shown in Fig.

23. As seen in Fig. 24, the biosensor unit 800 comprises a CMOS and/or BJT layer 830, an electrochemical layer 840 and a reagent containment layer 850, and is generally similar to the Fig. 22 embodiment already described.

[0114] Thus, as shown in Figs. 22, 23 and 24, the third aspect of the present invention is related to a biosensing system that allows for direct integration without chip-to-chip connection of the components in the sensor with other components needed for biological detection. The system does not require an external component (instrument) or requires only a minimum number of external components to constitute a complete system. Furthermore, this all-in-one biosensing system reduces the cost and noise level of biological sensing and simplifies the process of such sensing.

[0115] Referring now to Fig. 25, which shows an example of how an embodiment of the present biosensor (sensor-chip) can preferably be fabricated by integrated circuit (IC) technology with a CMOS device and/or devices. In addition, a BJT device and/or devices (not shown) may also be included. As shown in Fig. 25, an integrated circuit (IC) is fabricated on semiconductor substrate 900 with a layer of silicon dioxide 905 with a poly silicon gate 907 on top of a active well region 909. Poly silicon gate 907 is fabricated from an amorphous silicon and it is used for switching the transistor comprises low resistance source 917 and drain 919.

[0116] Referring now to Fig. 26, an oxide layer (5000Å) 920 is next deposited on the substrate 900 for electrical isolation. Referring now to Fig. 27, the silicon dioxide layer 920 is then selectively etched by using lithography and etching methods to form an electric connection hole 940. Referring now to Fig. 28, a conducting plug 950 is then applied into the contact hole 940. Conducting plug 950 is used as interconnection between conductive electrode 960 with low resistance source 917 and/or drain 919.

[0117] Fig. 29 shows a lift-off process for the fabrication of the necessary electrodes. The electrodes for biosensing are patterned on substrate 900 by using PR5214 photo resist layer 970 on silicon dioxide layer 920. Next, a mask 921 is used to transfer a desired pattern onto photo resist layer 970 by using reverse imaging process (which includes the removal of unwanted photo resist layer 970). A layer 960 of gold Au(2000Å) and/or Cr(200Å) is electron-beam deposited on silicon dioxide layer 920 with the desired photo resist pattern layer 970. Lastly,

referring to Fig. 30, any photo resist 970 and unwanted Au/Cr 960 are removed by dissolving the photo resist pattern layer 970.

[0118] Referring now to Fig. 31, this shows an example of how an embodiment of the present biosensor (sensor-chip) 1000 can preferably be used to detect an ionic molecule, such as iron (Fe). In this embodiment, the sensor surface 1010 is not modified and is ready to use after the post fabrication cleaning as shown in the above fabrication embodiment. The analyte used in this embodiment was potassium ferricyanide, $K_3Fe(CN)_6$ (329.26 g/mol), which contains an iron atom in the +3 oxidation state (Fe^{III}) in a buffer solution of potassium nitrate, KNO_3 (101.11 g/mol). As shown, in Fig. 31, the mixed solution 1020 with analytes (or reagent with electrolytes) is applied onto all three electrodes (working 1030, reference 1040 and counter electrode 1050). The volume of the solution 1020 is adjusted so the droplet is confined over all three electrodes by surface tension forces.

[0119] Next, referring to Fig. 32, the Cyclic Voltammetry (CV) current vs. bias potential was measured using a CH Instruments 660A Electrochemical Workstation with a picoamp booster and faraday cage. The potential is swept between 0.1 volt and –0.4 volt and the current is measured through working electrode 1030.

[0120] After the measurement, the Au surfaces were cleaned with acetone, alcohol, and concentrated "Piranha" solution (70 vol% H_2SO_4, 30 vol% H_2O_2) and thoroughly rinsed with deionized water (dH_2O) if the sensor 1000 is to be re-used.

[0121] Fig. 33 shows a preferred embodiment for macromolecules (e.g., DNA, RNA, protein) detection. Preferably, the detection of the concentration of macromolecules (DNA, RNA, protein) does include the sensor surface modification of biotin/Streptavidin layer. The sensor surface is modified with a proper biochemical solution to form a streptavidin layer after the post-fabrication cleaning as shown in the surface modification process described above. After the surface of the biosensor 1100 has been modified, the amperometric biosensing of pathogen is conducted by first adding 50 ml of lysis reagent (0.4 M NaOH) to a 250 ml sample of bacteria solution and incubated for 5 minute at room temperature. 100 ml of probe solution (anchoring and signaling probes) was then added, and the mixture was incubated for 10 min. at 65°C. 5 μL of the lysed E. coli/probe solution mixture 1120 is then placed on the streptavidin coated working electrode 1130 of the biosensor 1100 and incubated for 10 min. at room temperature.

[0122] Referring now to Fig. 34, the biosensor 1100 is then washed with biotin wash solution (Kirkegaard and Perry Laboratories, 50-63-06). Next, 5 μL 1140 of Anti-Fl-POD (Anti-fluorescein peroxidase, 150U, Roche Inc., 1 426 346), diluted to 0.75U/ml or 0.15 U/ml with dilutant (PBS/0.5%Casein) is placed on the working electrode 1130 and incubated for 10 minutes at room temperature.

[0123] Referring now to Fig. 35, the biosensor is then washed again with wash solution. After the wash, 10 μL 1160 of K-blue substrate (Neogen Corp., 300176) is placed on the biosensor in such a way that all three electrodes (working 1130, reference 1140, counter 1150) are covered by the substrate solution 1160.

[0124] Finally, the electrochemical (more specifically the redox) measurements are immediately taken. Amperometric current vs. time is measured using a CH Instruments 660A Electrochemical Workstation with a picoamp booster and faraday cage. Samples on the biosensor are to be measured sequentially. The voltage should be fixed at –0.1V (vs. reference), and a cathodic current (amperometric signal) reading should be taken in 20 seconds because at 20 seconds, the current values should reach steady-state. Cell concentration (cell number) is determined by using serial dilutions and culture plate counting.

[0125] After the measurement, the Au surfaces should then be cleaned with acetone, alcohol, and concentrated "Piranha" solution (70 vol% H_2SO_4, 30 vol% H_2O_2) and thoroughly rinsed with deionized water (dH_2O) if the sensor 1100 is to be re-used.

[0126] Preferably, in any of the above biosensor embodiments the biosensor is calibrated before actual sample detection. The biosensor is preferably calibrated with a calibrating solution that contain a known amount of target analyte(s) and another calibrating solution that contains an undetectable amount (e.g., none) of the target analyte(s). Optionally, the biosensor may be calibrated with a plurality of calibrating solutions. Each of the plurality of calibrating solutions respectively contains a known amount of the target analyte. Preferably, the calibrating solutions contain the target analytes at different level of concentrations. These calibrations solutions are measured on the biosensor by the above described detection process to obtain a reference signal and/or reference signals. The reference signal and/or signals are then compared with the measured signal from a sample solution to determine the presence and quantity of the analyte in

the sample reagent. The determination of the presence and quantity (e.g., concentration or absolute amount) of the analyte(s) can be determined by conventional biological interpolation methods.

[0127] Appendices A, B, and C provide additional material to further characterize the present invention.

[0128] All references herein to outside literature, including references made within the appendices of this application, are hereby incorporated by reference to the extent that they supplement, explain, provide a background for or teach methodology, techniques and/or compositions employed herein. In addition, the references listed below are also incorporated herein by reference to the extent that they supplement, explain, provide a background for or teach methodology, techniques and/or compositions employed herein.

[0129] References:

[0130] "USAF PAMPHLET ON THE MEDICAL DEFENSE AGAINST BIOLOGICAL MATERIAL - Medical Defense Against Biological Material" Defense Technical Information Center, released on 11 Feb 1997

[0131] Abbott, N.L.; Gorman, C.B.; Whitesides, G.M. "Active control of wetting using applied electrical potentials and self-assembled monolayers" *Langmuir* , **11**, Issue 1, January 1995, 16-18

[0132] Abbott, N.L.; Rolison, D.R.: Whitesides, G.M., "Combining micromachining and molecular self-assembly to fabricate microelectrodes" *Langmuir*, **10**, Issue 8, August 1994, 2672-2682

[0133] Abdel-Hamid, I. Ivnitski, D., Atanasov, P., Wilkins, E., 1998. Fast Amperometric Assay for E. coli 0157:H7 using partially immersed immunoelectrodes. Electroanalysis 10 (11), 758-763.

[0134] Abdel-Hamid, I., Ivnitski, D., Atanasov, P., Wilkins, E., 1999. Flow-through immunofiltration assay system for rapid detection of E. coli 0157:H7. Biosens. Bioelect. 14, 309-316.

[0135] Andrade, J.D., "Surface and Interface Aspects of Biomedical Polymers: Protein Adsorption" Plenum, New York, 1985

[0136] Bain, C. D.; Troughton, E. B.; Tao, Y.T.;Evall, J.; Whitesides, G. M.; Nuzzo, R. G., *J. Am. Chem.* Soc. **1989**, *111*, 321

[0137] Baxter, Ian; Cother, Lisa D.; Dupuy, Carole; Lickiss, Paul D.; White, Andrew J.P.; and Williams, David J. "Hydrogen Bonding to Silanols" Department of Chemistry, Imperial College of Science, Technology and Medicine, London SW7 2AY, UK

[0138] Beam, K.E. "Anisotropic Etching of Silicon," *IEEE Transactions on Electron Devices*, October, 1978

[0139] Becker, E.W.; Betz, H.; Ehrfeld, W.; Glashauser, W.; Heuberger, A.; Michel, H.J.; Munchmeyer, D.; Pongratz, S.; and Siemens, R.V. "Production of Separation Nozzle Systems for Uranium Enrichment by a Combination of X-Ray Lithography and Galvano-plastics," *Naturwissenschaften*, **69**, (1982), 520 to 523.

[0140] Blake, C., Gould, B.J., 1984. Use of enzymes in immunoassay techniques. A review. Analyst 109, 533–547.

[0141] Brody, J.P.; Yager, P.; Goldstein, R.E. and Austin, R.H. "Biotechnology at low Reynolds numbers" *J. Biophys.* **71**, 1996, 3430-3441

[0142] Chen, Y.F., Yang, J.M., Gau, J.J., Ho, C.M., Tai, Y.C., 2000. Microfluidic System for Biological Agent Detection. Proceedings of the 3rd International conference on the interaction of art and fluid mechanics, Zurich, Switzerland.

[0143] Chen, Y.F.; Yang, J.M.; Gau, J.J.; Ho, C.M.; and Tai, Y.C., "Microfluidic System for Biological Agent Detection" The 3rd International conference on the interaction of Art and Fluid Mechanics, Zurich, Switzerland , 2000.

[0144] Cooper, N. "The Human Genome Project," Los Alamos Lab, *Science,* **20**,1-338. 1992.

[0145] Cussler, E. L., Diffusion – mass transfer in fluid systems, 2nd edition, , Cambridge University Press, 1997

[0146] Darst, S.A.; Ahlers, M.; Meller, P.H.; Kubalek, E.W.; Blankenburg, R.; Ribi, H.O.; Ringsdorf, H.; Kornberg, R., "Two-Dimensional Crystals of Streptavidin on Biotinylated Lipid Layers," *Biophys J.* **59** (1991) 387-396.

[0147] Dunford, H.B., 1991. Horseradish peroxidase: structure and kinetic properties. In: Everse, J., Everse, K.E., Grisham, M.B. (Eds.), Peroxidases in Chemistry and Biology, vol. 2. CRC Press, Boca Raton, FL, pp. 1-24.

[0148] Ehteshami, G.; Rana, N.; Raghu, P.; and Shadman, F. "Interactions of impurities with Silicon and Silicon dioxide during oxidation", Center for Micro-contamination Control, NSF I/U CRC

[0149] Feynman, Richard P. "There's Plenty of Room at the Bottom" *Engineering and Science*, Caltech, February 1960

[0150] Gau, J.J., Lan, E. H., Dunn, B., Ho, C.M., 2000. Enzyme-based electrochemical biosensor with DNA array chip. Proceedings of the fourth International Symposium on Micro Total Analysis Systems (μTAS), Enschede, The Netherlands.

[0151] Ghindilis, A.L., Atanasov, P., Wilkins, E., 1997. Enzyme-catalyzed direct electron transfer: Fundamentals and analytical applications. Electroanalysis 9, 661–674.

[0152] Gorton, L., Lindgren, A., Larsson, T., Munteanu, F.D., Ruzgas, T., Gazaryan, I., 1999. Direct electron transfer between heme-containing enzymes and electrodes as basis for third generation biosensors. Anal. Chim. Acta 400, 91–108.

[0153] Hall, E.A.H., 1991. Biosensors. Prentice Hall, Englewood Cliffs, New Jersey.

[0154] Haussling, L., Ringsdorf, H., Schmitt, F.J., Knoll, W., 1991. Biotin-functionalized self-assembled monolayers on gold: surface plasmon optical studies of specific recognition reactions. Langmuir 7 (9), 1837-1840.

[0155] Ho, C.M., Tai, Y.C., 1996. Review: MEMS and its applications for flow control. J. Fluids Eng. 118, 437-447.

[0156] Ho, C.M., Tai, Y.C., 1998. Micro-electro-mechanical systems (MEMS) and fluid flows. Ann. Rev. Fluid Mech. 30, 579-612.

[0157] Hou, S.F., Yang, K.S., Fang, H.Q., Chen, H.Y., 1998. Amperometric glucose enzyme electrode by immobilizing glucose oxidase in multilayers on self-assembled monolayers surface. Talanta 47, 561-567.

[0158] Howe, R.T. and Muller, R.S. "Polycrystalline Silicon Micromechanical Beams," *Journal of the Electrochemical Society*: Solid State Science and Technology, June, 1983.

[0159] Ivnitski, D., Abdel-Hamid, I., Atanasov, P., Wilkins, E., 1999. Biosensors for detection of pathogenic bacteria. Biosens. Bioelect. 14, 599-624.

[0160] Ivnitski, D., Abdel-Hamid, I., Atanasov, P., Wilkins, E., Stricker, S., 2000. Application of Electrochemical Biosensors for Detection of Food Pathogenic Bacteria. Electroanalysis 12 (5), 317-325.

[0161] Jung, L.S., Nelson, K.E., Campbell, C.T., Stayton, P.S., Yee, S.S., Perez-Luna, V., Lopez, G.P., 1999. Surface plasmon resonance measurement of binding and dissociation of wild-type and mutant streptavidin on mixed biotin-containing alkylthiolate monolayers. Sensors Actuators B 54, 137-144.

[0162] Kane, R.S., Takayama, S., Ostuni, E., Ingber, D.E., Whitesides, G.M., 1999. Patterning proteins and cells using soft lithography. Biomaterials 20, 2363-2376.

[0163] Kevles, D., and L. Hood . "The Code of Codes: Scientific and Social Issues in the Human Genome Project", Harvard University Press, Cambridge, Mass., 1992.

[0164] Lahiri, J., Ostuni, E., Whitesides, G.M., 1999. Patterning Ligands on Reactive SAMs by Microcontact Printing. Langmuir 15 (6), 2055-2060.

[0165] Lindgren, A., Munteanu, F.-D., Gazaryan, I.G., Ruzgas, T., Gorton, L., 1998. Comparison of rotating disk and wall-jet electrode systems for studying the kinetics of direct and mediated electron transfer for horseradish peroxidase on a graphite electrode. J. Electroanal. Chem. 458, 113–120.

[0166] Marrazza, G.; Chianella, I.; Mascini, M., "Disposable DNA Electrochemical Biosensors for Environmental Monitoring", Analytica Chimica Acta 387 (1999), 297-307.

[0167] Motesharei, K., Myles, D.C., 1998. Molecular recognition on functionalized self-assembled monolayers of alkanethiols on gold. J. Am. Chem. Soc. 120 (29), 7328-7336.

[0168] Murthy, A.S.N, Sharma, J., 1998. Glucose oxidase bound to self-assembled monolayers of bis(4-pyridyl) disulfide at a gold electrode: Amperometric determination of glucose. Anal. Chim. Acta 363, 215-220.

[0169] Nathanson, H.C.; Newell, W.E.; Wickstrom, R.A.; and Davis, J.R., Jr., "The Resonant Gate Transistor," IEEE Transactions on Electron Devices, March, 1967.

[0170] Ooka, A. A., Kuhar, K.A., Cho, N., Garrell, G.L., 1999. Surface Interactions of a Homologous Series of a,w-Amino Acids on Colloidal Silver and Gold. Biospectroscopy 5, 9-17.

[0171] Ostuni, E., Yan, L., Whitesides, G.M., 1999. The interaction of proteins and cells with self-assembled monolayers of alkanethiolates on gold and silver. Colloids Surfaces B 15, 3-30.

[0172] Rao, J., Yan, L., Xu, B., and Whitesides, G.M., 1999. Using surface plasmon resonance to study the binding of vancomycin and its dimer to self-assembled monolayers presenting D-Ala-D-Ala. J. Am. Chem. Soc. 121 (11), 2029-2030.

[0173] Revell, D.J., Knight, J.R., Blyth, D.J., Haines, A.H., Russell, D.A., 1998. Self-assembled carbohydrate monolayers: formation and surface selective molecular recognition. Langmuir 14 (16) 4517-4524.

[0174] Ruzgas, T., Gorton, L., Emne´us, J., Marko-Varga, G., 1995. Kinetic models of horseradish peroxidase action on a graphite electrode. J. Electroanal. Chem. 391, 41–49.

[0175] Ruzgas, T.; Csöregi, E.; Emnéus, J.; Gorton, L.; Marko-Varga, G., "Peroxidase-modified electrodes: Fundamentals and application", Analytica Chimica Acta 330 (1996), 123-138.

[0176] Sieval, A.B.; Demirel, A.L.; Nissink, J.W.M.; Linford, M.R.; van der Maas, J.H.; de Jeu, W.H.; Zuilhof, H. and Sudhölter, E.J.R. "Highly stable Si-C linked functionalized monolayers on the silicon(100) surface." *Langmuir* 1998, **14**, 1759-1768.

[0177] Sieval, A.B.; Zuilhof, H.; Sudhölter, E.J.R.; Schuurmans, F.M.; and Sinke, W.C. "Surface passivation of silicon by organic monolayers." Proceedings of the 2nd World Conference and Exhibition on Photovoltaic Solar Energy Conversion, Vienna, 1998

[0178] Sigal, G.B., Bamdad, C., Barberis, A., Strominger, J., and Whitesides, G.M., 1996. A self-assembled monolayer for the binding and study of histidine-tagged proteins by surface plasmon resonance. Anal. Chem. 68, 490-497.

[0179] Spinke, J., Liley, M., Guder, H.J., Angermaier, L., Knoll, W., 1993. Molecular recognition at self-assembled monolayers: the construction of multicomponent multilayers. Langmuir 9 (7), 1821-1825.

[0180] Sun, X., He, P., Liu, S., Ye, Jiannog, Fang, Y., 1998. Immobilization of single-stranded deoxyribonucleic acid on gold electrode with self-assembled aminoethanethiol monolayer for DNA electrochemical sensor applications. Talanta 47, 487-495.

[0181] Taylor, Robert "Bioterrorism Special Report: All fall down", *New Scientist*, Volume **150**, Issue 2029, 11 May 1996

[0182] Trimmer, W.S.N. "Microrobots and Micromechanical Systems" *Sensors and Actuators*, **19**, Number 3, September 1989, 267 - 287

[0183] Trimmer, William "Grand in Purpose, Insignificant in Size" The tenth Annual International Workshop on MEMS, Nagoya, Japan, Proceedings IEEE Catalog Number 97CH36021, 1997, 9 – 13.

[0184] Ulman, A. Ultrathin Organic Films from Langmuir Blodgett to Self-Assembly; Academic Press: New York, 1991.

[0185] Ulman, A., An Introduction to Ultrathin Organic Films From Langmuir Blodgett to Self-Assembly, Academic Press, Inc., San Diego, CA, 1991

[0186] Ulman, A., Ed. Characterization of Organic Thin Films; Butterworth-Heinemann: Boston, 1995.

[0187] Voet, Donald; Voet, J. " Biochemistry, 2nd edition" Wiley, New York, 916-919

[0188] Wagner, P.; Hegner, M.; Guntherodt, H-J; Semenza, G., "Formation and in Situ Modification of Monolayers Chemisorbed on Ultraflat Template-Stripped Gold Surfaces," *Langmuir* **11** (1995) 3867-75.

[0189] Wang, J., Rivas, G., Cai, X., Palecek, E., Nielsen, P., Shiraishi, H., Dontha, N., Luo, D., Parrado, C., Chicharro, M., Farias, P.A.M, Valera, F.S., Grant, D.H., Ozsoz, M., Flair, M.N., 1997. DNA electrochemical biosensors for environmental monitoring. A Review. Anal. Chim. Acta 347, 1-8.

[0190] Wang, T.H., Chen Y.F., Masset S., Ho, C.M., Tai, Y.C., 2000. Molecular beacon based micro biological detection system. Proceedings of the 2000 International Conference on Mathematics and Engineering Techniques in Medicine and Biological Sciences (METMBS'2000) Las Vegas, Nevada.

[0191] Weber, P.C., Ohlendorf, D.H., Wendoloski, J.J., Salemme, F.R., 1989. Structural Origins of High-Affinity Biotin Binding to Streptavidin. Science 243, 85-88.

[0192] Whitesides, G. M.; Laibinis, P. E., *Langmuir* **1990**, *6*, 87.

[0193] Wink, Th.; van Zuilen, S.J.; Bult, A.; and van Bennekom, W.P., "Self-assembled Monolayers for Biosensors" *Analyst*, April 1997, **122**, 43R-50R

[0194] Wise, K.D.; Jackson, T.N.; Masnari, N.A.; Robinson, M.B.; Solomon, D.E.; Wuttke, G.H.; and Rensel, W.B. "Fabrication of Hemispherical Structures Using Semiconductor Technology for Use in Thermonuclear Fusion Research," *Journal of Vacuum Science Technology*, May/June, 1979.

[0195] Xia, Y., Whitesides, G.M., 1998. Soft Lithography. Angew. Chem. Int. Ed. 37, 550-575.

[0196] Yang, R.H., Wang, K.M., Xiao, D., Luo, K. and Yang, X.H., A renewable liquid drop sensor for di- or trinitrophenol based on fluorescence quenching of 3,3 A ,5,5 A –tetramethylbenzidine dihydrochloride, *Analyst*, 2000, 125, 877–882

[0197] Thus, a novel "bio-sensing" system has been shown and described. Various modifications may of course be made without departing from the sprit and scope of the invention. For example, it can be envisioned that the biosensor disclosed here can be used to sense or detect non-biological elements and compounds. The invention, therefore, should not be restricted, except by the intent of the following claims.

Appendix A.

Enzyme-based electrochemical DNA sensor chip

with MEMS technology

CHAPTER 1 INTRODUCTION TO MEMS BASED BIOSENSOR

1. Overview

Microfabrication technology has been successfully producing a wide range of miniature and micro-scale biosensors and actuators. Of particular interests is the application of micro electromechanical system (MEMS) technology to a biological system. A biological system is difficult to manipulate because of the feature size of the basic living components and the complexity of Mother Nature. We are down the road where the resolution and accuracy of our observing tools are close to the fundamental unit of the biological creature, this exploratory venture is only limited by time.

The ultimate goal of MEMS technology in biomedical application is not merely on "shrinking" the device size but to integrate individual functional modules in a whole. Therefore the design of each BioMEMS device should take into account of flexibility and capability of integration into micro total analysis system (μ-TAS).

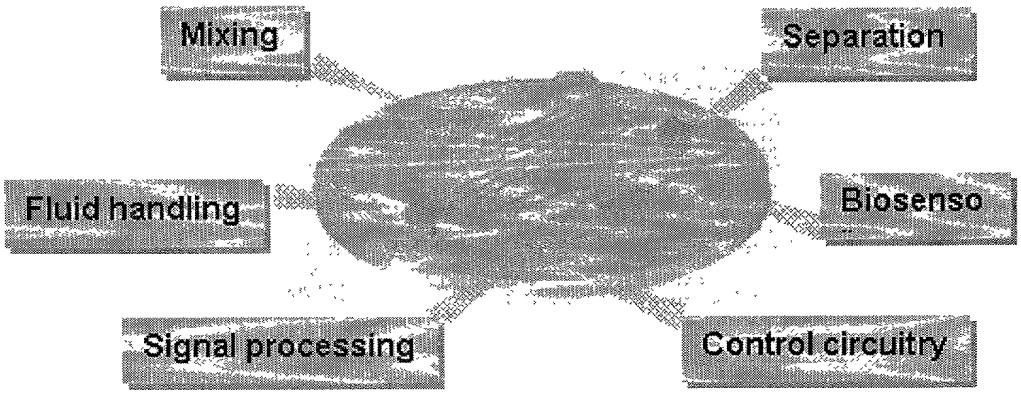

Figure. 1 Micro Total Analysis System

The development of low cost automated systems for DNA analysis that will obtain quantity and identity information of bioagents efficiently and accurately will impact many industry sectors. This work presents a MEMS-based DNA sensor array chip, which is highly

flexible to be adapted to the following biomedical applications.

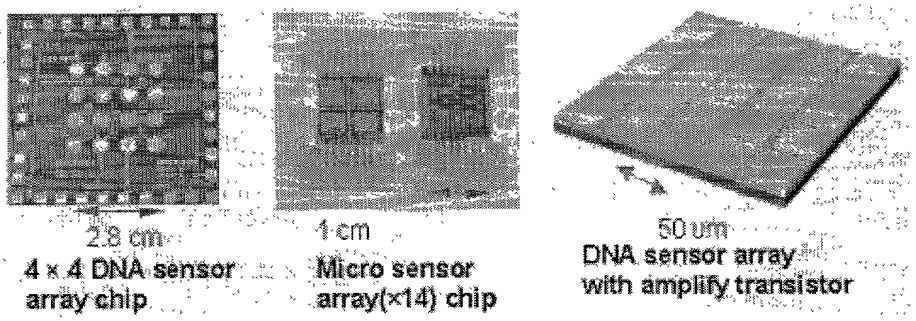

Figure. 2 Sensor Chip Revolution

2. Some Applications of BioMEMS to Biomedical detection

Bio-warfare

Background

Biological warfare (BW) is the use of microorganisms or toxins derived from living organisms to produce death or disease in humans, animals, or plants. In spite of the 1972 Biological Weapons Convention prohibiting the use of BW agents, concern over compliance still remains. A highly addressed issue is the possibility that the solders may be exposed to biological weapons in the field. Characteristics of many live biological agents and toxins make them potentially effective for offensive military use. These agents can provide a readily available and effective weapon in the hands of terrorists as well as assassins.

There are more than 10 countries that have, or are developing, a BW capability. The production of BW agents does not require specialized equipment or advanced technology. When comparing equivalent amounts of biological and chemical warfare agents, the biological agent is far more potent. Only small amounts can produce large numbers of casualties. [1,2]

Detection

Detection is vital in obtaining information on the risks. In order to reach decisions on the level of protection required, it is necessary to know the type of biological agent present in the area and whether the concentration exceeds the threshold level. An alarm detector must be capable of operating continuously for long periods. It should require no particular attention except for changing batteries, etc., and might be operated by personnel with short training periods. All these requirements deviate BW sensors from the main stream of conventional sensing system. Defense advanced research projects agency (DARPA) dedicate a special program to BW detection system and has pushed the classical science to another level.

E. coli Screening for Food Industry

Background

In 1994, USDA's Food Safety and Inspection Service classified bacterium E. coli O157:H7 on ground beef as an adulterant and classified products found to contain the bacteria as unfit for consumption unless it was cooked or further processed by the manufacturer.

E. coli O157 is a strain of the bacteria known to cause serious gastrointestinal illness, and usually is encountered in contaminated ground beef that has not been properly cooked. Outbreaks of E. coli O157 related illness have also been associated with the consumption of raw milk, tainted water and certain fruits and vegetables. Although symptoms of E. coli O157 infection typically disappear in 5-10 days, some people -- especially the very young and elderly -- may contract hemolytic uremic syndrome (HUB), which can result in kidney failure and even death. About 60,000 cases of E. coli O157 infection are reported each year in the US.

Policy and Initiative

In January 1997, President Clinton announced a new, national food safety initiative to fund a number of needed improvements in food safety, including those efforts already undergoing in USDA.

1. Early Warning System
2. Improve Responses to Foodborne Outbreaks
3. Risk Assessment
4. Research
5. Improve Inspections and Compliance
6. Education
7. Strategic Planning

This initiative supports the need for research to more quickly identify and characterize foodborne hazards, to provide the tools for regulatory enforcement, and to develop effective interventions that can be used to prevent hazards at each step from production to consumption. This research supports the needs not only of government agencies but the food industry as well.

One major bottleneck of the control over E. coli outbreak is the efficiency of the E. coli screening. The time and cost of the test limits the sampling number and the response time. Rapid and cost-effective test methods for a variety of pathogens such as Salmonella and E. coli O157:H7 need to be developed.

Medical Diagnosis (Otitis Media)

Background

Otitis Media, or middle ear infection, is an infection inside the eardrum that causes ear pain and fever. It is most common in children and there may be persisting deafness after the infection. Otitis Media remains the most frequent illness resulting in visits to physicians. Seven out of ten children will have at least one episode of this infection before the age of three. And one-third of these youngsters will have repeated bouts.

Although currently there is some debate as to whether antibiotics is a good idea or not, it can not be denied that it is the standard treatment for the acute middle ear infection in many countries. Clinical experience has proved that antibiotics are a very effective treatment. The risk of more serious spread of infection will be cut down and the pain is reduced. But everything has two aspects. Antibiotics can cause some side effects such as diarrhea, vomiting or rash. Since the current diagnosis can not distinguish the infection sources, usually all the antibiotics for each

possible bacteria and virus source are given to the patients. Therefore the patients take more than they need and pay for more than they should. And more terribly, it is increasingly awarded that unnecessary use of antibiotics can increase the risk of "superbugs" developing, which can resist the antibiotics. When people need antibiotics for more serious or urgent situation, they may be ineffective.

Diagnosis

Currently, an alarming increase in antibiotic resistance has been observed worldwide. But even today, determination of antibiotic resistance is made only after a course of antibiotic therapy fails to produce amelioration of the diseases. The patients have to suffer pains and danger for untimely diagnosis of antibiotic resistance status. Therefore, for otitis media patients, a rapid, effective way to determinate antibiotic resistance status is as important as pathogen identification.

The most efficient treatment for the middle ear infection is to screen for the types of bacteria or viruses that cause the specific infection and use the proper antibiotic. Since bacteria may be adapted into the harsh environment and become resistant to some antibiotics, it's also very important to probe the antibiotic resistant gene within the bacteria genome. After being informed the information of the bacteria responsible for the infection and the antibiotic resistance status, doctors can give the proper medicine with the least amount and the maximum strength.

A smart diagnosis system that can perform a rapid and highly accurate detection technique should be developed for clinical use. This system should be able to substitute the labor-intensive manual work with a minute sample and shorten the test time. Bacteria infection status and antibiotic resistance characteristics should be determined without a technician before the infection spreads out.

3. Summary and Objectives of this Work

It is apparent that micro electromechanical systems exhibit tremendous potential for growth in the next decade. It is also apparent, however, that the biological characteristics of MEMS structure need to be explored.

The objectives of this work are twofold. First, there are important scientific and technological issues that remain to be clarified in the study of MEMS-based biosensor. The scientific understanding of interface interaction of MEMS structure in biological environment must be expanded if possible to include the surface property and biocompatibility of the materials. Surface analytical experiments for characterizing binding events in MEMS structures must be designed and performed so that the interactions at bio and MEMS interface can be well predicted and controlled. From these fundamental measurements and the understanding gained, we can efficiently develop strategies for biosensor chip.

The second main objective of this work will entail the actual incorporation of various state-of-the-art technologies into the design process and fabrication of MEMS-based DNA sensor chip. This is also the most significant achievement of this work, integrating different disciplines via functionality and maintaining the simplicity and the integrity of the entire system.

Chapter one reviews, in general, the significance and background of the current applications of this work in three major fields. This chapter reveals the unique requirements for certain application and these expectations later become the guidelines of sensor design.

Chapter two focuses on the fundamental concepts of BioMEMS devices and the significance of the biocompatibility is pointed out. The interactions at the interface play an ineligible role in biosensing. The technical aspects of MEMS technology are briefly reviewed, followed by the detail study of biocompatibility of MEMS devices. Functional surface is proposed as a solution to implement a media layer between the mechanical structure and the biological environment.

Chapter three examines four state-of-the-art technologies used in this work. This chapter aims to further the understanding of the pros and cons of current techniques and to lay the foundations for the DNA sensor chip design. The specificity, sensitivity and speed of the new design are also illustrated as a benefit of integrating these disciplines.

Chapter four details the design aspects, fabrication process and experimental results. The process parameter optimization of each significant step is described stepwise. The preliminary results of this work are illustrated in each relating topic.

Chapter five introduces the surface plasmon resonance (SPR) and atomic force microscopy (AFM) for surface kinetic analysis. The motivation of kinetic study is to verify the

quality of the functional surface and to evaluate the potential of further improvement.

Finally, chapter six summarizes the work need to be done to compete this work, including kinetic analysis, dielectrophoresis control and integration with bipolar transistor.

CHAPTER 2 BIOMEMS FOR BIOMEDICAL APPLICATION — DNA CHIPS

1. Introduction

A variety of recent technological breakthroughs have made the development of DNA chips possible and more promising. Fundamentally, genetic chips, the driving force of all kinds of DNA chips, are the result of achievements in two fields: molecular biology and microfabrication technology. From engineering prospective, the aspects of this work start from the improvements of modern microbiology due to the contribution of microfabrication to the great success of biosensing made possible by micro- and nano-scale fabrication techniques.

Research on microfabricated devices for biomedical applications (BioMEMS) has rapidly advanced in the last few years. The functionality of such devices for laboratory and clinical application has been widely documented with extensive work and development efforts in many academic research centers as well as in the industrial sector. The majority of BioMEMS research has focused on the development of diagnostic tools such as electrophoretic, chromatographic, biosensor, and cell manipulation system.

2. Micro- and Nano-Scale Biology

Molecular biology has been catalyzed by the work of the Human Genome Project (HGP) within last decade. Without focusing too much on the ethical, legal and social implications of HGP, the satellite research efforts brought about by HGP have pushed the fundamental science research to another peak. [3,4]

The fast booming progress in molecular biology has built a solid groundwork for the development of clinical laboratory diagnosis and therapies involving genetic probes. Fundamental advances include the use of polymerase chain reaction (PCR) or other purification and amplification technique enable the study of only few copies of a nucleic acid sample. All these have brought the view of biology from macro, micro into nano world.

3. MEMS Technology

The micromachining field has been given the generic name microelectromechanical systems or MEMS. The second technological trend making DNA-chip products possible encompasses the improvements in MEMS techniques. Developed initially for semiconductor device manufacturing, these techniques are now being exploited in a variety of other disciplines, including DNA-chip manufacturing and other chip based biosensing system. These achievements have made possible the application of organic structures (e.g., segments of DNA and reagents) onto a substrate of inorganic materials. Most DNA microassays are fabricated onto glass or plastic substrates or are placed in tiny glass tubes and reservoirs. Some researchers are still putting the efforts on keeping the connection with very large scale integration (VLSI), which uses silicon-based wafers. The advantage of doing this is for the integration between the transducer and the control circuitry. This is even more important when converting whole system into μ-TAS level. (See Chapter 2.2 for detail)

The MEMS field is quite broad and includes integrated microsensors, microactuators, microinstruments, micro-optics and microfluidics. The applications range from accelerometers, which deploy an automobile airbag, ink jet printer heads, an array of movable mirrors for color projection displays, to probes for atomic force microscopy. MEMS can be defined as the fabrication or micromachining of materials to make stationary and moving structures, devices and systems of a nominal size-scale from a few centimeters to a few micrometers.

Scaling of the Device

Dr. Richard P. Feynman, Nobel Prize winning physicist, pointed in the direction of molecular nanotechnology in a talk at California Institute of Technology, "There's Plenty of Room at the Bottom" in 1959. [5] The following is quoted from his historical speech given forty years ago:

I don't know how to do this on a small scale in a practical way, but I do know that computing machines are very large; they fill rooms. Why can't we make them very small?

Perhaps things normally start small, and grow. Man's habitats have grown from houses, to buildings, to skyscrapers. Our ability to travel has increased from a few miles on foot, to horses, to trains, and now we can encircle the world in a few days. Individually we work to

make large accomplishments in hopes of enormous success. We are enthralled with the big and significant and substantial. [6]

The insignificant, insubstantial, and minuscule is usually beneath our concern.

— William Trimmer, 1997

Dr. William Trimmer proposed the *Trimmer's Vertical Bracket Notation* of scaling micromechanical devices in 1989. [7] He gave a very clear guideline to analyze how the classical phenomenons scale into small domain. In this notation, the size of the system is represented by a single scale variable, S, which represents the linear scale of the system. The choice of S for a system is a bit arbitrary. The S could be the separation between the plates of a capacitor, or it could be the length of one edge of the capacitor. Once chosen, however, it is assumed that all dimensions of the system are equally scaled down in size as S is decreased (isometric scaling). For example, nominally S = 1; if S is then changed to 0.1, all the dimensions of the system are decreased by a factor of ten.

It's very important to know how does physical phenomenon scale then you can have the control over it and furthermore take advantage of it in micro-scale system design. Followed is a table of the scaling factors of some examples:

Phenomenon	Dominate factor	Scaling Factor
Biological forces	cross section	S^2
Pneumatic	pressures	S^2
Hydraulic forces	pressures	S^2
Surface tension	length of the interface	S^1
Mass of the object	volume	S^2
Electrostatic forces	constant E field (E= S^0)	S^2
Electrostatic forces	smaller (E = S-0.5)	S^1

Table.1 Scaling factors of various forces

Sacrificial Releasing

Sacrificial releasing is the first developed MEMS related technique and is widely used today. In 1967, Nathanson described a structural-sacrificial fabrication technique in his resonant gate transistor paper. [8] In these initial experiments, gold was used as the structural material and photoresist was the sacrificial material. This is an extremely powerful technique that allows complete microstructures to be built without having to assemble components, a great advantage when dealing with components too small to be seen with the eye, or manipulate with the hand. In 1983, Howe and Muller extended this work to the polysilicon-silicon dioxide, a structural-sacrificial material we now normally describe as surface micromachining. [9]

High Aspect Ratio

A second powerful fabrication technique for making small things was discussed in the 1978 paper "Anisotropic Etching of Silicon" by K. E. Beam. [10] A year later K. D. Wise describes how to make micro spheres filled with deuterium-tritium using isotropic etching. [11] These anisotropic and isotropic etching techniques in silicon and related materials are now commonly referred to as bulk micromachining.

An early application for microfabrication techniques in the nuclear power generation industry was presented in 1982. [12] This technique is now called LIGA (in German Lithographie, Galvanoformung, Abformung), and makes plastic and metal parts with spectacular accuracy. The above techniques demonstrate novel approaches to the manufacturing of micro parts. Now the question is why do we need these techniques and how to use them for biological applications.

4. Biological Identification — Nucleic Acid Hybridization

DNA chips are designed to identify hybridization products in the same fashion as with traditional sequencers. The conventional and most commonly used identifying scheme is using optical detection. Once hybridization has been completed, phosphorescent chemicals that bind to the hybridized sequences are scanned with a light source, making it easy to detect their presence with automated colorimetric or fluorimetric equipment.

Nucleic acid hybridization is only one step of the whole DNA chip sensing system, but

the most significant one. The roots of gene probing technologies go back much further, to molecular biology discoveries made decades ago. Most important of these are the base pairing rules discovered in the 1950s by James Watson and Francis Crick. They determined that the DNA molecules found in living organisms are composed of a structure of two twisted strands (the famous *double helix*) linked together with pairs of nitrogenous bases: adenine (A), cytosine (C), guanine (G), and thymine (T). They also discovered that these bases always appear in the same two pairs: A with T, and C with G. Thus, by knowing part of the molecular structure of a specific genetic segment, one can determine the other part. In other words, if you know the sequence of the target strand, another strand (oligonucleotide) can be synthesized to probe the target DNA. If we extend this concept, we can detect the presence of a specific biological agent by probing the segment of sequence within the content. This is the basis of gene probe and it's also the source of the specificity of DNA based sensor. The process of one strand of DNA matching up with its counterpart strand is called hybridization.

Hybridization can be performed either in solution or on a solid support. In traditional gene probing, the most common format for hybridization is the Southern blot, which uses a nitrocellulose membrane. DNA-chip manufacturers are also exploring variations of both solid-phase and solution-based hybridization for use in their microassays. At present, however, most DNA-chip companies use a solid-phase technique.

5. Micro Total Analysis System (μTAS)

The significance of molecular biology and the characteristic features of MEMS technology are briefly summarized in the previous sections. The size reduction should not only work on the few parts of the entire system. For nucleic acid hybridization, the pre-process or sample preparation is more complicate and time consuming. Sample prep is a series of labor intensive laboratory procedures, mainly liquid handling (mixing, filtering, centrifuging, heating and pipetting). The shrinking of liquid handling systems to the micron and sub-micron size range brings the system into the area of small Reynolds numbers. The fluid dynamics in this regime is very different from the macroscale. Different physics of small Reynolds numbers flow, along with microscopic sizes, can influence microfabricated fluidic device design for biological processing. [13]

Micro total analysis system (μTAS) is a specific research field dedicated to the monolithic integration of micro-flume, micro-transducer and control circuitry onto the same chip. This is a challenge compared to the development of each individual module due to the difficulties of the interconnection between each sub-system. Most of the so-called micro- or nano-scale devices still need to be operated with many bulky accessory instruments. When every component can be fabricated on one silicon wafer, it won't be too far away to travel along the cardiac network inside the body as shown in scenes of sci-fi films.

6. Biocompatibility of MEMS Structure

Introduction of Biocompatibility

Is silicon biocompatible?

This wasn't a question before the concept of BioMEMS. Silicon chip fabrication process was developed for the computer chips. It wasn't meant to be operated in biological condition. On the other hand, sand, composed of silicon, appears in all types of biological environment.

Biocompatibility is a surface property, which are interactions between the functional structure and the biological environment that take place at the surface. The nature of the initial interface that is established between the structural material and the attached surface biochemical molecules determine the biocompatibility of the sensor system.

The objective of the study of biocompatibility of MEMS structure is firstly to improve the understanding of the surface activities that take place when a MEMS device is in contact with an in vitro biological environment, such as changes in thin film composition, adsorption of biomolecules, and interaction with cells. A second aim is to modify the surface of biomaterials to obtain specific properties or to improve the biocompatibility and biological functionality of a MEMS structure.

Requirements for Biomaterials

Due to the wide variety of the biomedical application, there is no such an absolute and clear general definition of biocompatibility. Take cell adhesion as an example, nerve cell monitoring device is biocompatible would mean that the cell can attach to the surface and grow

the processes on or root into the surface. On the other hand, an implantable device if biocompatible would mean that the cell would not attach to and attack the surface of the device. Different application requires different surface property and different characteristic. As shown in the Figure 3, for the in vitro biomedical devices, the long-term biocompatibility will not be considered. For the in vivo implantation parts, the lifetime of the device will be a major criterion. The bioactivity also depends on the function of the device. For implantable parts, we want them bio-inert, and we want drug-releasing device bioactive on the other end. So the function and the application determine the biocompatibility requirements.

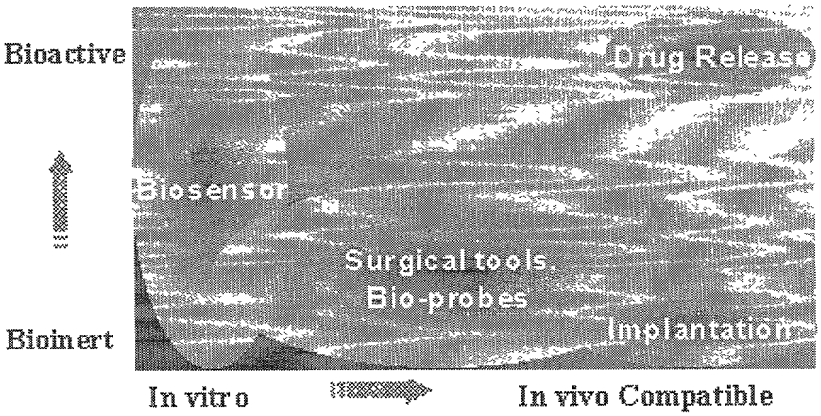

Figure. 3 Biocompatibility and Bioactivity

Silicon as a Biomaterial

Currently, most commercial biosensor products utilize glass or plastic substrate, not silicon wafer. The main constrain is lacking of understanding and control over the biocompatibility of silicon based MEMS devices. For example, *micro-bridge resonance sensor* has been developed for years and there're some remarkable paper published. The basic mechanism is to sense the change of resonant frequency due to target molecules bound to the micro-bridge. Its performance couldn't compete with the conventional detection methods, because it's difficult to eliminate the noise caused by non-specific binding onto the bridge surface. Silicon can be adhered to just about all kinds of biomolecules.

The other important issue of biocompatibility is the lifetime of biological product is

usually not as long as electronic of mechanic products. The degradation of the biological devices leads to the changing of the performance and the function. Unlike integrated circuit (IC) chips, biological components are simply composed of numerous chemical compounds and reactions, which are more sensitive to the surrounding condition. For some biomedical devices, such as a pacemaker, are almost zero tolerance for the degradation. That's makes the biocompatibility the most important parameter of a BioMEMS device.

To study the biocompatibility of MEMS structure, the aspects of surface activities of silicon should be evaluated. Some most common surface reactions that take place at biological and silicon interface are summarized below.

Surface hydrolysis

Silicon based structure will form a thin layer (~ a few tenths Å) of native silicon dioxide (S_iO_2) at the surface with the presence of moisture or water. This oxide layer is very critical and undesirable in VLSI fabrication. The native oxide residual would block the electrical contact hole and increase the resistance or cause an open circuit. The formation of the native oxide is referred to the hydrolysis of the silicon bulk substrate.

$$\mathbf{SiO_2 + 2H_2O \dashrightarrow Si(OH)_4}$$

The hydroxyl group attaches to the S_iO_2 and the proton might be released under certain condition, so the surface will be either hydroxyl-rich or oxygen-rich. This creates a binding site for many biomolecules by forming a hydrogen bond or due to electrostatic attraction. Followed with few examples of non-covalent binding of biomolecules onto S_iO_2 of a silicon substrate.

Butylated Hydroxytoluene Contamination

Butylated Hydroxytoluene (BHT) is the major organic contamination in VLSI industry. It

is used as additive in wafer box manufacturing, and it has high vapor pressure, relative high dipole moment and molecular weight. It will be trapped in gate oxide during the thermal oxidation and cause the shifting of C-V curve and failure of reliability. BHT attaches the S_iO_2 by forming two hydrogen bonds. [14]

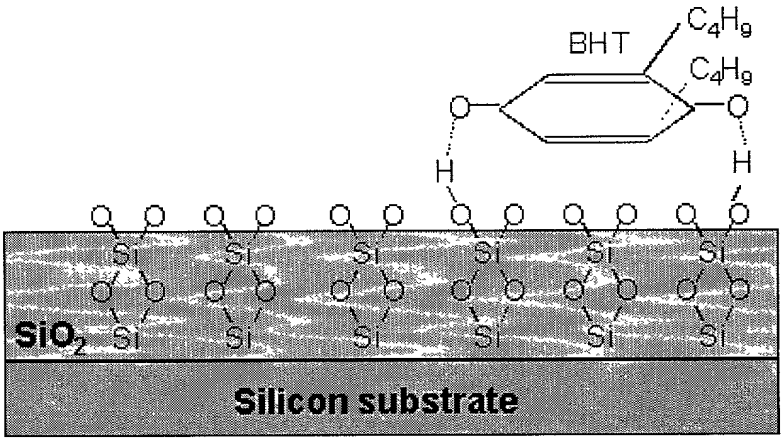

Figure. 4 BHT contamination on Silicon substrate

Polynucleotide, Polypeptide Chain

Polynucleotide and polypeptide chains (such as DNA, RNA and protein) are widely used for biomedical application. They are large molecular chains with charged or non-charged backbone. For DNA and RNA, they are usually negatively charged and tend to bind to positive charged surface. They all have many hydrogen bonds forming sites along the backbone, and play an important role in biological reaction and serve as a target or probe.

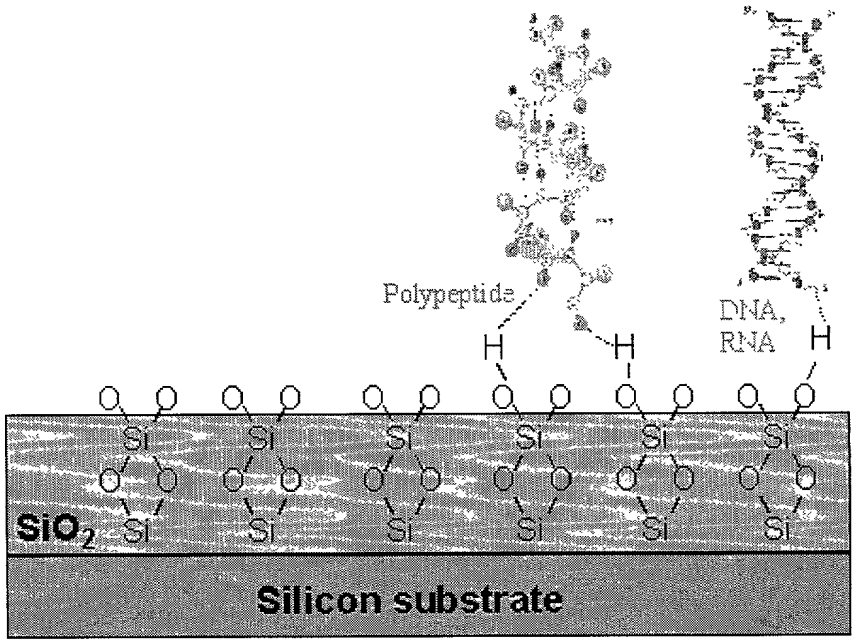

Figure. 5 DNA, RNA, Polypeptide chain attachment on Silicon substrate

Enzyme

Enzyme is a protein with the capability of catalyzing biological reactions. It's very active and could have many binding sites at the surface for other biomolecules. The enzyme could have many surface motifs with various functions and properties. They could be charged, polar, acidic or basic. A small amount of enzyme could significantly change the biological condition, so it's widely used as an amplifying or speeding element.

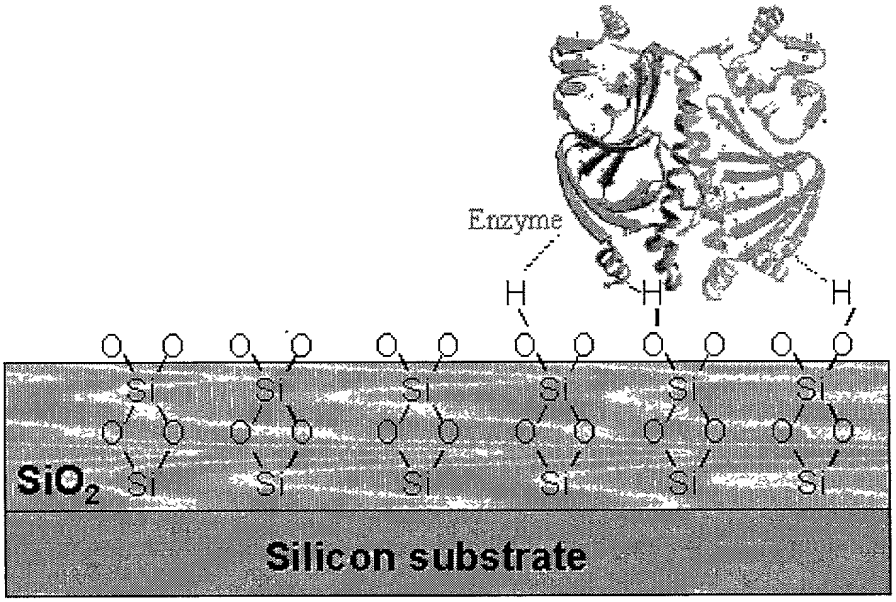

Figure. 6 Enzyme attachment on Silicon substrate

Performance limitation

One of the major commercial products utilizing BioMEMS is "On-chip Electrophoresis". Different biomolecules are separated in a silicon micro-channel due to the charge/mass ratio under a bias potential. It's widely studied and developed for fast DNA sequencing and it could fasten the building human genome library within a shorter time. The input sample still need to be high concentrated because the DNA tends to bind to the channel surface, and it would cause the sample loss and cross contamination.

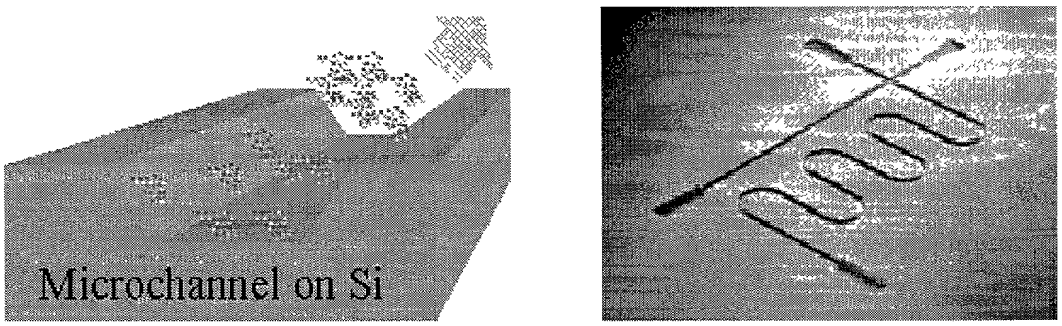

Figure. 7 Capillary Electrophoresis of Microfluidic system on Silicon substrate

7. Functional Surface

Working on surface property should not only improve the biocompatibility of the surface but also should set an ultimate goal to add to the functionality of it. Functional surface is the surface of the mechanical structure with more than one active function other than structural supporting.

Most work on functional surface focuses on new polymer biomaterials; Abbott and Whitesides first demonstrated the active functional surface applicable for MEMS devices in 1995. [15] In their work, electrical potentials were applied, in combination with self-assembled monolayers (SAMs) of alkanethiolates anchored on gold films to control the wettability of a surface over wide ranges. The time constant of the transition between hydrophobic and hydrophilic is about a second. The surface property is governed by the organic molecule in the monolayer and the competition binding of molecular adsorption is controlled by the biased potential.

The same binding competition can be found inside the nucleus at the molecular level. The expression of the *lac* operon is a well-studied model for transcription regulation. [16] The repressor has a higher affinity to the inducer over the operator region of the gene to be transcribed. Without the presence of the inducer, the repressor will anchor onto the operator gene and block the transcription. With the presence of the inducer, repressor will bind to the inducer and the operator gene will be available for transcription. Different binding events can be switched by one specific biomolecule or external field and this is the basic principle or implementation of functional surface.

It's always safe to design a biomedical device from the *bio-inspiration*, other control mechanisms could also be applied to implement the functional surface, such as the feedback inhibition and allosteric enzyme regulation.

Self-Assembled Monolayer (SAM)

Self-assembled monolayers (SAMs) are of great current interest because of potential applications in electronics, surface treatment, passivation, adhesion, and nanotechnology. These films are being used to create complex, multifunctional surface architectures, such as artificial receptor sites and controlled-size transport channels on electrodes. For all these applications the

structure, motion, and defects of these films on the nanometer scale are critically important. The ability to control the precise placement of selected functional groups on a flexible, substrate-bound molecular assembly will provide a means to replicate the physiochemical functions of biological surfaces and membranes.

SAM is widely used to modify the surface chemically to form a thin layer of uniform molecules with or without functional terminal groups on the top. [17,18] SAM of organosulfurs on gold films has been shown to form highly organized and ordered systems, which is suitable for utilization in membrane mimetic studies such as molecular recognition, catalysis, and cellular interactions.

The difference between SAM and other chemical binding techniques is that SAM provides a specific and uniform molecule binding. The surface could be hydrophilic or hydrophobic. Au is the typical material for conducting working electrode due to its inert characteristic. Au is stable, and it won't form an oxide layer on the surface easily, but biomolecules still can bind onto the surface. The major concern is the weak adhesion between the gold and silicon substrate. Therefore titanium of chromium is usually used as an adhesion layer between the gold film and the bulk substrate. Another approach, which relies on a direct surface modification of the silicon surface by silane-based molecules, has also been developed. SAM can also be formed on silicon substrate by HF oxide striping and forming Si-R, Si-O-R or Si-O-Si-R bonds. [19,20,21] This approach eliminates the intermediate stage of the gold coating and allows fabricating more robust modified surface. Surface property can be modified with different terminal function R group, such as alcoholic or phenolic, hydroxyl, amine, phenyl, carbonyl, and nitric group.

For the biosensor application, SAM formation could be a bottleneck technique because of the presence of the active biomolecule functional groups. Especially, the functional terminal linkage group (Sulfur group, Amino group, Silane-based group) of most biochemical reagents tends to bind to Au or even Silicon/Nitride/PolySilicon surface. In other words, there will be many different molecules on the surface with different binding efficiency and time constant. That is why the base line of the biosensor is always unpredictable. Therefore the kinetic analysis of the formation of functional surface is extremely important.

Surface Modification to Improve the Biocompatibility

Alkanethiols, $HS(CH_2)_nX$, can chemisorb on gold and silver and form self-assembled monolayers (SAMs). The ability to present a variety of functional organic groups, X, at the terminal position of the alkanethiol makes it possible to control the structure of the surface at the molecular level, and thus to control the interfacial properties of these organic surfaces. These SAMs constitute an exceptionally useful set of model surfaces with which to study the interaction of synthetic materials with biologically relevant systems.

Besides tethered with organic groups, alkanethiols can be terminated with oligo (ethylene glycol) groups and form SAMs that resist the adsorption of proteins (so-called 'inert surfaces'). These alkanethiols, when used in mixed SAMs that include alkanethiols that present other functional groups isolate the biomolecular interactions of interest from non-specific effects.

The performance of artificial materials in contact with biological systems is determined by the surface interactions of the two materials. Therefore considerable efforts have been made in the last few years to improve the "biocompatibility" of compounds used for biological and biomedical applications. The goal of most research activities is to tailor the surface properties of substrates in such a way, that a favorable interaction of the surface modified material and biological systems is achieved

Since the surface interaction could result in noise increasing and structure damage, surface modification is one way to go around this problem. The easiest way is to change the surface property of the structure or using plastic. By converting the surface into biocompatible or bio-inert, non-specific interaction will be limited to minimum or eliminated by the fabrication of a molecular layer firmly tethered to the surface. The most widely implemented approach uses SAM from thiol molecules by chemisorption onto a gold surface and silane molecules to form SAM on a silicon oxide surface according to well-established procedures developed in the 80s mostly by C. D. Bain, and G. M. Whitesides.

8. Non-Specific Binding — Protein Adsorption

Protein adsorption contributes most of the noise from non-specific binding. Protein adsorption is dominated by interactions other than hydrophilic force. The general protein

adsorption is due to ionic and hydrogen bonding of O^- groups at the surface. Protein could be used to modify the surface property for biomedical application, especially for eliminating the non-specific binding on biosensor surface by competitive replacement binding.

Protein adhesion onto solid surface could be accomplished by forming different bonds with the external ligands. Protein can form covalent or non-covalent bond with other molecules at the attachment site on protein surface.

Protein adsorption can be reduced by water-soluble, nontoxic, non-immounogenic polymer such as polyethylene oxide (PEO) or polyethylene glycol (PEG) treatment. Major protein binding mechanisms are described below.

Hydrogen Bonding

Protein or polypeptides contains numerous proton donors and acceptors both in their backbone and in the R-groups of the amino acids. Proteins are found to also contain the hydrogen bond donors and acceptors of the water molecule. Therefore, hydrogen bonding occurs not only within and between polypeptide chains but also with the surrounding aqueous medium.

Hydrophobic Forces

Proteins are composed of amino acids that contain either hydrophilic or hydrophobic R-groups. It is the nature of the interaction between different R-groups in the aqueous environment to play the major role in shaping protein structure and protein adhesion. The spontaneous folded state of globular proteins is a reflection of a balance between the opposing energetic of H-bonding between hydrophilic R-groups and the aqueous environment and the repulsion from the aqueous environment by the hydrophobic R-groups.

Electrostatic Forces

Electrostatic forces are mainly of three types: charge-charge, charge-dipole and dipole-dipole. Typical charge-charge interactions that favor protein folding are those between

oppositely charged R-groups or external molecules such as lysine (Lys, K) or arginine (Arg, R) and aspartic acid (Asp, D) or glutamic acid (Glu, E). A substantial component of the energy involved in protein folding/adhesion is charge-dipole interactions. This refers to the interaction of ionized R-groups of amino acids with the dipole of the water molecule. The slight dipole moment that exists in the polar R-groups of amino acid also influences their interaction with water. It is, therefore, understandable that the majority of the amino acids found on the exterior surfaces of globular proteins contain charged or polar R-groups.

Van der Waals Forces

There are both attractive and repulsive van der Waals forces that control protein folding. Attractive van der Waals forces involve the interactions among induced dipoles that arise from fluctuations in the charge densities that occur between adjacent uncharged non-bonded atoms. Repulsive van der Waals forces involve the interactions that occur when uncharged non-bonded atoms come very close together but do not induce dipoles. The repulsion is the result of the electron-electron repulsion that occurs as two clouds of electrons begin to overlap. Although van der Waals forces are extremely weak, relative to other forces governing conformation and adhesion, it is the huge number of such interactions that occur in large protein molecules that make them significant to the folding of proteins.

Covalent binding

The ionized caborxyl group and amino group would react with external molecules by forming a covalent bonding. It will happen at the active site of protein, and it's very specific. Because it only occurs at the certain site of protein and orientation of protein the conformation of the solid surface will determine the absorption efficiency and surface protein density.

CHAPTER 3 STATE OF THE ART TECHNOLOGIES FOR DNA CHIP

1. Introduction

Four state-of-the-art technologies (enzymatic reaction, nucleic acid hybridization, electrochemical detection, surface modification) used in this work are briefly reviewed in this chapter. The background and working principle of each technique is addressed and the contribution of each module to DNA sensor chips is also discussed.

2. Enzymatic Reaction

Characteristics of Enzyme — *Catalytic Reaction*

Enzymes are extraordinarily efficient and selective biological catalysts that accelerate the chemical reaction toward equilibrium. A catalyst cannot initiate a reaction that would not happen in its absence, but it can radically affect the reaction rate. Most enzymes are highly specific. They tend to accelerate only one or a group of related reactions. Enzyme-catalyzed reactions are stereoselective and stereospecific and these characteristics have resulted in frequent use of enzymes in analytical applications.

Several thousand enzymes have been isolated, and several hundred are available commercially. Enzymes are classified by the reactions they catalyze and oxidoreductase enzymes are most frequently used for electrochemical electrodes. Oxidoreductases catalyze the oxidation (removal of electrons) or reduction (addition of electrons) of the enzyme substrate.

Prosthetic Group and Mediator

Enzymes, like all proteins, are composed of amino acid chains folded into specific three-dimensional structures. They range in size from 10,000 to several million daltons. Besides, amino acids, many enzymes also contain prosthetic groups — nicotinamide adenine dinucleotide (NADH), flavin (FAD), heme, Mg2+, and Ca2+ — that enhance enzyme activity. With

oxidoreductases, the prosthetic groups serve as temporary traps of electrons or electron vacancies.

The prosthetic groups can be near the surface or deep within the enzyme's protein core structure. In the latter case, the trapped charge is not easily transferred to an electrode. According to Marcus theory, which is used to explain electrochemical reaction rate, electron transfer decays exponentially with distance. Therefore, the accessibility of the active site of a enzyme determines the practical functionality for electrochemical applications.

From a biological perspective, concealment of the active site is often necessary for selective targeting or redox reactions toward a specific synthetic or degradative route. For electrochemical biosensor applications, however, the difficulty of electron transfer into or out of the active site poses a real problem. Mediators capable of accessing the active site are frequently used to assist in the transduction of the enzyme activity into a measurable amperometric response.

3. Nucleic Acid Hybridization

Watson Base Pairing

Deoxyribose nucleic acid (DNA) is a structurally polymorphic macromolecule carrying genetic information. In 1953, James Watson and Francis Crick proposed the first correct structural model for DNA. It accounts for this pairing of bases and also explains how relatively simply the system of storing and transferring genetic information is. According to the Watson-Crick model, a DNA molecule consists of two polynucleotide strands coiled around each other in a helical "twisted ladder" structure. The sugar-phosphate backbone is on the outside of the double helix, and the bases are on the inside, so that a base on one strand points directly toward a base on the second strand. When using the twisted ladder analogy, think of the sugar-phosphate backbones as the two sides of the ladder and the bases in the middle as the rungs of the ladder. In effect, each strand of DNA is one-half of the double helix and called single strand DNA (ssDNA). The two halves come together to form the double helix structure.

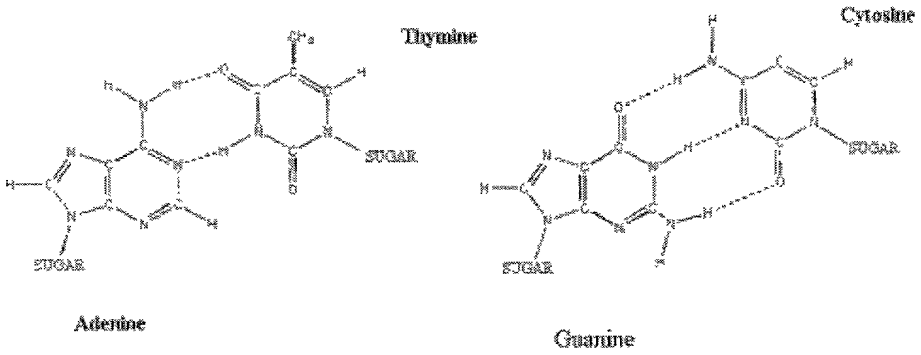

Figure. 8 A-T base pairing and G-C pairing

The strands are held together by hydrogen bonds between the nitrogenous bases. In the double helix, adenine and thymine form two hydrogen bonds to each other but not to cytosine or guanine. Similarly, cytosine and guanine form three hydrogen bonds to each other in the double helix, but not to adenine or thymine.

DNA Sensor

DNA based technologies are extremely important in molecular biology, genetics and molecular medicine, and are extensively used by academic research and biotechnology industry. DNA technology methods where first introduced into the area of in vitro diagnostics in 1986 when the polymerase chain reaction (PCR) were developed. Most methods based on DNA technology are used ex vivo and their development requires extensive skills in mathematics, physics, chemistry and engineering - more than in biology and medicine.

DNA technology is becoming very advanced and highly sophisticated, and it is almost always combined with advanced technology from other areas of science. Sensors are key components in instrument development for DNA technology. DNA technology is a highly interdisciplinary research area that requires extensive collaboration

Oligonucleotide Synthesis

Molecular probes to detect particular nucleic acid sequences are extremely important in many applications of DNA sensor technology. They are used on chips, for blotting in gels, for screening colonies, detect chromosomal abnormalities and most recently for direct detection of PCR products. In the future molecular probes will be developed for other applications, and they will also be based on other physical phenomena then radioactivity and fluorescence to generate detectable signal.

Bio-molecule Modification

The development of DNA technology, particularly in the area DNA probing in solution, goes towards more and more sensitive systems. Today, detection of nucleic acids for diagnostic purposes requires the nucleic acid to be amplified. Bio-molecule modification is widely used as a signal indicator in DNA sensor. The presence of nucleic acid can be detected optically or electrochemically by the biomolecules attached to it. Most bio-molecule modifications are various types of optical dye a wide range of emission wavelength for detection and visualization.

Amplification Technologies

The polymerase chain reaction (PCR), developed in 1986 and rewarded the Nobel price to Kary Mullis in 1993, revolutionized Molecular Biotechnology by making amplification of nucleic acids a reality. Since then other methods have been invented. For example, Nucleic Acid Sequence-Based Amplification (NASBA) developed at Akzo Nobel health care division, Organon Teknika, is superior to PCR for mRNA detection. The ligase chain reaction (LCR) was developed by the American company Abbot.

4. Electrochemical sensor

Basic Principles of Electrochemical Detection

Electrochemical Cell

Electrochemical cell is a device that converts chemical energy into electrical energy or vice versa when a chemical reaction is occurring in the cell. Typically, it consists of three metal electrodes immersed into an aqueous solution (electrolyte) with electrode reactions occurring at the electrode-solution surfaces.

It consist of two electronically conducting phases (e.g., solid or liquid metals, semiconductors, etc) connected by an ionically conducting phase (e.g. aqueous or nonaqueous solution, molten salt, ionically conducting solid). As an electrical current passes, it must change from electronic current to ionic current and back to electronic current. These changes of conduction mode are always accompanied by oxidation/reduction reactions. Each mode changing reaction is called a half-cell.

An essential feature of the electrochemical cell is that the simultaneously occurring oxidation-reduction reactions are spatially separated. The hydrogen is oxidized at the anode by transferring electrons to the anode and the oxygen is reduced at the cathode by accepting electrons from the cathode. The overall electrochemical reaction is the sum of the two electrode reactions. The ions produced in the electrode reactions, in this case positive hydrogen ions and the negative hydroxyl ions will recombine in the solution to form the final product of the reaction: water.

During this process the electrons are conducted from the anode to the cathode through an outside electric circuit where the electronic current can be measured. The reaction can also be reversed, water can be decomposed into hydrogen and oxygen by the application of electrical power in an electrolytic cell.

Electrochemical Reaction

Electrochemical reaction is an oxidation/reduction (redox) reaction that occurs in an

electrochemical cell. The essential feature is that the simultaneously occurring oxidation-reduction reactions are spatially separated. For example, in a spontaneous "chemical reaction" during the oxidation of hydrogen by oxygen to water, electrons are passed directly from the hydrogen to the oxygen. In contrast, in the spontaneous electrochemical reaction in a galvanic cell two separate electrode reactions occur.

Three Electrode System

Three electrode system is an electrochemical cell containing a working electrode, a counter electrode (or auxiliary electrode), and a reference electrode. A current may flow between the working and counter electrodes, while the potential of the working electrode is measured against the reference electrode. This setup can be used in basic research to investigate the kinetics and mechanism of the electrode reaction occurring on the working electrode surface, or in electroanalytical applications. The detection module in this work is based on a three-electrode system.

Counter Electrode (Auxiliary Electrode)

Counter electrode is used only to make an electrical connection to the electrolyte so that a current can be applied to the working electrode. The processes occurring on the counter electrode are unimportant, it is usually made of inert materials (noble metals or carbon/graphite) to avoid its dissolution. This is the case for cells used for research or for electroanalytical purposes. Of course, for many practically used cells, the processes occurring on both electrodes can be very important. From the observation in this work, small feature or small cross-section at the counter electrode will heat up the surrounding solution when a large current is pulled out from the counter electrode. Bubbles would come out if the current is continuously overflowed and it will end up with the dissolution of the electrode.

Reference Electrode

Reference electrode is used as a reference point against which the potential of other electrodes (typically that of the working electrode or measuring electrode) can be measured in an electrochemical cell. In principle it can be any electrode fulfilling the above requirements. In practice there are a few commonly used (and usually commercially available) electrode assemblies that has an electrode potential independent of the electrolyte used in the cell, such as silver/silver-chloride electrode, calomel electrode, and hydrogen electrode.

Working Electrode

Working electrode is where the action is. The reaction occurring on the working electrode may be used to perform an electrochemical analysis of the electrolyte solution. It can serve either as an anode or a cathode, depending on the applied polarity. One of the electrodes in some "classical two-electrode" cells can also be considered a "working" ("measuring," "indicator," or "sensing") electrode, e.g., in a potentiometric electroanalytical setup where the potential of the measuring electrode (against a reference electrode) is a measure of the concentration of a species in the solution.

Amperometry

Amperometric detection transduces the flux of electroactive product into a measured current. It is based on monitoring the oxidation or reduction of an electroactive compound at a working electrode of the sensor. A potentiostat is used to apply a constant potential to the working electrode with respect to the reference electrode. The applied potential is an electrochemical driving force that causes the oxidation or reduction reaction. In this work, electrochemical workstation Model 660A from CH instruments were use for all the amperometric measurements.

The current response of a redox reaction can be expressed mathematically using Faraday's Law:

$$I = n F (da/dt)$$

where the current in amperes (I) represents the electrochemical oxidation or reduction rate of the analyte at the working electrode, (da/at) is the oxidation or reduction rate in $mole^{-1}$. F is Faraday's constant, and n is the number of electrons transferred. The reaction rate depends on both the rate of electron transfer at the electrode surface and analyte mass transport.

With most redox reactions, the rate of electron transfer can be accelerated by increasing the potential at which the electrode is poised. As the potential is increased, the reaction reaches the point where the rate is limited by the mass transport of reactant to the electrode. When the reaction at the electrode surface is sufficiently fast, the concentration of analyte at the electrode is zero, and a maximum overall rate of reaction is reached. This overall rate is limited by the rate of mass transfer given by the following equation:

$$I = nAFD(dC/dX)_{x=0}$$

where dC/dX is the flux of C (electroactive species) to the electrode surface, A is the electrode surface area, and D is the diffusion coefficient. The rate of mass transport to the electrode surface depends on the bulk concentration of analyte, the electrode shape and area, and diffusion and convection conditions.

Electrochemical Work Station (CH Instrument)

The Model 660A series is designed for general-purpose electrochemical measurements. This instrument contains a fast digital function generator, a high speed data acquisition system, filters for the potential and the current signals, a secondary gain stage, iR compensation circuitry, a potentiostat and a galvanostst. The potential control range is ± 10V and the current range is ± 250mA. It is capable of measuring current down to tens of picoamperes. The steady state current of a 10 mm disk electrode can be readily measured without external adapters. With the CHI200 Picoamp Booster and Faraday Cage, currents down to 1 pA can be measured.

5. Surface Modification

The importance of surface and material science cannot be underestimated when designing a DNA sensor. Immobilization of biomolecules on to solid surface or synthetic materials and investigation of its relative characteristics relative to the native biomolecule are crucial in the development of solid-phase bioanalytical techniques. [22]

Self-Assembled Monolayer (SAM)

Control over the density, orientation and structure of the immobilized oligonucleotide probe is very important, and one promising route to accomplish this is self-assembled monolayers on gold surfaces.

Self-assembled monolayers (SAMs) formed by organosulfur compounds on gold and other surfaces have developed into an increasingly important research area at the frontier of analytical chemistry [23] and electrochemical biosensors.

Two primary analytical advantages associated with coating an electrode with a self-assembled monolayer (SAM) are as follows:

1. Non-Faradic background currents are dramatically reduced, largely because the monolayer prevents close approach of solvent and ions to the electrode surface and therefore decrease the double-layer capacitance and reduced background currents are usually desirable in electroanalytical chemistry because of improved sensitivity.
2. Self-assembled monolayers made it possible to bind enzymes covalently onto electrode surface for electrochemical sensor. This membrane-free type of sensor has high amperometric sensitivities and rapid response time because it's free from any diffusion problems of substrates or products through the enzyme membrane.

SAM is used in MEMS technology in different aspects, from biosensors to electrode patterning. [23,24] The attractive feature of SAM is the capability of forming the electrochemically active surfaces of the microelectrode. Therefore the conducting wires become multi-functional and increase the value of the device.

6. Integration

MEMS technology is not only to make structures small, but to push the limit of

macroscale physics for a better performance. The most significant achievement of this work is not to discover a unique scientific phenomenon or to invent a new sensing scheme. In this work, for the first time, four individual existing techniques previously described are successfully modified and integrated into a DNA sensor array chip with a better performance over the conventional DNA diagnostic sensor.

CHAPTER 4 DNA SENSOR ARRAY ON A SILICON CHIP — EXPERIMENTAL RESULTS

1. Introduction

A reusable DNA sensor array for rapid biological agent detection has been fabricated on a silicon chip. (Fig.9) The DNA-based probes target the DNA/RNA sequence of the analyte instead of indirect probing using antibodies. The sensitivity is greatly enhanced by combining the hybridization event with a signal enzyme. The formation of the self-assembled monolayer sensor surface, in-situ DNA hybridization, signal measuring and the sensor regeneration can be performed within 40 minutes. Even without using the PCR, as low as 1000 Escherichia coli (E. coli) cells through 16s rRNA can be detected using this sensor array. (Fig.9) The dimension of each sensor area ranges from 25 mm^2 to 160 μm^2.

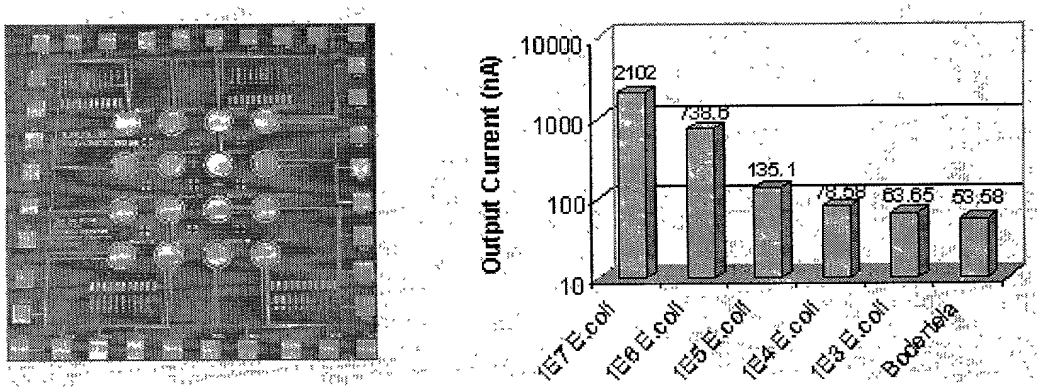

Figure. 9 DNA Sensor Chip and Sensitivity Curve

Background and Significance

The enzyme-based electrochemical biosensor is primarily motivated by the need for a highly sensitive and selective protocol capable of rapid monitoring the concentration of bacteria, virus or various biological species for field use. Such a protocol would operate remotely, and would be fully automated, compact, and robust [25]. Therefore the electrochemical transducer

with minimum power consumption and smaller size is preferred over the optical system [26]. High specificity can be achieved by using DNA hybridization to reduce false positive and false negative signals. DNA electrochemical biosensors have been previously reported [27,28] using graphite or carbon electrodes. Carbon-based electrodes, however, are generally not adaptable to MEMS technology when small (<μm) dimensions are needed. In this study, Au is used as electrodes, with a protein self-assembled monolayer (SAM) to capture the E. coli rRNA. An enzyme is used as a biological amplifier in this study to gain the high sensitivity without PCR. A sensitivity and specificity check for E. coli MC4100 versus Bordetella SB54 is shown in Fig.9.

Detection Principle

Horseradish peroxidase (HRP) is one of the most widely used enzymes for analytical purposes and biosensors application [29]. Enzymatic amplification occurs due to a high turnover number in reactions that can be detected electrochemically. We describe here an amperometric biosensor based on HRP with 3,3'5,5'-tetramethylbenzidine (TMB) as a mediator. (Fig.10) The electron transfer at the electrode surface is measured amperometrically to represent the number of the enzymes immobilized by DNA hybridization though the 16s ribosomal RNA of the target cell. Therefore, the output current is proportional to the number of the target cells in the solution.

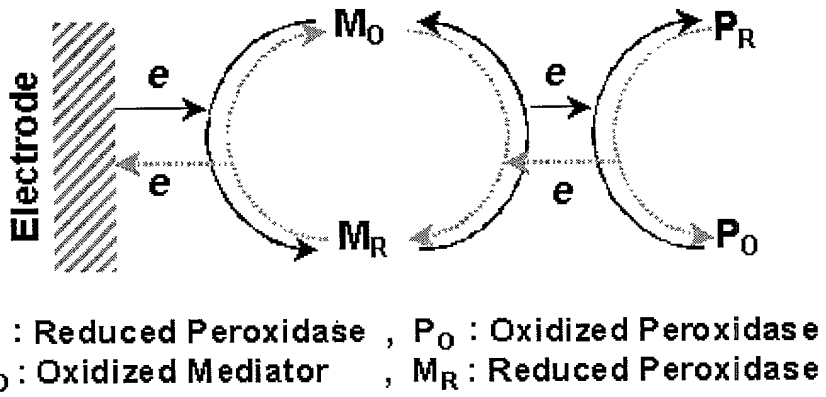

Figure 10 Electron transport of HRP enzymatic reaction

2. Sensor Chip Fabrication

Design Aspect

As described in Chapter 3, the main function of fabricating a DNA chip is to integrate nucleic acid hybridization, enzymatic reaction, electrochemical detection and surface modification into a complete functional sensor module. The new design should be able to minimize or eliminate the weakness of the current technique by taking advantages of MEMS technologies. If the performance of the new design is no better than the conventional device, then the efforts for the work are questionable. If the system integration is just putting all individual components together, then it would be an assembly work, not an engineering design.

The main issue here is the noise reduction or sensitivity in another term. We can prevent the noise from happening, reduce the level of the noise or amplify the signal to obtain a high signal-to-noise ratio. In the following sections, detail design aspects will be reviewed along with the experimental results to verify the design concept.

I Materials for Electrochemical Electrodes

Standard electrodes are used in conventional electrochemical experiments to provide an accurate and precise reference potential though a half-cell composed of an analyte/electrode interface. The commercial standard reference/counter electrode is about the size of a pen; therefore the reaction is often conducted in a one-liter beaker. Stirring is generally required in all cases to eliminate diffusion controlled effect.

Typical material combination for reference/counter complex is Ag/AgCl. Screen-printed sensors were reported using AgCl paste and Ag wire onto plastic board or silicon wafer. Screen-printing is not MEMS compatible process and its resolution is limited by the fineness of the screen matrix.

Several conducting materials available in MEMS technology were patterned on silicon substrate by lift-off process and the characteristic of the three-electrode system were tested by cyclic voltammetry with ferrocene solution. Different combination between gold, platinum, titanium and aluminum were tested and the Au/Au/Au three electrode system gave the best C-V curve and redox characteristics. Different shapes and areas were also tested to achieve the most optimum design.

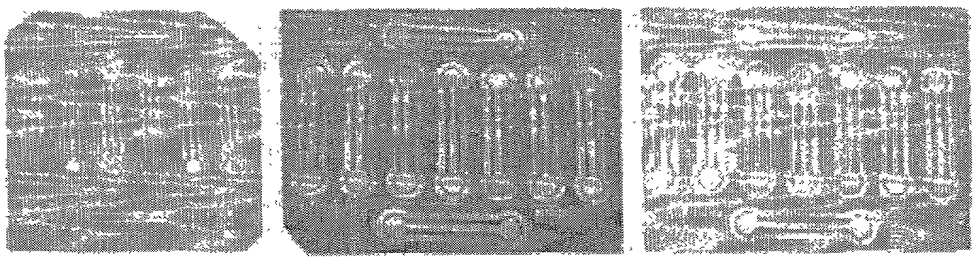

Figure 11 Different Electrode Material on Silicon Substrate

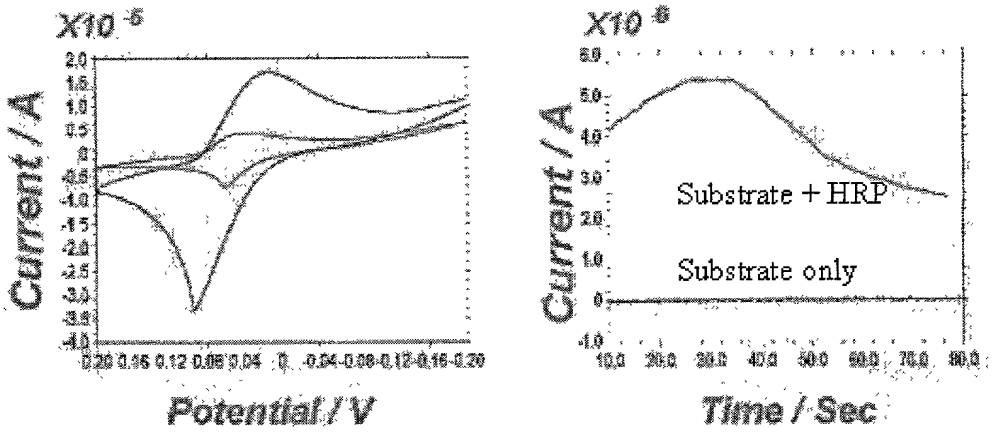

Figure 12 C-V characteristics of Sensor electrodes and Enzyme Response

II On-Chip Reaction Well for Reagent Confinement

The design concept of having a reaction well on silicon substrate was from the observation of the high level noise from the non-specific binding of HRP onto the periphery region of the working electrode. To verify that noise does come from the HRP residual at the surface, a simple test was done to estimate the contribution of this unwanted binding. HRP were introduced to bare silicon chip, followed with several wash steps before the addition of the substrate solution. A very high level of enzymatic reaction was observed right after adding the substrate solution.

As expected, HRP, like other proteins, sticks to the silicon surface easily and tightly. Several commercial wash solutions and blocking protein were tested without any significant improvement of reducing non-specific binding. The best way to reduce the number of the undesirable binding to a minimum is to prevent it from happening. The area outside the working electrode need not encounter the HRP solution. But it's almost a tradition to immerse all three electrodes in aqueous system all the time and all the reagents would flow through all the surface area.

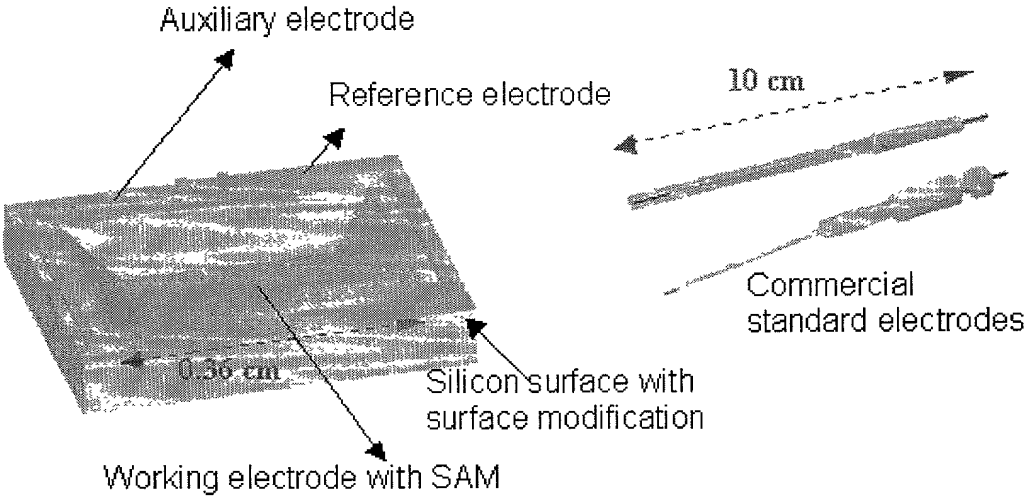

Figure 13. Comparison between microfabricated and commercial electrodes

The simplest way to confine certain reagent within a well-defined space is to build a well. As shown in Fig.13, a microfabricated well is bordered by (111) silicon planes after KOH etching. The working electrode defined by lift-off process covers the whole well surface.

III Surface Modification for Noise Reduction

Surface technology and material science

The importance of surface and material science cannot be underestimated when designing a DNA chip. An ineligible amount of non-specific binding still occurs during the washing process while the diluted reagent is flowing around the wafer surface. The time for the wash solution containing HRP to stay on the periphery region is much longer than the binding time constant. Besides fabricating the well structure, the surface of the periphery area must be protected by other mechanism.

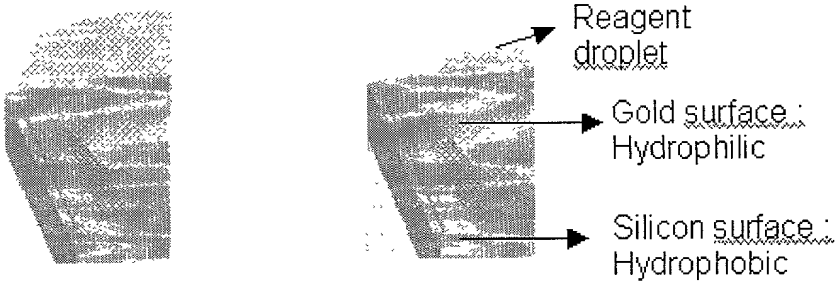

Figure 14. Reagent Confinement with Reaction Well

The most efficient way to keep the surface from contacting reagents is to make it hydrophobic. Silanation of silicon surface is widely used to prevent suspended structure sticking to substrate by surface tension. It was used here to prevent the direct contact of biomolecules to the periphery area of silicon substrate.

Silanation

Silane-based molecules with various functional terminal groups have been used to modify surface properties of silicon wafers, silicon nitride chips, and the SPM tips. Silane compounds for the surface modification form robust self-assembled monolayers (SAMs) chemically tethered to silicon oxide surfaces as a result of hydrolysis of terminal Si(Cl)n or SiO-C_2H_5 groups.

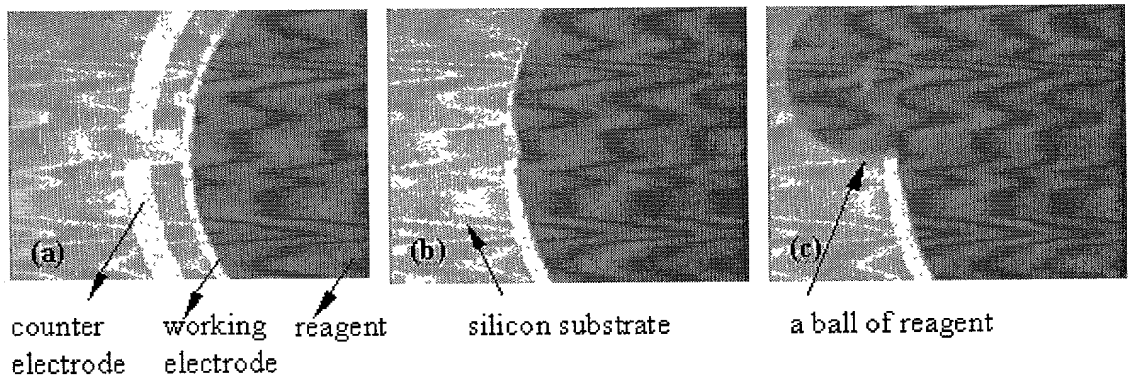

Figure 15. Reagent Confinement by Surface Treatment

(a) the reagent is shaped by the hydrophilic working electrode and a droplet is nicely formed over the Au surface (b) with increasing the volume of the reagent, the area covered by the reagent will gradually expand and then cover the other two electrodes (c) shoot out a stream of reagent by pipetteman, a ball of reagent will be formed in stead of spread out on the hydrophobic silicon substrate

Fabrication Process

A three-electrode electrochemical cell is constructed with a micro-fabricated reaction well for the working electrode (Fig.16a). Gold (Au) is deposited as a conducting layer and Si3N4/SiO2 as an isolation layer. (Fig.16b) The surrounding Si surface is modified to be hydrophobic. The three dimensional reaction well along with the hydrophobic nature of the surrounding area allows a liquid droplet to be well contained in the working electrode. This design minimizes non-specific binding of biomolecules to other areas of the sensor chip. The Au working electrode has a

monolayer of streptavidin immobilized on the surface via a thiolated-biotin SAM or through direct protein adsorption onto the gold. (Fig.16c).

A sample solution containing E. coli is treated with lysis buffer, the target DNA/RNA from the E. coli cells are hybridized with both an anchoring ssDNA probe and a labelling ssDNA probe at annealing temperature (~65°C) in the presence of cell debris. The anchoring probe (conjugated to biotin) and the labelling probe (conjugated to fluorescein) recognize two distinct conservative sequences, therefore, the hybrid forms only with the specific gene segment from the target bio-agent. The oligonucleic hybrid is then immobilized through biotin-streptavidin binding onto the working electrode and unbound components are washed away. A HRP-linked anti-fluorescein antibody is then loaded onto each hybrid (Fig.16d). After addition of substrate, enzymatic reaction causes a current signal which is measured amperometrically using the three-electrode cell. (Fig.16e) The entire protocol is completed in 40 minutes.

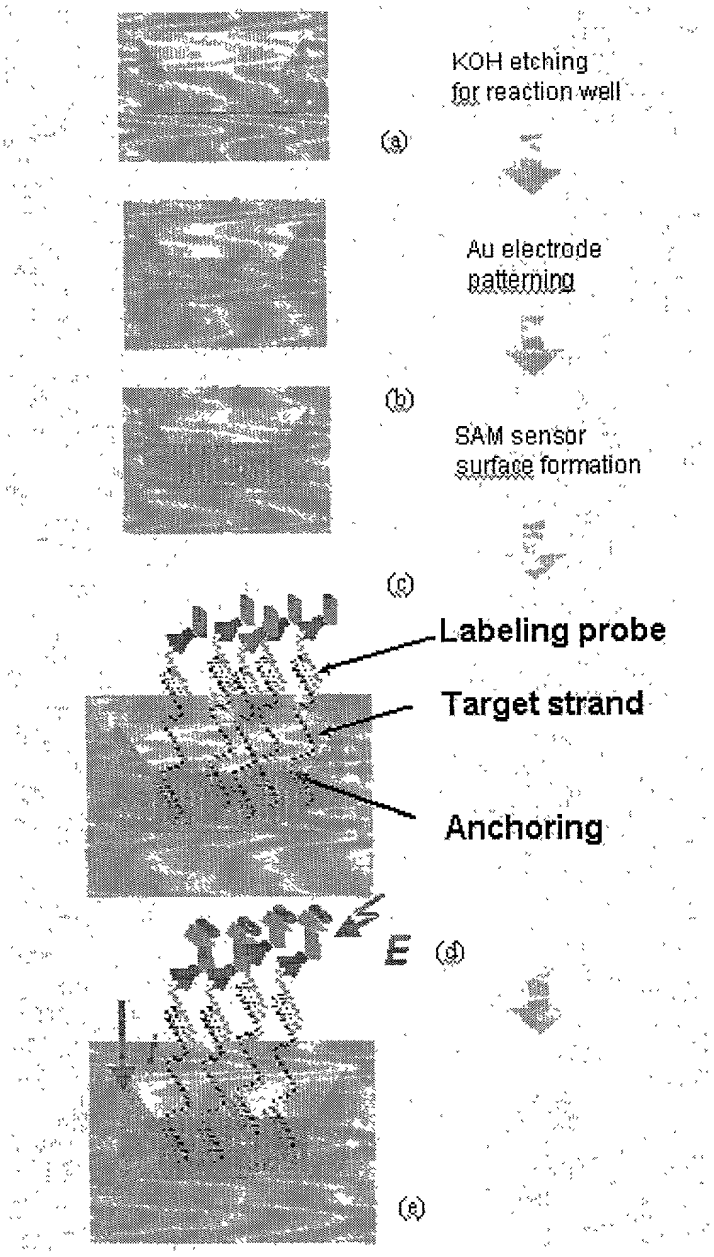

Figure 16. Sensor Chip Fabrication Process Flow

3. Chemical Sensor Surface Formation

Self-Assembled Monolayer

Three different approaches of immobilizing streptavidin SAMs on the Au surface were tested:

1) depositing the protein directly on bare Au, Fig. 17-1
2) depositing a monolayer of a biotin SAM using a thiol (R-SH) and then binding streptavidin to the biotin. Fig. 17-2
3) depositing a monolayer of a biotin SAM using a disulfide (R-S-S-R) and then binding streptavidin to the biotin. Fig. 17-3

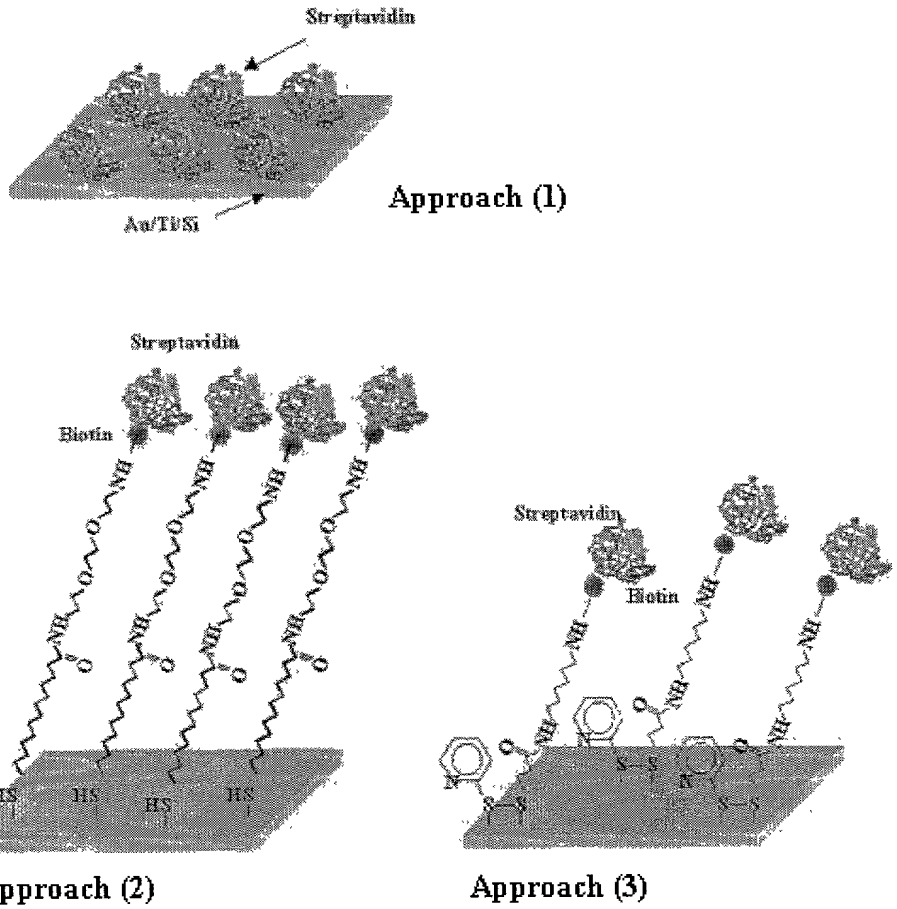

Figure 17. Different Approaches of Protein Deposition

4. Protocol

Fig.18 is the schematic drawing of the detection strategy. Two types of probes, labelling probes and anchoring probes, which are labeled with fluorescent and biotin respectively, are used in this application. Firstly, the cell is disrupted by base solution (NaOH) or other methods. Introduce the probe solution to the cell debris without any isolation process. (Fig. 18-1) Single-stranded 16s ribosomal RNA targets are hybridized to fluorescent-labeled labelling probes and biotin-labeled anchoring probes at its hybridization temperature (65°C). Then the biotin-tagged hybrids are captured on Gold/strepavidin sensors (Fig. 18-2) and loaded with an anti-Fluorescent-HRP antibody-enzyme conjugate. (Fig. 18-3) A few seconds following addition of the HRP substrate, a quantitative electrochemical signal, which is proportional to the activity of the HRP enzyme and thus the amount of immobilized hybrids on the surface, can be read on the monitor. In the mean time, two washing processes are employed to remove the extra reagents, including unhybridized sample, probes, enzyme and cell debris.

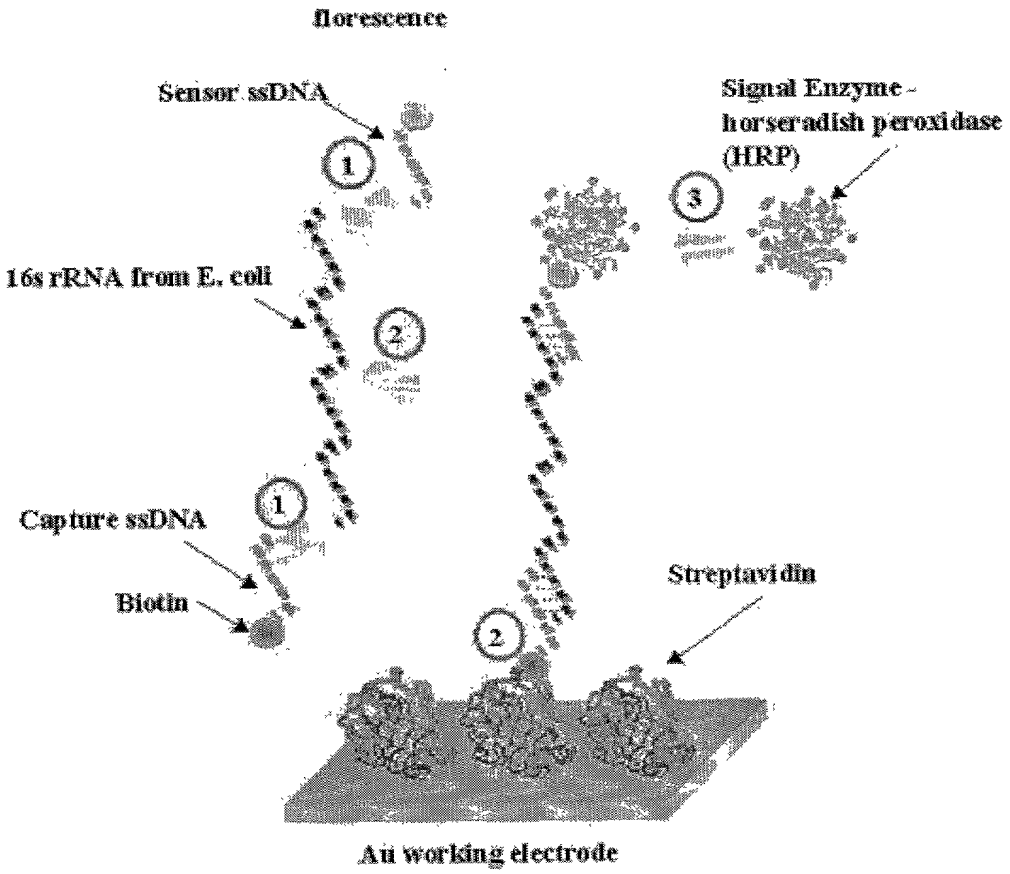

Figure 18. Schematic Drawing of Detection Method

A key feature of this work is the immobilization of a biomolecular monolayer on the sensor electrode to capture the ribosomal RNA of E. coli. This biomolecular layer was immobilized onto the Au surface of the working electrode using self-assembled monolayer (SAM) technology as described previously. The protein streptavidin was selected as the biomolecule due to its high affinity for biotin (~10^{15}M). In our sensor configuration, a SAM of streptavidin is immobilized on the Au working electrode. Biotin is conjugated to an anchoring oligonucleotide, which hybridizes to one end of the 16s rRNA of E. coli, thereby anchoring the E. coli rRNA on the sensor surface. A second labeling oligonucleotide hybridizes to the other end of the E. coli rRNA, and finally, the enzyme horseradish peroxidase (HRP) is attached to the hybrid. An electrical signal is generated by the enzymatic reaction, which is detected electrochemically using the MEMS biosensor.

Andcare Protocol

The sample preparation and hybridization scheme is originated from the commercial protocol from Andcare Inc. The detail of the protocol is illustrated below.

5

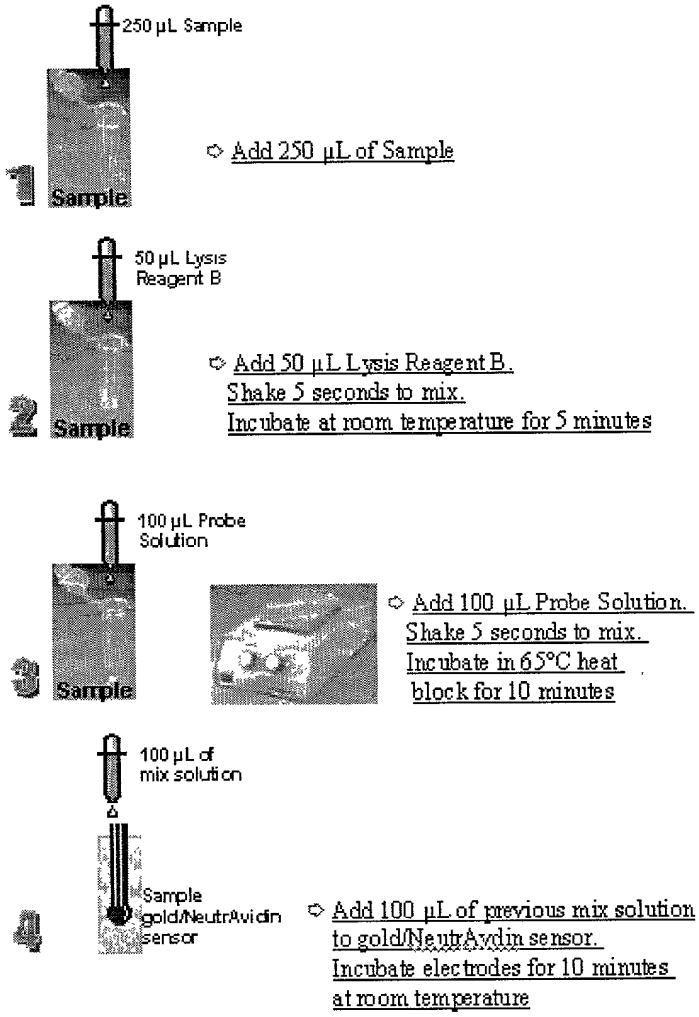

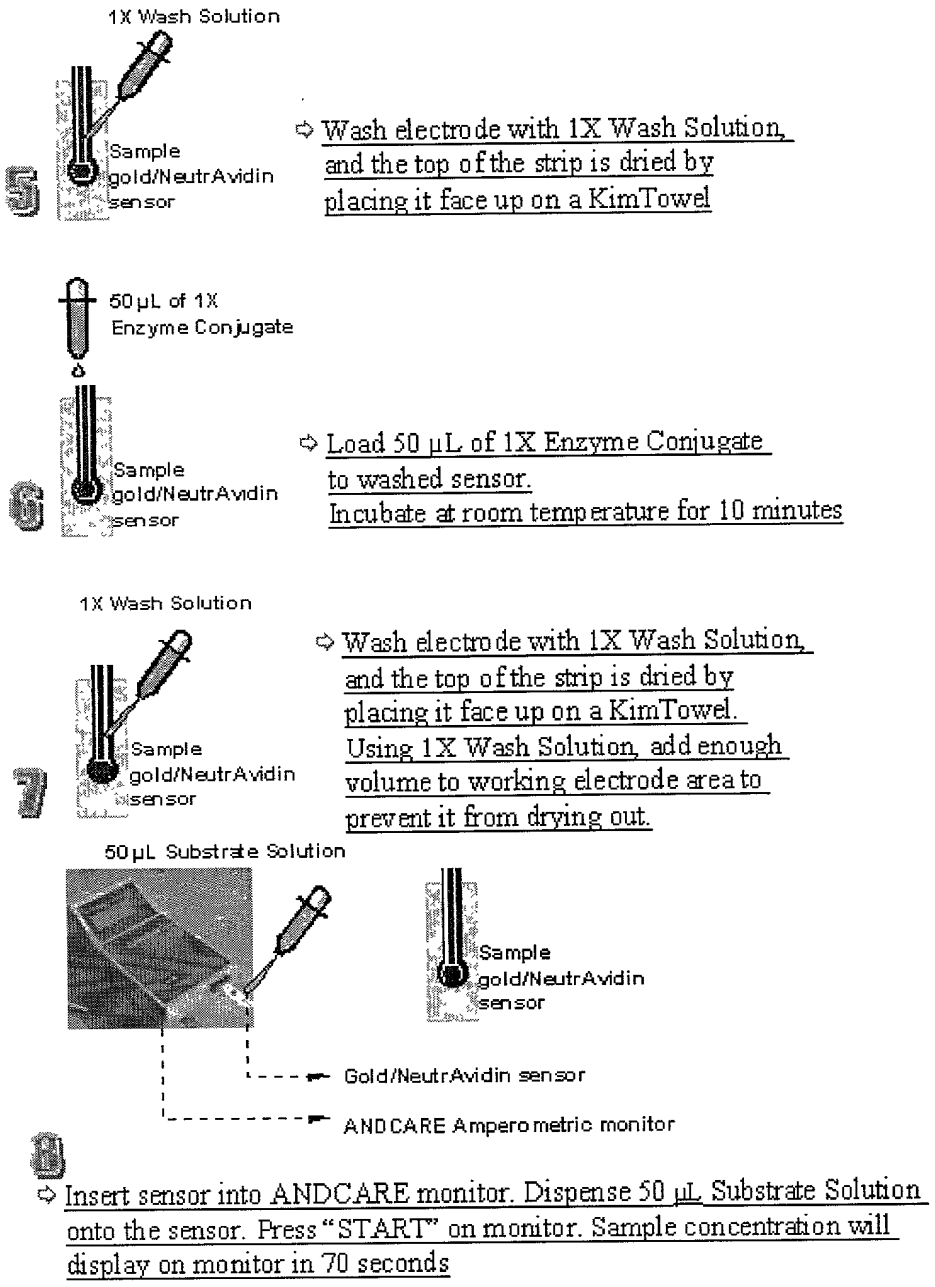

Figure 19. Commercial Available Andcare Protocol with Carbon Paste Sensor for E. coli Screening

Probe Design

Anchoring probe and labeling probe provide the specificity and the linkage between the target molecule with the transducer. The sequence design of the probe affects the detection performance directly. Therefore, many software tools are available to eliminate the human error and to assist optimizing the sequence alignment when dealing with a few thousand to few millions bases of genetic information.

I Gene Bank Searching

Entrez Nucleotides

Entrez is a search and retrieval system that integrates information from databases at National Center for Biotechnology Information (NCBI). These databases include nucleotide sequences, protein sequences, macromolecular structures, whole genomes, and MEDLINE, through the National Library of Medicine's search service, PubMed. *Entrez Nucleotides*, part of the *Entrez* system, is a collection of nucleotide entries from GeneBank.

To search in the GeneBack database, it is advised to key in as detail as possible, otherwise numerous matched results will be pooled out. In the example shown below, The strain name (MC4100) of the E. coli used in our experiment was typed as keyword to retrieve the gene of its 16s ribosomal RNA for sequence alignment. The sequence is shown in FASTA format, a standard format for a long written sequence. The FASTA sequence can be directly copied to the alignment tool for primer selection.

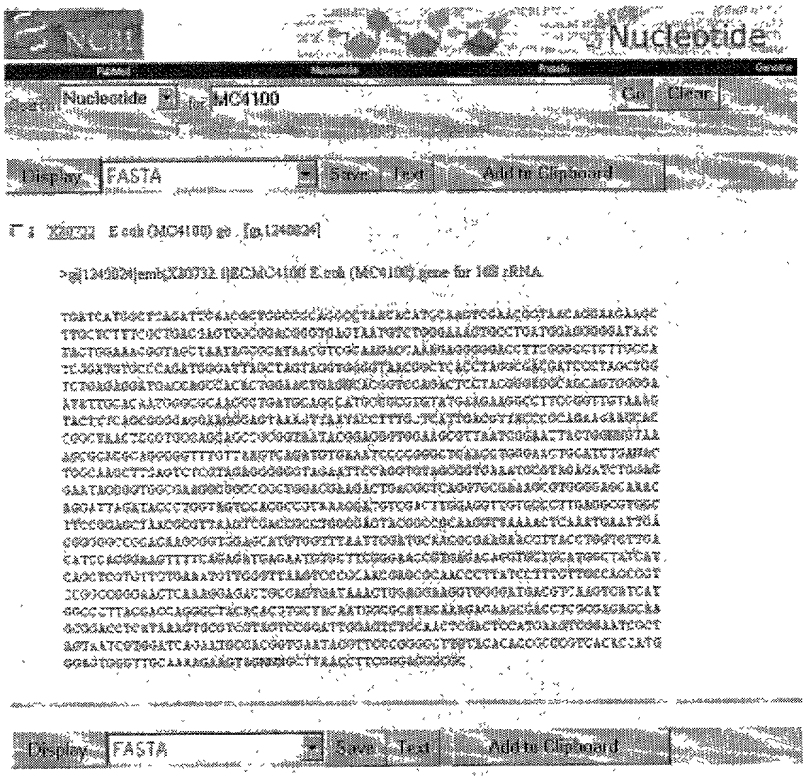

Figure 20. Entrez Nucleotides : Sequence Search Tool

II Sequence Alignment — Primer Selection

There are many commercial software, shareware or web-sites provide the function of primer selection. The term "primer" is specific for the oligonucleotide probe used in PCR. With a given target sequence, primer selector could search along the gene and then obtain two best regions for primer design based on the preset conditions. The upper and lower primer is for two complementary ssDNA probes respectively. Usually the one with the most unique sequence will be for the labeling probe and the conservative one is for the anchoring probe. A picture of the primer selection result is shown below.

Rank	Scores Model	Local	Sequence	(Position)
F1	6	1	GGTAACGGCTCACCTAGGC	(246)
F2	7	1	CCAGATGGGATTAGCTAGTAGG	(221)
F3	8	1	GACCAGGGCTACACACGTG	(1196)
F4	8	1	GTAACGGCTCACCTAGGCG	(247)
F5	9	1	GGGTAACGGCTCACCTAGG	(245)
F6	10	1	TAACGGCTCACCTAGGCGA	(248)
F7	10	1	CCCAGATGGGATTAGCTAGT	(220)
F8	11	1	AAACGATGTCGACTTGGAG	(797)
F9	11	1	AGGCGACGATCCCTAGCTG	(261)
F10	11	1	TAAACGATGTCGACTTGGAG	(796)
F11	12	1	GAAGTCGGAATCGCTAGTAAT	(1312)
F12	13	1	AAGACCAAAGAGGGGGACC	(176)

Rank	Scores Model	Local	Sequence	(Position)
R1	5	1	CCGTTACCCCACCTACTAGC	(253)
R2	6	1	TAGGGATCGTCGCCTAGGT	(275)
R3	7	1	GCCGTTACCCCACCTACTAG	(254)
R4	8	1	CTAGGGATCGTCGCCTAGG	(276)
R5	8	1	CGCCATTGTAGCACGTGTG	(1225)
R6	9	1	AGGGATCGTCGCCTAGGTG	(274)
R7	9	1	CGTTACCCCACCTACTAGCT	(253)
R8	10	1	CGTTACCCCACCTACTAGCTA	(252)
R9	11	1	CTGATCCACGATTACTAGCG	(1342)
R10	11	1	TCCTCTCAGACCAGCTAGG	(290)
R11	11	1	AAGGGCACAACCTCCAAGT	(826)
R12	12	1	TCATCCTCTCAGACCAGCTAG	(293)

Figure 21. Primer Selection Search Results

III Hybridization Temperature Calculation

Hybridization is usually few degrees lower than the melting temperature. There are many published models to calculate the melting temperature. Most of them are based on the following simplified equation:

$$Tm = 81.5 + 16.6*\log_{10}(C_{Na}) + 41*f_{GC} - 600/n_{total}$$

where Tm = melting temperature in degree Celsius

C_{Na} = concentration of sodium ions in molar (M).

f_{GC} = fraction of G+C bases in the oligonucleotide

n_{total} = total number of bases

$\log_{10}$ = common (base 10) log

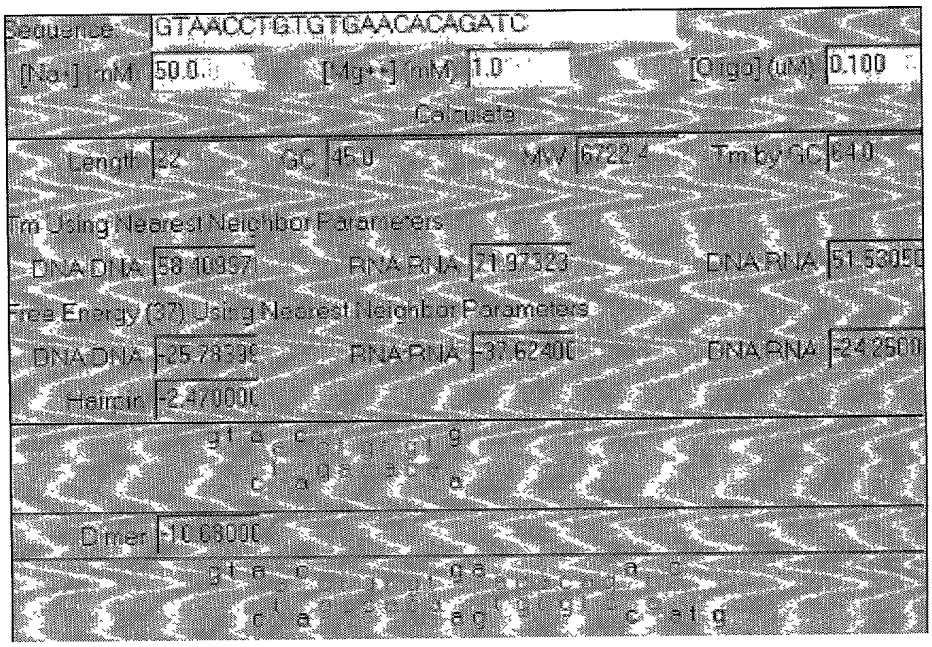

Figure 22. Calculation results of Melting Temperature

Materials

Lysis reagent, probe solution (containing a mixture of capture and detector probe), Anti-fluorescein-horseradish peroxidase (Anti-Fl-HRP), and enzyme diluant were purchased from Andcare, Inc. (Durham, NC). Wash solution was purchased from Substrate (K-blue substrate) for horseradish peroxidase (HRP) was purchased from Neogen Corp. Streptavidin was purchased from Sigma Chemical Co. Biotin-HPDP (N-[6-(Biotinamido)hexyl]-3'-(2'-pyridyldithio)propionamide) was purchased from Pierce, Inc. Biotin-DAD-C12-SH (12-

mercapto(8-biotinamide-3,6-dioxaoctyl)dodecanamide was purchased from Roche GmBH (Germany).

Methords

For deposition of SAMs on Au, three different SAMs were used. The first was depositing streptavidin on bare Au, the second was depositing a SAM of biotin-HPDP and then subsequently binding streptavidin, and the third was depositing a SAM of biotin-DAD-C12-SH and then subsequently binding streptavidin. In all cases, the Au surfaces were cleaned with concentrated "Piranha" solution (70 vol% H_2SO_4, 30 vol% H_2O_2. Note: this solution is highly reactive and must be handled with care) and thoroughly rinsed with deionized water. For depositing a SAM of streptavidin on bare Au, a 1.0 mg/ml streptavidin solution in 0.02M Na phosphate buffer, pH 7, was placed on the surface, allowed to stand for 10 minutes, and rinsed with deionized water. For depositing a SAM of biotin-HPDP, a 10mM solution of biotin-HPDP was prepared in DMSO, and then this solution was diluted with ethanol (or water) to form a final biotin-HPDP concentration of 50μM. Au surfaces were incubated in the 50μM solution for ~18 hours and then rinsed with deionized water. The surfaces were then exposed to a 1.0 mg/ml streptavidin solution for ~10 minutes and rinsed again with water. For depositing a SAM of biotin-DAD-C12-SH, the procedure of Spinke, et al. (1993) was used. The biotin-coated Au surfaces were then exposed to a 1.0 mg/ml streptavidin solution for ~10 minutes and rinsed again with water.

The protocol for amperometric detection of E. coli was conducted as follows: 1) 50 μl of lysis reagent was added to a 250 μl sample of E. coli in culture media and incubated for 5 min. at room temperature, 2) 100 μl of probe solution was then added and the mixture was incubated for 10 min. at 65°C, 3) 10 μl of the lysed E. coli/probe solution mixture was placed on the working electrode of the MEMs sensor chip and incubated for 10 min. at room temperature, 4) the MEMs sensor chip was washed with wash solution, 5) 10 μl of Anti-Fl-HRP was placed on the working

electrode and incubated for 10 minutes at room temperature, 6) the MEMs sensor chip was washed again with wash solution, 7) 10 µl of the K-blue substrate was placed on the sensor chip in such a way that all three electrodes (working, auxiliary, reference) were covered by the substrate solution, and 8) electrochemical measurements were then taken.

5

CHAPTER 5 SURFACE ANALYSIS

1. Introduction

The SAMs on the DNA sensor were characterized by surface plasmon resonance (SPR) and atomic force microscopy (AFM) to determine whether only a monolayer was deposited and also to determine the kinetics of protein deposition. From this data, the time scale required for in situ sensor surface formation in the integrated fluidic system could be ascertained.

2. Atomic Force Microscopy

Atomic force microscopy (AFM) provides topographic information down to the Angstrom (Å) level. Additional properties of the sample, such as thermal and electrical conductivity, magnetic and electric field strength, and sample compliance can simultaneously be obtained using a specialty probe. Many applications require little or no sample preparation.

A physical probe is scanned across the sample using piezoelectric ceramics or laser beam while a feedback loop is used to maintain a constant interaction between the probe and the sample. The position of the probe and the feedback signal are electronically recorded to produce a three dimensional map of the surface or other information depending on the specialty probe used.

Atomically Smooth Surface: Template-Stripped Gold Surface (TSG)

Gold is becoming a popular substrate for biological application on mechanical structures. Its surface is satisfactorily inert, but can be easily chemisorb dialkyl disulfides or alkanethiols, which spontaneously organize into functional SAMs. [28,29,30]

Sample Preparation

Atomic Force Microscopy (AFM) was performed using the AutoProbe CP from Park Scientific Instruments (Thermomicroscopes, Inc.). AFM was performed in the contact mode using ultralever tips with a force of 5.0nN. (Note: Forces of 0.5nN and 13nN were also used with no observable differences in the results). To ensure a flat Au surface, the method of Wagner, et al. (1995) [31] was used wherein Au was first deposited via e-beam evaporation on Mica and then transferred to Si. In our case, THF was not used to detach the Au from the Mica surface. By cleaving the Mica, it can be cleanly removed from the Au without solvent. Deposition of SAMs was performed as previously described. Four mica preparation methods are illustrated in Fig. 23.

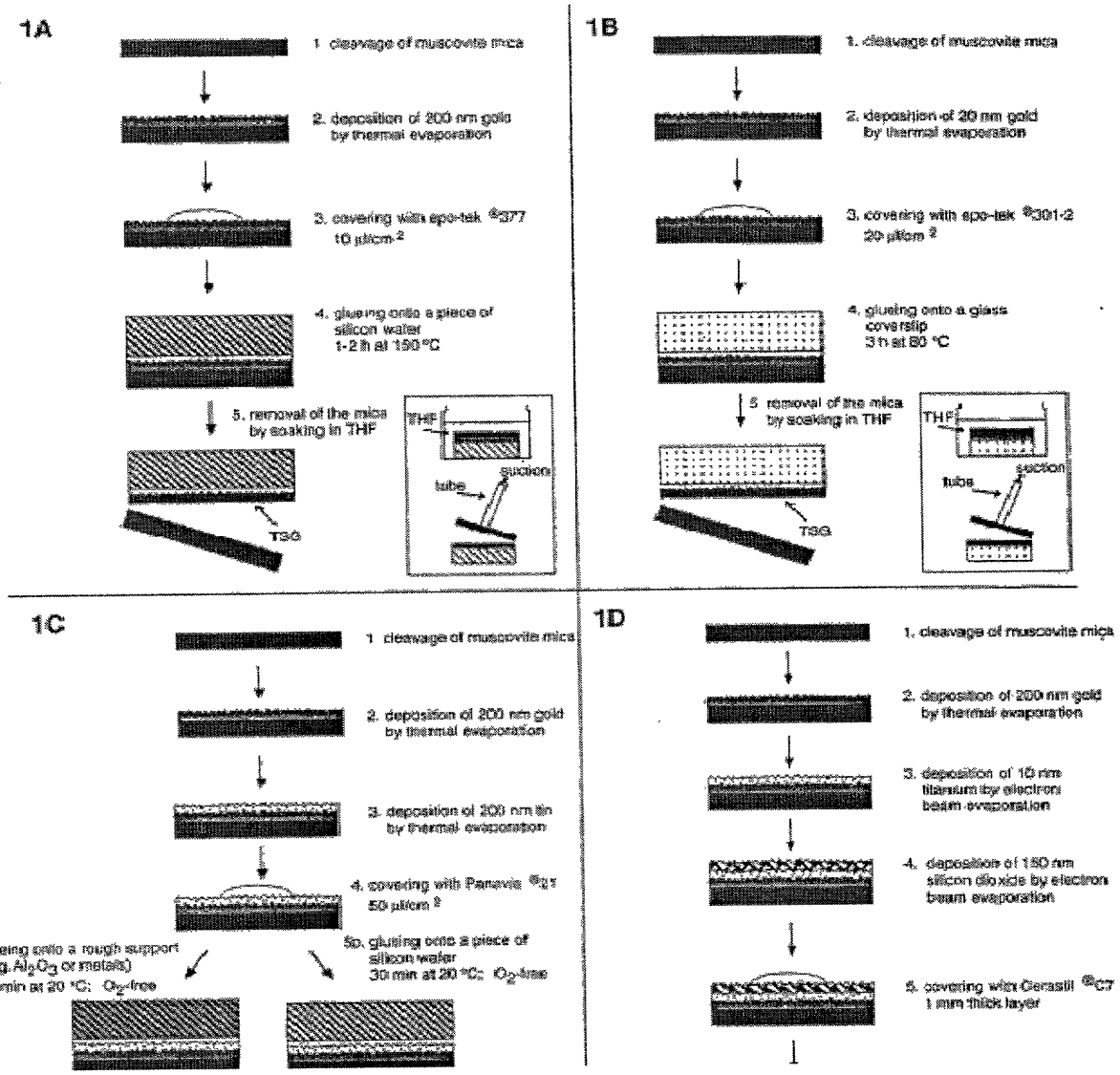

Figure 23. Mica Sample Preparation from Wagner, et al. (1995)

Experimental Results

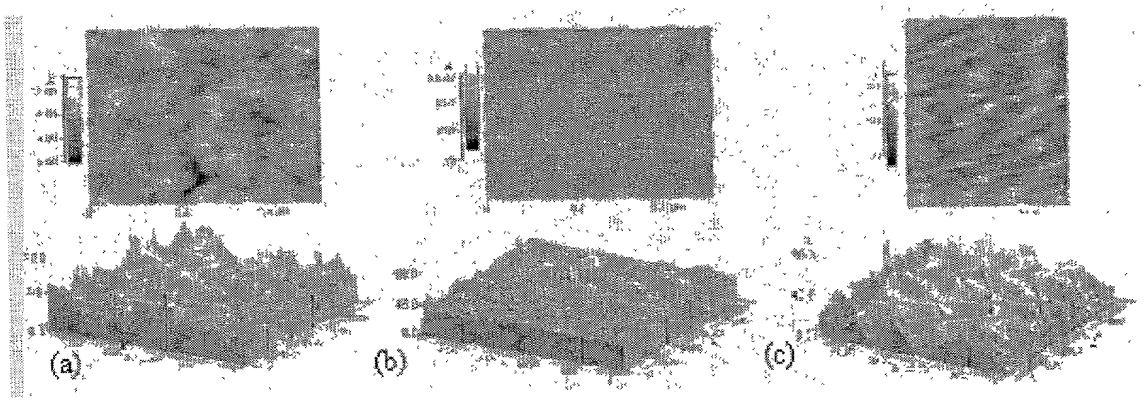

Figure 24. AFM of SAM formation on Au (a) bare Au only (b) full coverage with protein dragging (c) partial coverage with protein islands.

3. Surface Plasmon Resonance

Background and Principle

Surface plasmon resonance (SPR) is sensitive to changes in the index of refraction at and near the surface of a thin metal film. SPR is an in situ technique to observe the processes occurring between synthetic surfaces and complex biological solutions. It also allows the acquisition of data in real time without requiring fluorescent tagging of the analytes. SPR is most commonly used for obtaining both kinetic and thermodynamic parameters of binding events.

Sample Preparation

Surface Plasmon Resonance (SPR) was performed using the Biacore X system (Biacore, Inc.). Flow rates ranged from 5µl/min to 25µl/min and are stated in the Results section. For studies of streptavidin binding to bare Au, bare Au chips (J1 sensor chips from Biacore) were used. For studies of streptavidin binding to biotin-DAD-C-12-SH or biotin-HPDP on Au, a SAM of the biotinylated thiol was deposited on the bare Au chips as previously described. For best results, we used new chips cleaned with diluted "Piranha" solution for ~2 min. prior to use. In the regeneration studies, 25 µl of the following solutions were flowed through the channels at 25

μl/min (total exposure time of 1 min.): 1.0M KCl, 8M urea, 1.0% SDS, 0.1M NaOH, 0.1M HCl, and 40 vol% formamide.

Results

Two different methods were used to deposit the streptavidin SAM, one using a thiolated biotin and the other using direct protein adsorption. In both cases, SPR data shows that only one monolayer was deposited on the surface (Fig.25). A crystalline monolayer of streptavidin has an expected surface coverage of 2.8 ng/mm^2 [34]. Our results indicate that a full monolayer was obtained using the thiolated biotin and ~80% coverage was obtained by direct protein absorption. Moreover, protein binding/adsorption occurs within ~10 seconds.

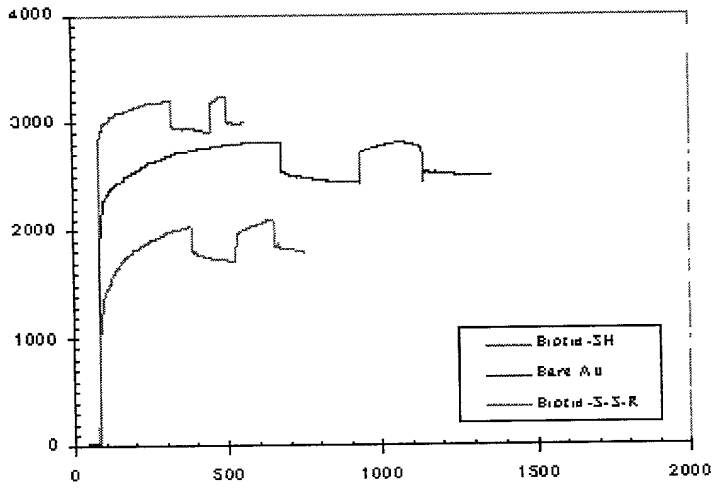

Figure 25. SPR Results of three Different Sensor Surface

CHAPTER 6 FUTURE WORK AND SUMMARY

To optimize the process parameters and the sensor performance, a complete and detail kinetic analysis will be done. There are two transfer functions should be obtained: firstly, from the numbers of target bio-agent to the numbers of the anchored signaling enzyme, and from the numbers of enzyme to the output current.

To implement a micro total analysis system (μTAS), the DNA sensor array chip will be integrated with bipolar transistor array for on-chip signal process. For the first time, a semiconductor amplifier is integrated with a DNA sensor without increasing the sensor area.

1. Kinetic Analysis

The ultimate goal of this work is not only to fabricate a DNA sensor chip but also to analyze the steady state of the enzyme-catalyzed reaction the kinetic analysis, validity of the steady-state assumption and then obtain the transfer function. Analysis of enzymatic kinetic data is not to characterize the nature of the enzyme (that's not our work) but to verify the performance of the DNA sensor and to know the potential of the sensor. The process of obtaining a simplified transfer function of the sensor can also benefit the optimization of experimental design: choice of substrate concentrations; choice of pH, temperature and other conditions.

Surface plasmon resonance (SPR) is a particularly valuable technique for measuring rates and equilibrium constants of processes that involve adsorption of proteins at surfaces and for characterizing mechanisms of protein adsorption. Since the techniques used in preparing SAMs for studies of protein adsorption are essentially the same as those used in preparing substrates for SPR, a common synthetic technology can be used with both. The combination of SAMs, AFM, SPR, MEMS lithography allows the study of the molecular-level interaction of solutions containing proteins (or enzyme) with synthetic surfaces.

2. Integration with Bipolar Transistor

ECBJT *(Electrochemical Bipolar Transistor)*

MEMS devices have distinctive properties as a result of small features but the signal level from MEMS-based sensor is relative low compared to conventional sensor. Best sensitivity can be achieved by using off-chip amplification module but it also increases the noise and the system size. On-chip amplification circuit can reduce the inter-chip interference but the sensor array density is limited by the on-chip circuitry and the limitation of CMOS-compatible MEMS process also reduce the flexibility of the MEMS structure.

We propose an on-chip amplification device underneath the working electrode, which is the largest area of the electrochemical sensor cell. Analogues to the open-base BJT photosensor, the base area receives the current from the transducer with the current gain beta β, which ranges from 80-150. There're two types of BJT can be implemented with electrochemical cell, vertical BJT and horizontal BJT. The current gain is determined by the length of base region. In vertical BJT, this is a function of ion implementation energy and doping concentration. While in horizontal BJT, the length is a function of lithography resolution, ion implementation angle and thermal diffusion. So the vertical BJT is more reliable in term of chip-to-chip or within chip gain uniformity.

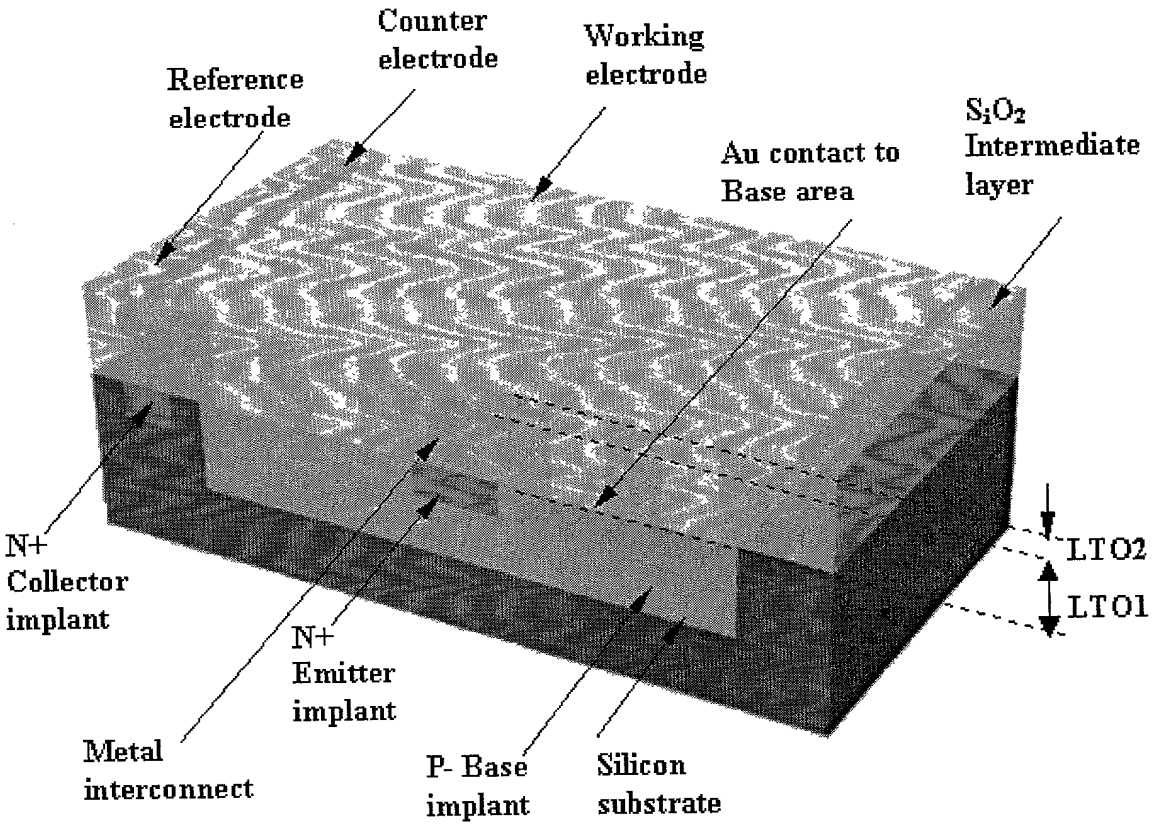

Figure 26. Schematic Drawing of Electrochemical Bipolar Transistor

Conventional in-chip amplify circuitry requires three-metal CMOS process and large area for interconnection and isolation. ECBJT can stack two stages (sensing and amplify) and the Au working electrode can act as an electromagnetic shield for the BJT device. Fig.26 is one approach to realize ECBJT. The working electrode contacts to the base area can also increase the surface area of the working electrode for higher signal. All the structures can be done with one metal and one last Au patterning.

In Fig.26, Metal1 connects to signal output and emitter of the ECBJT. Gold working electrode connects to base through LTO2 via etching. LTO1 isolate the BJT and signal line while LTO2 isolate three electrodes. The via array on working electrode increases the surface area and

also forms a solid contact with BJT. The dimension of the via (~a few μm) is much larger than the size of the protein SAM (~ few tenths Å) on working electrode so the protein adsorption will not be affected.

The structural design of the DNA sensor chip array with bipolar device is shown in Fig.27 and the process flow of the BiCMOS fabrication procedures is in

Fig.28.

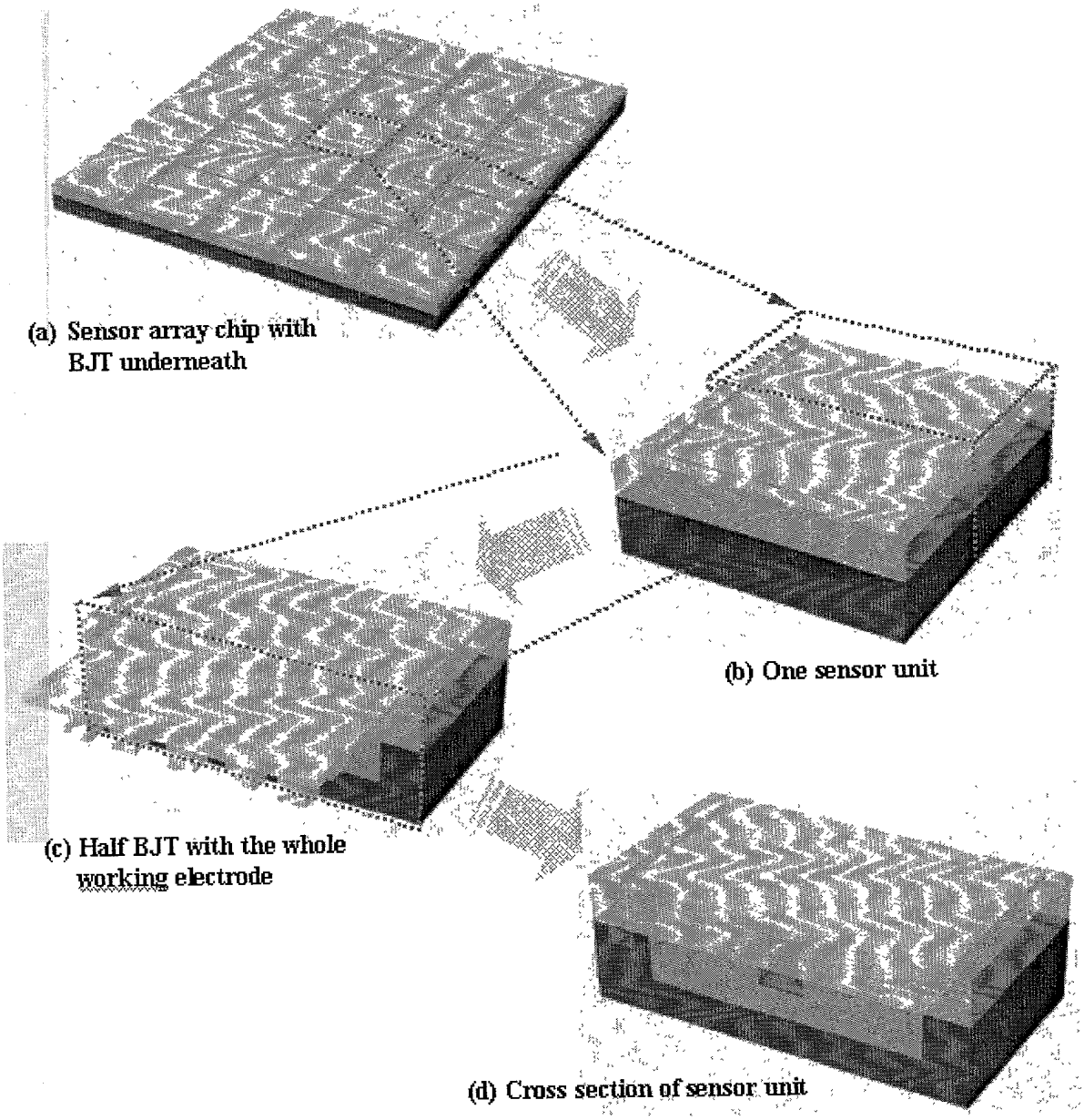

Figure. 27 STRUCTURAL DESIGN OF SENSOR ARRAY CHIP WITH BURIED BJT

5

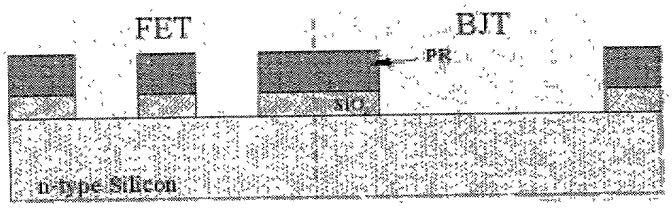

6. Oxide etching

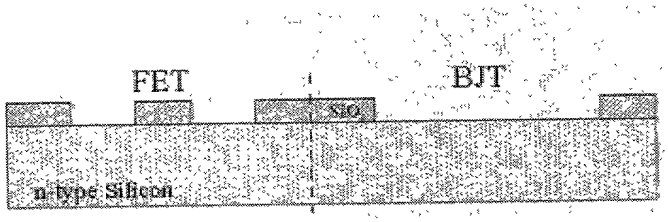

7. PR removal

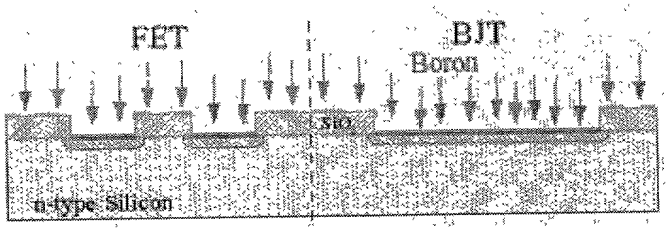

8. Boron predeposition

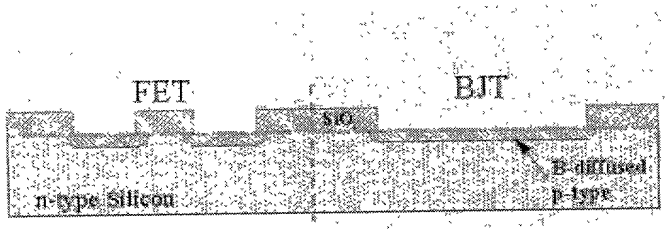

9. Borosilicate glass removal

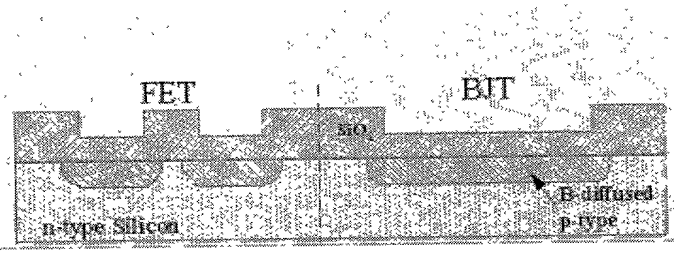

10. Boron drive-in

5

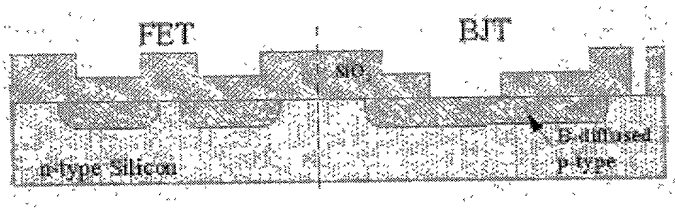

11. Phosphorus mask patterning and etching

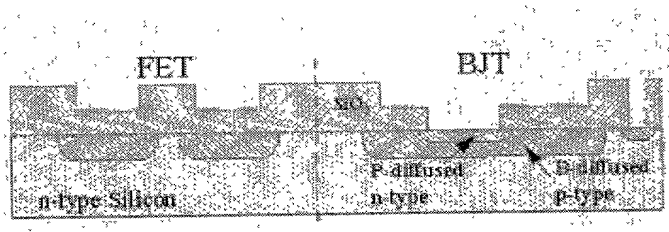

12. Phosphorus predeposition and drive-in

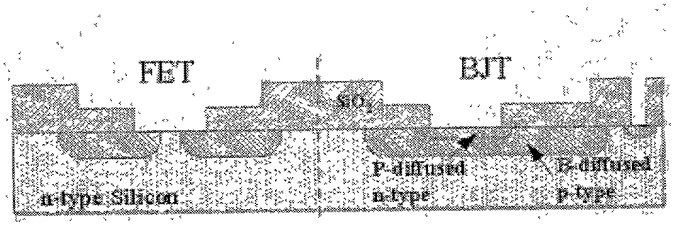

13. Gate mask lithography and etching

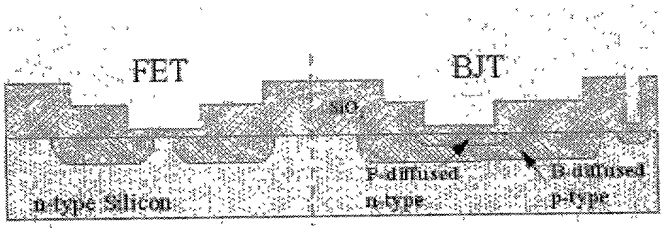

14. Gate oxidation

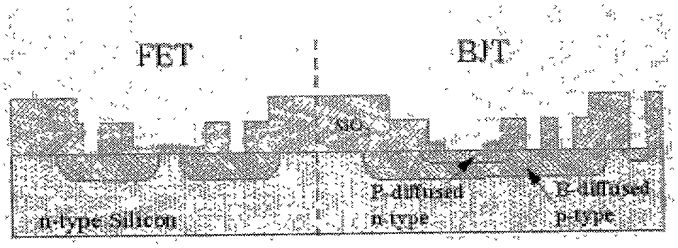

15. Contact hole lithography and etching

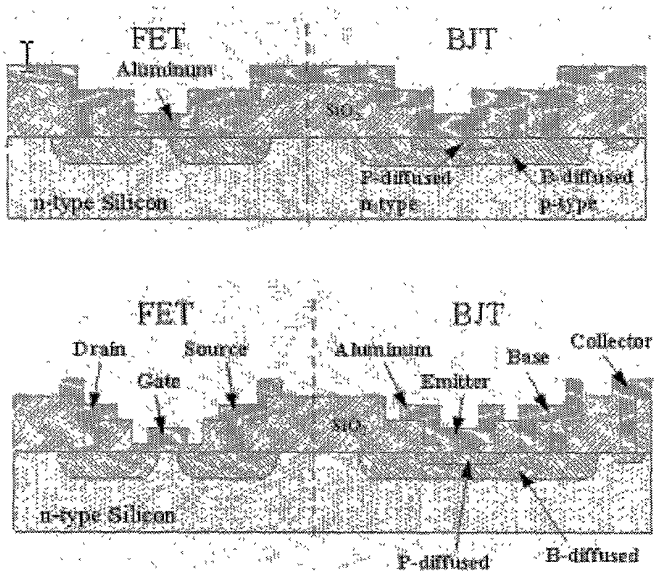

Figure. 28 PROCESS FLOW OF BiCMOS FABRICATION PROCEDURE

To provide a better understanding of the spatial arrangement of the DNA sensor electrodes and the bipolar transistor device, one sensor unit is decomposed layer by layer to show the inner structure of the design in Fig. 29

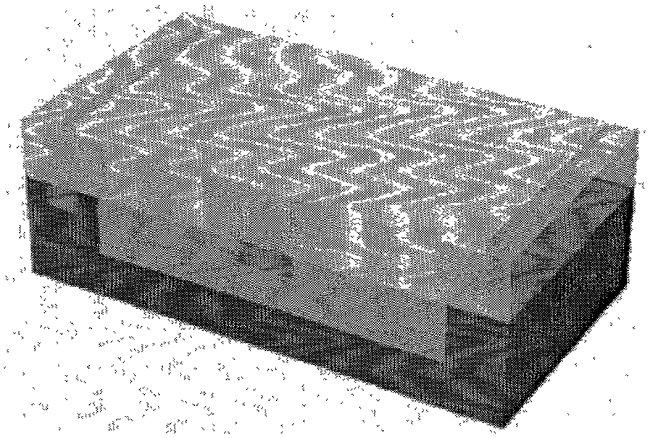

(a) Sensor unit with all layers

5

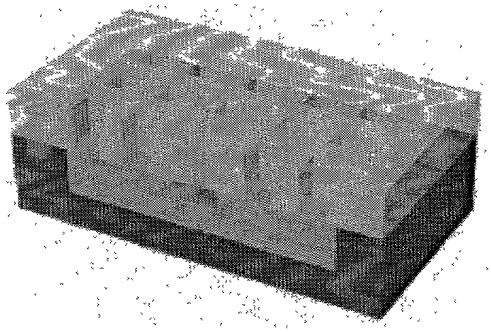

(b) Sensor unit without Au electrodes

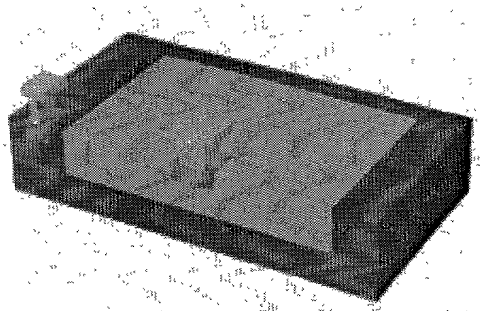

(c) Sensor unit without Au electrodes and two oxide layers (LTO1, LTO2)

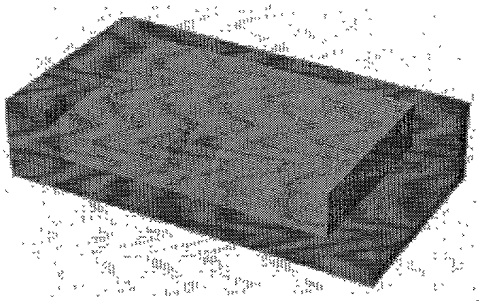

(d) Sensor unit without Au electrodes two oxide layers (LTO1, LTO2) and metal

Figure. 29 DECOMPOSITION OF SENSOR UNIT

3. Summary

This work has shown experimental evidence of successful coupling of nucleic acid recognition event with electrochemical transducers. Various approaches of noise reduction have been discussed in the previous sections, with special attention given to non-specific binding of biomolecules onto MEMS structures. Such enzyme-based DNA sensor chips thus add new dimensions of selectivity and sensitivity to the MEMS based biosensors.

Particular attention was given to factors influencing the kinetics and efficiency of the formation of functional surface, including protein concentration, deposition flow rate, substrate surface condition, dielectrophoresis control and temperature. Additional improvements in the sensitivity have been achieved by modifying the sensor array structure and overcoming the fabrication difficulties.

A novel method for constructing electrochemical biosensor electrodes based on microfabrication and protein adsorption has been demonstrated with better sensitivity (over two order of magnitude) than carbon paste electrodes. The use of microfabricated DNA analysis tools utilizing microfluidics will provide the next generation of inexpensive DNA diagnostics.

REFERENCE :

1) "USAF PAMPHLET ON THE MEDICAL DEFENSE AGAINST BIOLOGICAL MATERIAL - Medical Defense Against Biological Material" Defense Technical Information Center, released on 11 Feb 1997

2) Robert Taylor , "Bioterrorism Special Report: All fall down", *New Scientist*, Volume **150**, Issue 2029, 11 May 1996

3) Cooper, N. "The Human Genome Project," Los Alamos Lab, *Science,* **20**,1-338. 1992.

4) Kevles, D., and L. Hood . "The Code of Codes: Scientific and Social Issues in the Human Genome Project", Harvard University Press, Cambridge, Mass., 1992.

5) Richard P. Feynman "There's Plenty of Room at the Bottom" *Engineering and Science*, Caltech, February 1960

6) William Trimmer, "Grand in Purpose, Insignificant in Size" The tenth Annual International Workshop on MEMS, Nagoya, Japan, Proceedings IEEE Catalog Number 97CH36021, 1997, 9 – 13.

7) W. S. N. Trimmer "Microrobots and Micromechanical Systems" *Sensors and Actuators*, **19**, Number 3, September 1989, 267 - 287

8) H. C. Nathanson, W. E. Newell, R. A. Wickstrom, and J. R. Davis, Jr., "The Resonant Gate Transistor," IEEE Transactions on Electron Devices, March, 1967.

9) R. T. Howe and R. S. Muller, "Polycrystalline Silicon Micromechanical Beams," *Journal of the Electrochemical Society*: Solid State Science and Technology, June, 1983.

10) K. E. Beam, "Anisotropic Etching of Silicon," *IEEE Transactions on Electron Devices*, October, 1978

11) K. D. Wise, T. N. Jackson, N. A. Masnari, M. B. Robinson, D. E. Solomon, G. H. Wuttke, and W. B. Rensel, "Fabrication of Hemispherical Structures Using Semiconductor Technology for Use in Thermonuclear Fusion Research," *Journal of Vacuum Science Technology*, May/June, 1979.

12) E. W. Becker, H. Betz, W. Ehrfeld, W. Glashauser, A. Heuberger, H. J. Michel, D. Munchmeyer, S. Pongratz, and R.v. Siemens, "Production of Separation Nozzle Systems for Uranium Enrichment by a Combination of X-Ray Lithography and

Galvano-plastics," *Naturwissenschaften*, **69**, (1982), 520 to 523.

13) JP Brody, P Yager, RE Goldstein, and RH Austin "Biotechnology at low Reynolds numbers" *J. Biophys.* **71**, 1996, 3430-3441

14) G.Ehteshami, N. Rana, P.Raghu and F. Shadman, "Interactions of impurities with Silicon and Silicon dioxide during oxidation", Center for Micro-contamination Control, NSF I/U CRC

15) N. L. Abbott, C. B. Gorman, , G. M. Whitesides "Active control of wetting using applied electrical potentials and self-assembled monolayers" *Langmuir* , **11**, Issue 1, January 1995, 16-18

16) Donald Voet, J. Voet " Biochemistry, 2nd edition" Wiley, New York, 916-919

17) Ulman, A. Ultrathin Organic Films from Langmuir Blodgett to Self-Assembly; Academic Press: New York, 1991.

18) Ulman, A., Ed. Characterization of Organic Thin Films; Butterworth-Heinemann: Boston, 1995.

19) Ian Baxter, Lisa D. Cother, Carole Dupuy, Paul D. Lickiss, Andrew J. P. White and David J. Williams, "Hydrogen Bonding to Silanols" Department of Chemistry, Imperial College of Science, Technology and Medicine, London SW7 2AY, UK

20) A.B. Sieval, A.L. Demirel, J.W.M. Nissink, M.R. Linford, J.H. van der Maas, W.H. de Jeu, H. Zuilhof, and E.J.R. Sudhölter. "Highly stable Si-C linked functionalized monolayers on the silicon(100) surface." *Langmuir* 1998, **14**, 1759-1768.

21) A.B. Sieval, H. Zuilhof, E.J.R. Sudhölter, F.M. Schuurmans, and W.C. Sinke." Surface passivation of silicon by organic monolayers." Proceedings of the 2nd World Conference and Exhibition on Photovoltaic Solar Energy Conversion, Vienna, 1998

22) J. D. Andrade, "Surface and Interface Aspects of Biomedical Polymers: Protein Adsorption" Plenum, New York, 1985

23) Th. Wink, S. J. van Zuilen, A. Bult and W. P. van Bennekom, "Self-assembled Monolayers for Biosensors" *Analyst*, April 1997, **122**, 43R-50R

24) N. L. Abbott, D. R. Rolison, G. M. Whitesides "Combining micromachining and molecular self-assembly to fabricate microelectrodes" *Langmuir*, **10**, Issue 8, August 1994, 2672-2682

25) Y.F. Chen, J.M Yang, J.J. Gau, C.M. Ho and Y.C. Tai. "Microfluidic System for Biological Agent Detection" The 3rd International conference on the interaction of Art and Fluid Mechanics, Zurich, Switzerland , 2000.

26) D. Ivnitski, I. Abdel-Hamid, P. Atanasov, E. Wilkins, "Review: Biosensors for Detection of Pathogenic Bacteria", Biosensors & Bioelectronics 14 (1999), 599-624.

27) G. Marrazza, I. Chianella, M. Mascini, "Disposable DNA Electrochemical Biosensors for Environmental Monitoring", Analytica Chimica Acta 387 (1999), 297-307.

28) J. Wang, et. al., "DNA Electrochemical Biosensors for Environmental Monitoring", A Review", Analytica Chimica Acta 347 (1997), 1-8.

29) T.Ruzgas, E. Csöregi, J. Emnéus, L Gorton, G. Marko-Varga, "Peroxidase-modified electrodes: Fundamentals and application", Analytica Chimica Acta 330 (1996), 123-138.

30) Ulman A. "An Introduction to Ultrathin Organic Films From Langmuir-Blodgett to Self-Assembly" Academic Press, Inc: San Diego, CA, 1991

31) Whitesides, G. M.; Laibinis, P. E., *Langmuir* **1990**, *6*, 87.

32) Bain, C. D.; Troughton, E. B.; Tao, Y.T.;Evall, J.; Whitesides, G. M.; Nuzzo, R. G., *J. Am. Chem.* Soc. **1989**, *111*, 321

33) P. Wagner, M. Hegner, H-J Guntherodt, G. Semenza, "Formation and in Situ Modification of Monolayers Chemisorbed on Ultraflat Template-Stripped Gold Surfaces," *Langmuir* **11** (1995) 3867-75.

34) S.A.Darst, M. Ahlers, P.H. Meller, E.W. Kubalek, R. Blankenburg, H.O. Ribi, H. Ringsdorf, R. Kornberg, "Two-Dimensional Crystals of Streptavidin on Biotinylated Lipid Layers," *Biophys J.* **59** (1991) 387-396.

Appendix B.

Enzyme-based electrochemical DNA detector chip using MEMS technology

by

Jen-Jr Gau

2001

ABSTRACT OF THE DISSERTATION

Enzyme-based electrochemical DNA detector chip
using MEMS technology
by

Jen-Jr Gau
Doctor of Philosophy in Biomedical Engineering
University of California, Los Angeles, 2001
Professor Chih-Ming Ho, Chair

We developed a system for amperometric detection of pathogen based on the integration of microelectromechanical systems (MEMS), self-assembled monolayers (SAMs), DNA hybridization, and enzyme amplification. Using MEMS technology, a detector array was fabricated which has multiple electrodes deposited on a Si wafer and was fully reusable. Using SAMs, a monolayer of the protein streptavidin was immobilized on the working electrode (Au) surface to capture rRNA from E. coli. Three different approaches can be used to immobilize streptavidin onto Au, direct adsorption of the protein on bare Au, binding the protein to a biotinylated thiol SAM on Au, and binding the protein to a biotinylated disulfide monolayer on Au. The biotinylated thiol approach yielded the best results. High specificity for E. coli was achieved using ssDNA-rRNA hybridization and high sensitivity was achieved using enzymatic amplification with peroxidase as the catalyst. The analysis protocol can be conducted with solution volumes on the order of a few microliters and completed in 40 minutes. The detection system was capable of detecting single Escherichia coli cell without polymerase chain reaction with high specificity for E. coli vs. the bacteria Bordetella bronchiseptica. The kinetics of SAM formation onto electrode surface is investigated with surface plasmon resonance (SPR) and 80% of the protein deposition can be achieved within four seconds. The quality of the protein

monolayer can be monitored based on topographical information from atomic force microscopy (AFM).

CHAPTER 7 INTRODUCTION

1. Overview

A variety of biosensors, both optical and electrochemical, have been developed for the detection of pathogenic bacteria (Ivnitski, et al., 1999, 2000). While conventional methods for detecting bacteria usually involve a morphological evaluation of the organisms as well as testing their ability to grow, such methods are very time consuming and are not feasible under field conditions. The need for rapid detection as well as portability has led to the development of systems that couple pathogen recognition with signal transduction. Both optical and electrochemical detection of bacteria have been reported, although electrochemical methods have an advantage in that they are more amenable to miniaturization (Ivnitski, et. al., 1999, T. Wang, et. al., 2000). Requirements for an ideal detector include high specificity and high sensitivity using a protocol that can be completed in a relatively short time. Moreover, systems that can be miniaturized and automated offer a significant advantage over current technology, especially if detection is needed in the field.

Microelectromechanical systems (MEMS) technology provides transducers to perform sensing and actuation in various engineering applications. The significance of MEMS technology is that it makes possible mechanical parts of micron size that can be integrated with electronics and batch fabricated in large quantities. MEMS devices are fabricated through the process of micromachining, a batch production process employing lithography. Micromachining relies heavily on the use of lithographic methods to create 3-dimensional structures using pre-designed resist patterns (masks) (Ho and Tai, 1996, 1998). MEMS is an enabling technology for making miniaturized devices, and in this work, we integrate MEMS technology with biosensing methods to detect E. coli bacteria.

One of the most effective means of achieving high specificity is to detect the bacteria's genetic material (e.g. rRNA, mRNA, denatured DNA). By choosing a single-stranded DNA (ssDNA) probe whose sequence is complementary only to the target bacteria's rRNA or ssDNA, monitoring the hybridization event allows selective sensing of target cells. To maximize sensitivity, coupling the hybridization event with an enzymatic reaction leads to signal amplification, as each substrate-to-product turnover contributes to the overall signal. Bioassays to detect DNA hybridization that are amplified by enzymatic reaction can still be completed within a reasonably short time. Finally, the miniaturization and portability inherent in electrochemical probes make them excellent candidates for integration into MEMS devices.

A prototype amperometric detector has been developed for Escherichia coli (E. coli) based on combining several, well-established technologies into one detection system (Chen, et. al., 2000, Gau, et. al., 2000). The technologies of MEMS, self-assembled monolayers (SAMs), DNA hybridization, and enzyme amplification all contribute to the design of a miniaturized, specific, and sensitive E. coli detector. DNA electrochemical probes have been reported previously (Wang, et al., 1997, Marrazza, et al., 1999), with graphite or carbon electrodes typically used. Commercial units for amperometric detection of DNA from E. coli using screen-printed carbon electrodes on disposable test strips are also available. Screen-printing has the advantage of low cost, however, achieving high dimensional precision is not easy. Using lithography, thin films of a wide range of materials, including metals (Au, Ag) and carbon, can be accurately patterned in mm size dimensions. Moreover, utilizing a SAM is an elegant method of selectively immobilizing molecules on MEMS surfaces. The bonding of SAMs to Au, Ag and other metals has been well studied (Revell, et al., 1998, Motesharei, et al., 1998, Xia, et al., 1998, Lahiri, et al., 1999), and proteins and other biomolecules can be easily immobilized onto surfaces such as Au using SAMs (Ostuni, et al., 1999, Kane, et al., 1999, Spinke, et al., 1993, Haussling, et al., 1991). Amperometric methods using SAMs on electrodes have demonstrated the ability to detect target analytes successfully (Sun, et al., 1998, Hou, et al., 1998, Murthy, et al., 1998).

In our E. coli detection system, we take advantage of the benefits inherent in each

technology. Using DNA hybridization and enzyme amplification, we achieve the required specificity and sensitivity. Using MEMS and SAMs, we fabricate a miniaturized system that can be developed into a portable instrument. Finally, we demonstrate that the present detection system is applicable to a broad range of pathogenic bacteria. For example, the detection module and assay protocol can be adapted to detect uropathogenic E. coli and identify microorganisms causing otitis media (middle ear infection).

2. Summary and Objectives of this Work

The main objective of this dissertation entails the incorporation of various state-of-the-art technologies into the design and fabrication of a MEMS-based, DNA microarray chip. This is also the most significant achievement of this work – integrating different disciplines via functionality while maintaining the simplicity and integrity of the entire system. Throughout the whole paper, experimental results will be presented at various checkpoints with gold standard testing methods to validate the performance and the quality of our proprietary MEMS based electrochemical sensor.

Chapter one provides an overview of the various types of gene-based detectors developed by other groups while highlighting the fundamental uniqueness of our work. This chapter outlines the significance of various techniques used in our work while focusing on the integration of each functional component.

Chapter two details the design aspects, fabrication process, experimental methods and results. Optimization of process parameter at each significant step is described. The analytical and characteristic results of this work are illustrated in each relating topic.

Chapter three focuses on the fundamental mechanism of the enzymatic reaction and summarizes the electron transfer pathway. The kinetic aspects of peroxidase reactions are briefly

reviewed, followed by a detail reaction analysis of the Horseradish peroxidase/3,3',5,5'tetramethylbenzidine (HRP/TMB) redox couple. A first order approximation of the sensitivity limitation is derived and shown to match the best sensitivity of our detector. To further improve the sensitivity of our current detector array, efforts should be addressed regarding diffusion-controlled effects.

Chapter four examines the reproducibility and stability of the detector using standard electroanalytical techniques. The aim of the chapter is to develop a further understanding of the error factor and the limitation of this MEMS based electrochemical cell, in an attempt to lay the foundation for the future DNA detector chip design.

Chapter five introduces SPR and AFM for surface kinetic analysis and detector characterization. The motivation for the kinetic study is to verify the quality of the functionalized surface and to evaluate the potential for further improvement.

CHAPTER 8 EXPERIMENTAL DESIGN

1. Fabrication of MEMS based DNA microarray

A layer of silicon dioxide (SiO_2, 1000Å) was deposited on a bare Si wafer (prime grade, p-type <100>, thickness 500-550mm) and served as a pad layer underneath the silicon nitride (Si_3N_4, 1000Å) to release stress and improve adhesion. MEMS microarrays were fabricated with working electrodes of various dimensions etched to form wells up to 350mm depth.

The nitride wafer was patterned and bulk etched using KOH along the [111] and [100] crystal planes, and the depth of the well was controlled by KOH etching time and temperature. The 100mm wide auxiliary and reference electrodes are separated from their corresponding working electrode by 200mm. **Figure 1** shows a schematic of the pattern used in generating the MEMS array.

The nitride and oxide were removed by HF etching to release internal stress, and another oxide layer (5000Å) was deposited for electrical isolation. Electrodes were patterned by PR5214 photo resist reverse imaging and lift-off process with e-beam deposition of Au(2000Å)/Cr(200Å). Finally the wafer was bathed in hexamethyldisilazane (HMDS) vapor for three minutes after ten minutes of a 150°C hot bake to generate a hydrophobic

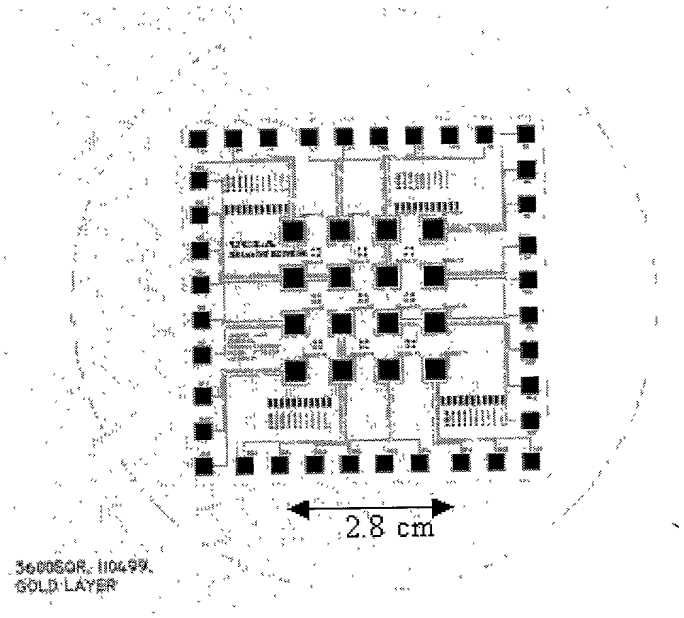

Figure 1. Schematic design of DNA microarray chip

surface on the surrounding Si areas. The hydrophobic nature of the surrounding area, along with the 3-dimensional nature of the working electrode, allows containment of a liquid droplet on the working electrode. This design effectively minimized non-specific binding of biomolecules to other areas of the MEMS array.

2. Deposition of streptavidin SAMs on Au

Three different methods were used to deposit streptavidin monolayers on Au:

1) directly adsorbing streptavidin on bare Au
2) depositing a SAM of a biotinylated thiol, biotin-DAD-C12-SH, and subsequently binding streptavidin
3) depositing a SAM of a biotinylated disulfide, biotin-HPDP, and subsequently binding streptavidin

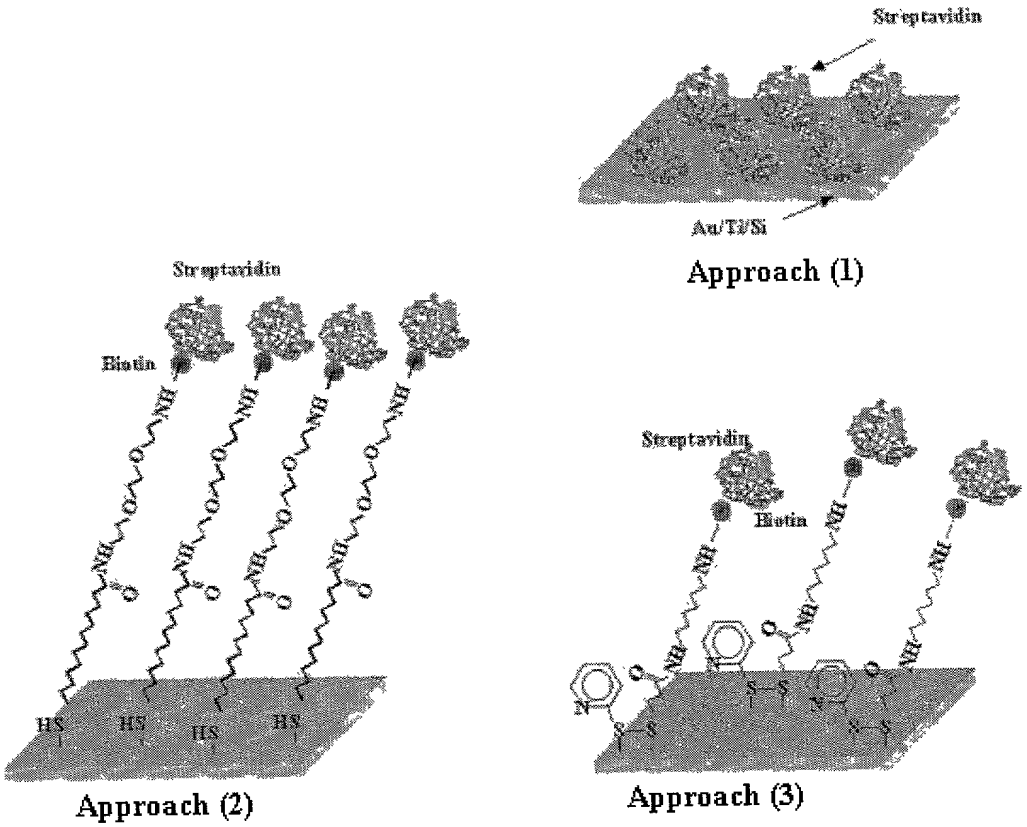

Figure 2. Different approaches for protein deposition

In all cases, the Au surfaces were cleaned with concentrated "Piranha" solution (70 vol% H_2SO_4, 30 vol% H_2O_2) and thoroughly rinsed with deionized water (dH_2O). For depositing streptavidin on bare Au, a solution of 1.0 mg/ml streptavidin (Sigma Chemical Co., S0677) in 0.02M Na phosphate buffer, 0.15M NaCl, pH 7.2, was placed on the surface, allowed to stand for 10 minutes, and rinsed with dH_2O. For depositing a SAM of biotin-DAD-C12-SH (12-mercapto(8-biotinamide-3,6-dioxaoctyl)dodecanamide, Roche GmBH, Germany), the procedure of Spinke, et al. (1993) was used wherein samples were incubated for ~18 hours in a 50mM solution of biotin-DAD-C12-SH in ethanol with $4.5x10^{-4}$M 11-mercapto-1-undecanol (Aldrich Chemical Co., 44,752-8) and rinsed with ethanol and water. The biotin-coated Au surfaces were then exposed to a 1.0 mg/ml streptavidin solution for ~10 minutes and rinsed again with dH_2O. For

depositing a SAM of biotin-HPDP, (N-[6-(biotinamido)hexyl]-3'-(2'-pyridyldithio)propionamide, Pierce Inc., 21341) samples were incubated for ~18 hours in a 50mM biotin-HPDP solution in ethanol (with or without $4.5x10^{-4}$M mercaptopropanol) and rinsed with ethanol and dH_2O. The surfaces were then exposed to a 1.0 mg/ml streptavidin solution for ~10 minutes and rinsed again with dH_2O.

3. Assay protocol for amperometric detection of pathogen

The assay protocol was conducted as follows:

1) 50 ml of lysis reagent (0.4 M NaOH) was added to a 250 ml sample of bacteria in culture media and incubated for 5 min. at room temperature
2) 100 ml of probe solution (anchoring & signaling probes) was then added, and the mixture was incubated for 10 min. at 65°C
3) 5 ml of the lysed E. coli/probe solution mixture was placed on the streptavidin coated working electrode of the MEMS detector array and incubated for 10 min. at room temperature
4) The MEMS DNA detector array was washed with biotin wash solution (Kirkegaard and Perry Laboratories, 50-63-06)
5) 5 ml of Anti-Fl-POD (Anti-fluorescein peroxidase, 150U, Roche Inc., 1 426 346), diluted to 0.75U/ml or 0.15 U/ml with dilutant (PBS/0.5%Casein) was placed on the working electrode and incubated for 10 minutes at room temperature
6) The MEMS array chip was washed again with wash solution
7) 10 ml of K-blue substrate (Neogen Corp., 300176) was placed on the detector array in such a way that all three electrodes (working, auxiliary, reference) were covered by the substrate solution
8) Electrochemical measurements were immediately taken.

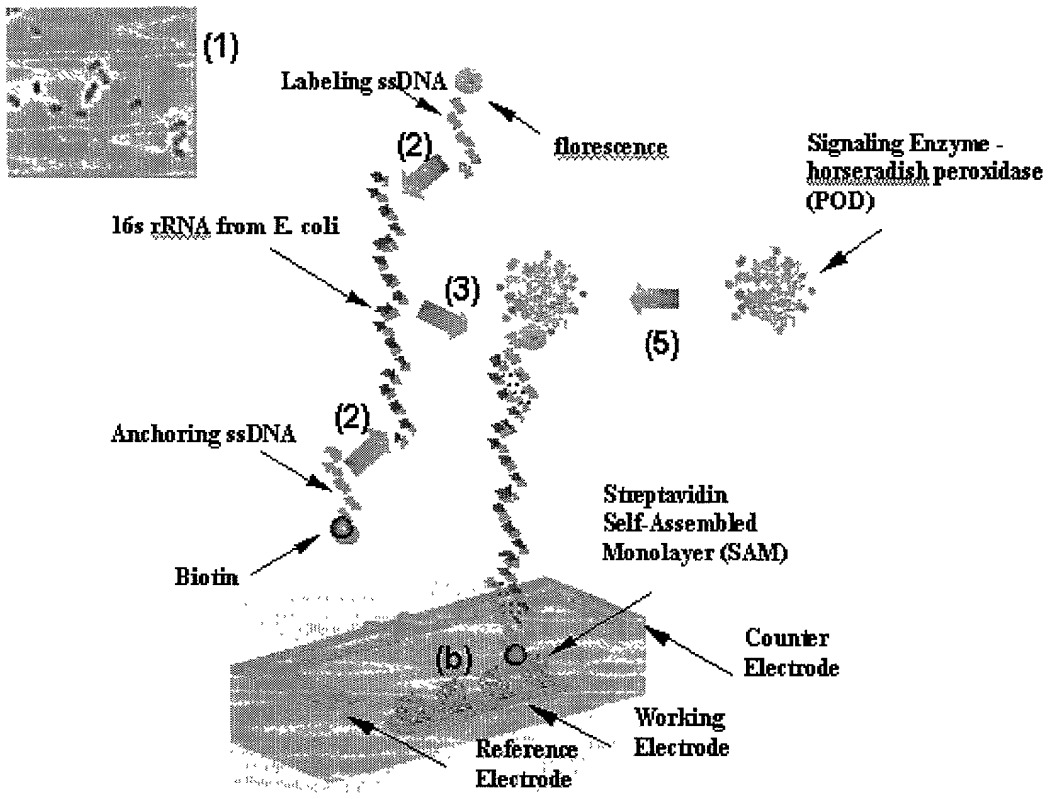

Figure 3. Sensor and protocol process flow (1) lysis (2) hybridization (3) immobilization (4) washing (5) POD loading

The entire protocol was completed within 40 minutes. Amperometric current vs. time was measured using a CH Instruments 660A Electrochemical Workstation with a picoamp booster and faraday cage. Samples on the MEMS detector array were measured sequentially. The voltage was fixed at –0.1V (vs. reference), and a cathodic current (amperometric signal) reading was taken at 20 seconds. At 20 seconds, current values had reached steady-state. Cell concentration (cell number) was determined using serial dilutions and culture plate counting.

4. Materials for Electrochemical Electrodes

Standard electrodes are used in conventional electrochemical experiments to provide an accurate and precise reference potential though a half-cell composed of an analyte/electrode interface.

The commercial standard reference/counter electrode is about the size of a pen; therefore the reaction is often conducted in a one-liter beaker. Stirring is generally required in all cases to eliminate diffusion controlled effect.

Typical material combination for reference/counter complex is Ag/AgCl. Screen-printed sensors were reported using AgCl paste and Ag wire onto a plastic board or silicon wafer. Screen-printing is not a MEMS compatible process and its resolution is limited by the size of the screen matrix.

Several conducting materials, available in MEMS technology, were patterned on a silicon substrate by the lift-off process, and the characteristic of the three-electrode system were tested by cyclic voltammetry with ferrocene solution. Different combinations between gold, platinum, titanium and aluminum were tested and the Au/Au/Au, three-electrode system gave the best C-V curve and redox characteristics. Different shapes and areas were also tested to achieve the optimum design.

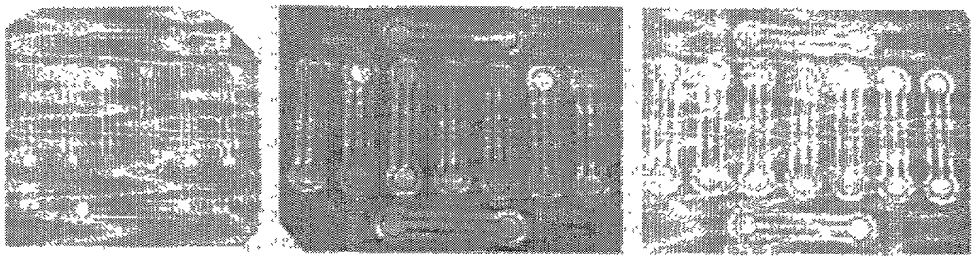

Figure 4. Different electrode material on silicon substrate

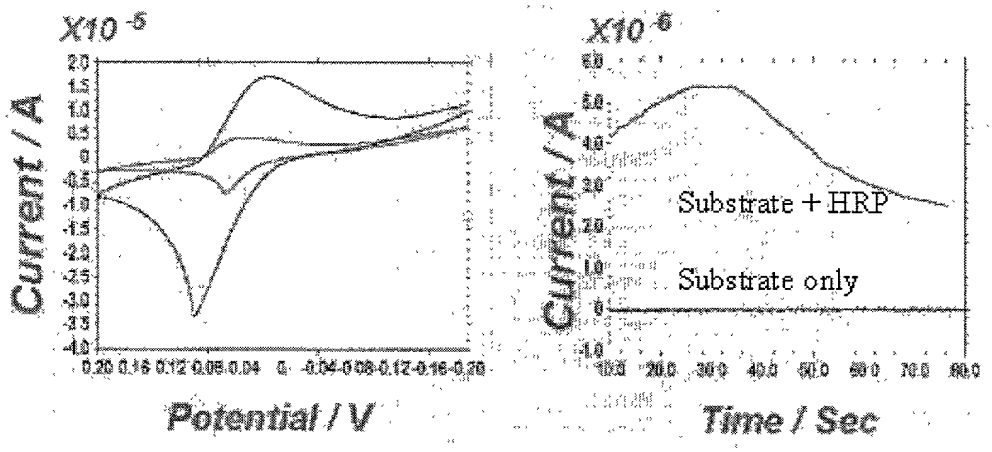

Figure 5. C-V characteristics of sensor electrodes and enzyme response

5. On-Chip Reaction Well for Reagent Confinement

The design concept of having a reaction well on the silicon substrate was taken from the observation of the high level noise from the non-specific binding of HRP onto the periphery region of the working electrode. To verify that noise does come from the HRP residual at the surface, a simple test was done to estimate the contribution of this unwanted binding. HRP were introduced to a bare silicon chip, followed with several wash steps before the addition of the substrate solution. A very high level of enzymatic reaction was observed immediately after addition of the substrate solution.

As expected, HRP, like other proteins, sticks to the silicon surface easily and tightly. Several commercial wash solutions and blocking protein were tested without any significant improvement of reducing non-specific binding. The best way to reduce undesirable binding is to prevent it from happening. The area outside the working electrode need not encounter the HRP

solution, however, it is almost always a tradition to immerse all three electrodes in the aqueous system during the protocol.

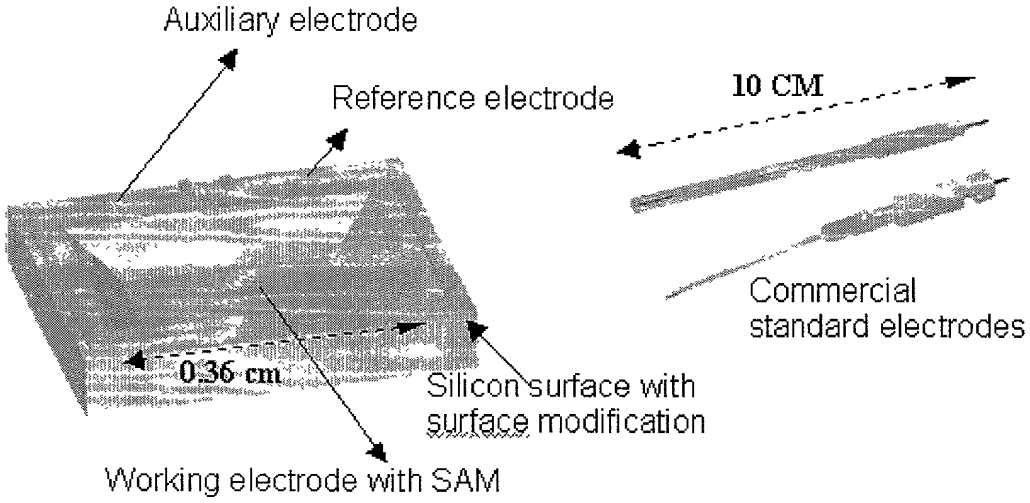

Figure 6. Comparison between microfabricated and commercial electrodes

The simplest way to confine certain reagents within a well-defined space is to build a well. As shown in **Figure 6**, a microfabricated well is bordered by (111) silicon planes after KOH etching. The working electrode, defined by the lift-off process, covers the entire well surface.

6. Surface Modification for Noise Reduction

Surface technology and material science

The importance of material science cannot be underestimated when designing a DNA chip. An unacceptable amount of non-specific binding still occurs during the washing process

while the diluted reagent is flowing around the wafer surface. The time for the wash solution, containing HRP, to stay on the periphery region is much longer than the binding time constant. Besides fabricating the well structure, the surface of the periphery area must be protected by another mechanism.

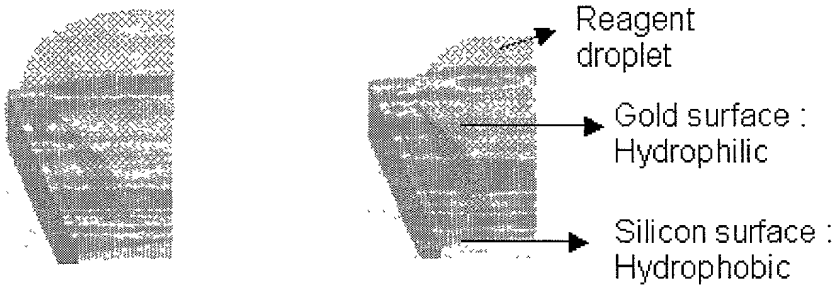

Figure 7. Reagent Confinement with Reaction Well

The most efficient way to keep the surface from contacting reagents is to make it hydrophobic. Silanation of the silicon surface is widely used to prevent suspended structure sticking to the substrate by surface tension. In our case, it was used to prevent the direct contact of biomolecules to the periphery area of silicon substrate.

Silanation

Silane-based molecules with various functional terminal groups have been used to modify surface properties of silicon wafers, silicon nitride chips, and the scanning probe microscopy (SPM) tips. Silane compounds, from the surface modification, form robust self-assembled monolayers (SAMs), which chemically tether from the silicon oxide surfaces. This behavior is a result of hydrolysis of the terminal Si(Cl)n or $SiO\text{-}C_2H_5$ groups.

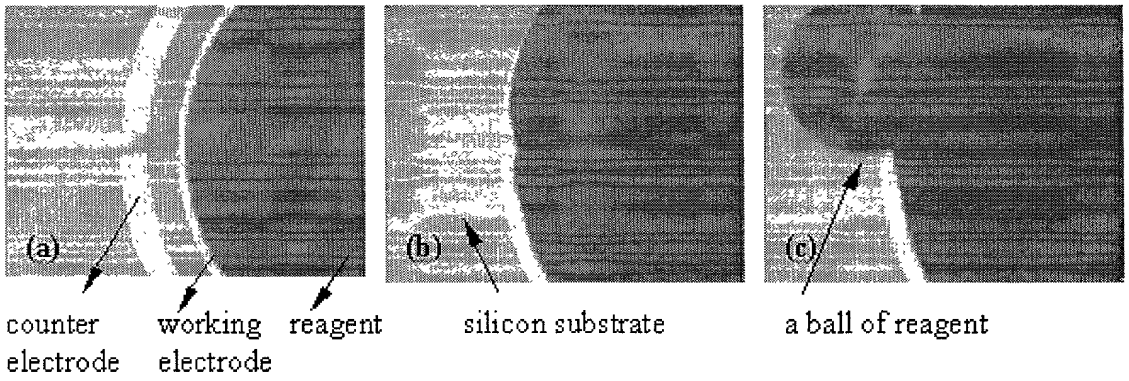

Figure 8. Reagent Confinement by Surface Treatment

(a) The reagent is shaped by the hydrophilic working electrode and a droplet is nicely formed over the Au surface (b) By increasing the volume of the reagent, the area covered by the reagent will gradually expand and cover the remaining two electrodes (c) stream of reagent is dispensed by a pipetteman, and a ball of reagent is formed instead of spreading over the hydrophobic silicon substrate

7. Results

Micro electromechanical system (MEMS)

Figure 9 shows a photograph of the MEMS detector array. Sixteen working electrodes with their corresponding auxiliary and reference electrodes were patterned in a 2.8 cm x 2.8 cm area. The detector array was fully reusable as the surface can be cleaned using the Piranha solution. We have reused the same MEMS detector array multiple times by appropriately cleaning the surface and redepositing the SAMs on the working electrode.

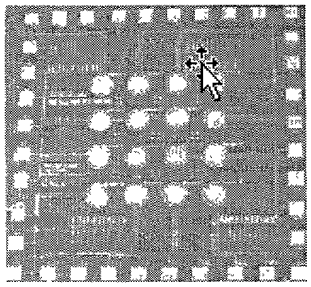

4 × 4 DNA sensor array

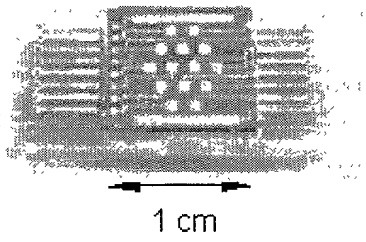

Micro sensor array (×14) chip

Figure 9. Different types of DNA microarray detector chip

Detection of pathogen

For the amperometric detection of E. coli rRNA, we first compared the performance of the three different streptavidin monolayer surfaces. Streptavidin was immobilized on the Au using the three different approaches previously described, and the assay protocol was conducted for the bacteria E. coli and Bordetella bronchiseptica (Bordetella). Since the ssDNA probes are specific for E. coli, the Bordetella bacteria served as the negative control sample. The purpose of this experiment was to compare the efficiancy of the immobilized streptavidin to capture the biotin-rRNA-POD hybrid. Two concentrations of E. coli were used, with one sample having ten times the concentration of the other. Moreover, the signal from the negative control (Bordetella) indicates the level of non-specific binding or the achievable "baseline".

Since the same bacterial solutions (E. coli or Bordetella) were used, a direct comparison can be made of the different surfaces. The result shows that streptavidin immobilized via the biotinylated thiol to Au was the best condition for E. coli detection. Using the biotin-thiol SAM, we obtained good signals for the E. coli while achieving a low baseline signal from the

Bordetella. For streptavidin immobilized via the biotin-disulfide to Au, current signals for the E. coli (both concentrations) were significantly lower, while the baseline was the same as that for the biotin-thiol/streptavidin. In the case of streptavidin directly adsorbed to Au, the signal from the Bordetella was much higher, indicating a higher level of non-specific binding of POD to the surface.

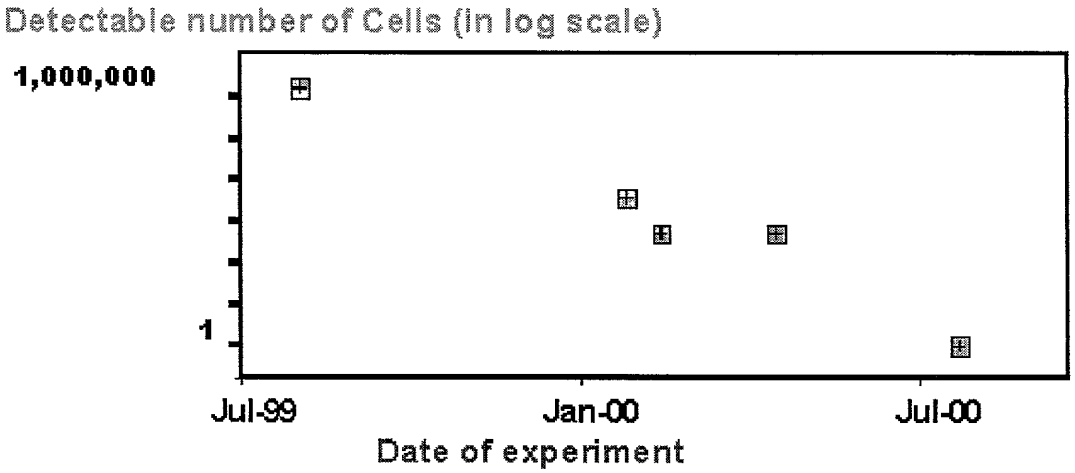

Figure 10. Sensitivity evolution of DNA detector microarray

After ascertaining Au/biotin-SH/streptavidin to be the optimal streptavidin surface, we repeated the protocol using E. coli and Bordetella to determine the sensitivity of our system. We immobilized streptavidin via the biotin-SH SAM and performed the assay on a series of E. coli dilutions along with Bordetella as the negative control. The improvement of the sensitivity over time is shown in **Figure 10**. The data indicate that as few as single E. coli cells can be detected using our MEMS system. As expected, the current signal increased as a function of increasing number of E. coli cells in the sample solution. Moreover, by lowering the POD concentration used in the assay protocol (from 0.75 U/ml to 0.15 U/ml), we achieved better discrimination in signals at lower E. coli cell numbers. As seen in **Fig. 11**, the current signal for 0.4 atto (1E-18) mole was four times more than twice that for 2.0×10^6 Bordetella cells. The results using our MEMS system confirm that E. coli bacteria was successfully detected using amperometry and SAMs to capture the bacteria rRNA.

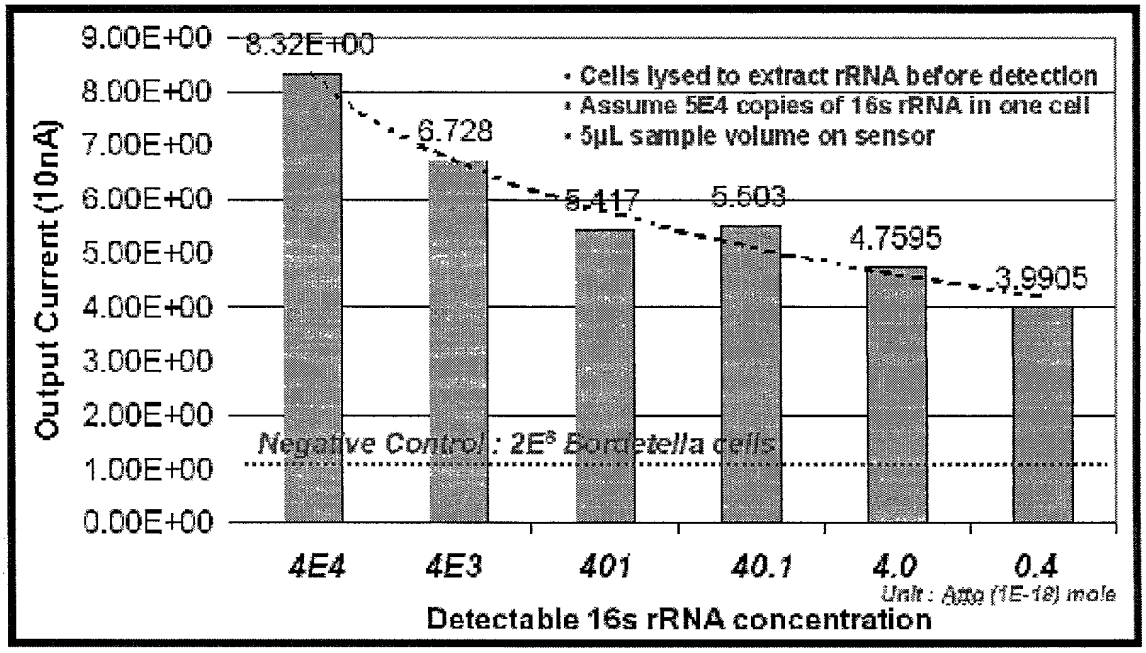

Figure 11. Sensitivity check of E.coli over Bordetella cells through 16s rRNA

E. coli Detection Using DNA Hybridization

In our MEMS system, E. coli detection is based on DNA hybridization followed by enzymatic reaction. A schematic illustrating the electrode surface is shown in **Figure 12**. A streptavidin monolayer is immobilized on the Au working electrode surface to capture the rRNA from E. coli. Two ssDNA segments are used in this system. The capture ssDNA, which is conjugated to biotin for streptavidin binding, hybridizes to one end of the E. coli rRNA. The detector ssDNA, which is conjugated to fluorescein for binding to anti-fluorescein linked to the enzyme peroxidase (POD), hybridizes to the other end of the E. coli rRNA. The capture and detector ssDNA recognize two distinct conservative sequences, and therefore, the hybrid forms only with the specific gene segment from E. coli. The oligonucleic hybrid is immobilized through biotin-streptavidin binding onto the Au, working electrode and unbound components are washed away.

Streptavidin binds biotin with unusually high affinity (Kd ~10^{-15}M) (Weber, et. al., 1989). After loading the POD onto the hybrid (through Anti-fluorescein binding), substrate is added and the enzymatic reaction is detected amperometrically. The substrate solution contains both the substrate H_2O_2 and a mediator, 3,3',5,5'tetramethylbenzidine (TMB).

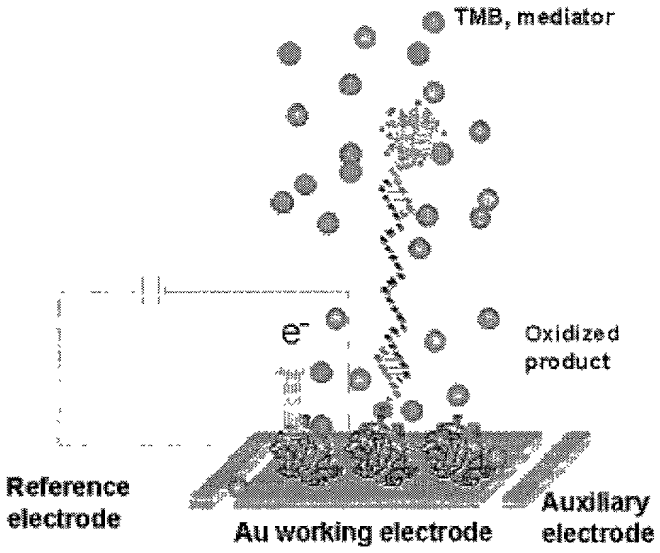

Figure 12. A schematic illustrating the electrode surface

CHAPTER 9 ENZYMATIC REACTION MECHANISMS

1. Introduction

The enzymatic reaction plays a significant role in our detection scheme. In order to derive the correlation between the target molecule and the current readout, the detailed reaction mechanism is described in this chapter. Enzymes have the capability of accelerating chemical reaction toward equilibrium and hence are extraordinarily efficient and selective biological catalysts. A catalyst is a substance that typically accelerates the rate of a chemical reaction while

remaining unharmed in the process. Most enzymes are highly specific to their substrate and consequently have been referred to as having a "lock and key" relationship. They tend to accelerate one or a group of related reactions. Enzyme-catalyzed reactions are stereoselective and stereospecific and these characteristics have resulted in their frequent use in analytical applications. Enzymes are widely used for molecular recognition in biosensors due to their highly specific nature and catalytic behavior. They act as a "capturer" as well as a "reporter".

Several thousand enzymes have been isolated from mammals, fungi, bacteria and plants, and hundreds are commercially available. Enzymes are classified by the reactions they catalyze and peroxidases (or oxidoreductase enzymes) are frequently used for electrochemical electrodes. Peroxidases catalyze the oxidation and reduction of the enzyme substrate. In controlled experiments, the charge transfer event can be quantitatively measured at the working electrode.

2. Peroxidase

Peroxidases (PODs) are important enzymatic tools in analytical biochemistry. They are widely used to construct biosensors (Ruzgas et al., 1996) and are also commonly used in enzyme-linked immunoassays (ELISA) and biological isolation techniques (Blake and Gould, 1984). Peroxidases' wide spectrum of activity and functionality in biochemistry and physiological pathways has lead to fundamental research, which has advanced our understanding of their molecular structure, functionality and reaction mechanisms. Peroxidases catalyze the oxidation of various electron donor substrates (e.g. phenols and aromatic amines) with hydrogen peroxide (H_2O_2) (Dunford et al., 1991). The core technology of our electrochemical sensor for DNA identification is based on the electron transfer of a redox reaction catalyzed by a peroxidase. Consequently, the nature of peroxidases is fully studied in this work.

3. Electrochemical Reaction of Horseradish Peroxidase (HRP)

Horseradish peroxidase (HRP, EC 1.11.1.7) is the most studied member of the heme-containing superfamily of plant peroxidases. Its commercial availability, high purity and low cost make it a versatile enzyme for sensing applications. HRP is a relatively small ferric enzyme derived from the root of the horseradish. It has been used extensively for biological detections and life science researches such as ELISA assay and blotting. When used with a variety of substrates, HRP's high turnover number (high catalytic activity) leads to the generation of large signals from the production of colored products in the presence of hydrogen peroxide. For this reason it is commonly analyzed using optical detection schemes.

HRP uses H_2O_2 as the electron acceptor to catalyze a number of oxidative reactions. Our approach differs from that of optical detection in that, the mediated electron transfer is electrochemically detected instead of monitored by the change of absorbance at a certain frequency (655nm, or 450nm upon acid stop) of the product. The enzymatic reaction can be looped either by direct electron transfer or mediated electron transfer. The direct electron transfer involves the physical contact of the acting site with the electrode potential. In general, the redox center of the enzyme is usually buried in the thick protein shell, and hence the direct electron transfer between the enzyme and a common electrode is very slow. Orientation and accessibility are major limiting factors in its practical application. The mediated electron transfer has a much faster reaction since it utilizes free moving mediators for the electron transfer. These mediators are typically small molecules that can directly access the redox center of the enzyme, and can then diffuse to the electrode surface where charge transfer occurs.

Mediated Electron Transfer

The generalized reaction of peroxidases is an irreversible ping-pong mechanism that can be described by three sequential steps:

$$Fe^{III}(porphyrin) + H_2O_2 \xrightarrow{k_1} Fe^{IV} = O^{-II}(porphyrin)^{\bullet+} + H_2O \qquad (1)$$

$$Fe^{IV}=O^{-II}(porphyrin)^{\bullet+}+AH_2 \xrightarrow{k_2} Fe^{IV}=O^{-II}(porphyrin)H^{+}+AH^{\bullet} \quad (2)$$

$$Fe^{IV}=O^{-II}(porphyrin)H^{+}+AH_2 \xrightarrow{k_3} Fe^{III}(porphyrin)+AH^{\bullet}+H_2O \quad (3)$$

In this mechanism, the resting state ferric enzyme $Fe^{III}(porphyrin)$ (the original form of HRP) is oxidized by one equivalent of H_2O_2 to give an active intermediate (compound I), where the iron is oxidized to a ferryl ($Fe^{IV}=O^{-II}$) species. Compound I is an orphyrin-cation radical containing Fe^{IV}, with one oxidizing equivalent ($\bullet^{+}$) stored as an organic radical. This is a two-electron oxidation/reduction reaction where H_2O_2 is reduced to water and the enzyme is oxidized. One oxidizing equivalent resides on iron, giving rise to the oxyferryl ($Fe^{IV}=O$) intermediate.

Figure 13. Oxidation of the heme group in HRP to compound I. (The heme is represented as a square of nitrogens)

The oxidized form of HRP is reduced back to its native form in two steps. In each step, one organic mediator (AH_2) is oxidized. In our protocol, TMB (3,3',5,5' tetramethylbenzidine – $C_{16}H_{20}N_2$) is used as the organic substrate to compound I. First, compound I accepts a TMB molecule into its active site and carries out its oxidation. In the process, a free radical ($AH^{\bullet}$) is produced and released into solution. Compound I then undergoes an one-electron oxidation reaction with one molecule of TMB yielding compound II, which contains an oxyferryl center coordinated to a normal (dianionic) porphyrin ligand. Compound II is finally reduced back to its native ferric state with concomitant one-electron substrate oxidation. The mediator (AH_2) is

oxidized to a free radical product ($AH^{\bullet}$). The overall charge on the resting state of compound I is +1, while compound II is neutral.

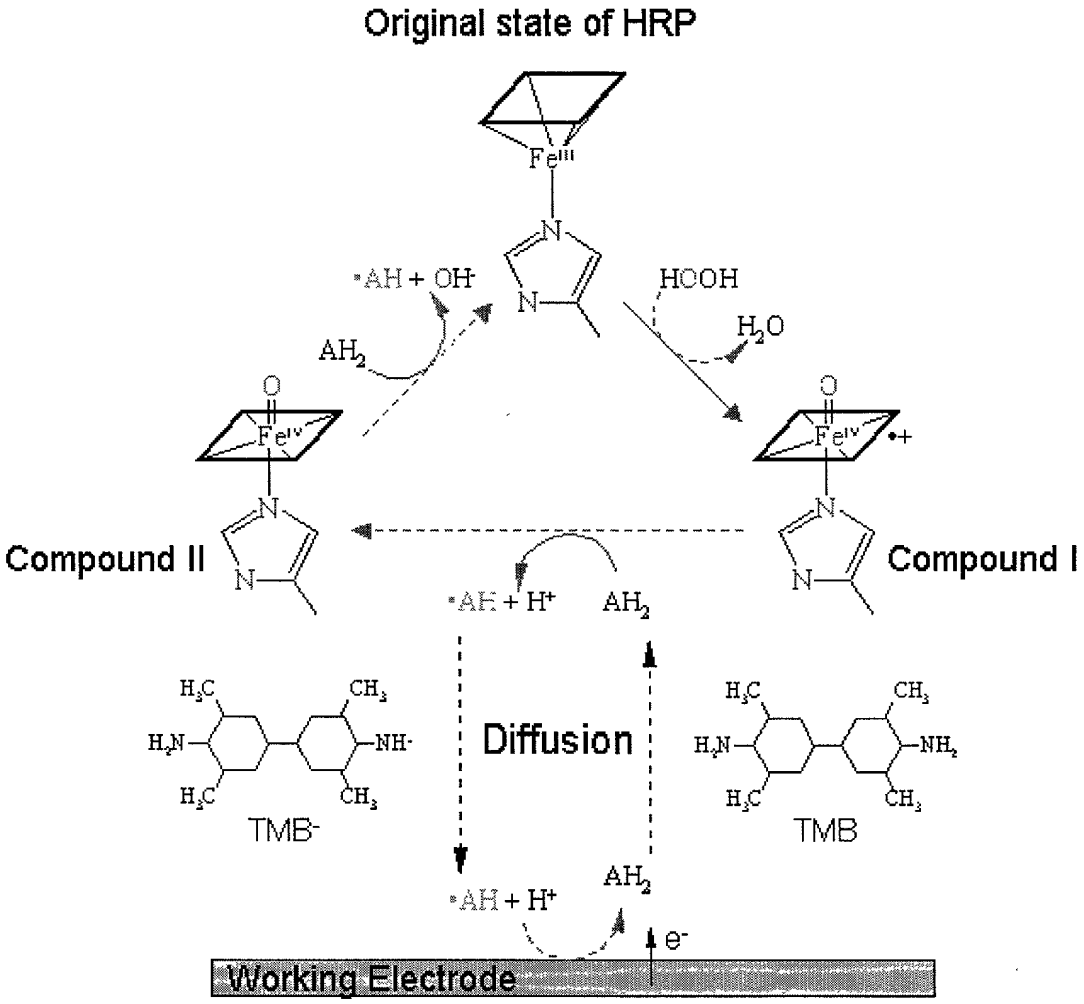

Figure 14. Schematic drawing of HRP enzymatic reaction with TMB

The entire reaction will be limited by the depletion of the mediator (TMB), unless the free radical product ($AH^{\bullet}$) can be reduced to its original form. The free radicals ($AH^{\bullet}$), formed during the reaction, can be transferred into its non-radical form in various ways. Our approach is to bias the electrode at a certain potential which actively drives the reduction of the free radical. The HRP takes electrons from the electron donor (TMB), and the oxidized mediator is

electrochemically reduced back to its initial form. The mediated electron transfer can be observed at the working electrode through the measurement of current (electrons). In order to measure the flow of current in an efficient manner, the diffusion distance of the TMB must be reduced. This is achieved by anchoring the HRP close to the working electrode. The distance between the HRP and the working electrode in our protocol is about 320Å.

When both H_2O_2 and an electron donor (TMB) are present at a peroxidase electrode, direct electron transfer coexists with the mediated enzymatic reaction. The oxidized formed TMB ($AH^{\bullet}$) is rapidly reduced at the biased electrode according to the following reaction:

$$AH^{\bullet} + e^{-} + H^{+} \xrightarrow{k_{s,m}} AH_2 \qquad (4)$$

The reaction from equations (1) and (4) is known as mediated electron transfer, which is usually more efficient than direct electron transfer (Ruzgas et al., 1995; Lindgren et al., 1998).

When using TMB as a substrate for HRP, the sensitivity is high compared to other mediators. Additionally, the product of the TMB reaction is stable, insoluble and is superior to others for the application of precipitation.

Direct Electron Transfer

Reversible redox transformations of peroxidases at an electrode can be used to drive enzyme-catalyzed reactions for analytical purposes. Electrical contact of peroxidases with electrode surfaces is a critical process in the design of enzyme electrodes for bioelectronics and biosensor application utilizing direct electron transfer of peroxidase. Achieving direct electron exchange between electrodes and enzymes simplifies the enzymatic reaction by eliminating the need for a chemical mediator. The major obstacles of direct electron transfer are the extended three-dimensional structure and the inaccessibility of the electro-active center. On the other hand, electron transfer reactions provide an alternative means by which the oxidized form of HRP can

return to its rest state without the need of a mediator. Compound I and II are the oxidized intermediates of peroxidase. AH_2 and $AH^{\bullet}$ are the electron donor substrate and the radical product of its one-electron oxidation, respectively. When peroxidases are immobilized on a working electrode, the direct electron transfer reaction is commonly described as the peroxidase reaction cycle, in which the electron donor (AH_2) is created when the acceptor ($AH^{\bullet}$) gains an electron in the charge transfer reaction. (Ghindilis et al., 1997; Gorton et al., 1999)

Peroxidase is oxidized by hydrogen peroxide according to reaction equation (1), and then subsequently reduced by electrons provided by the electrode as shown in reaction equation (5):

$$Fe^{IV}=O^{-II}(porphyrin)^{\bullet+}+2e^{-}+2H^{+}\xrightarrow{k_s}Fe^{III}(porphyrin)+H_2O \qquad (5)$$

Consequently, after hybridization and immobilization, HRP should be tethered to the sensor surface at a relative close distance but not in contact with the working electrode. If the oxidized form of HRP is in contact with the working electrode (by non-specific binding) direct electron transfer will occur. This effect contributes to the overall electron signal (current measurement) and can make quantitative analysis difficult.

4. First Order Approximation of Sensitivity Limitation

In this section, a first order approximation of the sensor sensitivity is derived. The detailed mechanism is discussed in the following sections. After understanding the working mechanism of the detection protocol, we focus on systematically addressing how the limiting factors in our protocol relate to sensor sensitivity. Our ultimate goal is to determine the physical limitation of our system. A number of the key parameters will be compared with those published in literature to verify the accuracy of this calculation.

Noise level

Two leakage currents are major noise sources for this DNA sensor chip design. One is the Johnson noise from the silicon substrate and the other is the baseline current from the substrate solution. A series of characterization experiments, conducted by Shannon Huang, using different electrochemical sensor chips conclude that the average Johnson noise level is 6.49 nA and the baseline current from the substrate solution is 32.9 nA. If we set the noise level to be the sum of these two currents then we assume the noise to be 40 nA. This is a very conservative assumption since the non-Faradic, background current (due to the substrate solution) can be dramatically reduced by the self-assembly monolayer modification and optimization of the physical properties of the solution.

Assumption number one : Noise level is fixed at 40 nA

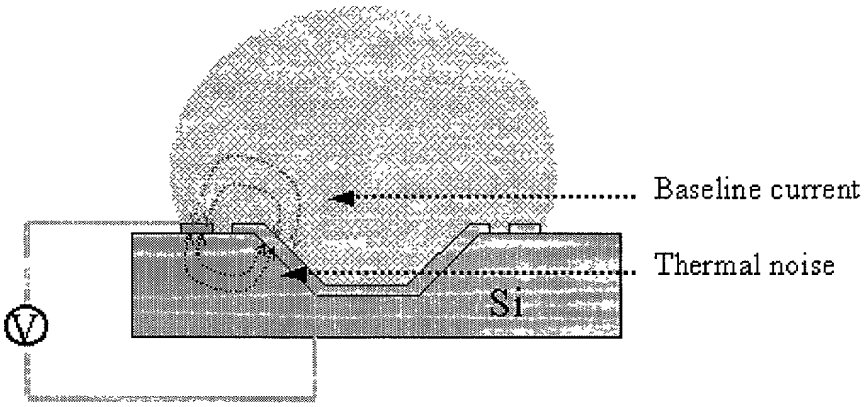

Figure 15. Sources of background noise: thermal noise through Si substrate and leakage current through electrolyte

Signal limit

The signal current must be higher than the noise level in order to be distinguishable. Consequently, the minimum signal current must be 50 nA. Assuming each target

macromolecule can be captured and immobilized onto the sensor surface without loss, the output current would be determined by HRP's turnover number, which is dominated by diffusion control of TMB.

Assumption number two : Hybridization efficiency is 100%

The reaction rate constants of the enzymatic reaction are extremely fast compared to mass diffusion, so k_1, k_2 and $k_3 >> k_s$. The turnover number is ultimately determined by the time it takes for the oxidized form of TMB to diffuse from the electroactive site of the HRP to the working electrode.

Use Einstein's formula for the diffusion coefficient of a substance, in terms of the radius of the diffusing particles or molecules and other known parameters:

$$D = \frac{RT}{6\pi N v r} \qquad (6)$$

R = gas constant (8 in SI units)

T = absolute temperature (300 K for room temperature)

$\pi = 3.14159$

N = number of molecules in a mole (6×10^{23})

v = viscosity of the solvent (0.001 for water in SI units)

r = radius of the particle or molecule (in meter)

The diffusion coefficient is inversely proportional to the radius of a particle, or the cube root of the volume. Thus, if the mass of one spherical particle is 8 fold greater than another, its diffusion coefficient is only 2 fold smaller. The molecular weight of TMB is about 240; and if we assume it is spherical with a radius of 1 Å, by substitution of these values into equation (6), the diffusion coefficient (D) is calculated as $2.12\text{x}10^{-9}$ m^2/sec.

Now if we examine the structure of the hybrid that the HRP is loaded onto, the distance from HRP to the sensor surface is about 322 Å. It would take TMB $9.66x10^{-6}$ second to get to the surface, therefore the turnover number is $1.04x10^{5}$. This means that each hybrid immobilized onto the sensor will generate $10.4x10^{4}$ electrons per second.

Each hybrid can contribute $10.4x10^{4}$ electrons per second, which is equal to $1.66x10^{-14}$ amperes (C/sec). In order to reach the minimum current limit of 50nA, 3.02E6 hybrids are needed. Consequently, the sensitivity is $3.02x10^{-6}$ molecules or 5 atto mole. The minimum detectable number of molecules derived from this approximation matches the latest sensitivity check results in this research.

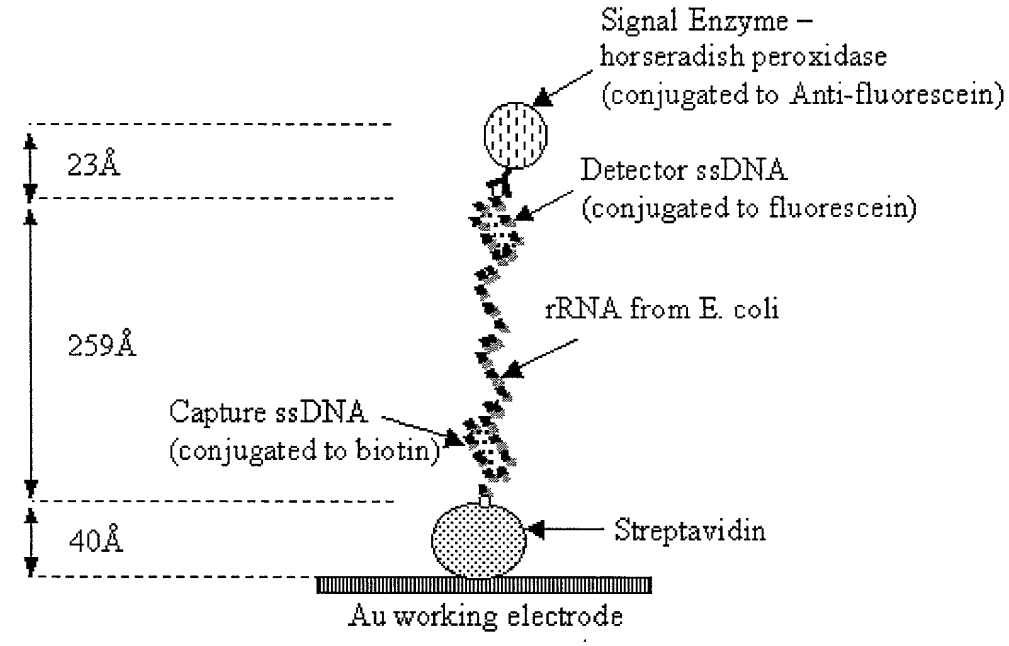

Figure 16. Distance between HRP and electrode is the dimension of the hybrid

5. Diffusion constant derivation

To investigate the diffusion-limited effect, it is first necessary to measure the diffusion constant. Here, we use chronoamperometry and the Cottrell equation to measure the diffusion constant of $K_3Fe(CN)_6$. We then can calculate the diffusion constant of the oxidized form of TMB.

In this plot, the x-axis is $1/\sqrt{t}$, so the equation for the slope can be derived from (17) and expressed as:

$$Solpe = nFAC\left(\frac{D}{\pi}\right)^{1/2} \qquad (7)$$

Where, slope = $7.99E^{-6} = 1 \times 96{,}485 \times 0.0706 \times 2E^{-6} \times (\boldsymbol{D} / 3.14159)^{1/2}$.

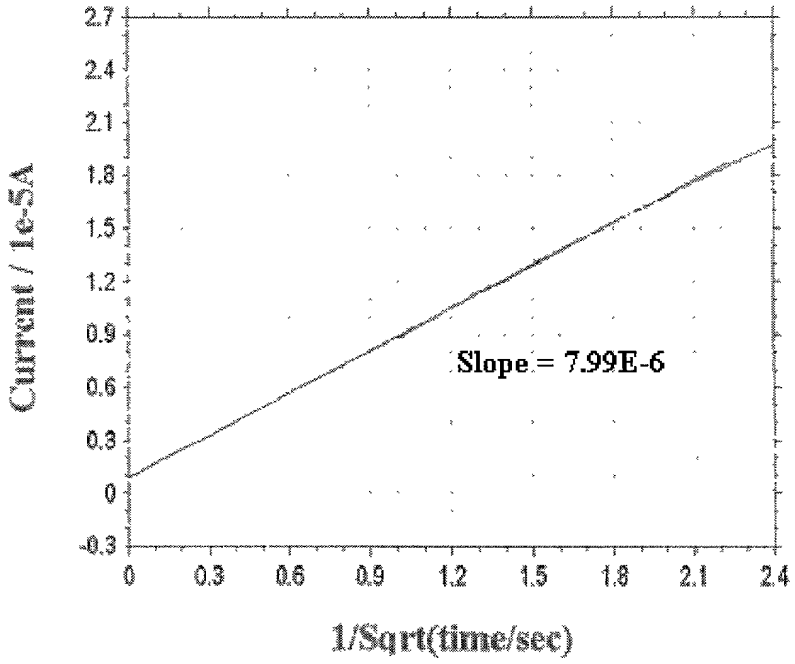

Figure 17. Cottrel plot of $K_3Fe(CN)_6$ using DNA detector chip

With a sensor area = 0.15 cm × 0.15 cm ×π , $[K_3Fe(CN)_6]$ = 2mM = $2E^{-6}$ mole/cm^3 ,we can get solve (7) for the diffusion constant: D = **$1.08E^{-6}$** cm^2 sec. for potassium ferricyanide.

This is very close to the published value of $0.98E^{-5}$ cm^2/sec. (E.L. Cussler 1997). We can thus conclude that the electrochemical DNA detector is accurate enough to conduct analytical measurement. We can also use the microarray chip to measure the diffusion constant of TMB.

It is a somewhat complicated when using TMB, since it is the oxidized form of TMB that reacts with the biased electrode and diffuses away from the electrode to react with compounds I & II. In order to make certain most species in the solution are the oxidized form of TMB, an excess amount of HRP is added into the bulk TMB/H_2O_2 solution and allowed to sit overnight. This provides sufficient time for the peroxidase and peroxide to oxidize all the TMB. We can then take the Cottrel plot on the oxidized TMB solution.

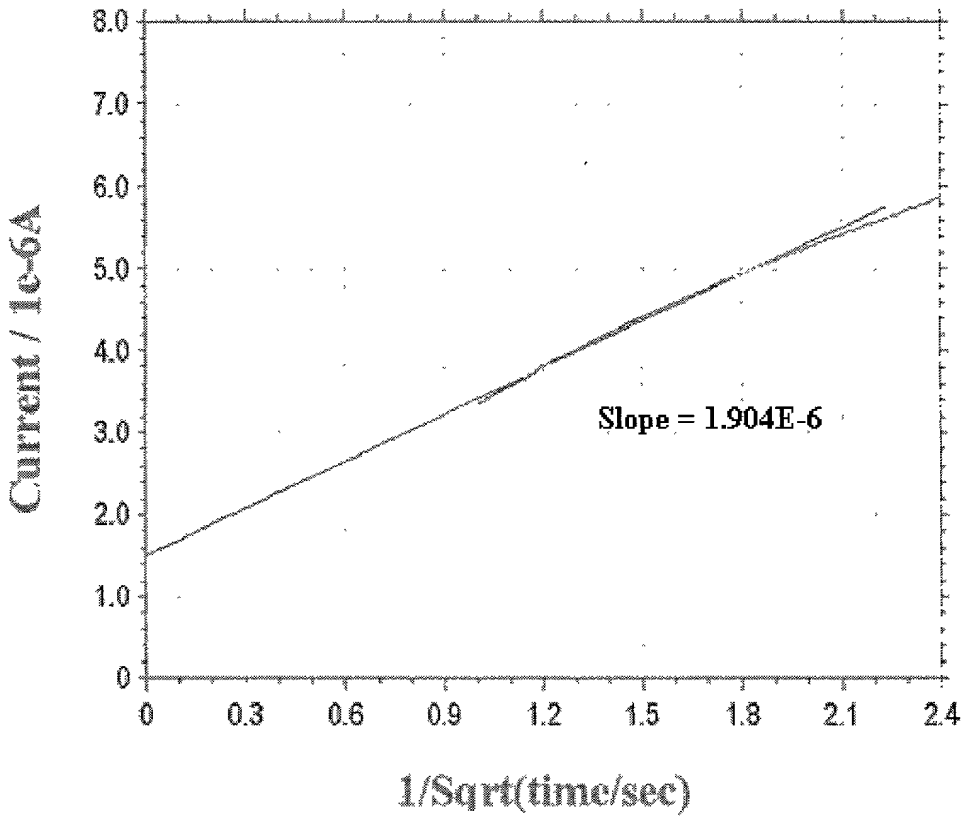

Figure 18. Cottrel plot of oxidized TMB using DNA detector chip

By substituting the slope into equation (7) with [TMB] = 200uM, we get the diffusion constant of TMB_{ox} to be $6.7E^{-6}$ cm^2/sec, which is slightly less than our assumption in chapter three. This technique, however, can be crosschecked with other electroanalytical methods.

6. Diffusion model with optimizing geometrical design

The geometrical design of the working electrode used in this work is a typical planar cell. The simplicity of the design would help the characterization of the detector but would not benefit the sensitivity. Applications of the lithography technology to the construction of microelectrodes for amperometric detection have resulted in the production of uniform electrode array at micro-scale, expanding new horizons for electrochemical sensing. Although reducing the electrode size would decrease the measured current, it also results in an increased signal to noise ratio due to the phenomena of nonlinear diffusion which is the dominant mode of mass transport to the microelectrode. The current is proportional to the concentration of the analyte in the solution, as described in the Cottrell equation, with the addition of a correction term due to the nonlinear diffusion, after Bard and Faulkner (Brad et al., 1980):

$$i = nFADC\left[\frac{1}{\sqrt{\pi Dt}} + \frac{1}{r}\right] \qquad (8)$$

where, n = number of electrons appearing in half-reaction for the redox couple

F = Faraday's constant (96,485 C/mol)

A = electrode area (cm^2)

D = analyte's diffusion coefficient (cm^2/sec.)

C = concentration of analyte (mole/L)

$\pi = 3.14159$

t = time the current was measured (sec.)

r = radius of circular working electrode (cm)

The first term is proportional to the electrode surface area and decays to zero at time $\rightarrow \infty$, whereas the second term is inverse proportional to the electrode radius and represents a steady state current due to a constant flux of material to the surface. As the radius is decreased and the

ratio of the second term to the first becomes larger, resulting in a decreased current magnitude with an increased signal to noise ratio.

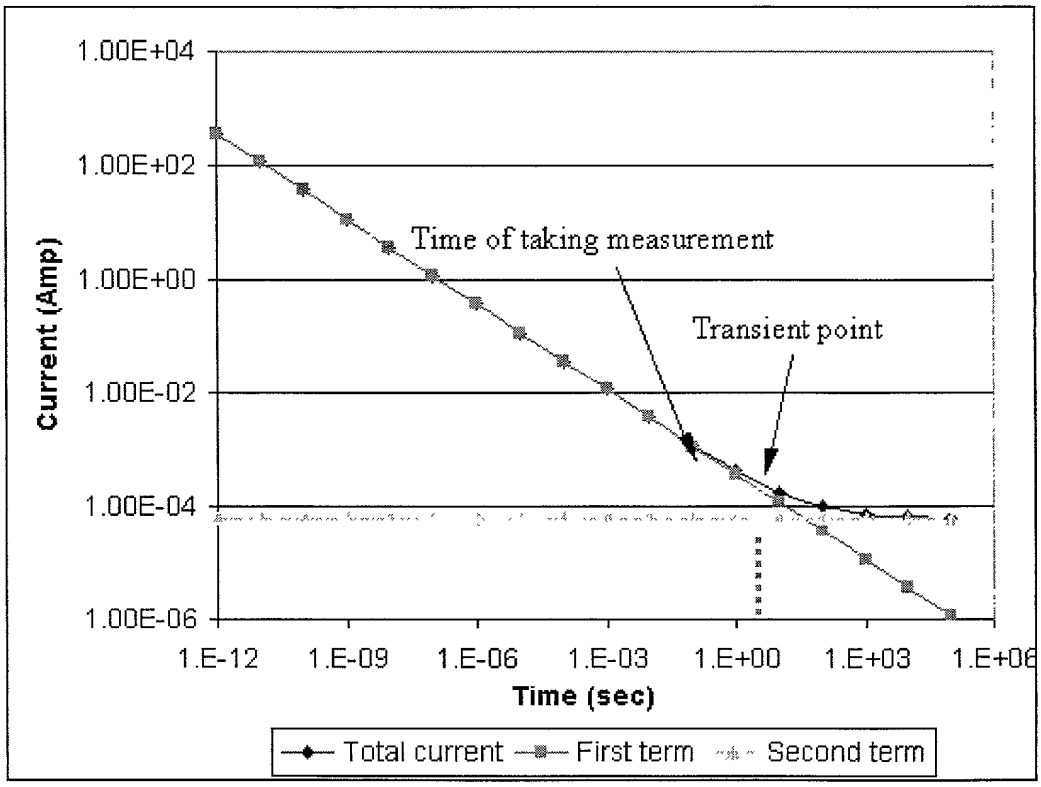

Figure 19. Contribution of both terms to total current based on current design of working electrode (r = 0.16 cm, D = 6.7E-6 cm2/sec, [TMB] = 200uM)

We take the amperometric measurement at the time of time of twenty seconds after applying the bias potential. As shown in **Figure 19**, it is right at the transient point. This adds a potential of fluctuations to the accuracy of the output current, since both terms are sensitive to different factors. As discussed in the chapter two, the baseline current from the solution dominate the noise current in a flux form to the electrode and it has the same geometrical dependence with the first term of equation (8). Shrinking the radius of working electrode would decrease both noise current and the first term of the equation (8) at the same fashion. But the second term would catch up pretty quick and a steady state current can be reached after one second, **Figure 20**.

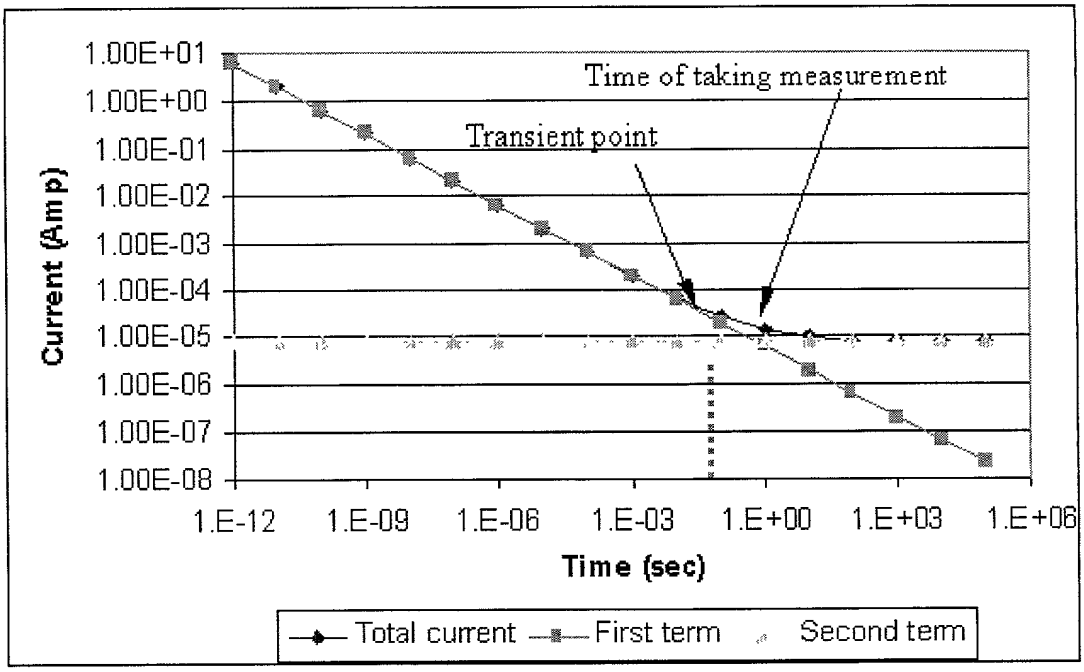

Figure 20. Contribution of both terms to total current based on prposed design of working electrode (r = 200 μm, D = 6.7E-6 cm2/sec, [TMB] = 200uM)

To deduce the equation (8) to a simply form, a dimensionless time parameter τ is introduced for different time scale (Shoup et al., 1980);

$$\tau = \frac{4Dt}{r^2} \qquad (9)$$

Equation (8) can be simplified to equation (10) to (12),

$$i = 4nrFDC \qquad (\tau >> 1) \qquad (10)$$

$$i = nFAC\sqrt{\frac{D}{\pi t}} \qquad (\tau << 1) \qquad (11)$$

$$i = 4nrFDC + nFAC\sqrt{\frac{D}{\pi t}} \qquad (0.01 < \tau < 100) \qquad (12)$$

Microelectrodes are easy to construct; nevertheless, they do not present a uniform flux over their surface since the rate of diffusion to the edge is always higher than to the center. The edge effects become more important and dominate the response of very small electrode even at times of one second or less. However, when $t >> r^2 / D$ (or $\tau >> 1$), the shape of the electrode becomes irrelevant.

A schematic drawing of the concentration distribution is shown in **Figure 21**. Usually, the enzyme layer is relatively thin and can be neglected and the diffusion thickness depends on the bilk concentration and the diffusion coefficient of the analyte. This is based on the dimension diffusion process without considering the edge effect. In **figure 22**, the effect of the dimension of the electrode is demonstrated in the form of concentration distribution. When the diameter of the working electrode is close to the diffusion thickness, then the lateral diffusion from the edge would change the diffusion model significantly.

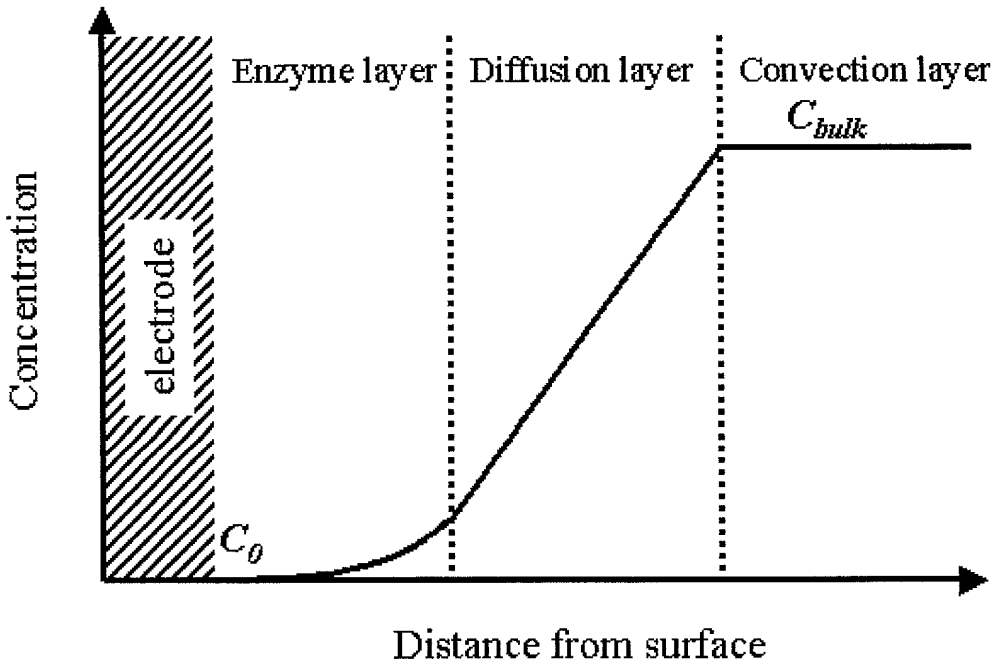

Figure 21. Concentration distribution along the normal direction of the electrode

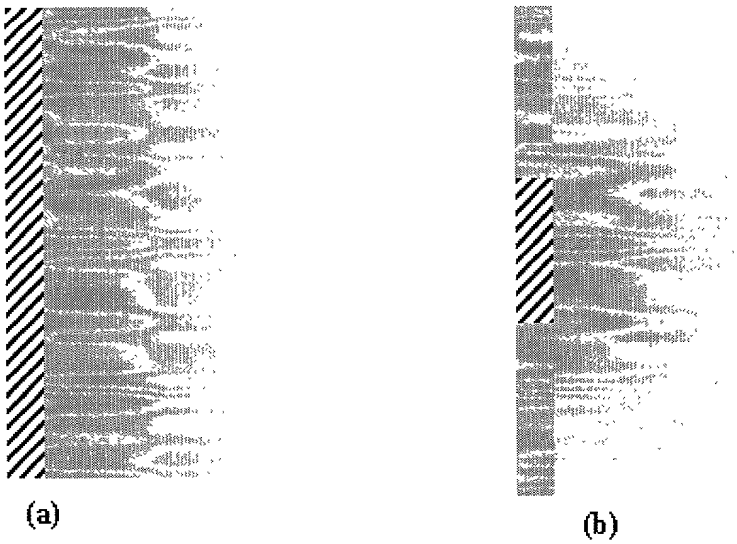

Figure 22. Concentration distribution of (a) planar electrode (b) microelectrode

Chapter 10 Analytical Electrochemistry

The major difference between the DNA sensor discussed in this paper, and the DNA microarrays presently available on the market, is the detection mechanism applied. Our on-chip sensor is based on an enzymatic reaction and electrochemical detection, while others rely mainly on off-chip optical detection with imaging processing. A number of analytical techniques were used in the characterization of our DNA sensor and detection scheme. The sensor was first developed at UCLA in 1998 on a silicon wafer using standard MEMS fabrication processing. Since no literature was found on the fabrication and characterization of a complete, electrochemical cell consisting of a working, auxiliary and reference electrode, a thorough investigation on the analytical functionality of our sensor was critical for further application in quantitative measurement.

In this chapter, we initially use a well-studied, inorganic compound with standard electrochemical analysis tools to demonstrate the functionality, stability and reproducibility of the sensor. The limitations of the present, electrochemical biosensor design are also addressed. This same sensor is used to study the kinetics of the enzymatic reaction as applied to the detection protocol. All of the experimental result presented in this paper were taken using the MEMS-based, electrochemical sensor fabricated at the UCLA nanolab facility.

In order to derive a quantitative correlation between the current readout and the concentration of the analyte, detailed description of cyclic voltammetry and chronoamperometry are summarized in the following paragraphs and a series of electroanalytical validations were performed based on these techniques.

1. Cyclic Voltammetry

Cyclic Voltammetry (CV) is one of the most versatile, analytical techniques used in the study of electroactive species and the characterization of biosensors. It is widely used as both an industrial and academic research tool in the fundamental characterization of electrochemical systems. In cyclic voltammetry, the potential is ramped from an initial potential (E_o) to a maximum potential (E_m) at a fixed sweep rate (V/sec.). **Figure 23**

illustrates this concept. Repeated cycles of reduction and oxidation of the analyte generate alternating anodic and cathodic currents in and out of the working electrode. Since the solution is not stirred, diffusion effects are observed at different analyte concentrations and different scan rates.

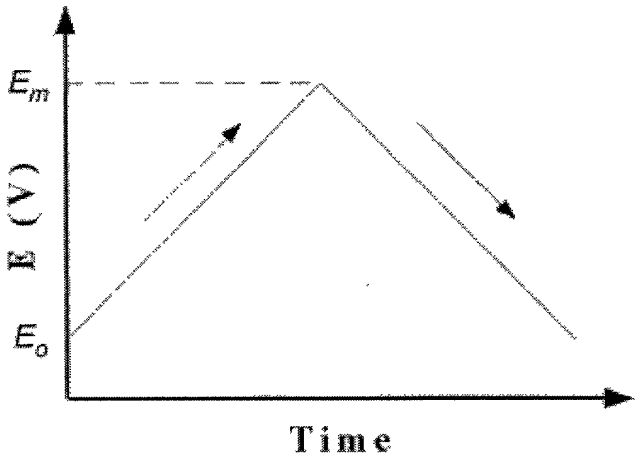

Figure 23. Cyclic voltammetry scans potential over time

Separation of the anodic (i_{pa}) and cathodic (i_{pc}) current peaks can be used to predict the number of electrons involved in the redox reaction. The peak current is also directly proportional to the analyte concentration, C and scan rate, v. Experimental results are usually plotted as current versus potential, similar to the graph shown in **Figure 24.**

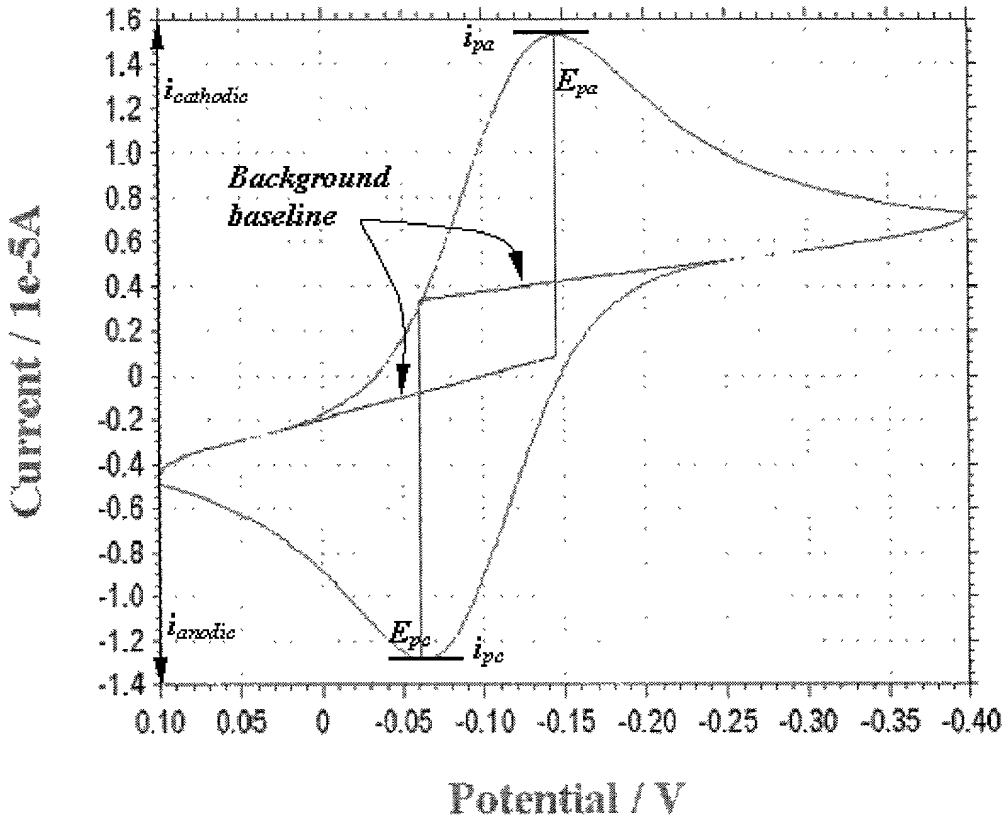

Figure 24. Typical cyclic voltammetry (one cycle) taken by DNA sensor on $K_3Fe(CN)_6$

In this CV scan, the potential is graphed along the x-axis with more positive (or oxidizing) potentials plotted to the right, and more negative (or reducing) potentials to the left. The current is plotted on the y-axis with cathodic (i.e., reducing) currents plotted down along the negative direction, and anodic (i.e. oxidizing) currents plotted in the positive direction.

Redox reaction of potassium ferricyanide

The analyte used in the following control experiment was potassium ferricyanide, $K_3Fe(CN)_6$ (329.26 g/mol), which contains an iron atom in the +3 oxidation state (Fe^{III}) in a buffer solution of potassium nitrate, KNO_3 (101.11 g/mol). At the surface of a working electrode, a single electron can be added to the ferricyanide anion. This will cause it to be reduced to the

ferricyanide anion, $Fe^{II}(CN)_6^{4-}$, which contains an iron atom in the +2 oxidation state (Fe^{II}). This simple, one electron exchange between the analyte and the electrode is a well behaved, reversible reaction. This means that the analyte can be easily reduced to $Fe^{II}(CN)_6^{4-}$ and then easily oxidized back to $Fe^{III}(CN)_6^{3-}$.

A redox couple is a pair of analytes differing only in oxidation state. The electrochemical half-reaction for the $Fe^{III}(CN)_6^{3-}$ / $Fe^{II}(CN)_6^{4-}$ redox couple can be written as follows:

$$Fe^{III}(CN)_6^{3-} + e^- \Leftrightarrow Fe^{II}(CN)_6^{4-} \qquad E_o = +0.358V(NHE). \qquad (13)$$

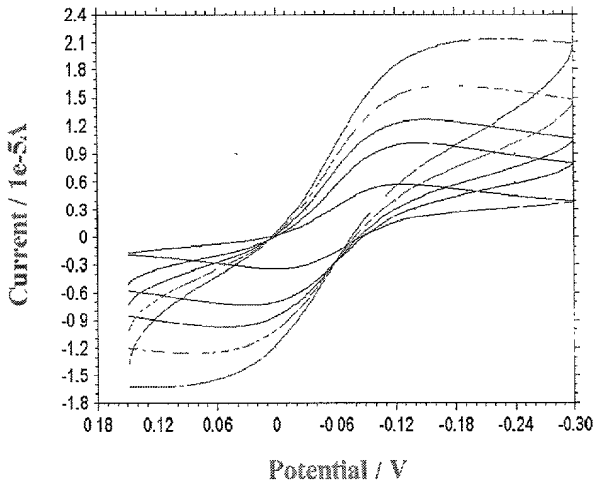

Figure 25. Cyclic Voltammetry at different scan rate (taken by electrochemical DNA sensor on $K_3Fe(CN)_6$)

The voltammogram in **Figure 25** exhibits two asymmetric peaks, one cathodic (i_{pc}) and the other anodic (i_{pa}). Using a standard reference electrode, such as the normal hydrogen electrode (NHE), the formal potential associated with this half-reaction is near *+358* mV. If the working electrode is held at a potential more positive than *+400* mV, then the analyte tends to be oxidized to the $Fe^{III}(CN)_6^{3-}$ form. This oxidation at the working electrode causes electrons to go into the electrode from the solution resulting in an anodic current. At potentials more negative than *+400* mV, the analyte tends to be reduced to $Fe^{III}(CN)_6^{4-}$. This reduction at the working electrode causes electrons to flow out of the electrode into the solution resulting in a cathodic current. Our

sensor design does not utilize a standard reference electrode like NHE, silver/silver chloride (Ag/AgCl) or saturated calomel electrode (SCE). Since all three electrodes are in our design are Au, the rest (unbiased) potential in our experiment is close to zero volts.

Randles-Sevcik equation

The important parameters of a cyclic voltammogram are the magnitudes of the cathodic and anodic peak currents (i_{pc} and i_{pa} , respectively) and the potentials at which these currents are observed (E_{pc} and E_{pa} , respectively). Using these parameters, it is possible to calculate the formal reduction potential (E_o – which is centered between E_{pa} and E_{pc}) and the number of electrons (n) transferred in the charge transfer reaction.

The peak current (i_{pa} or i_{pc}) can be expressed by the Randles-Sevcik equation:

$$i_p = 0.4463nFAC\left(\frac{nF\nu D}{RT}\right)^{\frac{1}{2}} \qquad (14)$$

where, n = number of electrons appearing in half-reaction for the redox couple

F = Faraday's constant (96,485 C/ mol)

A = electrode area (cm^2)

ν = rate at which the potential is swept (V/sec)

D = analyte's diffusion coefficient (cm^2/sec)

R = universal gas constant (8.314 J / mol K)

T = absolute temperature (K)

At 25°C, the Randles-Sevcik equation can be reduced to the following:

$$i_p = (2.687\times 10^5)n^{3/2}\nu^{1/2}D^{1/2}AC \qquad (15)$$

where the constant has units (i.e., $2.687\text{x}10^5$ C mol^{-1} $V^{-1/2}$).

The Randles-Sevcik equation predicts that the peak current should be proportional to the square root of the sweep rate when voltammograms are taken at different scan rates. As shown in **Figure 26**, the plot of peak current versus the square root of sweep rate yields a straight line. The Randles-Sevcik equation can be modified to give an expression for the slope of this straight line as follows,

$$Slope = (2.687 \times 10^5 C mol^{-1} V^{-1/2}) n^{3/2} D^{1/2} AC \qquad (16)$$

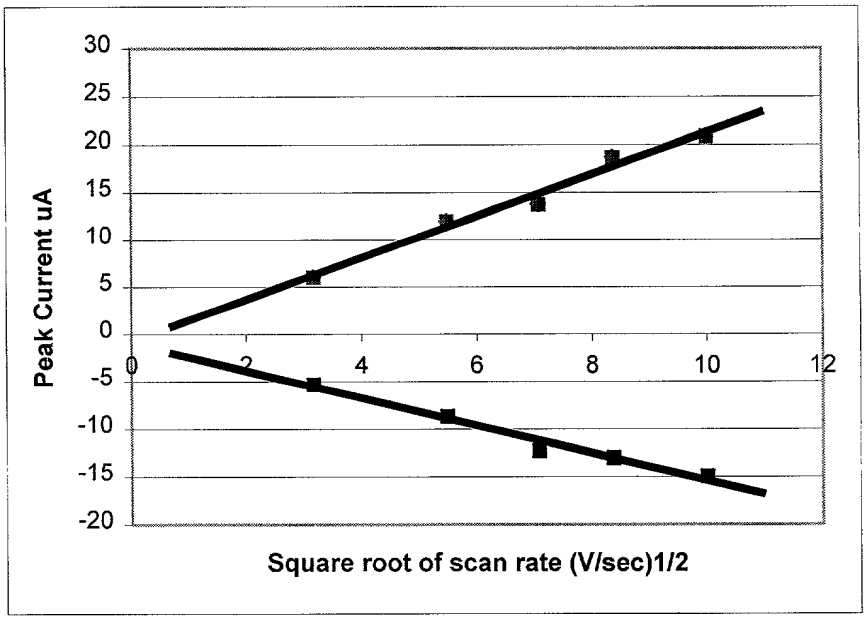

Figure 26. Scan rate dependence of peak current (taken by DNA sensor on $K_3Fe(CN)_6$)

The scan rate dependence of the peak potentials and peak currents are used to evaluate the number of electrons participating in the redox reaction as well as provide a qualitative account of the degree of reversibility in the overall reaction. The number of electrons transferred in the electrode reaction (***n***) for a reversible redox couple is determined from the separation between the peak potentials ($\Delta Ep = Epa - Epc$). For a simple, reversible (fast) redox couple, the ratio of the anodic and cathodic peak currents should be equal to one. Our results slightly deviate from unity, however, large deviations would indicate interfering chemical reactions coupled to the electrode processes. Slight deviations from unity merely suggest a non-ideal system. **Figure 27**

shows the CV scan for 12 consecutive cycles with minor deviations from the first cycle. These results clearly indicate a highly reversible systems and robust cell design.

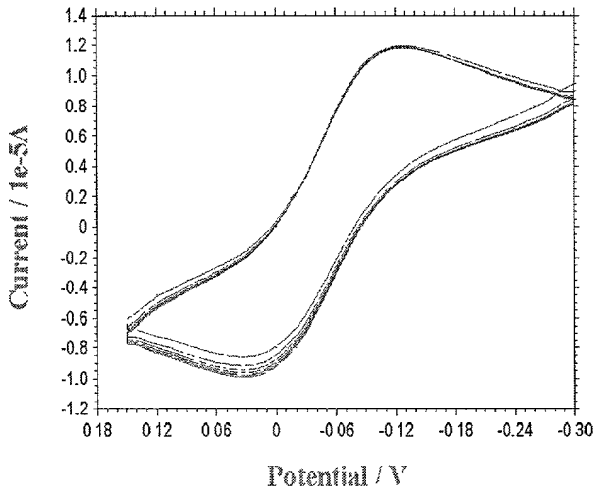

Figure 27. 12 consecutive CV scan

2. Chronoamperometry

Another useful electroanalytical technique is called chronoamperometry. This technique involves stepping the bias potential at the working electrode from an initial potential to a final potential and holding that potential while the current is recorded at the electrode. These potentials are chosen so that they bracket the formal potential, E_o of the analyte. At the initial potential, no significant current flows. Once the potential is stepped to the final potential, the analyte is consumed at the electrode surface via oxidation or reduction (depending on the direction of the step). This depletes the concentration of the analyte near the electrode. The current response is thus a rapid increase followed by a decay as the analyte is depleted and equilibrium is reached.

The analysis of chronoamperometry data is based on the Cottrell equation, which defines the current-time dependence for linear diffusion control. In chronoamperometry (or amperometry), the bias potential at the working electrode is pre-conditioned at an initial potential and then

stepped to a fixed potential at time zero. The step usually crosses the formal potential of the analyte. The solution is not stirred so a transient state is obtained. The initial potential is chosen such that no current flows (a potential that neither oxidizes or reduces the analyte). The potential is then stepped to a potential that either oxidizes or reduces the analyte, and a current begins to flow at the electrode. This potential is determined such that the baseline current generated from electrolyte oxidation or reduction is minimized. This helps yield a better signal-to-noise ratio. The current is quite large at first, but it rapidly decays as the analyte near the electrode is consumed, and a transient condition is reached.

If the point in time when the potential is stepped is taken at time zero, then the Cottrell equation describes how the current, $i(t)$ decays as a function of time, t.

$$i(t) = nFAC\left(\frac{D}{\pi}\right)^{1/2} t^{-1/2} \qquad (17)$$

where, n = number of electrons appearing in half-reaction for the redox couple

F = Faraday's constant (96,485 C/mol)

A = electrode area (cm^2)

C = concentration of analyte (mole/L)

D = analyte's diffusion coefficient (cm^2/sec.)

$\pi = 3.14159$

t = time the current was measured (sec.)

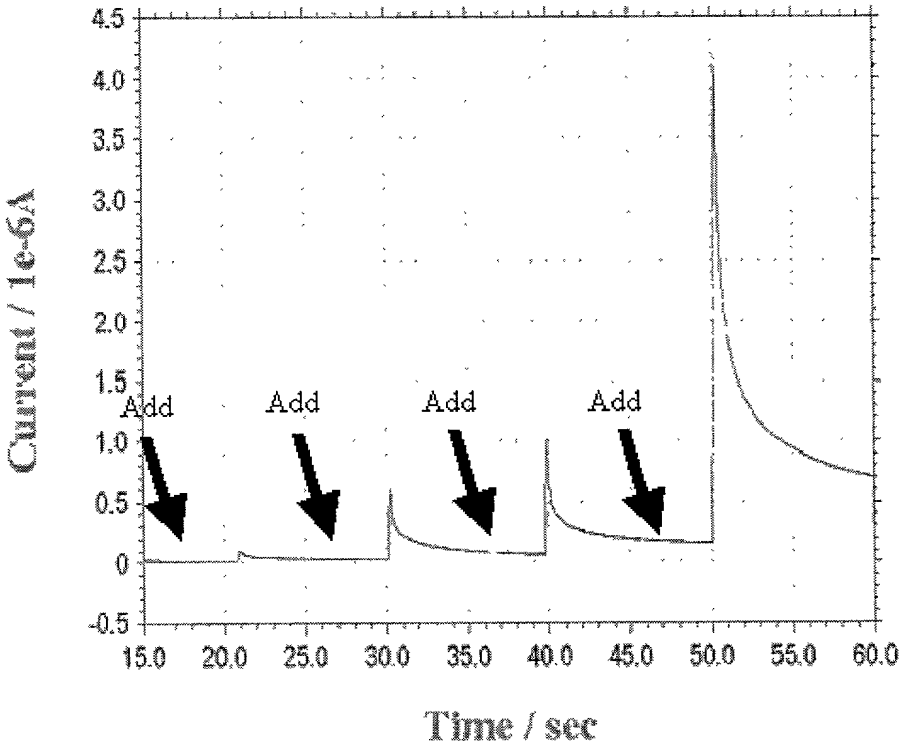

Figure 28. Addition of incremental concentration of oxidized form of TMB to the electrochemical DNA sensor

Although the current decay may appear to be exponential **(Figure 28)**, it actually decays as the reciprocal of the square root of time. This dependence on the square root of time reflects the fact that physical diffusion is responsible for transport of the analyte to the electrode surface. The experimental data is usually plotted as $i(t)$ vs. $t^{-1/2}$, yielding a straight line graph called a Cottrell plot. In addition to being used to determine concentration, the Cottrell plot is also commonly used to determine the working electrode area or an analyte's diffusion coefficient.

3. Electrode Polarization

Polarization occurs in an electrolytic cell when a potential is applied between the working and auxiliary electrode until a redox reaction is forced to occur. At the anode, the electrode potential is low enough to "pull" electrons from the analyte (oxidation occurs) while at the cathode, the potential is high enough to "force" the solution to accept electrons (reduction). The working electrode can either be the anode or cathode depending on the bias potential applied. If the redox reaction kinetics are infinitely fast, then the slope of the ***i*** vs. ***E*** plot would be determined by the solution resistance.

In **Figure 29,** the current passing through an electrolytic cell, with an infinitely fast redox reaction, is controlled by the solution resistance. Little current flows until the redox reaction begins, and then the current increases with a slope of $1/R_{solution}$. In fact, the current will be controlled by the rate of the redox reaction at one (or perhaps both) of the electrodes. As a higher larger polarization is applied to the cell, the current reaches a maximum value at which the reaction is at a maximum. The potential, above which the current through an electrochemical cell is limited by the rate of the redox reaction at one of the electrodes, is called the polarization potential. Voltammetry is based on measuring the current limited by the rate of analyte reaction at an electrode.

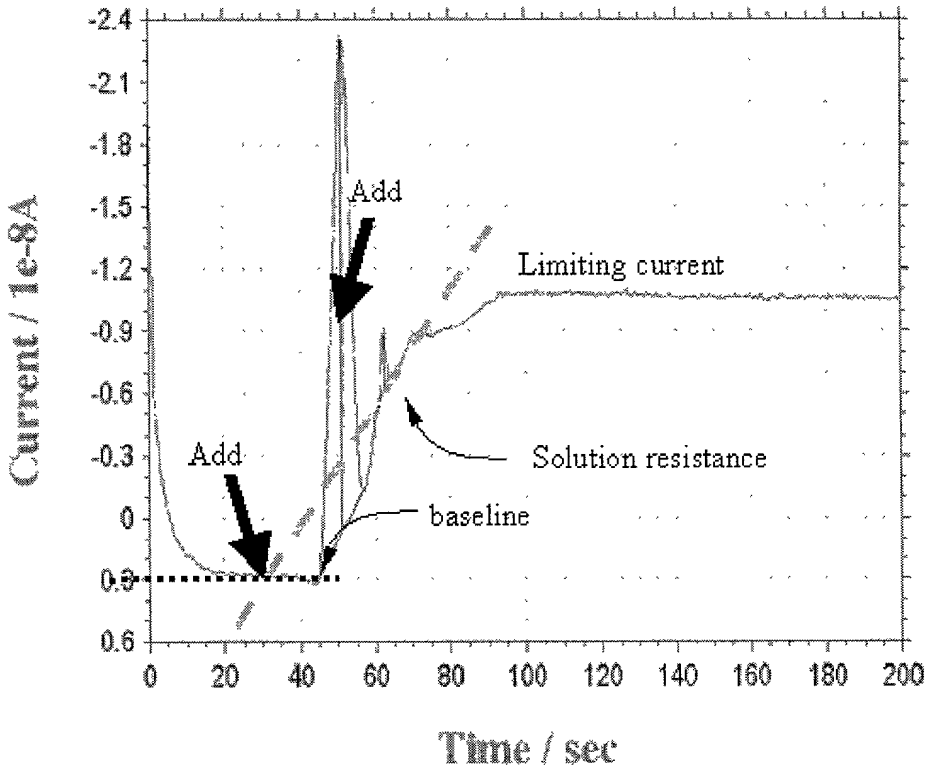

Figure 29. Electrode polarization of $Fe^{III}(CN)_6^{3-}$ on electrochemical DNA sensor

4. Diffusion constant derivation

To investigate the diffusion limited effect; first we need to measure the diffusion constant. Here, we will use chronoamperometry and Cottrell equation to measure the diffusion constant of $K_3Fe(CN)_6$ first and then see can we get the diffusion constant of the oxidized form of TMB. Cause it's the diffusion process of TMB moving between HRP and TMB limits the reaction constant, therefore the turnover number.

In this plot, the x-axis is one over square root of the time, so the equation for the slope can be derived from (17) and expressed as:

$$Slope = n\,F\,A\,C\,(D/\pi)^{1/2} \qquad (18)$$

Where, slope = 7.99E-6 = 1 × 96485 × 0.0706 × 2E-6 × $(D / 3.14159)^{1/2}$

(Sensor area = 0.15 cm × 0.15 cm ×π , $[K_3Fe(CN)_6]$ = 2mM = 2E-6 mole/cm^3)

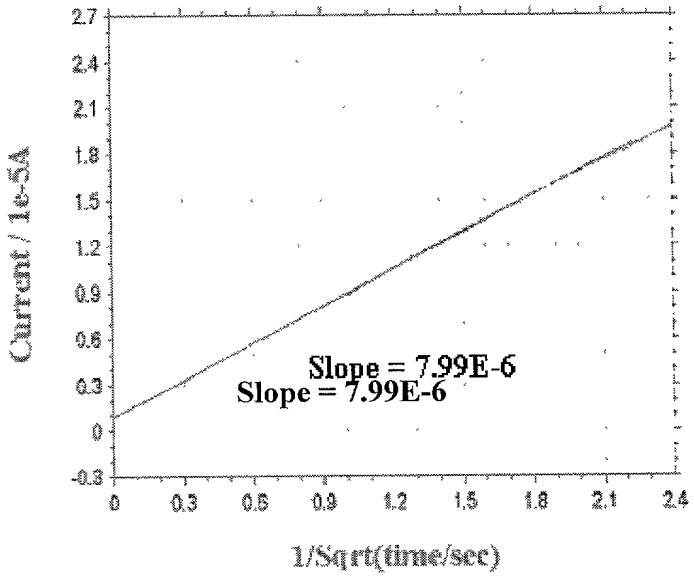

Figure 30. Cottrel plot of $K_3Fe(CN)_6$ using DNA detector chip

Then we can get the diffusion constant:

D = **1.08E-6** cm^2 / sec for potassium ferricyanide

This is very close to the one published by the literature (0.98E-5 cm^2 / sec by E.L. Cussler 1997). This means the electrochemical DNA detector is accurate enough to conduct analytical measurement and also we could use the microarray chip to measure the diffusion constant of TMB.

It is a little bit complicate with TMB since it's the oxidized form of TMB would react with the biased electrode and then diffuse away from the electrode to react with compound I & II. In

order to make sure most species in the solution are oxidized form of TMB, excess amount of HRP is added into bulk TMB/H2O2 solution and sit for overnight let the peroxidase and peroxide have enough time to oxidize all the TMB. Then take the Cottrel plot on oxidized TMB solution.

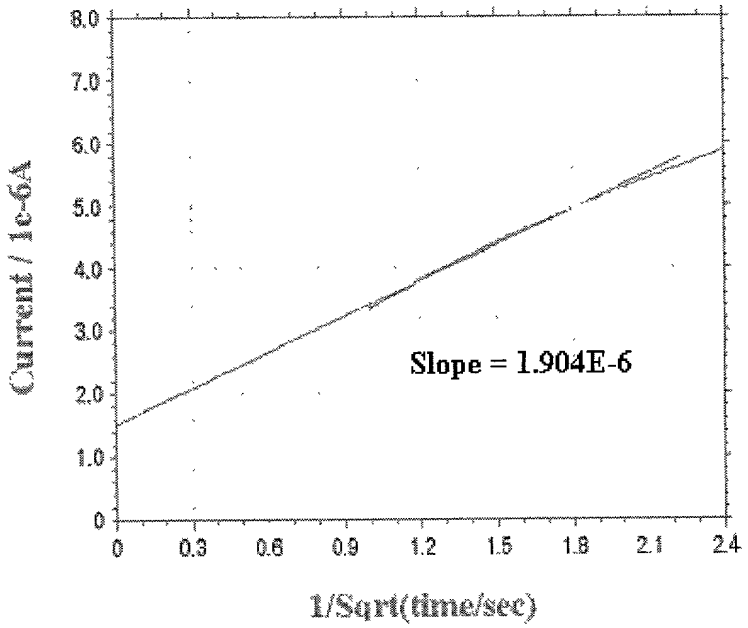

Figure 31. Cottrel plot of $K_3Fe(CN)_6$ using DNA detector chip

Substitute the slope into equation (12) with [TMB] = 200uM, then we can get the diffusion constant of TMB_{ox} is 6.7E-6 cm^2/sec, which is a little bit less than our assumption in chapter three. But there is a uncertainty of the accuracy of TMB solution. This technique can be cross checked with other electroanalytical methods.

CHAPTER 11 DNA CHIP CHARACTERIZATION

1. Characterization of Self-Assembled Monolayers

The performance of the detector depends heavily on the properties of the immobilized streptavidin monolayer. We performed SPR (Biacore X system, Biacore, Inc.) and AFM (AutoProbe CP, Park Scientific Instruments) to characterize the monolayers. For SPR studies of streptavidin binding to bare Au, bare Au chips (J1 sensor chips) were used. For studies of streptavidin binding to biotin-DAD-C-12-SH/Au or biotin-HPDP/Au, the biotin SAM was deposited on the bare Au chips as previously described before in the SPR experiments. For best results, new chips were cleaned with diluted Piranha solution for ~2 min. before performing SPR with bare Au or depositing the biotin SAM. In all cases, 1.0 mg/ml streptavidin in 0.02M Na phosphate, 0.15 M NaCl, pH 7.2 buffer was used. In adsorption experiments with streptavidin on bare Au, flow rates ranged from 1 to 5 ml/min. In the experiments with streptavidin and biotin-DAD-C12-SH/Au, flow rates ranged from 10 to 25 ml/min. In experiments with streptavidin and biotin-HPDP/Au, flow rates ranged from 5 to 10 ml/min. In the adsorption experiments, 25 ml of the following solutions were flowed sequentially through the channels at 25 ml/min (total exposure time of 1 min.): 1.0M KCl, 8M urea, 0.5% SDS, 0.1M HCl, 0.1M NaOH, and 40 vol% formamide.

AFM was performed in the contact mode using ultralever tips with a force of 5.0nN. To ensure a flat Au surface, the method of Wagner, et al. (1995) was used wherein Au was first deposited via e-beam evaporation on mica and then transferred to Si. In our case, the mica was cleaved to cleanly remove it from the Au without the use of a solvent.

Streptavidin Self Assembled Monolayers for rRNA Capture

We used three different approaches to immobilize a streptavidin monolayer on the electrode surface, as shown in Figure 2. In the first approach, a streptavidin monolayer was deposited on bare Au via protein adsorption. In the second approach, a SAM of biotin was deposited on the Au using a biotinylated thiol and streptavidin was subsequently bound to the biotin. In the third approach, a SAM of biotin was deposited on the Au using a biotinylated disulfide and streptavidin was subsequently bound to the biotin.

Characterization of Streptavidin Monolayers

The streptavidin monolayers were characterized using both SPR and AFM. SPR has been demonstrated to be a viable technique for monitoring interactions of molecules with metallic (Au, Ag) thin films at the solution-metal interface. This technique can be used to estimate the thickness of a deposited layer as well as to measure the kinetics of association and dissociation (Haussling, et al., 1991, Spinke, et al., 1993, Sigal, et al., 1996, Rao, et al., 1999, Jung, et al., 1999). We performed SPR to monitor deposition of streptavidin on Au using all three approaches. SPR results are shown in Figure 19. Based on calibrations by the manufacturer (Biacore), 1000 resonance units (RU) in the SPR signal is equivalent to a change of ~1 ng/mm^2 in surface protein concentration. Streptavidin has dimensions of ~ 55 x 45 x 50 Å (Darst, et al., 1991). A full monolayer of streptavidin has an expected density of ~2.8 ng/mm^2, based on a 2-dimensional crystalline monolayer (Jung, et al., 1999, Darst, et al., 1991).

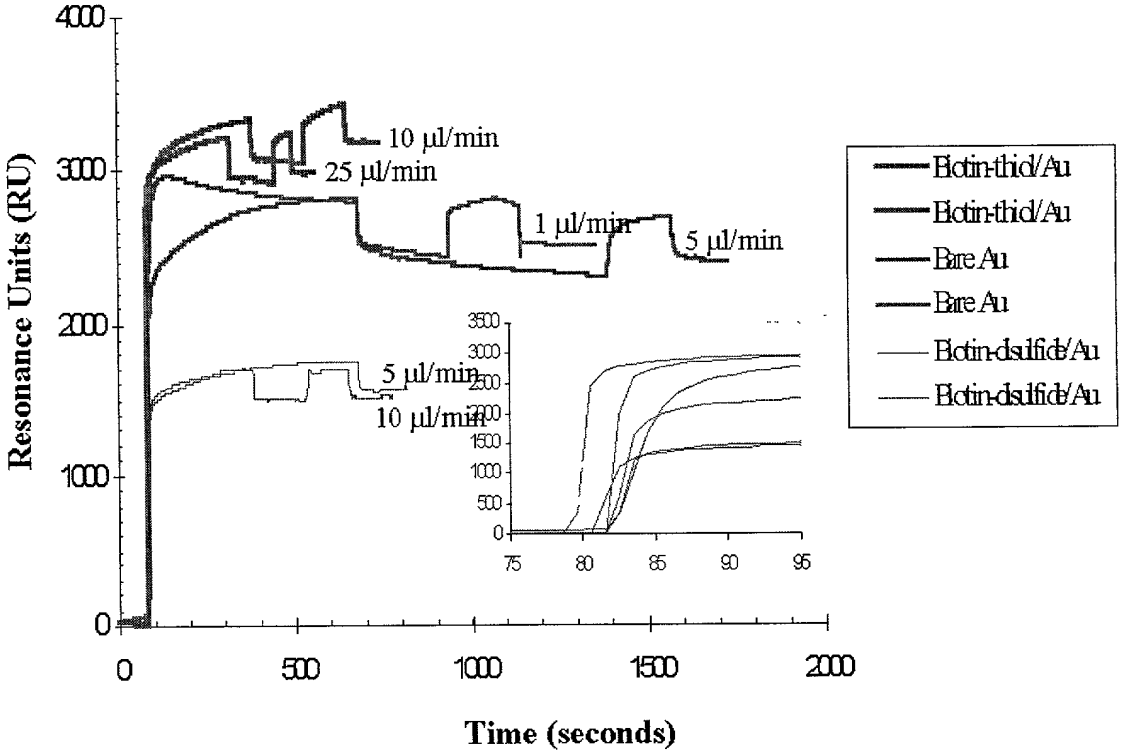

Figure 32. Surface plasmon resonance result of protein deposition

From the data presented in **Figure 32**, it was determined that essentially a complete monolayer of streptavidin was deposited on the biotinylated thiol SAM/Au (~3000 RU), ~80% coverage was obtained with streptavidin deposited on bare Au (~2400 RU), and ~52% coverage was obtained with streptavidin deposited on the biotinylated disulfide SAM/Au (~1550 RU). For the biotinylated disulfide, the presence of mercaptopropanol in the solution had a negligible effect on surface coverage as the SPR signal increased only ~10% (~1700 RU, data not shown). In all cases, additional protein deposition upon a second injection of protein solution was minimal. Moreover, flow rates had negligible effects on the rate or amount of protein deposited. The SPR results indicate that, in all three approaches, only a monolayer of streptavidin, and not multilayers, was deposited on the Au. Finally, these results establish that most of the streptavidin-biotin binding and streptavidin adsorption on bare Au occurs within seconds and can be completed on the order of minutes.

We performed experiments to determine whether streptavidin can be desorbed, i.e. whether streptavidin can be dissociated from the bare Au or from binding to biotin to regenerate the surface. Table I lists the loss in SPR signal (RU) after treatment with various reagents that are known to dissociate protein-ligand binding and/or denature proteins. As seen in Table I, only 8M urea, 0.5% SDS, and 0.1M NaOH were somewhat effective in desorbing streptavidin from the surface. 1.0M KCl, 0.1M HCl, and 40% formamide were not effective. Streptavidin could not be completely desorbed by any of the reagents, and some protein remained after subjecting the surface to all reagents. These results show that streptavidin has excellent binding to both the biotin SAM as well as to bare Au and that the streptavidin monolayers were relatively stable.

Treatment Condition	Streptavidin on Bare Au ~2400 RU deposited Loss in Signal (RU)		Streptavidin on biotin-DAD-C12-SH/Au ~3000 RU deposited Loss in Signal (RU)		Streptavidin on biotin-HPDP/Au ~1700 RU deposited Loss in Signal (RU)	
1.0 M KCl	0	0	0	0	0	0
8M Urea	280 (12%)	370 (15%)	790 (26%)	1050 (35%)	360 (21%)	300 (18%)
0.5% SDS	40 (2%)	150 (6%)	390 (13%)	230 (8%)	330 (19%)	690 (40%)
0.1M HCl	0	0	0	0	0	0
0.1 M NaOH	400 (17%)	550 (23%)	630 (21%)	690 (23%)	400 (24%)	200 (12%)
40% Formamide	0	0	0	0	0	0

Table I

Comparison of various reagents for the desorption of streptavidin from surface as determined by surface plasmon resonance

The use of AFM enables us to further characterize the surface by imaging streptavidin directly adsorbed on bare Au. Bare Au had topographic features <10 Å, whereas protein islands on a "partial" monolayer was ~45 Å, consistent with the dimensions of streptavidin (Figure 20). The AFM results confirm the SPR findings that only one monolayer was deposited on the Au. AFM in the contact mode for a "full" protein monolayer showed a featureless surface with evidence of protein dragging (data not shown), and therefore, did not provide any additional information as

to surface coverage. As previously reported, monolayer deposition is also obtained when using biotinylated SAMs and subsequently binding streptavidin (Spinke, et. Al., 1993, Jung, et. Al., 1999).

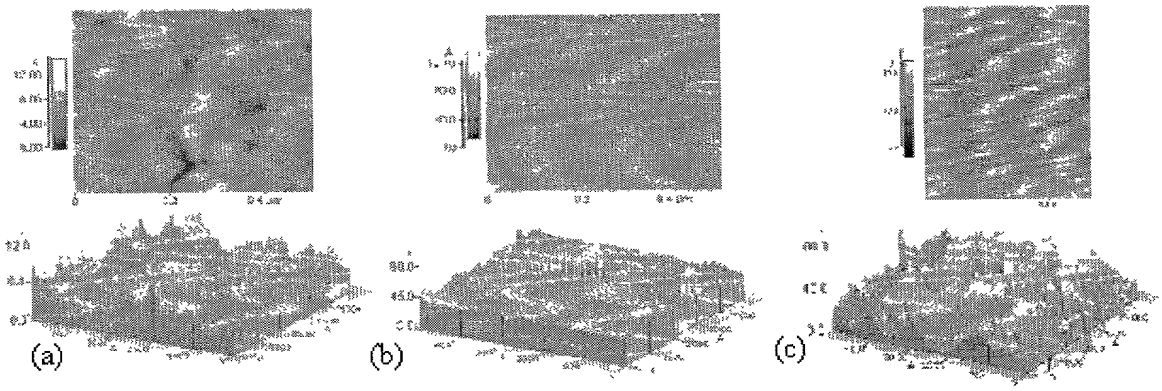

Figure 33. AFM of SAM formation on Au. (a) bare Au only (b) full coverage with protein dragging (c) partial coverage with protein islands

Electrochemical Measurements with MEMS Detector Array

In our MEMS detector array, we used a three-electrode system with Au for all three electrodes, i.e. working, auxiliary, and reference electrodes. Typically, Ag/AgCl or saturated calomel

electrode (SCE) is used as the reference electrode so that a reliable reference point is established. This enables reversible oxidation/reduction at a fixed potential to occurs at the working electrode. In our MEMS detector array, however, we used Au as the reference electrode to simplify fabrication and to permit a fully reusable array. Maintaining a constant potential is made possible by the use of a 3-electrode system (vs. a 2-electrode system). In our particular application where the reduction of TMB was monitored, Au can be successfully used as the reference electrode because a low voltage difference (-0.1V) was maintained for short periods of time (<1 min).

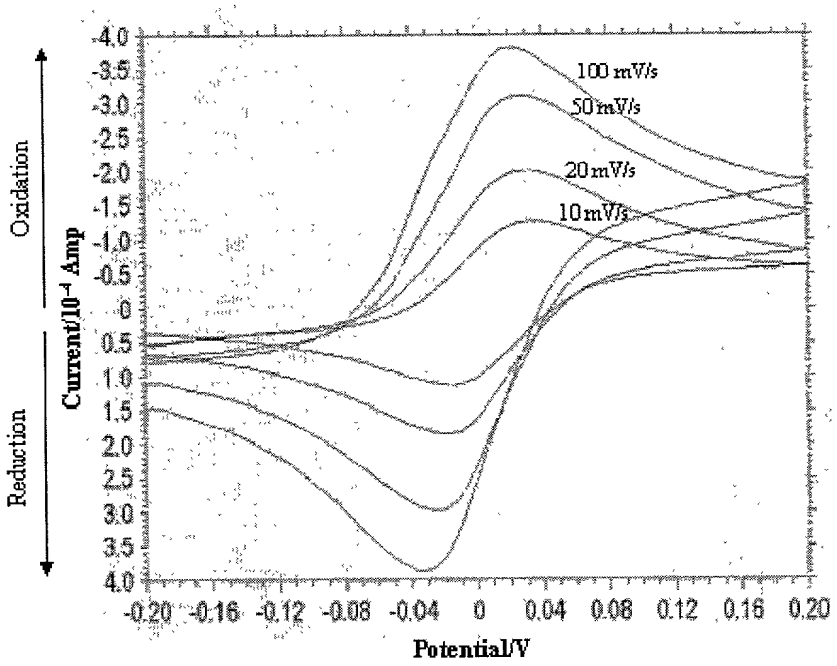

Figure 34. Voltammograms with ferrocene at different scan rate

We characterized the Au/Au/Au electrode system for electrochemical detection by two separate experiments. In the first experiment, a ferrocene film was placed on the electrodes and cyclic voltammetry was conducted to monitor the redox reactions. Cyclic voltammetry for a classic, reversible, one electron transfer reaction is characterized by a peak separation of ~57 mV between the anodic and cathodic peaks, the same peak currents at peak maximum, and a linear relationship between peak current vs. [scan rate]$^{1/2}$ (Hall, 1991). **Figure 34** shows the

voltammograms obtained with ferrocene at different scan rates. As seen in **Fig. 25**, classical redox behavior was observed and a plot of the peak current vs. [scan rate]$^{1/2}$ is linear.

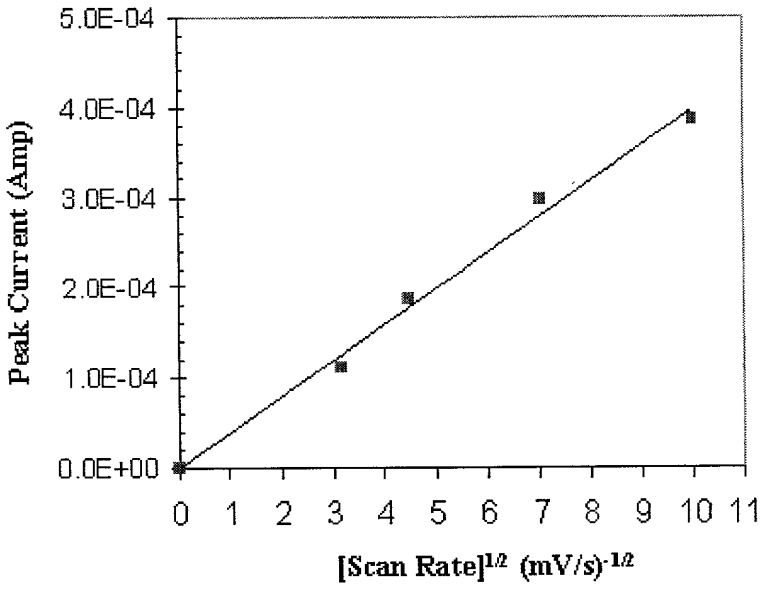

Figure 35. Peak current – scan rate dependence

In a second experiment with the Au/Au/Au electrode system, cyclic voltammetry was conducted on the substrate solution only (H_2O_2 + TMB) and then again on the same solution with POD enzyme. Cycling between –0.2V to +0.50V, at a scan rate of 10mV/s, the substrate solution showed the two electron redox behavior of TMB (**Figure 36**). The addition of POD to the substrate solution resulted in an increase in the reduction current. A constant potential of –0.10V (vs. reference) was then selected for measurement of POD enzymatic activity. At this potential, the current background was near zero and no substrate oxidation occurred. This potential was optimum for determining the enzymatic activity in which a small amount of product (oxidized TMB) was to be measured in the presence of a high concentration of substrate.

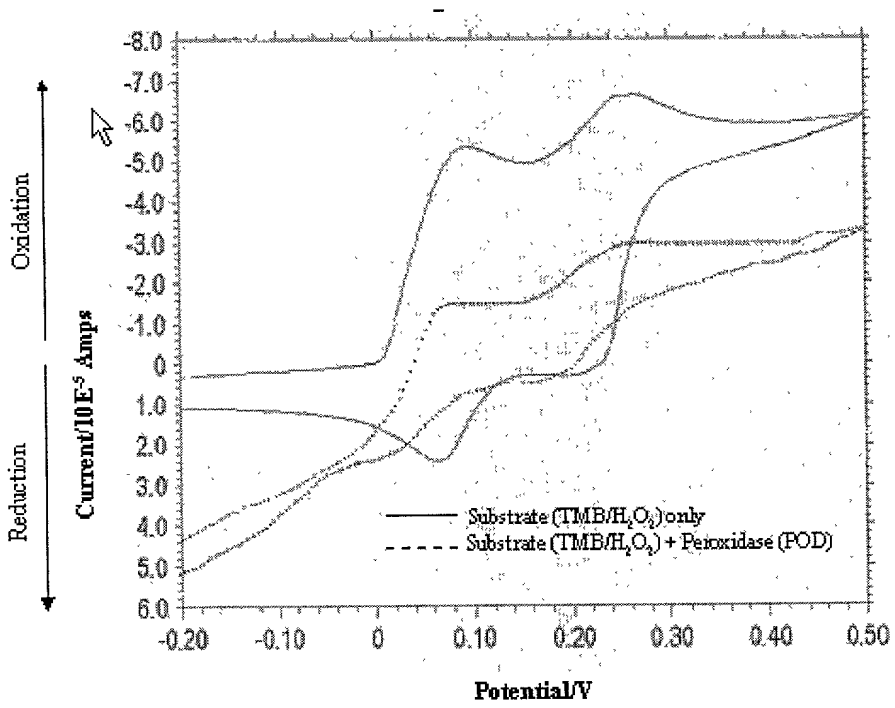

Figure 36. CV scan of TMB and POD reaction

2. Discussion

Our results show that combining MEMS technology with SAMs, DNA hybridization, and enzymatic amperometry leads to a highly specific and sensitive electrochemical detector for bacteria such as E. coli. The contribution from each component is critical to the overall success of the system. MEMS technology enables an array of multiple, three-electrode "cells" to be deposited on a Si wafer. The MEMS detector array we have described is fully reusable as the SAMs can be removed and the Au surfaces regenerated with appropriate cleaning. Moreover, with micromachined channels, valves, pumps and integrated electronics, one can fully automate the sample preparation and assay protocol.

SAMs provide an effective means of functionalizing the Au working electrode to capture biomolecules. DNA hybridization permits high specificity for pathogenic bacteria as the

sequence of the ssDNA probes can be carefully selected to complement only the target. Coupling the hybridization event with an enzymatic reaction provides signal amplification and enhances the sensitivity. Finally, by using electrochemical transduction, a miniaturized portable system with minimum power consumption can be developed.

Rapid detection and a portable instrument is desirable for pathogen sensing. We have demonstrated that detection can be achieved within ~40 minutes using this system. Due to the small dimensions and small sample volumes, it is possible to further reduce the assay time by reducing the incubation times (10 minutes) currently used for DNA hybridization and enzyme binding. A distinct advantage of MEMS is the ability to use very small volumes (a few μl) and electrode surface areas (currently 0.13 cm^2 for the working electrode, <0.02 cm^2 for the auxiliary and reference electrodes). Our results show that as little as one single cell can be detected using this system without polymerase chain reaction (PCR) amplification. Due to the small volumes and working electrode surface area in the MEMS system, reporting the detection limit in terms of absolute cell numbers is more appropriate than reporting the detection limit in terms of cell concentration (cells/ml). Detection limits on the order of 10^2 to 10^3 cells/ml have been reported, however, sample volumes of ~ 1.0 ml with working electrode surface areas ~1cm^2 were typically used (Abdel-Hamid, et. al., 1998, 1999). In amperometric, enzyme immunofiltration assays, the signal was more than an order of magnitude less when using a 0.1 ml sample than when using a 1.0 ml sample (Abdel-Hamid, 1999).

Results from amperometric experiments to detect E. coli rRNA have shown that the streptavidin monolayer immobilized via the biotinylated thiol SAM approach yielded the best results. This finding is not surprising as SPR data indicated the highest streptavidin surface density or coverage when using the biotinylated thiol. It is likely that a well-ordered, SAM is formed only with the biotinylated thiol, leading to the highest streptavidin surface density. In the case of the biotinylated disulfide, although attachment of the biotin to the Au surface occurs via the Au-S bond, the additional organic group probably hinders the formation of a densely packed monolayer. Streptavidin immobilized via direct adsorption to Au resulted in significantly higher non-specific binding of the POD enzyme to the working electrode. Protein adsorption to Au has

been well known as colloidal Au particles attached to various proteins (e.g. streptavidin, immunoglobulins) are commercially available (Nanoprobes, Inc., Yaphank, NY). Streptavidin does not contain cysteine or methionine residues (Weber, et. al., 1989) and therefore, does not attach to Au via an Au-S bond. Protein adsorption to Au can occur via interaction of carboxylate groups with Au (Ooka, et. al., 1999) and is the likely mechanism for streptavidin-Au attachment. Although a streptavidin monolayer can be attached to Au via direct adsorption, whether self-assembly or molecular ordering occurs is questionable. SPR adsorption experiments showed the streptavidin-Au attachment to be as robust as streptavidin-biotin binding, i.e. the amount of streptavidin removed due to urea, SDS, and NaOH were similar for streptavidin directly adsorbed on Au as compared to streptavidin attached to biotin. When conducting the assay protocol for E. coli, however, sample solutions contained oligonucleotides as well as cell debris from the lysed E. coli. Our data suggests that the presence of other proteins and biomolecules accelerated the adsorption of streptavidin from Au, leading to increased non-specific binding of the enzyme POD to the surface.

3. Conclusions

E. coli bacteria were successfully detected by incorporating MEMS with SAMs, DNA hybridization, and enzyme amplification. We demonstrated a MEMS-based detection system that is specific for E. coli and capable of detecting a single cell without PCR. The process time can be 40 minutes or less. Moreover, the assay can be conducted with solution volumes on the order of a few microliters. The integration of SAMs, DNA hybridization, and enzyme amplification methodologies with MEMS technology makes possible a new generation of devices for pathogenic detection.

This work has shown experimental evidence of successful coupling of nucleic acid recognition event with electrochemical transducers. Various approaches of noise reduction have been discussed in the previous sections, with special attention given to non-specific binding of biomolecules onto MEMS structures. This enzyme-based DNA detector chips thus add new dimensions of selectivity and sensitivity to the MEMS-based biosensors.

Particular attention was given to factors influencing the kinetics and efficiency of the formation of functional surface, including protein concentration, deposition flow rate, substrate surface condition, dielectrophoresis control and temperature. Additional improvements in the sensitivity have been achieved by modifying the sensor array structure and overcoming the fabrication difficulties.

A novel method for constructing electrochemical biosensor electrodes based on microfabrication and protein adsorption has been demonstrated with better sensitivity than carbon paste electrodes. The integration of DNA sensor array with bipolar transistor array is proposed to achieve on-chip amplification with increasing the chip area.

4. Future work

MEMS devices have distinct properties as a result of small features. The signal level from these MEMS-based sensors is relative low compared to conventional sensors. The best sensitivity can be achieved by using off-chip amplification, however, this approach increases the noise and the overall system size. On-chip amplification circuits can reduce the inter-chip interference, but the sensor array density is limited by the on-chip circuitry. The limitations of CMOS-compatible, MEMS processing also reduces the flexibility of the MEMS structure.

We propose an on-chip amplification device, underneath the working electrode, which is constitutes the largest area of the electrochemical sensor cell. Analogues to the open-base BJT photosensor, the base area receives the current from the transducer with the current gain beta β, ranging from 80-150. There are two types of BJTs that can be implemented with an electrochemical cell – vertical BJT and horizontal BJT. The length of the base region determines the current gain. In vertical BJT, this is a function of the ion implementation energy and doping concentration; while in horizontal BJT, the length is a function of lithography resolution, ion implementation angle and thermal diffusion. Thus, the vertical BJT is more reliable in terms of chip-to-chip or within-chip gain uniformity.

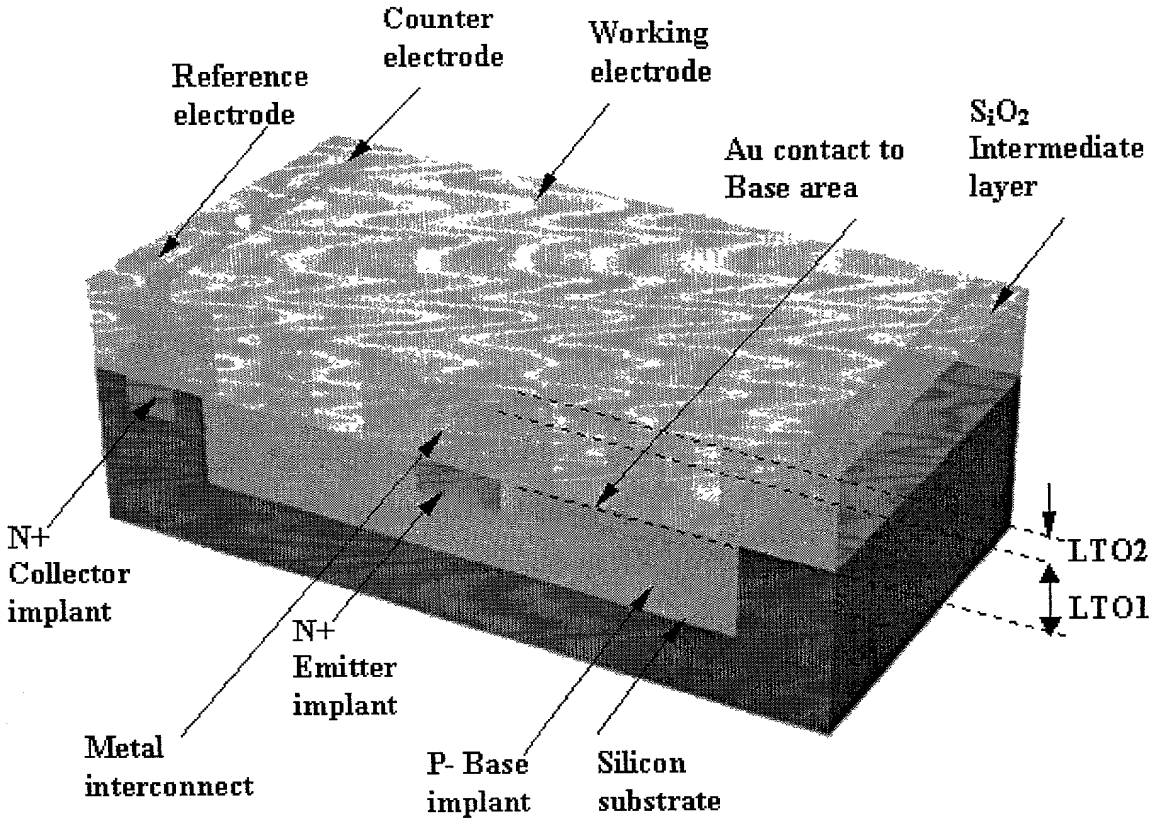

Figure 37. Schematic drawing of DNA microarray integrated with BJT circuitry

References

Abdel-Hamid, I. Ivnitski, D., Atanasov, P., Wilkins, E., 1998. Fast Amperometric Assay for E. coli 0157:H7 using partially immersed immunoelectrodes. Electroanalysis 10 (11), 758-763.

Abdel-Hamid, I., Ivnitski, D., Atanasov, P., Wilkins, E., 1999. Flow-through immunofiltration assay system for rapid detection of E. coli 0157:H7. Biosens. Bioelect. 14, 309-316.

Chen, Y.F., Yang, J.M., Gau, J.J., Ho, C.M., Tai, Y.C., 2000. Microfluidic System for Biological Agent Detection. Proceedings of the 3rd International conference on the interaction of art and fluid mechanics, Zurich, Switzerland.

Cussler, E. L., Diffusion – mass transfer in fluid systems, 2nd edition, , Cambridge University Press, 1997

Darst, S.A., Ahlers, M., Meller, P.H., Kubalek, E.W., Blankenburg, R., Rib, H.O., Ringsdorf, H., Kornberg, R.D., 1991. Two-dimensional crystals of streptavidin on biotinylated lipid layers and their interactions with biotinylated macromolecules. Biophys. J. 59, 387-396.

Dunford, H.B., 1991. Horseradish peroxidase: structure and kinetic properties. In: Everse, J., Everse, K.E., Grisham, M.B. (Eds.), Peroxidases in Chemistry and Biology, vol. 2. CRC Press, Boca Raton, FL, pp. 1–24.

Gau, J.J., Lan, E. H., Dunn, B., Ho, C.M., 2000. Enzyme-based electrochemical biosensor with DNA array chip. Proceedings of the fourth International Symposium on Micro Total Analysis Systems (μTAS), Enschede, The Netherlands.

Ghindilis, A.L., Atanasov, P., Wilkins, E., 1997. Enzyme-catalyzed direct electron transfer: Fundamentals and analytical applications. Electroanalysis 9, 661–674.

Gorton, L., Lindgren, A., Larsson, T., Munteanu, F.D., Ruzgas, T., Gazaryan, I., 1999. Direct electron transfer between heme-con-taining enzymes and electrodes as basis for third generation biosensors. Anal. Chim. Acta 400, 91–108.

Hall, E.A.H., 1991. Biosensors. Prentice Hall, Englewood Cliffs, New Jersey.

Haussling, L., Ringsdorf, H., Schmitt, F.J., Knoll, W., 1991. Biotin-functionalized self-assembled monolayers on gold: surface plasmon optical studies of specific recognition reactions. Langmuir 7 (9), 1837-1840.

Ho, C.M., Tai, Y.C., 1996. Review: MEMS and its applications for flow control. J. Fluids Eng. 118, 437-447.

Ho, C.M., Tai, Y.C., 1998. Micro-electro-mechanical systems (MEMS) and fluid flows. Ann. Rev. Fluid Mech. 30, 579-612.

Hou, S.F., Yang, K.S., Fang, H.Q., Chen, H.Y., 1998. Amperometric glucose enzyme electrode by immobilizing glucose oxidase in multilayers on self-assembled monolayers surface. Talanta 47, 561-567.

Ivnitski, D., Abdel-Hamid, I., Atanasov, P., Wilkins, E., 1999. Biosensors for detection of pathogenic bacteria. Biosens. Bioelect. 14, 599-624.

Ivnitski, D., Abdel-Hamid, I., Atanasov, P., Wilkins, E., Stricker, S., 2000. Application of Electrochemical Biosensors for Detection of Food Pathogenic Bacteria. Electroanalysis 12 (5), 317-325.

Jung, L.S., Nelson, K.E., Campbell, C.T., Stayton, P.S., Yee, S.S., Perez-Luna, V., Lopez, G.P., 1999. Surface plasmon resonance measurement of binding and dissociation of wild-type and

mutant streptavidin on mixed biotin-containing alkylthiolate monolayers. Sensors Actuators B 54, 137-144.

Kane, R.S., Takayama, S., Ostuni, E., Ingber, D.E., Whitesides, G.M., 1999. Patterning proteins and cells using soft lithography. Biomaterials 20, 2363-2376.

Lahiri, J., Ostuni, E., Whitesides, G.M., 1999. Patterning Ligands on Reactive SAMs by Microcontact Printing. Langmuir 15 (6), 2055-2060.

Lindgren, A., Munteanu, F.-D., Gazaryan, I.G., Ruzgas, T., Gorton, L., 1998. Comparison of rotating disk and wall-jet electrode systems for studying the kinetics of direct and mediated electron transfer for horseradish peroxidase on a graphite electrode. J. Electroanal. Chem. 458, 113–120.

Marrazza, G., Chianella, I., Mascini, M., 1999. Disposable DNA electrochemical biosensors for environmental monitoring. Anal. Chim. Acta 387, 297-307.

Motesharei, K., Myles, D.C., 1998. Molecular recognition on functionalized self-assembled monolayers of alkanethiols on gold. J. Am. Chem. Soc. 120 (29), 7328-7336.

Murthy, A.S.N, Sharma, J., 1998. Glucose oxidase bound to self-assembled monolayers of bis(4-pyridyl) disulfide at a gold electrode: Amperometric determination of glucose. Anal. Chim. Acta 363, 215-220.

Ooka, A. A., Kuhar, K.A., Cho, N., Garrell, G.L., 1999. Surface Interactions of a Homologous Series of a,w-Amino Acids on Colloidal Silver and Gold. Biospectroscopy 5, 9-17.

Ostuni, E., Yan, L., Whitesides, G.M., 1999. The interaction of proteins and cells with self-assembled monolayers of alkanethiolates on gold and silver. Colloids Surfaces B 15, 3-30.

Rao, J., Yan, L., Xu, B., and Whitesides, G.M., 1999. Using surface plasmon resonance to study the binding of vancomycin and its dimer to self-assembled monolayers presenting D-Ala-D-Ala. J. Am. Chem. Soc. 121 (11), 2029-2030.

Revell, D.J., Knight, J.R., Blyth, D.J., Haines, A.H., Russell, D.A., 1998. Self-assembled carbohydrate monolayers: formation and surface selective molecular recognition. Langmuir 14 (16) 4517-4524.

Ruzgas, T., Cs regi, E., Emneéus, J., Gorton, L., Marko-Varga, G., 1996. Peroxidase-modified electrodes. Fundamentals and application. Anal. Chim. Acta 330, 123–138.

Blake, C., Gould, B.J., 1984. Use of enzymes in immunoassay techniques. A review. Analyst 109, 533–547.

Ruzgas, T., Gorton, L., Emne´us, J., Marko-Varga, G., 1995. Kinetic models of horseradish peroxidase action on a graphite electrode. J. Electroanal. Chem. 391, 41–49.

Sigal, G.B., Bamdad, C., Barberis, A., Strominger, J., and Whitesides, G.M., 1996. A self-assembled monolayer for the binding and study of histidine-tagged proteins by surface plasmon resonance. Anal. Chem. 68, 490-497.

Spinke, J., Liley, M., Guder, H.J., Angermaier, L., Knoll, W., 1993. Molecular recognition at self-assembled monolayers: the construction of multicomponent multilayers. Langmuir 9 (7), 1821-1825.

Sun, X., He, P., Liu, S., Ye, Jiannog, Fang, Y., 1998. Immobilization of single-stranded deoxyribonucleic acid on gold electrode with self-assembled aminoethanethiol monolayer for DNA electrochemical sensor applications. Talanta 47, 487-495.

Wagner, P., Hegner, M., Guntherodt, H.J., Semenza, G., 1995. Formation and in situ modification of monolayers chemisorbed on ultraflat template-stripped gold surfaces. Langmuir 11, 3867-3875.

Wang, T.H., Chen Y.F., Masset S., Ho, C.M., Tai, Y.C., 2000. Molecular beacon based micro biological detection system. Proceedings of the 2000 International Conference on Mathematics and Engineering Techniques in Medicine and Biological Sciences (METMBS'2000) Las Vegas, Nevada.

Wang, J., Rivas, G., Cai, X., Palecek, E., Nielsen, P., Shiraishi, H., Dontha, N., Luo, D., Parrado, C., Chicharro, M., Farias, P.A.M, Valera, F.S., Grant, D.H., Ozsoz, M., Flair, M.N., 1997. DNA electrochemical biosensors for environmental monitoring. A Review. Anal. Chim. Acta 347, 1-8.

Weber, P.C., Ohlendorf, D.H., Wendoloski, J.J., Salemme, F.R., 1989. Structural Origins of High-Affinity Biotin Binding to Streptavidin. Science 243, 85-88.

Xia, Y., Whitesides, G.M., 1998. Soft Lithography. Angew. Chem. Int. Ed. 37, 550-575.

Yang, R.H., Wang, K.M., Xiao, D., Luo, K. and Yang, X.H., A renewable liquid drop sensor for di- or trinitrophenol based on fluorescence quenching of 3,3 A ,5,5 A –tetramethylbenzidine dihydrochloride , ,*, *Analyst*, 2000, 125, 877–882

Appendix C :

Micro Total Analysis System 2000 Manuscript

Enzyme-Based Electrochemical Biosensor with DNA Array Chip

Abstract

A reusable DNA sensor array for rapid biological agent detection has been fabricated on a silicon chip.(Fig.1) The DNA-based probes target the DNA/RNA sequence of the analyte instead of indirect probing using antibodies. The sensitivity is greatly enhanced by combining the hybridization event with a signal enzyme. The formation of the self-assembled monolayer sensor surface, in-situ DNA hybridization, signal measuring and the sensor regeneration can be performed within 40 minutes. Even without using the PCR, as low as 1000 Escherichia coli (E. coli) cells through 16s rRNA can be detected using this sensor array.(Fig.2) The dimension of each sensor area ranges from 25 mm^2 to 160 μm^2.

Keywords: Electrochemical sensor, Microelectromechanical system (MEMS), Self-assembled monolayers (SAMs), DNA hybridization

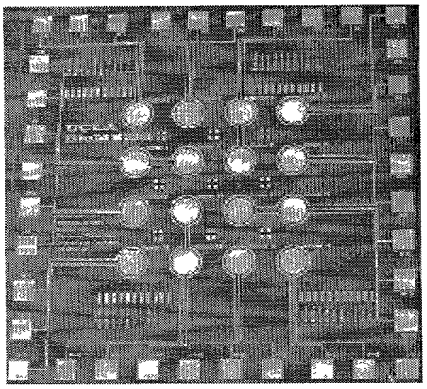

Fig. 1 DNA sensor array chip

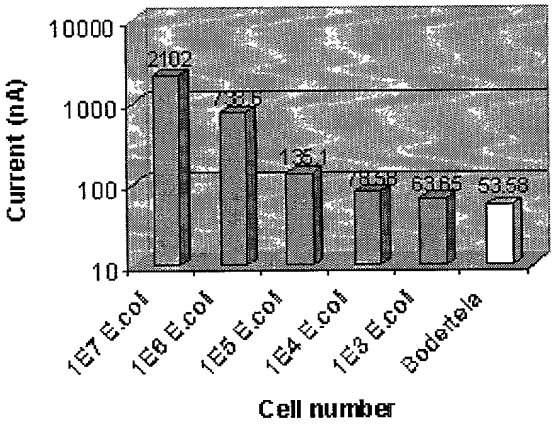

Fig. 2 Sensitivity and specificity check

1. Introduction

The enzyme-based electrochemical biosensor is primarily motivated by the need for a highly sensitive and selective protocol capable of rapid monitoring the concentration of bacteria, virus or various biological species for field use. Such a protocol would operate remotely, and would be fully automated, compact, and robust [1]. Therefore the electrochemical transducer with minimum power consumption and smaller size is preferred over the optical system [2]. High specificity can be achieved by using DNA hybridization to reduce false positive and false negative signals. DNA electrochemical biosensors have been previously reported [3,4] using graphite or carbon electrodes. Carbon-based electrodes, however, are generally not adaptable to MEMS technology when small (<μm) dimensions are needed. In this study, Au is used as electrodes, with a protein self-assembled monolayer (SAM) to capture the E. coli rRNA. An enzyme is used as a biological amplifier in this study to gain the high sensitivity without PCR. A sensitivity and specificity check for E. coli MC4100 versus Bordetella SB54 is shown in Fig.2.

2. Detection Principle

HRP is one of the most widely used enzymes for analytical purposes and biosensors application [5]. Enzymatic amplification occurs due to a high turnover number in reactions that can be detected electrochemically. We describe here an amperometric biosensor based on horseradish peroxidase (HRP) with 3,3'5,5'-tetramethylbenzidine (TMB) as a mediator. (Fig.3) The electron transfer at the electrode surface is measured amperometrically to represent the number of the enzymes immobilized by DNA hybridization though the 16s ribosomal RNA of the target cell. Therefore, the output current is proportional to the number of the target cells in the solution.

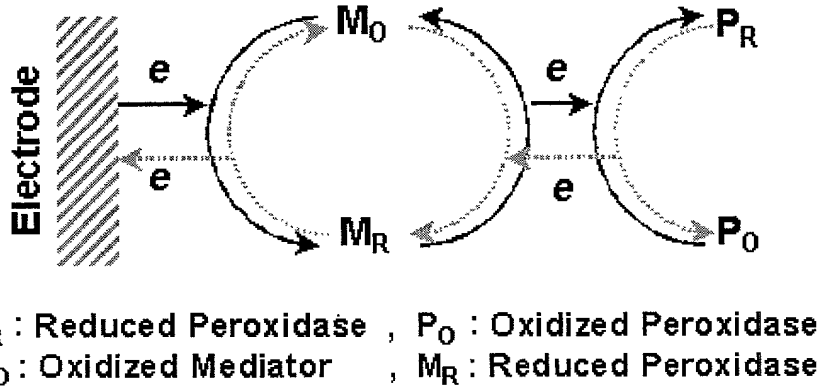

Fig. 3 Electron transport of HRP enzymatic reaction

3. Experimental

A three-electrode electrochemical cell is constructed with a micro-fabricated reaction well for the working electrode (Fig.4a). Gold (Au) is deposited as a conducting layer and Si_3N_4/SiO_2 as an isolation layer. (Fig.4b) The surrounding Si surface is modified to be hydrophobic. The three dimensional reaction well along with the hydrophobic nature of the surrounding area allows a liquid droplet to be well contained in the working electrode. This design minimizes non-specific binding of biomolecules to other areas of the sensor chip. The Au working electrode has a monolayer of streptavidin immobilized on the surface via a thiolated-biotin SAM or through direct protein adsorption onto the gold. (Fig.4c). A sample solution containing E. coli is treated with lysis buffer, the target DNA/RNA from the E. coli cells are hybridized with both an anchoring ssDNA probe and a labelling ssDNA probe at annealing temperature (~65°C) in the presence of cell debris. (Fig.4d) The anchoring probe (conjugated to biotin) and the labelling probe (conjugated to fluorescein) recognize two distinct conservative sequences, therefore, the hybrid forms only with the specific gene segment from the target bio-agent. The oligonucleic hybrid is then immobilized through biotin-streptavidin binding onto the working electrode and unbound components are washed away. A HRP-linked anti-fluorescein antibody is then loaded onto each hybrid (Fig.4e). After addition of substrate, enzymatic reaction causes a current signal which is measured amperometrically using the three-electrode cell. (Fig.4f) The entire protocol is completed in 40 minutes.

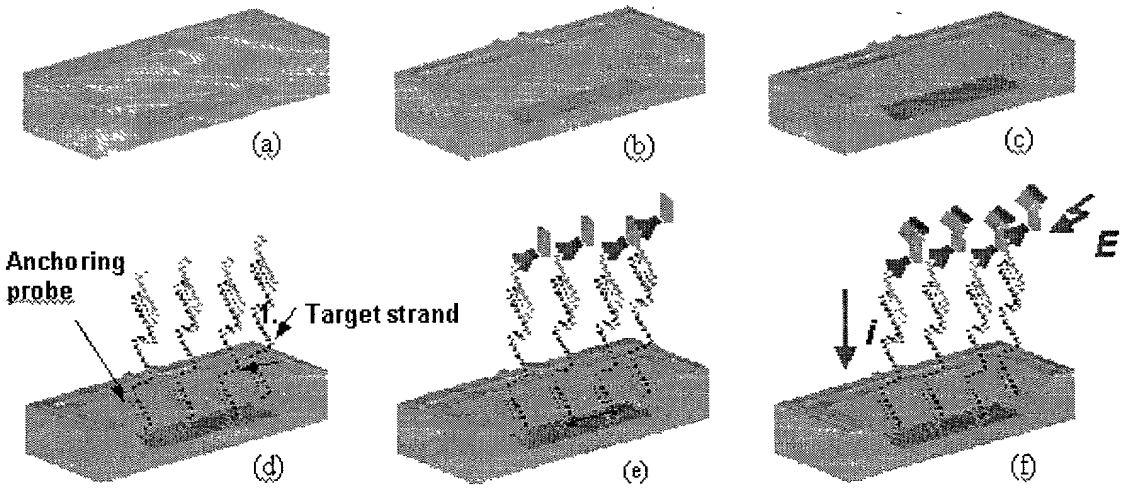

Fig. 4 Sensor unit process flow

4. Experimental Results

The SAMs on the DNA sensor were characterized by surface plasmon resonance (SPR) and atomic force microscopy (AFM) to determine whether only a monolayer was deposited and also to determine the kinetics of protein deposition. From this data, the time scale required for in situ sensor surface formation in the integrated fluidic system can be ascertained. Two different methods were used to deposit the streptavidin SAM, one using a thiolated biotin and the other using direct protein adsorption. In both cases, SPR data shows that only one monolayer was deposited on the surface (Fig.5). A crystalline monolayer of streptavidin has an expected surface coverage of 2.8 ng/mm^2 [6]. Our results indicate that a full monolayer was obtained using the thiolated biotin and ~80% coverage was obtained by direct protein absorption. Moreover, protein binding/adsorption occurs within ~10 seconds.

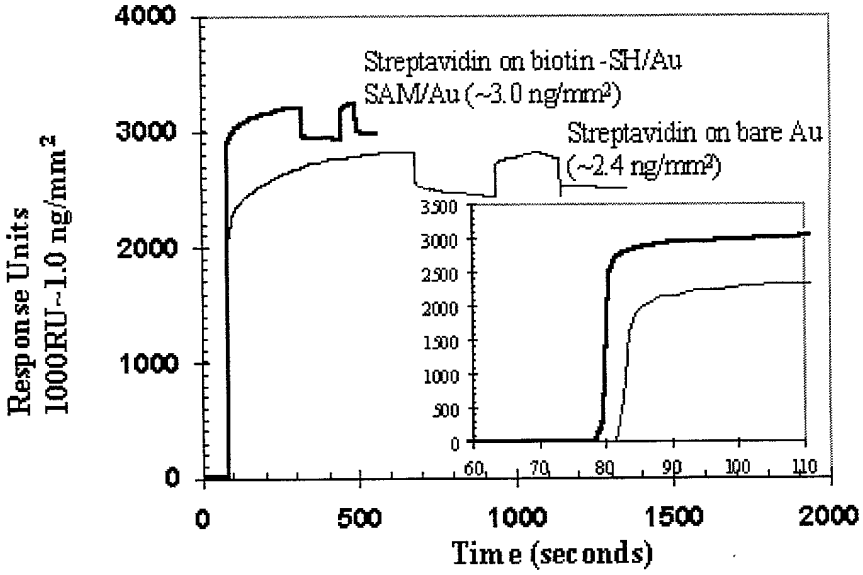

Fig. 5 Surface Plasmon Resonance of Streptavidin on Biotin-SH/Au or Bare Au

Atomic Force Microscopy (AFM) was performed in the contact mode using ultralever tips with a force of 5.0nN. The Au substrate was prepared following the method of Wagner, et al. [7]. The bare Au has topographic features <10Å (Fig.6a) and contact AFM of a "full" monolayer showed a smooth surface with evidence of protein dragging (Fig.6b). The height of protein islands on a "partial" monolayer was ~45Å, consistent with the dimensions of the streptavidin protein. The AFM observations confirm the SPR results that only one monolayer was deposited.

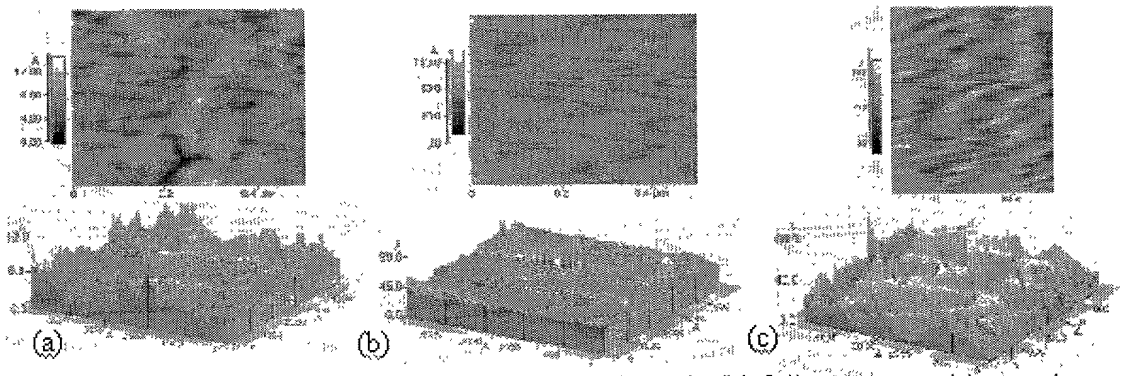

Fig. 6 AFM of SAM formation on Au. (a) bare Au only (b) full coverage with protein dragging (c) partial coverage with protein islands.

5. Conclusions

The combination of MEMS technology with established DNA technology leads to a highly specific and sensitive detector for pathogenic bacteria. Biological identification using electrochemical detection with SAMs was successfully incorporated into a silicon wafer with a sensitivity that can detect less than 1,000 E. coli cells.

References

1. Y.F. Chen, J.M Yang, J.J. Gau, C.M. Ho and Y.C. Tai. "Microfluidic System for Biological Agent Detection" The 3rd International conference on the interaction of Art and Fluid Mechanics, Zurich, Switzerland , 2000.
2. D. Ivnitski, I. Abdel-Hamid, P. Atanasov, E. Wilkins, "Review: Biosensors for Detection of Pathogenic Bacteria", *Biosensors & Bioelectronics* **14** (1999), 599-624.
3. G. Marrazza, I. Chianella, M. Mascini, "Disposable DNA Electrochemical Biosensors for Environmental Monitoring", *Analytica Chimica Acta* **387** (1999), 297-307.
4. J. Wang, et. al., "DNA Electrochemical Biosensors for Environmental Monitoring", A Review", *Analytica Chimica Acta* **347** (1997), 1-8.
5. T.Ruzgas, E. Csöregi, J. Emnéus, L Gorton, G. Marko-Varga, "Peroxidase-modified electrodes: Fundamentals and application", *Analytica Chimica Acta* **330** (1996), 123-138.
6. S.A.Darst, M. Ahlers, P.H. Meller, E.W. Kubalek, R. Blankenburg, H.O. Ribi, H. Ringsdorf, R. Kornberg, "Two-Dimensional Crystals of Streptavidin on Biotinylated Lipid Layers," *Biophys J.* **59** (1991) 387-396.
6. P. Wagner, M. Hegner, H-J Guntherodt, G. Semenza, "Formation and in Situ Modification of Monolayers Chemisorbed on Ultraflat Template-Stripped Gold Surfaces, " *Langmuir* 11 (1995) 3867-75.

ASME paper

OptimiZAtion of DNA microsensor arrays for biological detection

Abstract

This paper describes the characterization and optimization of a reusable DNA microsensor array for rapid biological agent detection developed in previous publications. (Fig.1) [1-3] This MEMS based DNA sensor utilizes a standard three-electrode electrochemical cell configuration with novel micro fabricated structure design to minimize non-specific binding. The sensor module is easily to be adapted to various protocols and can be used for rapid detection of macromolecules (DNA, RNA) from targets such as uropathogenic Escherichia coli (E. coli) in urine and microorganisms causing otitis media (middle ear infection). Less than 10^5 E. coli cells can be detected from the urine sample of a patient with urine tract infection. The sensitivity is enhanced by appropriate sensor characterization and surface modification. The total detection time including sample preparation can be reduced to 25 minutes by using a POD conjugated oligonucleotide.

Introduction

Conventional electrochemical detection is not quite compatible with MEMS technology and fabrication processes due to system requirements and configuration. An electrochemical cell must consist of at least two electrodes (working electrode, reference electrode) and an electrolyte. An electrochemical electrode is an interface at which the mechanism of charge transfer changes between electronic transport and ionic transport. [4] An electrolyte is a medium through which charge transfer can take place by the movement of ions. Electrochemical detection requires a second unvarying potential supplied by a reference electrode, forming a half battery. A typical reference electrode is Ag/AgCl. Currently, it is difficult to fabricate this reference electrode on a silicon substrate. Most MEMS based electrochemical sensors focus on micro fabrication of only the working electrode. This work investigates the characteristics and application of a MEMS based electrochemical sensor on silicon fabricated by standard MEMS processes. Testing of clinical urine samples with DNA hybridization on the electrochemical sensor demonstrates that MEMS based sensor on silicon can be used for biomedical detection.

Detection scheme

Nucleic acid molecules (RNA/DNA) from chemically disrupted target cells are hybridized with both an anchoring ssDNA probe (conjugated to biotin) and a labeling ssDNA probe (conjugated

to fluorescein) in the presence of cell debris. (Fig.2a) These two probes recognize two distinct conservative sequences, and therefore, the hybrid forms only with the specific genetic segment from the target bio-agent. The oligonucleic hybrid is then immobilized through biotin-streptavidin binding onto the working electrode and unbound components are washed away. (Fig.2b) A peroxidase (POD)-linked anti-fluorescein antibody is then loaded onto each hybrid. (Fig.2c) After addition of substrate with a mediator (tetramethylbenzidine, TMB), enzymatic reaction causes a current signal which is measured amperometrically from the REDOX reaction shown in Fig.3. The entire protocol can be completed in 40 minutes and the sensor reactivated after a cleaning process.

Sensor characterization

Most biosensor chips utilize off-chip optical detection. Our work is directed at on-chip electrochemical detection with sensor optimization and surface modification for signal-noise-ratio improvement. MEMS technology makes possible the development of miniaturized electrochemical cells since conductive metallic electrodes in small dimensions can be accurately deposited and patterned on a silicon substrate. From our studies, Au was a suitable candidate for all three electrodes (working, auxiliary, and reference), and characterization of the Au/Au/Au electrode cell using a well-known one-electron system such as ferrocene confirmed that classic reversible one-electron transfer was obtained.

Cyclic voltammetry

Cyclic voltammetry for reversible one-electron transfer of ferrocene is characterized by a peak separation of ~57 mV between the anodic and cathodic peaks, the same peak maximum, and a linear relationship between peak current vs. $[\text{scan rate}]^{1/2}$ [4]. As seen in Figure 4, voltammograms of ferrocene using MEMS based electrochemical sensor at different scan rates show the expected behavior and a plot of the peak current at peak maximum vs. $[\text{scan rate}]^{1/2}$ is linear. Further characterization of the electrochemical cell using peroxidase confirmed that enzymatic amperometry is also feasible. Cyclic voltammetry conducted on the mediator shows a two-electron redox transfer, as expected for TMB (Fig 5), and addition of the peroxidase enzyme

results in an increase in the reduction current that can be clearly measured at –0.1V bias potential.

Reduction of non-specific bonding

The sensor surface has a protein self-assembled monolayer to capture the target RNA/DNA onto the working electrode, and the SAMs have been characterized by atomic force microscopy (AFM) and surface plasmon resonance (SPR). [2] The signal-to-noise can be improved significantly by appropriate surface modifications to reduce non-specific binding. The first approach is to introduce a surface blocking protein to eliminate potential bonding sites for non-specific binding. (Fig 6) The second approach is adding a hydrophobic modification of the periphery region with silanation treatment or thin-film coatings of Teflon® or polyimide. With the hydrophilic nature of protein-covered Au working electrode, reagents will be confined to the working electrode only, minimizing deposition of enzyme to the periphery and other two electrodes. (Fig 7,8) In both cases, noise due to non-specific binding was reduced. Typically, the second approach (hydrophobic modification) is used in MEMS fabrication and the first one is incorporated into probe reagent.

Protocol simplification

Sample preparation is the most time consuming step for most biosensors. Any additional protocol steps will require more fluidic devices and a longer detection time. A simplified protocol is shown in Fig.9 whereby the step of the enzyme loading with POD conjugation onto detector DNA probe is eliminated. The hybridization condition was controlled to retain the enzymatic activity of POD after heating to 65°C. The protocol can then be shortened fro m 40 to 25 minutes while reducing the required number of reagents by one.

Result

Previous work has demonstrated the sensitivity of micro DNA sensor to be ~10^3 E. coli cells. Recent data show it has the capability to detect less than 10 E. coli cells from cell culture at stationary stage through ribosomal RNA content. The sensor was then subjected to clinical urine sample from Division of Infectious Disease at UCLA for testing. As shown in Figure 10, the

minimum detectable cell number of E. coli in urine sample is 10^5 from our preliminary result without isolation. Sensitivity with urine sample can be improved with further optimization. Another type of bacteria, Bordetella, was used as a negative control and all E. coli samples, including dilutions, have higher signal than the negative control.

Micro DNA sensor can be used for electrochemical detection without utilizing a conventional reference electrode because the bias potential is reasonable low (-0.1V) and the detection is short enough (20 seconds) to avoid the accumulation of charge at auxiliary electrode. This was confirmed with voltammograms of ferrocene and POD solution.

We have demonstrated that micro DNA sensor can be used for electrochemical detection of pathogens such as E. coli. The Au/Au/Au three electrode cells patterned on silicon by MEMS technology were successfully used in amperometric measurement of enzymatic reactions. These sensors show promise that they can be incorporated into micro total analysis system (μ-TAS) or "Lab on a Chip".

Conclusion

A micro DNA sensor was fabricated that can detect enzymatic reaction amperometrically and was characterized by using cyclic voltammetry with ferrocene and POD to demonstrate the capability of conducting electrochemical detection without a conventional Ag/AgCl electrode. Noise reduction was accomplished by surface modification and introducing blocking protein. The structural design of a well in the working electrode and surface treatment on silicon substrate enable reagent confinement over the working electrode. The reagent-electrode contact can be controlled to reduce non-specific binding, not possible with a conventional beaker setup. Urine sample testing shows this DNA sensor is suitable for clinical diagnosis with a short detection time and smaller system size.

References

1. Chen, Y.F., Yang, J.M., Gau, J.J., Ho, C.M., Tai, Y.C., 2000. "Microfluidic System for Biological Agent Detection" Proceedings of the 3rd International conference on the interaction of art and fluid mechanics, Zurich, Switzerland, 2000.

2. Gau, J.J., Lan, E. H., Dunn, B., Ho, C.M., 2000. "Enzyme-based electrochemical biosensor with DNA array chip" Proceedings of the fourth International Symposium on Micro Total Analysis Systems (μTAS), Enschede, The Netherlands.
3. Gau, J.J., Lan, E. H., Dunn, B., Ho, C.M., 2000. "A MEMS Based Amperometric Detector for E. Coli Bacteria - Using Self-Assembled Monolayers" Proceedings of the sixth World Congress on Biosensors, San Diego, USA
4. Eggins, B., 1996 *Biosensors*, John Wiley and Sons, New York.
5. Hall, E. A. H., Biosensors, Prentice Hall, Eaglewood Cliffs, NJ, pp. 97-139, 1991.

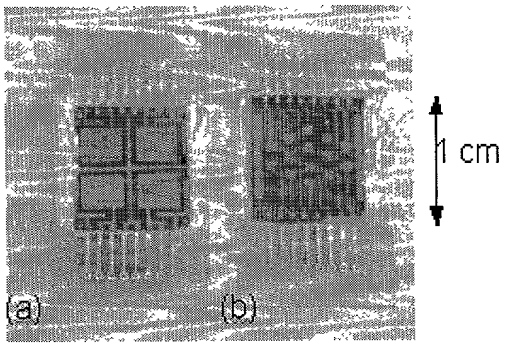

Fig.1 DNA microsensor array chip
(a) 4 sensors with surface feature to increase surface-volume-ratio
(b) 14 sensors in $1cm^2$

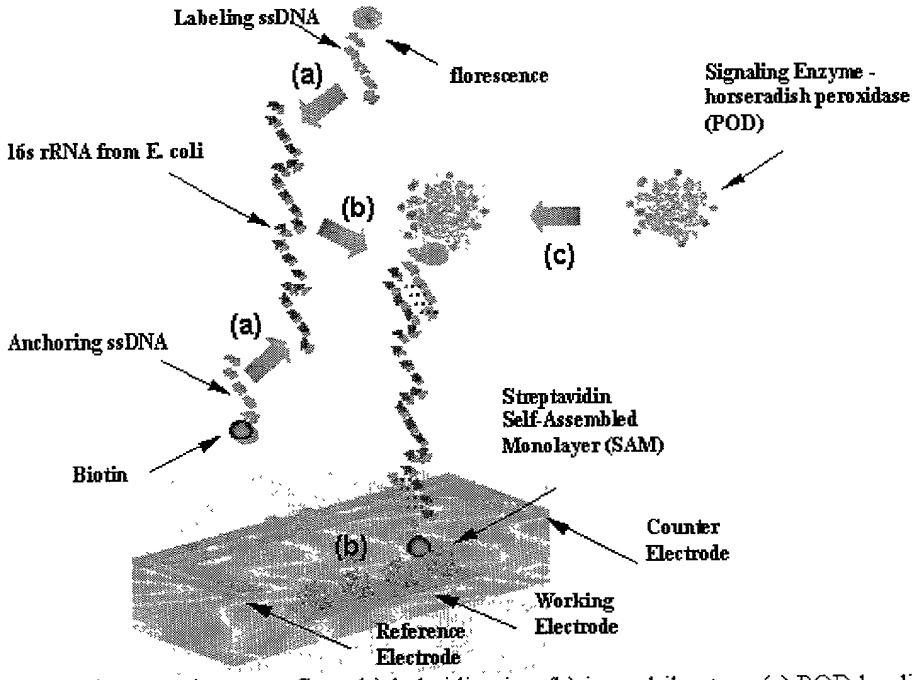

Fig.2 Sensor and protocol process flow (a) hybridization (b) immobilization (c) POD loading

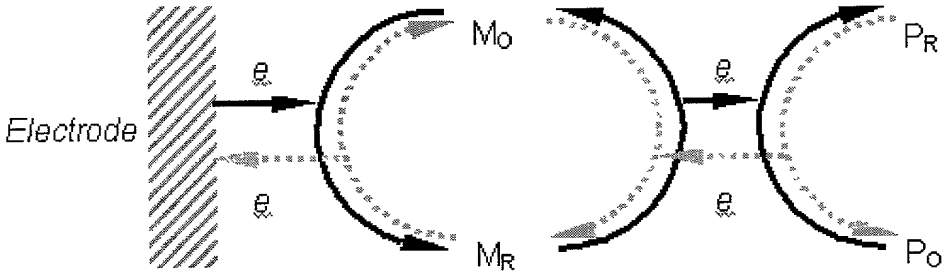

P_R: Reduced Peroxidase , P_O : Oxidized Peroxidase

M_O: Oxidized Mediator , M_R: Reduced Mediator

Fig.3 Electron transfer of enzymatic reaction of horseradish peroxidase

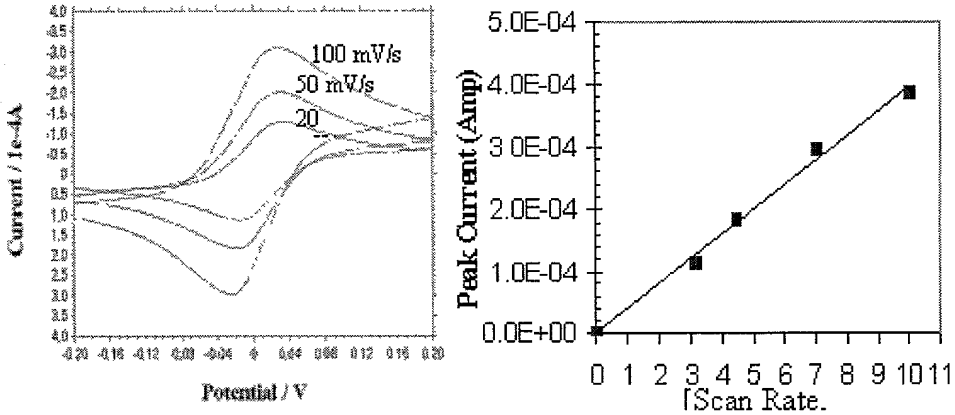

Fig.4 Sensor characterization by cyclic voltammetry

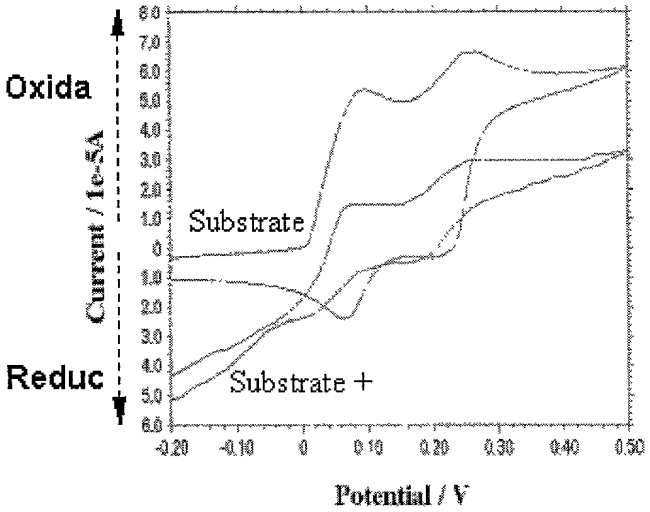

Fig.5 Sensor characterization with HRP enzymatic

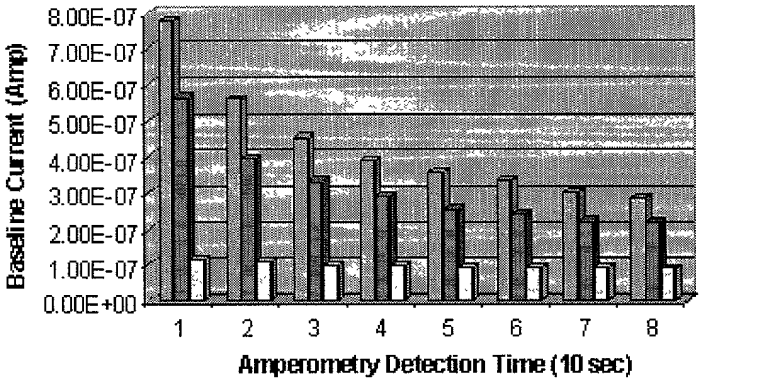

Fig.6 Noise reduction by adding blocking proteins to eliminate non-specific binding

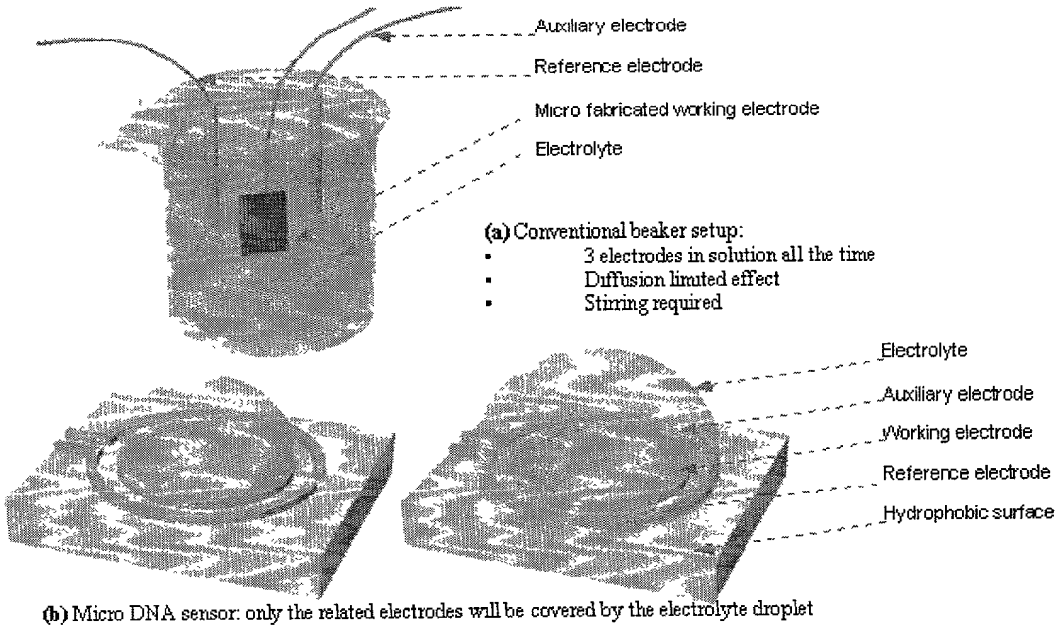

Fig.7 Comparison of electrode-reagent contact between (a) conventional and (b) micro DNA sensor

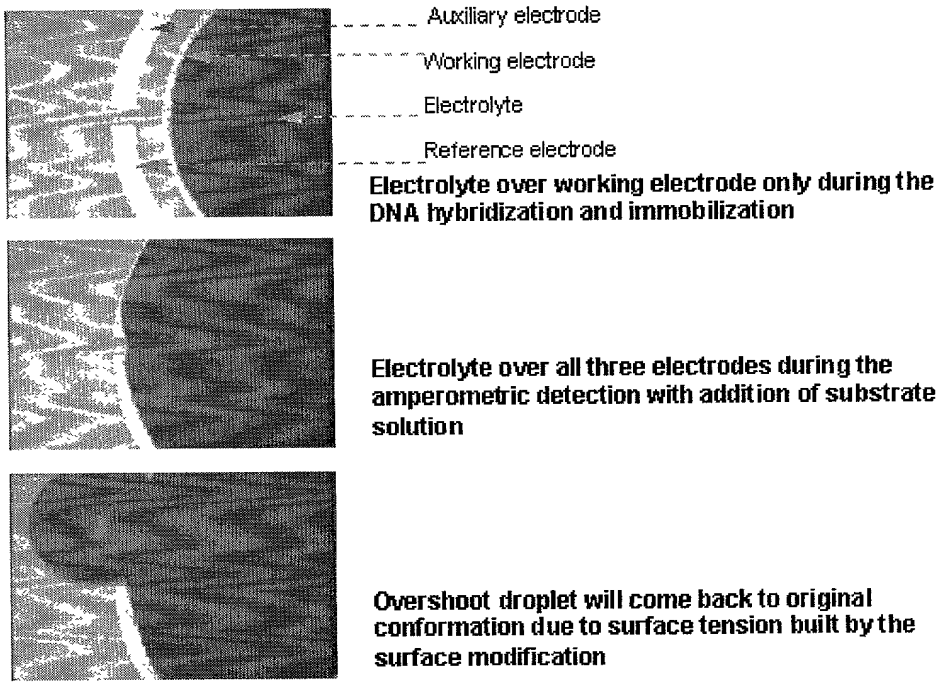

Fig.8 Image of electrolyte confinement over electrodes of micro DNA

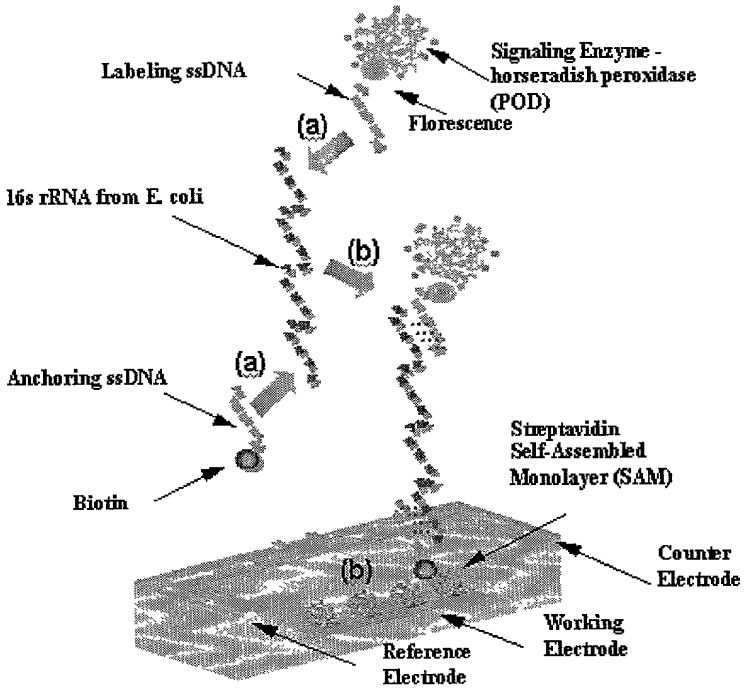

Fig.9 Simplified protocol with POD conjugated labeling probe (a) hybridization (b) immobilization

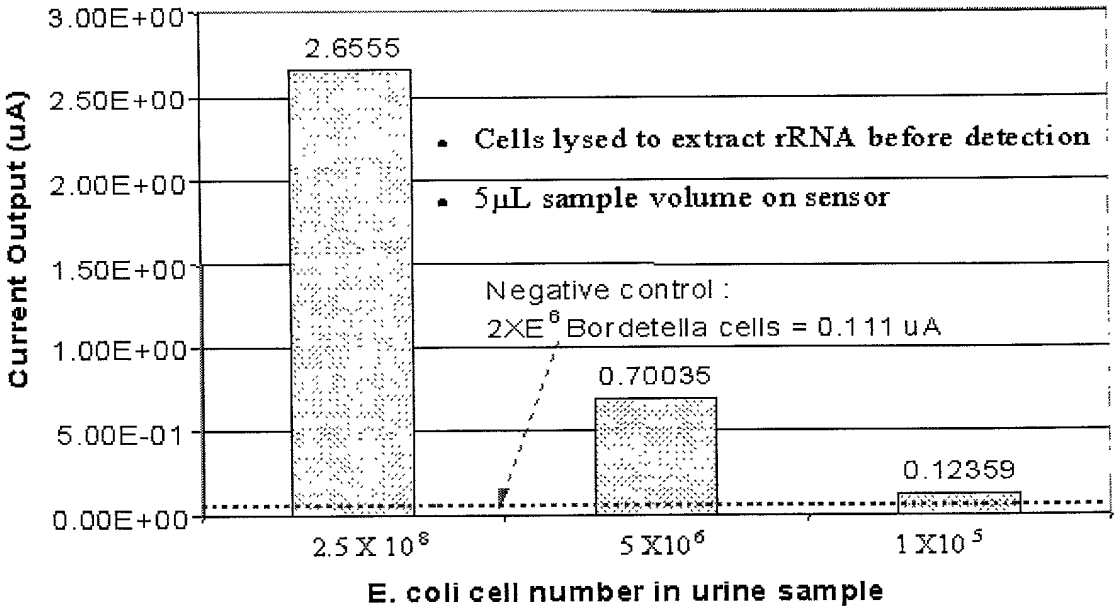

Fig.10 Sensitivity check of micro DNA sensor with urine sample

A MEMS BASED AMPEROMETRIC DETECTOR FOR E. COLI BACTERIA

USING SELF-ASSEMBLED MONOLAYERS

Abstract

We developed a system for amperometric detection of *Escherichia coli* (E. coli) based on the integration of microelectromechanical systems (MEMS), self-assembled monolayers (SAMS), DNA hybridization, and enzyme amplification. Using MEMS technology, a detector array was fabricated which has multiple electrodes deposited on a Si wafer and was fully reusable. Using SAMs, a monolayer of the protein streptavidin was immobilized on the working electrode (Au) surface to capture rRNA from E. coli. Three different approaches can be used to immobilize streptavidin onto Au, direct adsorption of the protein on bare Au, binding the protein to a biotinylated thiol SAM on Au, and binding the protein to a biotinylated disulfide monolayer on Au. The biotinylated thiol approach yielded the best results. High specificity for E. coli was achieved using ssDNA-rRNA hybridization and high sensitivity was achieved using enzymatic amplification with peroxidase as the enzyme. The analysis protocol can be conducted with solution volumes on the order of a few microliters and completed in 40 minutes. The detection system was capable of detecting 1000 E. coli cells without polymerase chain reaction with high specificity for E. coli vs. the bacteria *Bordetella bronchiseptica.*

Key words:
Microelectromechanical systems (MEMS), self-assembled monolayers (SAMs), amperometric detection, Escherichia coli bacteria, DNA hybridization

1. Introduction

A variety of biosensors, both optical and electrochemical, have been developed for the detection of pathogenic bacteria (Ivnitski, et al., 1999, 2000). While conventional methods for detecting bacteria usually involve a morphological evaluation of the organisms as well as testing their ability to grow, such methods are very time consuming and are not feasible under field conditions. The need for rapid detection as well as portability has led to the development of systems that couple pathogen recognition with signal transduction. Both optical and electrochemical detection of bacteria have been reported, although electrochemical methods have an advantage in that they are more amenable to miniaturization (Ivnitski, et. al., 1999, T. Wang, et. al., 2000). Requirements for an ideal detector include high specificity and high sensitivity

using a protocol that can be completed in a relatively short time. Moreover, systems that can be miniaturized and automated offer a significant advantage over current technology, especially if detection is needed in the field.

Microelectromechanical systems (MEMS) technology provides transducers to perform sensing and actuation in various engineering applications. The significance of MEMS technology is that it makes possible mechanical parts of micron size that can be integrated with electronics and batch fabricated in large quantities. MEMS devices are fabricated through the process of micromachining, a batch production process employing lithography. Micromachining relies heavily on the use of lithographic methods to create 3-dimensional structures using pre-designed resist patterns (or masks) and then selectively etching the undesirable parts away (Ho and Tai, 1996, 1998). MEMS is an enabling technology for making miniaturized devices, and in this work, we integrate MEMS technology with biosensing methods to detect E. coli bacteria.

One of the most effective means of achieving high specificity is to detect the bacteria's genetic material (e.g. rRNA, mRNA, denatured DNA). By choosing a single-stranded DNA (ssDNA) probe whose sequence is complementary only to the target bacteria's rRNA or ssDNA, monitoring the hybridization event allows selective sensing of target cells. To maximize sensitivity, coupling the hybridization event with an enzymatic reaction leads to signal amplification, as each substrate-to-product turnover contributes to the overall signal. Bioassays to detect DNA hybridization that are amplified by enzymatic reaction can still be completed within a reasonably short time. Finally, the miniaturization and portability inherent in electrochemical probes make them excellent candidates for incorporation in MEMS devices.

We developed a prototype amperometric detector for *Escherichia coli* (E. coli) based on combining several well-established technologies into one detection system (Chen, et. al., 2000, Gau, et. al., 2000). The technologies of MEMS, self-assembled monolayers (SAMs), DNA hybridization, and enzyme amplification all contribute to the design of a miniaturized, specific, and sensitive E. coli detector. DNA electrochemical probes have been reported previously (Wang, et al., 1997, Marrazza, et al., 1999), with graphite or carbon electrodes typically used. Commercial units for amperometric detection of DNA from E. coli using screen-printed carbon electrodes on disposable test strips are also available (Andcare Inc., Durham, NC). Screen-printing has the advantage of low cost, but achieving high dimensional precision is not easy .

Using lithography, thin films of a wide range of materials, including metals (Au, Ag) and carbon, can be accurately patterned in μm size dimensions. Moreover, SAMs is an elegant method of selectively immobilizing molecules on MEMS surfaces. The bonding of SAMs to Au, Ag and other metals has been well studied (Revell, et al., 1998, Motesharei, et al., 1998, Xia, et al., 1998, Lahiri, et al., 1999), and proteins and other biomolecules can be easily immobilized onto surfaces such as Au using SAMs (Ostuni, et al., 1999, Kane, et al., 1999, Spinke, et al., 1993, Haussling, et al., 1991). Moreover, amperometric methods using SAMs on electrodes have demonstrated the ability to detect target analytes successfully (Sun, et al., 1998, Hou, et al., 1998, Murthy, et al., 1998).

In our E. coli detection system, we take advantage of the benefits inherent in each technology. Using DNA hybridization and enzyme amplification, we achieve the required specificity and sensitivity. Using MEMS and SAMs, we fabricate a miniaturized system that can lead to a portable instrument. Finally, we demonstrate that the present detection system is applicable to a broad range of pathogenic bacteria. For example, the detection module and assay protocol can be adapted to detect uropathogenic E. coli and identification of microorganisms causing otitis media (middle ear infection).

2.Experimental

2.1.MEMS detector array

A layer of silicon dioxide (S_iO_2, 1000Å) was deposited on a bare Si wafer (prime grade, p-type <100>, thickness 500-550μm) and served as a pad layer underneath the silicon nitride (Si_3N_4, 1000Å) to release stress and improve adhesion. MEMS arrays were fabricated with working electrodes of 3.6mm x 3.6 mm etched to form wells of 350μm depth. The nitride wafer was patterned and bulk etched using KOH along [111] and [100] crystal planes, and depth of the well was controlled by KOH etching time and temperature. The 100μm wide auxiliary and reference electrodes are separated from their corresponding working electrode by 200μm. Figure 1 shows a schematic of the pattern used in generating the MEMS array. The nitride and oxide were removed by HF etching to release internal stress, and another oxide layer (5000Å) was deposited for electrical isolation. Electrodes were patterned by PR5214 photo resist reverse imaging and lift-off process with e-beam deposition of Au(2000Å)/Cr(200Å). Finally the wafer was bathed in

hexamethyldisilazane (HMDS) vapor for three minutes after ten minutes of a 150°C hot bake to generate a hydrophobic surface on the surrounding Si areas. The hydrophobic nature of the surrounding area along with the 3-dimensional nature of the working electrode allows containment of a liquid droplet in the working electrode. This design effectively minimized non-specific binding of biomolecules to other areas of the MEMS array.

2.2.Deposition of streptavidin SAMs on Au

Three different methods were used to deposit streptavidin monolayers on Au: 1) directly adsorbing streptavidin on bare Au, 2) depositing a SAM of a biotinylated thiol, biotin-DAD-C12-SH, and subsequently binding streptavidin, 3) depositing a SAM of a biotinylated disulfide, biotin-HPDP, and subsequently binding streptavidin. In all cases, the Au surfaces were cleaned with concentrated "Piranha" solution (70 vol% H_2SO_4, 30 vol% H_2O_2) and thoroughly rinsed with deionized water. For depositing streptavidin on bare Au, a solution of 1.0 mg/ml streptavidin (Sigma Chemical Co., S0677) in 0.02M Na phosphate buffer, 0.15M NaCl, pH 7.2, was placed on the surface, allowed to stand for 10 minutes, and rinsed with deionized water. For depositing a SAM of biotin-DAD-C12-SH (12-mercapto(8-biotinamide-3,6-dioxaoctyl)dodecanamide, Roche GmBH, Germany), the procedure of Spinke, et al. (1993) was used wherein samples were incubated for ~18 hours in a 50μM solution of biotin-DAD-C12-SH in ethanol with $4.5x10^{-4}$M 11-mercapto-1-undecanol (Aldrich Chemical Co., 44,752-8) and rinsed with ethanol and water. The biotin-coated Au surfaces were then exposed to a 1.0 mg/ml streptavidin solution for ~10 minutes and rinsed again with water. For depositing a SAM of biotin-HPDP, (N-[6-(biotinamido)hexyl]-3'-(2'-pyridyldithio)propionamide, Pierce Inc., 21341) samples were incubated for ~18 hours in a 50μM biotin-HPDP solution in ethanol (with or without $4.5x10^{-4}$M mercaptopropanol) and rinsed with ethanol and water. The surfaces were then exposed to a 1.0 mg/ml streptavidin solution for ~10 minutes and rinsed again with water.

2.3 Assay protocol for amperometric detection of E. coli

The assay protocol was conducted as follows: 1) 50 μl of lysis reagent (Andcare Inc., 4002-11) was added to a 250 μl sample of bacteria in culture media and incubated for 5 min. at room temperature, 2) 100 μl of probe solution (Andcare Inc., 4002-13) was then added and the mixture was incubated for 10 min. at 65°C, 3) 5 μl of the lysed E. coli/probe solution mixture was placed

on the streptavidin coated working electrode of the MEMS detector array and incubated for 10 min. at room temperature, 4) the MEMS detector array was washed with biotin wash solution (Kirkegaard and Perry Laboratories, 50-63-06), 5) 5 µl of Anti-Fl-POD (Anti-fluorescein peroxidase, 150U, Roche Inc., 1 426 346), diluted to 0.75U/ml or 0.15 U/ml with diluant (Andcare Inc., 4002-14) was placed on the working electrode and incubated for 10 minutes at room temperature, 6) the MEMS array chip was washed again with wash solution, 7) 10 µl of K-blue substrate (Neogen Corp., 300176) was placed on the detector array in such a way that all three electrodes (working, auxiliary, reference) were covered by the substrate solution, and 8) electrochemical measurements were immediately taken. The entire protocol was completed within 40 minutes. Amperometric current vs. time was measured using a CH Instruments 660A electrochemical workstation with picoamp booster and faraday cage. Samples on the MEMS detector array were measured sequentially. The voltage was fixed at –0.1V (vs. reference), and the cathodic current at 20 seconds was taken as the amperometric signal. At 20 seconds, current values reached steady-state. Cell concentration (cell number) was determined using serial dilutions and culture plate counting.

2.4 Characterization of Self-Assembled Monolayers

The performance of the detector depends heavily on the properties of the immobilized streptavidin monolayer. We performed surface plasmon resonance (SPR, Biacore X system, Biacore, Inc.) and atomic force microscopy (AFM) to characterize the monolayers. For SPR studies of streptavidin binding to bare Au, bare Au chips (J1 sensor chips) were used. For studies of streptavidin binding to biotin-DAD-C-12-SH/Au or biotin-HPDP/Au, the biotin SAM was deposited on the bare Au chips as previously described before the SPR experiments. For best results, new chips were cleaned with diluted H_2SO_4/H_2O_2 solution for ~2 min. before performing SPR with bare Au or depositing the biotin SAM. In all cases, 1.0 mg/ml streptavidin in 0.02M Na phosphate, 0.15 M NaCl, pH 7.2 buffer was used. In adsorption experiments with streptavidin on bare Au, flow rates ranged from 1 to 5 µl/min. In the experiments with streptavidin and biotin-DAD-C12-SH/Au, flow rates ranged from 10 to 25 µl/min. In experiments with streptavidin and biotin-HPDP/Au, flow rates ranged from 5 to 10 µl/min. In the desorption experiments, 25 µl of the following solutions were flowed sequentially through

the channels at 25 µl/min (total exposure time of 1 min.): 1.0M KCl, 8M urea, 0.5% SDS, 0.1M HCl, 0.1M NaOH, and 40 vol% formamide.

AFM (AutoProbe CP, Thermomicroscopes, Inc.) was performed in the contact mode using ultralever tips with a force of 5.0nN. To ensure a flat Au surface, the method of Wagner, et al. (1995) was used wherein Au was first deposited via e-beam evaporation on mica and then transferred to Si. In our case, the mica was cleaved to cleanly remove it from the Au without the use of solvent.

3 Results

3.1 Microelectromechanical system (MEMS)

Figure 2 shows a photograph of the MEMS detector array. Sixteen working electrodes with their corresponding auxiliary and reference electrodes were patterned in a 2.8 cm x 2.8 cm area. The detector array was fully reusable as the surface can be cleaned using H_2SO_4/H_2O_2 solutions. We have reused the same MEMS detector array multiple times by appropriately cleaning the surface and redepositing the SAMs on the working electrode.

3.2 E. coli Detection Using DNA Hybridization

In our MEMS system, E. coli detection is based on DNA hybridization followed by enzymatic reaction. A schematic illustrating the electrode surface is shown in Figure 3. A streptavidin monolayer is immobilized on the Au working electrode surface to capture the rRNA from E. coli. Two ssDNA segments are used in this system. The capture ssDNA, which is conjugated to biotin for streptavidin binding, hybridizes to one end of the E. coli rRNA. The detector ssDNA, which is conjugated to fluorescein for binding to anti-fluorescein linked to the enzyme peroxidase (POD), hybridizes to the other end of the E. coli rRNA. The capture and detector ssDNA recognize two distinct conservative sequences, and therefore, the hybrid forms only with the specific gene segment from E. coli. The oligonucleic hybrid is immobilized through biotin-streptavidin binding onto the Au working electrode and unbound components are washed away. Streptavidin binds biotin with unusually high affinity ($K_d \sim 10^{-15}$M) (Weber, et. al., 1989). After loading the POD onto the hybrid (through Anti-Fl-fluorescein binding), substrate is added and enzymatic reaction is detected amperometrically. The substrate solution contains both the substrate H_2O_2 and a mediator, 3,3',5,5'tetramethylbenzidine (TMB). The enzyme and electrode reactions are depicted in Figure 4.

3.3 Streptavidin Self Assembled Monolayers for rRNA Capture

We used three different approaches to immobilize a streptavidin monolayer on the electrode surface, as shown in Figure 5. In the first approach, a streptavidin monolayer was deposited on bare Au via protein adsorption. In the second approach, a SAM of biotin was deposited on the Au using a biotinylated thiol and streptavidin was subsequently bound to the biotin. In the third approach, a SAM of biotin was deposited on the Au using a biotinylated disulfide and streptavidin was subsequently bound to the biotin.

3.4 Characterization of Streptavidin Monolayers

The streptavidin monolayers were characterized using both surface plasmon resonance (SPR) and atomic force microscopy (AFM). SPR has been demonstrated to be a viable technique for monitoring interactions of molecules with metallic (Au, Ag) thin films at the solution-metal interface. This technique can be used to estimate the thickness of a deposited layer as well as to measure the kinetics of association and dissociation (Haussling, et al., 1991, Spinke, et al., 1993, Sigal, et al., 1996, Rao, et al., 1999, Jung, et al., 1999). We performed SPR to monitor deposition of streptavidin on Au using all three approaches. SPR results are shown in Figure 6. Based on calibrations by the manufacturer (Biacore), 1000 resonance units (RU) in the SPR signal is equivalent to a change of ~1 ng/mm^2 in surface protein concentration. Streptavidin has dimensions of ~ 55 x 45 x 50 Å (Darst, et al., 1991). A full monolayer of streptavidin has an expected density of ~2.8 ng/mm^2, calculated based on a 2-dimensional crystalline monolayer (Jung, et al., 1999, Darst, et al., 1991). From Figure 6, essentially a complete monolayer of streptavidin was deposited on the biotinylated thiol SAM/Au (~3000 RU), ~80% "coverage" was obtained with streptavidin deposited on bare Au (~2400 RU), and ~52% "coverage" was obtained with streptavidin deposited on the biotinylated disulfide SAM/Au (~1550 RU). For the biotinylated disulfide, the presence of mercaptopropanol in the solution had a negligible effect on surface coverage as SPR signal increased only ~10% (~1700 RU, data not shown). In all cases, additional protein deposition upon a second injection of protein solution was minimal. Moreover, flow rates had negligible effects on the rate or amount of protein deposited. The SPR results indicate that in all three approaches, only a monolayer of streptavidin, and not multilayers, was deposited on the Au. Finally, these results establish that most of the

streptavidin-biotin binding and streptavidin adsorption on bare Au occurs within seconds and can be completed on the order of minutes.

We performed experiments to determine whether streptavidin can be desorbed, i.e. whether streptavidin can be dissociated from the bare Au or from binding to biotin to regenerate the surface. Table I lists the loss in SPR signal (RU) after treatment with various reagents that are known to dissociate protein-ligand binding and/or denature proteins. As seen in Table I, only 8M urea, 0.5% SDS, and 0.1M NaOH were somewhat effective in desorbing streptavidin from the surface. 1.0M KCl, 0.1M HCl, and 40% formamide were not effective. Streptavidin could not be completely desorbed by any of the reagents, and some protein remained after subjecting the surface to all reagents. These results show that streptavidin had rather good binding to both the biotin SAM as well as to bare Au and that the streptavidin monolayers were relatively stable.

The use of AFM enables us to further characterize the surface by imaging streptavidin directly adsorbed on bare Au. Bare Au had topographic features <10 Å, whereas protein islands on a "partial" monolayer was ~45 Å, consistent with the dimensions of streptavidin (Figure 7). The AFM results confirm the SPR findings that only one monolayer was deposited on the Au. AFM in the contact mode for a "full" protein monolayer showed a featureless surface with evidence of protein dragging (data not shown), and therefore, did not provide any additional information as to surface coverage. As previously reported, monolayer deposition is also obtained when using biotinylated SAMs and subsequently binding streptavidin (Spinke, et. Al., 1993, Jung, et. Al., 1999).

3.5 Electrochemical Measurements with MEMS Detector Array

In our MEMS detector array, we used a three-electrode system with Au for all three electrodes, i.e. working, auxiliary, and reference electrodes. Typically, Ag/AgCl or saturated calomel electrode (SCE) is used as the reference electrode so that reversible oxidation/reduction at fixed potential occurs at the reference electrode. In our MEMS detector array, however, we used Au as the reference electrode to simplify fabrication and to permit a fully reusable array. Maintaining a constant potential is made possible by the use of a 3-electrode system (vs. a 2-electrode system). In our particular application where the reduction of TMB was monitored, Au can be successfully used as the reference electrode because a low voltage difference (-0.1V) was maintained for short periods of time (<1 min).

We characterized the Au/Au/Au electrode system for electrochemical detection by two separate experiments. In the first experiment, a ferrocene film was placed on the electrodes and cyclic voltammetry was conducted to monitor the redox reactions. Cyclic voltammetry for a classic reversible one electron transfer is characterized by a peak separation of ~57 mV between the anodic and cathodic peaks, the same peak currents at peak maximum, and a linear relationship between peak current vs. [scan rate]$^{1/2}$ (Hall, 1991). Figure 8 shows the voltammograms obtained with ferrocene at different scan rates. As seen in Fig. 8, classical redox behavior was observed and a plot of the peak current vs. [scan rate]$^{1/2}$ is linear (Figure 9).

In a second experiment with the Au/Au/Au electrode system, cyclic voltammetry was conducted on the substrate solution only (H_2O_2 + TMB) and then again on the same solution with POD enzyme. Cycling between –0.2V to +0.50V at a scan rate of 10mV/s, the substrate solution showed the two electron redox behavior of TMB (Figure 10). The addition of POD to the substrate solution resulted in an increase in the reduction current. A constant potential of –0.10V (vs. reference) was then selected for measurement of POD enzymatic activity. At this potential, the current background was near zero and no substrate oxidation occurred. This potential was optimum for enzymatic activity determination in which a small amount of product (oxidized TMB) was to be measured in the presence of high concentrations of substrate.

3.6 Detection of E. coli

For the amperometric detection of E. coli rRNA, we first compared the performance of the three different streptavidin monolayer surfaces. Streptavidin was immobilized on the Au using the three different approaches previously described, and the assay protocol was conducted for the bacteria E. coli and *Bordetella bronchiseptica* (Bordetella). Since the ssDNA probes are specific for E. coli, the Bordetella bacteria served as the negative control sample. The purpose of this experiment was to compare the efficacy of the immobilized streptavidin to capture the biotin-rRNA-POD hybrid. Two concentrations of E. coli were used, with one sample having ten times the concentration of the other. Moreover, the signal from the Bordetella indicates the level of non-specific binding or the achievable "baseline". Results from this experiment are shown in Figure 11. Since the same bacterial solutions (E. coli or Bordetella) were used, a direct comparison can be made of the different surfaces. As seen in Fig. 11, streptavidin immobilized

via the biotinylated thiol to Au was the best condition for E. coli detection. Using the biotin-thiol SAM, we obtained good signals for the E. coli while achieving a low baseline signal from the Bordetella. For streptavidin immobilized via the biotin-disulfide to Au, current signals for the E. coli (both concentrations) were significantly lower, while the baseline was the same as that for the biotin-thiol/streptavidin. In the case of streptavidin directly adsorbed to Au, the signal from the Bordetella was much higher, indicating a higher level of non-specific binding of POD to the surface.

After ascertaining Au/biotin-SH/streptavidin to be the optimal streptavidin surface, we repeated the protocol using E. coli and Bordetella to determine the sensitivity of our system. We immobilized streptavidin via the biotin-SH SAM and performed the assay on a series of E. coli dilutions along with Bordetella as the negative control. Results are shown in Figure 12. The data indicate that as few as 1000 E. coli cells can be detected using our MEMS system. As expected, current signal increased as a function of increasing number of E. coli cells in the sample solution. Moreover, by lowering the POD concentration used in the assay protocol (from 0.75 U/ml to 0.15 U/ml), we achieved better discrimination in signals at lower E. coli cell numbers (Figure 13). As seen in Fig. 13, the current signal for 1000 E. coli cells was more than twice that for 2.5×10^5 Bordetella cells. The results using our MEMS system confirm that E. coli bacteria was successfully detected using amperometry and SAMs to capture the bacteria rRNA.

4. Discussion

Our results show that combining MEMS technology with SAMs, DNA hybridization, and enzymatic amperometry leads to a highly specific and sensitive electrochemical detector for bacteria such as E. coli. The contribution from each component is critical to the overall success of the system. MEMS technology enables an array of multiple three-electrode "cells" to be deposited on a Si wafer, and the MEMS detector array we have described is fully reusable as the SAMs can be removed and the Au surfaces regenerated with appropriate cleaning. Moreover, with micromachined channels, valves, pumps and integrated electronics, one can fully automate the sample preparation and assay protocol.

SAMs provide an effective means of functionalizing the Au working electrode to immobilize capture biomolecules, for example, streptavidin. DNA hybridization permits high specificity for pathogenic bacteria as the sequence of the ssDNA probes can be carefully selected to

complement only the target. Coupling the hybridization event with an enzymatic reaction provides signal amplification and enhances the sensitivity. Finally, by using electrochemical transduction, a miniaturized portable system with minimum power consumption can be developed.

Rapid detection and a portable instrument is desirable for pathogen sensing. We have demonstrated that detection can be achieved within ~40 minutes using this system. Due to the small dimensions and small sample volumes, it is possible to further reduce the assay time by reducing the incubation times (10 minutes) currently used for DNA hybridization and enzyme binding. A distinct advantage of MEMS is the ability to use very small volumes (a few μl) and electrode surface areas (currently 0.13 cm^2 for the working electrode, <0.02 cm^2 for the auxiliary and reference electrodes). Our results show that as few as ~10^3 cells can be detected using this system without polymerase chain reaction (PCR). Due to the small volumes and working electrode surface area in the MEMS system, reporting the detection limit in terms of absolute cell numbers is more appropriate than reporting the detection limit in terms of cell concentration (cells/ml). Detection limits on the order of 10^2 to 10^3 cells/ml have been reported, however, sample volumes of ~ 1.0 ml with working electrode surface areas ~1cm^2 were typically used (Abdel-Hamid, et. al., 1998, 1999). In amperometric enzyme immunofiltration assays, the signal was more than an order of magnitude less when using a 0.1 ml sample than when using a 1.0 ml sample (Abdel-Hamid, 1999).

Results from amperometric experiments to detect E. coli rRNA have shown that the streptavidin monolayer immobilized via the biotinylated thiol SAM approach yielded the best results. This finding is not surprising as SPR data indicated the highest streptavidin surface density or "coverage" when using the biotinylated thiol. It is likely that a well-ordered self-assembled monolayer is formed only with the biotinylated thiol, leading to highest streptavidin surface density. In the case of the biotinylated disulfide, although attachment of the biotin to the Au surface occurs via the Au-S bond, the additional organic group probably hinders the formation of a densely packed monolayer. Streptavidin immobilized via direct adsorption to Au resulted in significantly higher non-specific binding of the POD enzyme to the working electrode. Protein adsorption to Au has been well known as colloidal Au particles attached to various proteins (e.g. streptavidin, immunoglobulins) are commercially available (Nanoprobes, Inc., Yaphank, NY).

Streptavidin does not contain cysteine or methionine residues (Weber, et. al., 1989) and therefore, does not attach to Au via an Au-S bond. Protein adsorption to Au can occur via interaction of carboxylate groups with Au (Ooka, et. al., 1999) and is the likely mechanism for streptavidin-Au attachment. Although a streptavidin monolayer can be attached to Au via direct adsorption, whether self-assembly or molecular ordering occurs is questionable. SPR desorption experiments showed the streptavidin-Au attachment to be as robust as streptavidin-biotin binding, i.e. the amount of streptavidin removed due to urea, SDS, and NaOH were similar for streptavidin directly adsorbed on Au as compared to streptavidin attached to biotin. When conducting the assay protocol for E. coli, however, sample solutions contained oligonucleotides as well as cell debris from the lysed E. coli. Our data suggests that the presence of other proteins and biomolecules accelerated the desorption of streptavidin from Au, leading to increased non-specific binding of the enzyme POD to the surface.

5. Conclusions

E. coli bacteria were successfully detected by incorporating MEMS with SAMs, DNA hybridization, and enzyme amplification. We demonstrated a MEMS-based detection system that is specific for E. coli and capable of detecting 1000 cells without PCR. The process time can be 40 minutes or less. Moreover, the assay can be conducted with solution volumes on the order of a few microliters. The integration of SAMs, DNA hybridization, and enzyme amplification methodologies with MEMS technology makes possible a new generation of devices for pathogenic detection.

References

Abdel-Hamid, I. Ivnitski, D., Atanasov, P., Wilkins, E., 1998. Fast Amperometric Assay for E. coli 0157:H7 using partially immersed immunoelectrodes. Electroanalysis 10 (11), 758-763.

Abdel-Hamid, I., Ivnitski, D., Atanasov, P., Wilkins, E., 1999. Flow-through immunofiltration assay system for rapid detection of E. coli 0157:H7. Biosens. Bioelect. 14, 309-316.

Chen, Y.F., Yang, J.M., Gau, J.J., Ho, C.M., Tai, Y.C., 2000. Microfluidic System for Biological Agent Detection. Proceedings of the 3rd International conference on the interaction of art and fluid mechanics, Zurich, Switzerland.

Darst, S.A., Ahlers, M., Meller, P.H., Kubalek, E.W., Blankenburg, R., Rib, H.O., Ringsdorf, H., Kornberg, R.D., 1991. Two-dimensional crystals of streptavidin on biotinylated lipid layers and their interactions with biotinylated macromolecules. Biophys. J. 59, 387-396.

Gau, J.J., Lan, E. H., Dunn, B., Ho, C.M., 2000. Enzyme-based electrochemical biosensor with DNA array chip. Proceedings of the fourth International Symposium on Micro Total Analysis Systems (μTAS), Enschede, The Netherlands.

Hall, E.A.H., 1991. Biosensors. Prentice Hall, Englewood Cliffs, New Jersey.

Haussling, L., Ringsdorf, H., Schmitt, F.J., Knoll, W., 1991. Biotin-functionalized self-assembled monolayers on gold: surface plasmon optical studies of specific recognition reactions. Langmuir 7 (9), 1837-1840.

Ho, C.M., Tai, Y.C., 1996. Review: MEMS and its applications for flow control. J. Fluids Eng. 118, 437-447.

Ho, C.M., Tai, Y.C., 1998. Micro-electro-mechanical systems (MEMS) and fluid flows. Ann. Rev. Fluid Mech. 30, 579-612.

Hou, S.F., Yang, K.S., Fang, H.Q., Chen, H.Y., 1998. Amperometric glucose enzyme electrode by immobilizing glucose oxidase in multilayers on self-assembled monolayers surface. Talanta 47, 561-567.

Ivnitski, D., Abdel-Hamid, I., Atanasov, P., Wilkins, E., 1999. Biosensors for detection of pathogenic bacteria. Biosens. Bioelect. 14, 599-624.

Ivnitski, D., Abdel-Hamid, I., Atanasov, P., Wilkins, E., Stricker, S., 2000. Application of Electrochemical Biosensors for Detection of Food Pathogenic Bacteria. Electroanalysis 12 (5), 317-325.

Jung, L.S., Nelson, K.E., Campbell, C.T., Stayton, P.S., Yee, S.S., Perez-Luna, V., Lopez, G.P., 1999. Surface plasmon resonance measurement of binding and dissociation of wild-type and mutant streptavidin on mixed biotin-containing alkylthiolate monolayers. Sensors Actuators B 54, 137-144.

Kane, R.S., Takayama, S., Ostuni, E., Ingber, D.E., Whitesides, G.M., 1999. Patterning proteins and cells using soft lithography. Biomaterials 20, 2363-2376.

Lahiri, J., Ostuni, E., Whitesides, G.M., 1999. Patterning Ligands on Reactive SAMs by Microcontact Printing. Langmuir 15 (6), 2055-2060.

Marrazza, G., Chianella, I., Mascini, M., 1999. Disposable DNA electrochemical biosensors for environmental monitoring. Anal. Chim. Acta 387, 297-307.

Motesharei, K., Myles, D.C., 1998. Molecular recognition on functionalized self-assembled monolayers of alkanethiols on gold. J. Am. Chem. Soc. 120 (29), 7328-7336.

Murthy, A.S.N, Sharma, J., 1998. Glucose oxidase bound to self-assembled monolayers of bis(4-pyridyl) disulfide at a gold electrode: Amperometric determination of glucose. Anal. Chim. Acta 363, 215-220.

Ooka, A. A., Kuhar, K.A., Cho, N., Garrell, G.L., 1999. Surface Interactions of a Homologous Series of a,w-Amino Acids on Colloidal Silver and Gold. Biospectroscopy 5, 9-17.

Ostuni, E., Yan, L., Whitesides, G.M., 1999. The interaction of proteins and cells with self-assembled monolayers of alkanethiolates on gold and silver. Colloids Surfaces B 15, 3-30.

Rao, J., Yan, L., Xu, B., and Whitesides, G.M., 1999. Using surface plasmon resonance to study the binding of vancomycin and its dimer to self-assembled monolayers presenting D-Ala-D-Ala. J. Am. Chem. Soc. 121 (11), 2029-2030.

Revell, D.J., Knight, J.R., Blyth, D.J., Haines, A.H., Russell, D.A., 1998. Self-assembled carbohydrate monolayers: formation and surface selective molecular recognition. Langmuir 14 (16) 4517-4524.

Sigal, G.B., Bamdad, C., Barberis, A., Strominger, J., and Whitesides, G.M., 1996. A self-assembled monolayer for the binding and study of histidine-tagged proteins by surface plasmon resonance. Anal. Chem. 68, 490-497.

Spinke, J., Liley, M., Guder, H.J., Angermaier, L., Knoll, W., 1993. Molecular recognition at self-assembled monolayers: the construction of multicomponent multilayers. Langmuir 9 (7), 1821-1825.

Sun, X., He, P., Liu, S., Ye, Jiannog, Fang, Y., 1998. Immobilization of single-stranded deoxyribonucleic acid on gold electrode with self-assembled aminoethanethiol monolayer for DNA electrochemical sensor applications. Talanta 47, 487-495.

Wagner, P., Hegner, M., Guntherodt, H.J., Semenza, G., 1995. Formation and in situ modification of monolayers chemisorbed on ultraflat template-stripped gold surfaces. Langmuir 11, 3867-3875.

Wang, T.H., Chen Y.F., Masset S., Ho, C.M., Tai, Y.C., 2000. Molecular beacon based micro biological detection system. Proceedings of the 2000 International Conference on Mathematics and Engineering Techniques in Medicine and Biological Sciences (METMBS'2000) Las Vegas, Nevada.

Wang, J., Rivas, G., Cai, X., Palecek, E., Nielsen, P., Shiraishi, H., Dontha, N., Luo, D., Parrado, C., Chicharro, M., Farias, P.A.M, Valera, F.S., Grant, D.H., Ozsoz, M., Flair, M.N., 1997. DNA electrochemical biosensors for environmental monitoring. A Review. Anal. Chim. Acta 347, 1-8.

Weber, P.C., Ohlendorf, D.H., Wendoloski, J.J., Salemme, F.R., 1989. Structural Origins of High-Affinity Biotin Binding to Streptavidin. Science 243, 85-88.

Xia, Y., Whitesides, G.M., 1998. Soft Lithography. Angew. Chem. Int. Ed. 37, 550-575.

Table I

Comparison of various reagents for the desorption of streptavidin from surface as determined by surface plasmon resonance

Treatment Condition	Streptavidin on Bare Au ~2400 RU deposited Loss in Signal (RU)		Streptavidin on biotin-DAD-C12-SH/Au ~3000 RU deposited Loss in Signal (RU)		Streptavidin on biotin-HPDP/Au ~1700 RU deposited Loss in Signal (RU)	
1 0 M KCl	0	0	0	0	0	0
8M Urea	280 (12%)	370 (15%)	790 (26%)	1050 (35%)	360 (21%)	300 (18%)
0 5% SDS	40 (2%)	150 (6%)	390 (13%)	230 (8%)	330 (19%)	690 (40%)
0 1M HCl	0	0	0	0	0	0
0 1 M NaOH	400 (17%)	550 (23%)	630 (21%)	690 (23%)	400 (24%)	200 (12%)
40% Formamide	0	0	0	0	0	0

Figure 1

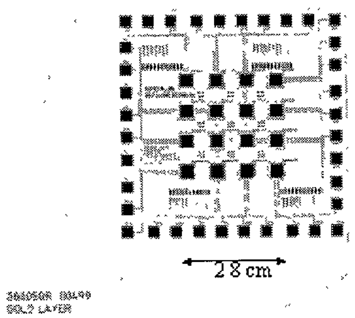

Figure 2

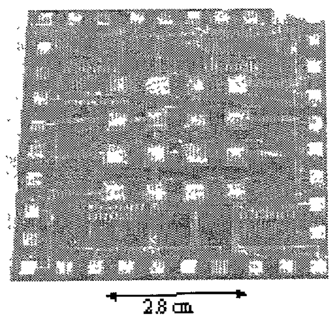

Figure 3

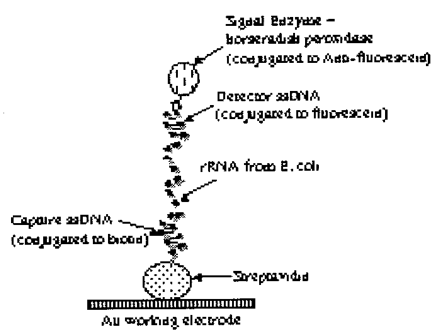

Figure 4

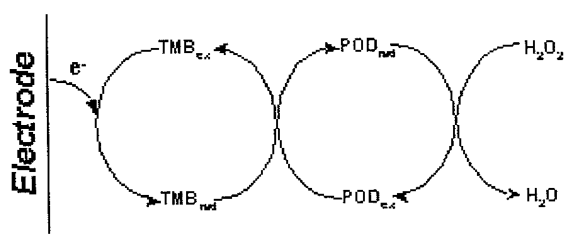

Figure 5

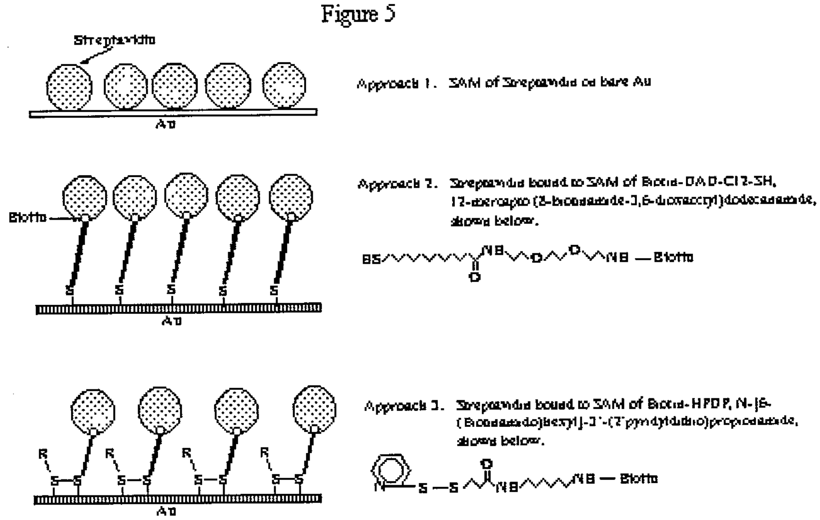

Figure 6

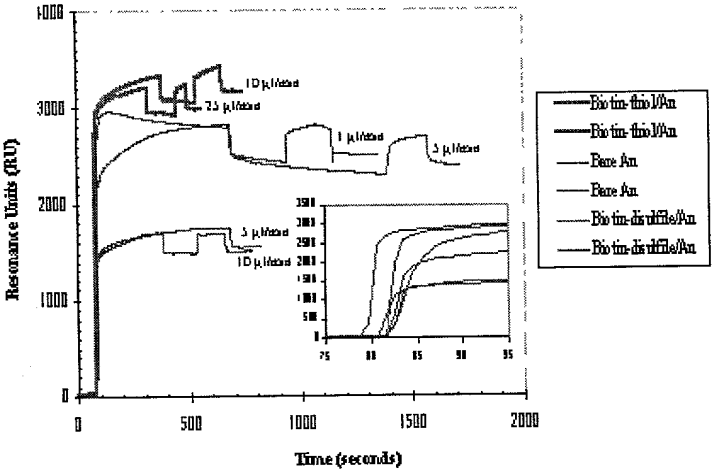

Figure 7

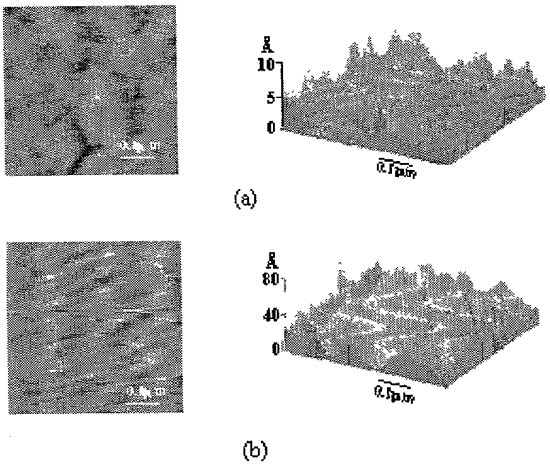

Figure 8

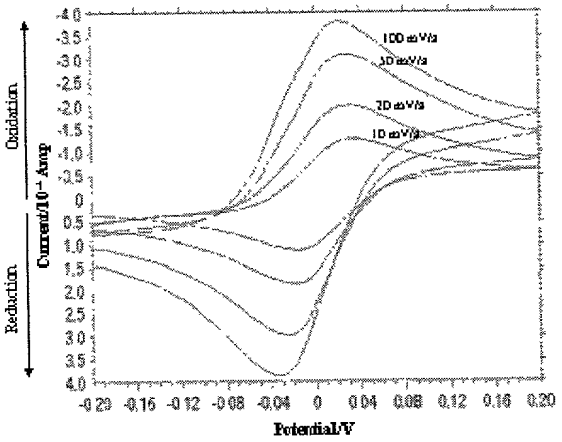

Figure 9

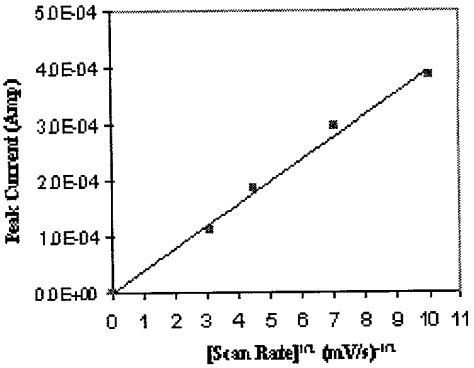

Figure 10

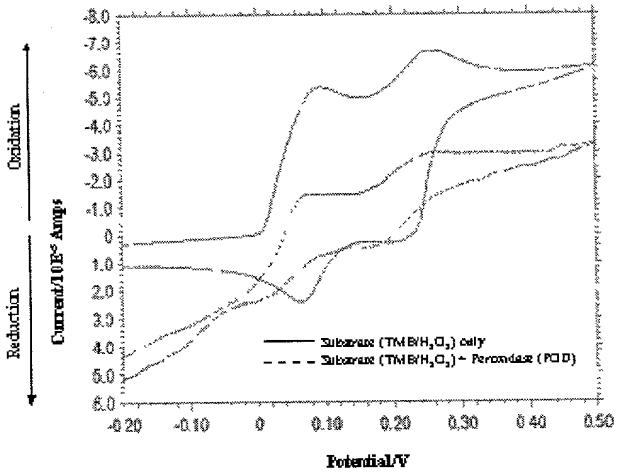

Figure 11

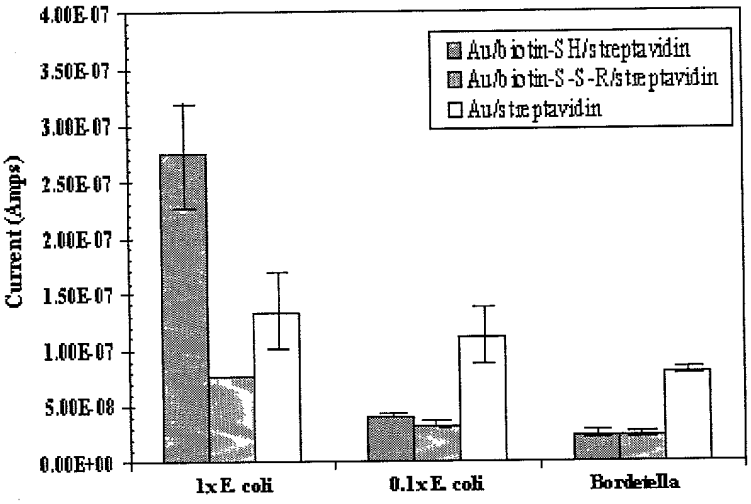

Figure 12

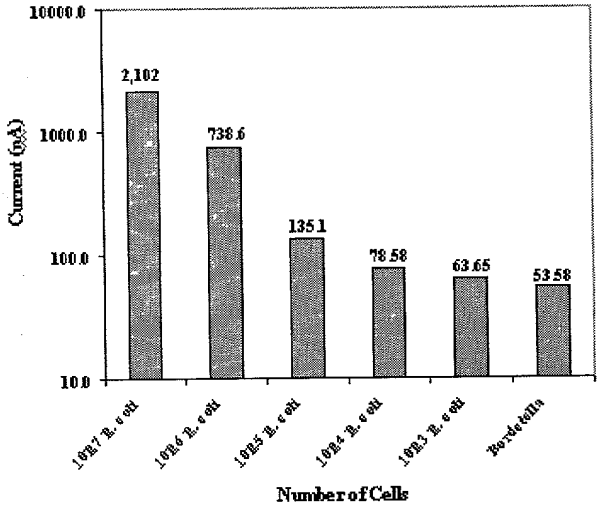

Figure 13